Role of glycerol-3-phosphate phosphatase (G3PP) in pancreatic β-cells and liver

Anfal Al-Mass

Division of Experimental Medicine

Faculty of Medicine

McGill University, Montreal

August 2022

A thesis submitted to McGill University in partial fulfillment of the requirements of the degree of Doctor of Philosophy.

Table of Contents

Abstract

Chronic nutritional excess results in metabolic disorders such as obesity, type 2 diabetes and fatty liver disease. Hyperglycemia is a frequent characteristic of these disorders; and chronic hyperglycemia can damage different cells and tissues including the pancreatic β-cells and liver cells through a process called glucotoxicity. Detoxification pathways that eliminate excess glucose carbons can help protect cells and tissues from damage. The glycerolipid/free fatty acid (GL/FFA) cycle is a critical detoxification pathway that plays an important role in the overall regulation of glucose and lipid metabolism. Glycerol-3-phosphate (Gro3P), which is formed from glucose during glycolysis, is at the crossroads of glucose and lipid metabolism and one of the starting substrates for the GL/FFA cycle. Gro3P is hydrolyzed by glycerol-3-phosphate phosphatase (G3PP) to glycerol, which suggests that G3PP could be an important metabolic regulator and raises the possibility that defective G3PP activity could lead to metabolic dysfunction. We have shown recently that G3PP, by regulating cytosolic Gro3P levels, can play a role in the control of glycolysis, glucose oxidation, cellular redox and ATP production, gluconeogenesis and glycerolipid synthesis in β-cells and hepatocytes *in vitro*. In this thesis I studied the potential role of G3PP in β-cells and liver *in vivo* and viewing G3PP as a potential detoxification enzyme that eliminate excess glucose carbon to glycerol.

In Chapter II, I demonstrated that G3PP play an important role in regulating β-cells insulin secretion and preventing glucotoxicity *in vivo* and *ex vivo*. β-cell specific G3PP-KO mouse (BKO) fed normal diet for 20 weeks showed increased body weight gain, fed insulinemia, and enhanced insulin secretion in response to glucose load. GSIS response *ex vivo* is higher in BKO islets only at high glucose. BKO islets show reduced glucose-induced glycerol release and elevated O_2 consumption and ATP production only at high glucose levels. Metabolites like Gro3P, DHAP, ATP, acetyl-CoA and malonyl-CoA were increased in BKO islets only at high glucose. Glucotoxicity at 30 mM glucose for 7 days led to increased apoptosis, reduced insulin content and expression of *Pdx-1* and *Ins-2* genes in BKO islets.

In Chapter III, I demonstrated that G3PP play an important role in regulating glucose metabolism and lipogenesis in mouse liver *in vivo*. Hepatocyte specific G3PP-KO (LKO) mice fed normal diet for 10 weeks showed no major phenotype. However, when challenged with a glucose infusion for 55h, LKO mice showed an accumulation of liver TG, glycogen and cholesterol and

increased liver weight. In addition, chronic hyperglycemia led to increased mRNA levels of pro-inflammatory cytokines and macrophage markers in LKO mice. LKO mice showed an increase in plasma markers levels of the metabolic syndrome, including TG, LDL, VLDL, urea and uric acid. Targeted metabolomics studies in livers of chronically hyperglycemic LKO mice showed increased levels of Gro3P, which drives lipogenesis/fatty acid esterification, and metabolites linked to *de novo* lipogenesis, including Krebs cycle intermediates, acetyl-CoA and malonyl-CoA.

In Chapter IV, I investigated the effects of 3-fold overexpression of human G3PP in mouse. To examine if G3PP overexpression protects against glucotoxicity and fat accumulation *in vivo*; and found no major effect on liver metabolism *in vivo* or *ex vivo*. This demonstrates that a higher level of G3PP overexpression is needed to study the effects of G3PP in liver *in vivo* using transgenic mice or G3PP activator in the future.

Overall, I have obtained evidence that the glycerol shunt promoted by G3PP is an important metabolic pathway implicated in glucodetoxification that can play a role in preventing insulin hypersecretion and excess body weight gain and contributes to β-cell mass preservation in the face of hyperglycemia and also plays a role in preventing fatty liver and its complications.

Résumé

Un excès nutritionnel chronique entraîne des troubles métaboliques tels qu'obésité, T2D et stéatose hépatique. L'hyperglycémie est une caractéristique fréquente de ces troubles métaboliques et l'hyperglycémie chronique peut endommager diverses cellules et tissus, dont les cellules β pancréatiques et les cellules du foie, en provoquant une glucotoxicité. Les voies de détoxification éliminant les glucides en excès peuvent aider à protéger les cellules et les tissus contre ces dommages. Le cycle GL/FFA est une voie critique de détoxification et joue un rôle important dans la régulation globale du métabolisme du glucose et des lipides. Le glycérol-3-phosphate (Gro3P), formé à partir du glucose lors de la glycolyse, se retrouve au carrefour du métabolisme du glucose et des lipides et est l'un des principaux substrats de départ du cycle GL/FFA. Gro3P est directement hydrolysé en glycérol par la glycérol-3-phosphate phosphatase (G3PP), suggérant que G3PP soit un important régulateur métabolique et soulevant la possibilité que l'activité défectueuse de G3PP pourrait conduire à un dysfonctionnement métabolique. Ici, j'ai étudié le rôle potentiel de G3PP dans les cellules β et le foie in-vivo et la possibilité que G3PP agisse comme une enzyme de détoxification potentielle pour l'excès de glucides.

Dans le chapitre II, j'ai démontré que G3PP joue un rôle important en régulant la sécrétion d'insuline par les cellules β et en prévenant la glucotoxicité in-vivo et ex-vivo. Un modèle de souris G3PP-KO spécifique pour les cellules β (BKO) nourri avec une diète normale pour 20 semaines présente une augmentation du gain de poids corporel et de l'insulinémie non à jeûn et une augmentation de la sécrétion d'insuline en réponse à une charge de glucose. La réponse GSIS ex-vivo est plus élevée dans les îlots de souris BKO uniquement à un taux élevé de glucose. Les îlots BKO présentent une libération réduite de glycérol induite par le glucose et une augmentation de la consommation d'O_2 et production d'ATP uniquement à des taux de glucose élevés. Les métabolites tels Gro3P et DHAP sont augmentés dans les îlots BKO à un taux de glucose élevé. La glucotoxicité entraîne une augmentation de l'apoptose, une réduction du contenu en insuline et une réduction de l'expression des gènes Pdx-1 et Ins-2 dans les îlots BKO.

Dans le chapitre III, j'ai démontré que G3PP joue un rôle important dans la régulation du métabolisme du glucose et la lipogenèse dans le foie de souris in-vivo (LKO). LKO sur diète normale pour 10 semaines ne présentent pas de phénotype majeur. Toutefois, en conditions d'hyperglycémie, les souris LKO ont montré une accumulation de TG hépatique, glycogène et

cholestérol. De plus, l'hyperglycémie chronique entraîne une augmentation des niveaux d'ARNm de cytokines pro-inflammatoires et des marqueurs des macrophages chez les souris LKO. Des modifications des marqueurs plasmatiques du syndrome métabolique comme TG and VLDL ont également été notées. Des études métabolomiques ciblées dans le foie des souris LKO chroniquement hyperglycémiques ont montré des niveaux accrus de Gro3P qui entraîne la lipogenèse/estérification des acides gras, et des métabolites liés à la lipogenèse de novo.

Dans le chapitre IV, j'ai étudié les effets d'une augmentation d'environ 3 fois de l'expression de G3PP humain dans les hépatocytes de souris afin d'examiner si la surexpression de G3PP protège contre la glucotoxicité et l'accumulation de graisses *in-vivo*. Aucun effet majeur au niveau du métabolisme hépatique *in-vivo* ou *ex-vivo* n'a pu être détecté.

En conclusion, j'ai réussi à démontrer que le shunt G3PP/glycérol est une voie métabolique impliquée dans la glucodétoxification qui peut jouer un rôle dans la prévention de l'hypersécrétion d'insuline et de l'excès de poids corporel et ainsi contribuer à la préservation de la masse des cellules β face à l'hyperglycémie, en plus de jouer un rôle dans la prévention de la stéatose hépatique.

Acknowledgements

First and foremost I would like to express my sincere thanks and gratitude to both of my supervisors Dr. Marc Prentki and Dr. Rob Sladek for their continued support during the past years and for their patience, enthusiasm, motivation and immense knowledge. Thank you Dr. Prentki for believing in me and guiding me through tough times in my PhD especially during COVID times. Your passion for science have inspired me to think bigger, aim higher and work harder. Thank you Dr. Sladek for all your remarkable and outstanding guidance and experience that you gave to me. Discussing with you always gave me a great insight on how to think outside the box and challenging me to be better in everything I do in science and in life. For everything you have given me, I sincerely thank you both.

Second, I would like to thank the senior scientists in the lab: Dr. Marie-Line Peyot and Dr. Murthy Madiraju. Thank you Marie-Line for you tremendous guidance and support, thank you for everything you taught me and for begging a great role model for me in science and I am glad to have you as one of my closest friend for life. Murthy thank you for your guidance, kindness and patience. I will always cherish our discussions in science and in life. Thank you for sharing your knowledge with me and always pushing me to be better.

Special thank you to Roxane Lussier, I would never survive this PhD without you. Thank you for being by myside everyday helping and guiding me through. Working with was the best thing, words can never do you justice so thank you for everything I will really miss working with you.

A sincere thank you to Dr. Alix Zutter, for making the lab feels like a big family, for always caring, encouraging and for being there for the good and bad days. Thank you for being the buffer that kept us going especially during COVID times. Thanks to Dr. Pegah Poursharifi and Dr. Yves Mugabo to their amazing support in my journey, working with you made the difference. It was a great pleasure sharing the good, the bad and the ugly with you guys and I wouldn`t choose a better people to share this with. Thank you for being a true friends and hope that I will be able to work with you in the future.

Thanks to everyone in the Prentki and Sladek laboratory, past and present, it was a pleasure working with you in the past years. A special thank you to Isabelle Chénier and Henry Leung for

the help, the support and the friendship. Thanks to the CRCHUM family for their help when needed and for they support and friendship. Thanks to McGill University for making is easy for us during the difficult times of COVID, this was really appreciated.

Last but not least, I must express my very profound gratitude to my family and friends for their tremendous love and support throughout my PhD. Especially to my parents for their unfailing support and continuous encouragement throughout my PhD. This accomplishment would have not been possible without them, so I would like to dedicate this doctoral thesis to them.

Publications arising from PhD study

Publications presented in the thesis:

- **Al-Mass, A.**, Poursharifi, P., Peyot, M. L., Lussier, R., Levens, E. J., Guida, J., Mugabo, Y., Possik, E., Ahmad, R., Al-Mulla, F., Sladek, R., Madiraju, S., & Prentki, M. (2022). Glycerol-3-phosphate phosphatase operates a glycerol shunt in pancreatic β-cells that controls insulin secretion and metabolic stress. **Molecular Metabolism.** 60:101471. PMID: 35272070.
- **Al-Mass, A**., Poursharifi, P., Peyot, M. L., Lussier, R., Chenier, I., Leung, YH., Oppong, A., Ghosh, A., Possik, E., Mugabo, Y., Possik, E., Sladek, R., Madiraju, S., & Prentki, M. (2022). Glycerol-3-phosphate phosphatase/glycerol shunt prevents hyperglycemia driven lipogenesis and inflammation in mouse liver. Submitted to **Molecular Metabolism.** 66:101609**.** PMID: 36198384.
- Possik E., **Al-Mass A.**, Peyot M. L., Ahmad R., Al-Mulla F., Madiraju S. R. M., Prentki M. New Mammalian Glycerol-3-Phosphate Phosphatase: Role in β-Cell, Liver and Adipocyte Metabolism. **Front Endocrinol (Lausanne).** 2021 Jul 13; 12:706607. PMID: 34326816. (Review).

Publications indirectly related to the thesis:

- Possik E, Schmitt C, **Al-Mass A**, Bai Y, Côté L, Morin J, Erb H, Oppong A, Kahloan W, Parker JA, Madiraju SRM, Prentki M. Phosphoglycolate phosphatase homologs act as glycerol-3-phosphate phosphatase to control stress and healthspan in C. elegans. **Nature Communications**. 2022 Jan 11; 13(1):177. PMID: 35017476.
- Lounis MA, Ouellet V, Péant B, Caron C, Li Z, **Al-Mass A**, Madiraju SRM, Mes-Masson AM, Prentki M, Saad F. Elevated Expression of Glycerol-3-Phosphate Phosphatase as a Biomarker of Poor Prognosis and Aggressive Prostate Cancer. **Cancers** (Basel). 2021 Mar 13; 13(6):1273. PMID: 33805661.
- Poursharifi P, Attané C, Mugabo Y, **Al-Mass A**, Ghosh A, Schmitt C, Zhao S, Guida J, Lussier R, Erb H, Chenier I, Peyot ML, Joly E, Noll C, Carpentier AC, Madiraju SRM, Prentki M. Adipose ABHD6 regulates tolerance to cold and thermogenic programs. **JCI Insight.** 2020 Dec 17;5(24):e140294. PMID: 33201859.

Contributions to original knowledge

Chapter II:

- G3PP operates a glycerol shunt in β-cells to remove excess glucose as glycerol.
- Inducible β-cell specific G3PP-KO (BKO) mice show hyperinsulinemia.
- BKO mice show enhanced body weight and glucose induced insulin secretion.
- BKO isolated islets show elevated insulin secretion only at high glucose.
- Chronic exposure of BKO isolated islets to high glucose enhances glucotoxicity.

Chapter III:

- LKO mice under normal diet show elevated plasma TG with only a small increase in liver TG levels and no changes in body weight and food intake.
- LKO mice under normal diet show elevated liver glucose production upon glycerol load
- Decreased glycerol shunt with reduced glycerol release and increased gluconeogenesis and lactate production from isolated hepatocytes from the LKO mice
- LKO mice show enhanced TG, LDL and VLDL and cholesterol levels in plasma following glucose infusion-induced hyperglycemia
- LKO mice show increased liver weight, TG and glycogen content and expression of inflammatory markers following glucose infusion-induced hyperglycemia
- Glucose infusion-induced hyperglycemia lead to increase levels of Gro3P, DHAP, acetyl-CoA, malonyl-CoA, Krebs cycle intermediates and NADP/NADPH ratio in LKO mouse livers.

Chapter IV:

- Using AAV8-TBG-h-PGP, 3-fold overexpression of G3PP was achieved in mouse liver (LOVX mice).
- LOVX mice show no specific phenotype *in vivo* after 10 weeks on normal diet.
- Three-fold overexpression of G3PP in LOVX mouse hepatocytes has no major impact on hepatocyte metabolism *ex vivo*.

Contribution of Authors

Chapter II:

The experiments were designed with the help of Marie-Line Peyot, S. R. Murthy Madiraju and Marc Prentki. I took care of the mice, their diet, weight, health and preformed all TMX injections with the technical help of Roxane Lussier, who did most of the genotyping. I was responsible for grouping the mice and planning the experiments. IPGTT, ITT, sacrificing the mice, islet isolation, blood and tissue collection and GSIS were done with the help of Pegah Poursharifi, Marie-Line Peyot, Roxane Lussier, Emily Levens and Julian Guida. I preformed all Western blots, glycerol release, glucotoxicity, RNA extraction, quantitative PCR and targeted metabolomics experiments. Oxygen consumption and mitochondrial function were done with the help of Yves Mugabo. I did all the data analysis with the help of Marie-Line Peyot, S. R. Murthy Madiraju and Marc Prentki. I wrote the manuscript with the help of Marie-Line Peyot, S. R. Murthy Madiraju and Marc Prentki. Elite Possik, Rasheed Ahmad, Fahd Al-Mulla, Robert Sladek reviewed the manuscript.

Chapter III:

The experiments were designed with the help of Marie-Line Peyot, S .R. Murthy Madiraju and Marc Prentki. I took care of the mice, there diet, weight, health and prepared the virus for IV injections with the technical help of Roxane Lussier, who did most of the genotyping. I was responsible of grouping the mice and planning the experiments. Oral glycerol load and pyruvate load tests, sacrificing the mice, hepatocyte isolation and blood and tissue collection were done with the help of Pegah Poursharifi, Roxane Lussier, Isabelle Chenier and Yat Hei Leung. I preformed all western blots, glycerol release, gluconeogenesis, RNA extraction, quantitative PCR and targeted metabolomics experiments. TG content and lactate measurements were done with the help of Roxane Lussier and Abel Oppong. In vivo glucose infusion was done with the help of Roxane Lussier and Isabelle Chenier. I did all the data analysis with the help of Marie-Line Peyot, S. R. Murthy Madiraju and Marc Prentki. I wrote the manuscript with the help of Robert Sladek, S. R. Murthy Madiraju and Marc Prentki.

Chapter IV:

The experiments were designed with the help of Marie-Line Peyot, S. R. Murthy Madiraju and Marc Prentki. I took care of the mice, their diet, weight, health and prepared the virus for IV injections with the technical help of Roxane Lussier. I was responsible of grouping the mice and planning the experiments. Oral glycerol load test, pyruvate load test, sacrificing the mice, hepatocytes isolation and blood and tissue collection were done with the help of Pegah Poursharifi, Roxane Lussier and Isabelle Chenier. I preformed all western blots, glycerol release and gluconeogenesis. TG content and lactate measurements were done with the help of Roxane Lussier and Abel Oppong. In vivo glucose infusion was done with the help of Roxane Lussier and Isabelle Chenier. I did all the data analysis with the help of Marie-Line Peyot, S. R. Murthy Madiraju and Marc Prentki. I wrote the manuscript with the help of Robert Sladek.

List of Figures

Chapter I:

List of tables

List of Abbreviations:

2-PG : 2-phosphoglycolate

4-PE : 4-phosphoerythronate

ABCA1 : ATP-binding cassette transporter-A1

ABHD6 : α / β-domain containing hydrolase-6

ACC : acetyl-CoA carboxylase

ACSL : long-chain acyl-CoA synthetase

ADP : adenosine di-phosphate

AGEs : advanced glycation end products

AGPAT : 1-acyl-sn-glycerol-3-phosphate acyltransferase

AKT : protein kinase B

AMP : adenosine monophosphate

AQPs : aquaglyceroporins

ASCVD : atherosclerotic cardiovascular disease

ATF6 : activating transcription factor 6

ATGL : adipose triglyceride lipase

ATP : adenosine triphosphate

AUM : Mg2+-dependent phosphatase

cAMP : cyclic adenosine monophosphate

Chop : C/EBP homologous protein

ChREBP : carbohydrate-responsive element-binding protein

CPT-1 : carnitine palmitoyltransferase 1

CREB : cAMP-response element binding protein

CRTC2 : CREB Regulated Transcription Coactivator 2

CVD : cardiovascular disease

DAG : diacylglycerol

DAGL : diacylglycerol lipase

DHAP : dihydroxyacetone-3-phosphate

DIO : diet-induced obese

DNA : deoxyribonucleic acid

ER stress : endoplasmic reticulum stress

ETC : electron transport chain

F1,6P : fructose 1,6-bisphosphate

F2,6P : fructose 1,6-bisphosphate

F6P : fructose-6-phosphate

FA-CoA : fatty acyl-CoA

FAD : flavin adenine dinucleotide

FADH2 : flavin adenine dinucleotide reduce

FAS : fatty acid synthase

FBPase : fructose 1,6-bisphoshpatase

FFA : free fatty acid

FFAR-1 : free fatty acid-activated receptor-1

FOXO1 : forkhead box protein O1

G3PP : glycerol-3-phosphate phosphatase

G6P : glucose-6-phosphate

G6Pase : glucose-6-phosphatase

GA3P : glyceraldehyde-3-phosphate

GAPDH : glyceraldehyde-3-phosphate dehydrogenase

GCK : glucokinase

GCKR : glucokinase regulator

GIP : gastric inhibitory polypeptide

GK : glycerol kinase

GL/FFA cycle : glycerolipid / free fatty acid cycle

GLP-1 : glucagon-like-peptide-1

GLUT : glucose transporter

GPAT : glycerol-3-phosphate acyl transferase

GPD1 : cytosolic Gro3P dehydrogenase

GPD2 : mitochondrial Gro3P dehydrogenase

GPDH : Gro3P dehydrogenase

GPR120 : G protein-coupled receptor 120

GPR40 : G protein-coupled receptor 40

Gro3P : glycerol-3-phosphate

GSIS : glucose-stimulated insulin secretion

GTP : guanosine triphosphate

HAD : haloacid dehalogenase

HDL : high density lipoproteins

HGP : hepatic glucose production

HIF1 α : hypoxia-inducible factor-1 alpha

HSCs : hepatic stellate cells

HSD17B13 : hydroxysteroid 17β- dehydrogenase

HSL : hormone-sensitive lipase

IGF1: insulin-like growth factor 1

IGF2 : insulin-like growth factor 2

IKKβ : kappa-B kinase subunit beta

IL-10 : interleukin-10

IL-6 : interleukin-6

IP3 : inositol triphosphate

IR : insulin resistance

IRS : insulin receptor substrates

JNK : c-Jun N-terminal kinase

LDL : low density lipoproteins

LPA : lysophosphatidic acid

LXR : liver X receptor

MafA : MAF BZIP Transcription Factor A

MAG : monoacylglycerol

MAGL : monoacylglycerol lipase

Mal-CoA : malonyl-CoA

MBOAT7 : membrane bound O-acyltransferase domain-containing 7

MCF : metabolic coupling factor

MetS : metabolic syndrome

mTOR : mammalian target of rapamycin

NAD : nicotinamide adenine dinucleotide

NADH : nicotinamide adenine dinucleotide reduce

NADP : nicotinamide adenine dinucleotide phosphate

NAFLD : non-alcoholic fatty liver disease

NASH : non-alcoholic steatohepatitis

NeuroD1 : Neurogenic differentiation 1 (also called β2)

PA : phosphatidic acid

PAP : phosphatidic acid phosphatase

Pax6 : paired box 6

PAX6 : paired box gene 6

PC : pyruvate carboxylase

PCOS : polycystic ovary syndrome

PDH : pyruvate dehydrogenase

PDK : PIP3-dependent protein kinase

PDX-1 : pancreatic and duodenal homeobox-1

PEP : phosphoenolpyruvate

PEPCK : phosphoenolpyruvate carboxykinase

PFK1 : phosphofructokinase 1

PGC-1α : proliferator-activated receptor gamma coactivator 1-alpha

PGP : phosphoglycolate phosphatase

PI3K : phosphatidylinositol 3,4,5 kinase

PIP2 : phosphatidylinositol (4,5)-bisphosphate

PIP3 : phosphatidylinositol (3,4,5)-trisphosphate

PK : pyruvate kinase

PKA : protein kinase A

PKD1 : protein kinase D

Pl : phosphatidylcholine

PNPLA3 : patatin-like phospholipase domain containing protein-3

PPARs : peroxisome proliferator-activated receptors

RBC : red blood cell

ROS : reactive oxygen species

SAT : subcutaneous adipose tissue

SNPs : single-nucleotide polymorphisms

SREBP : sterol regulatory element-binding protein

T2D : type 2 diabetes

TCA cycle : tricarboxylic acid cycle

TG : triglycerides

TM6SF2 : transmembrane 6 superfamily member 2

TNFa : tumor necrosis factor alpha

TPI : triose phosphate isomerase

Txnip : thioredoxin-interacting protein

UPR : unfolded protein response

VAT : visceral adipose tissue

VLDL : very low-density lipoprotein

Chapter I. Introduction

1.1. Metabolic syndrome: an overview

A sedentary lifestyle, easy access to calorie-dense food and genetic predisposition are major contributors to the progression of metabolic syndrome (MetS), a term used to describe a state of poor metabolic health that represents a group of metabolically related symptoms (Smith, Mittendorfer et al. 2019). Central obesity, glucose intolerance, dyslipidemia and hypertension are the main characteristics of MetS and the presence of all or some of these risk factors in one person represents MetS (Aguilar-Salinas and Viveros-Ruiz 2019). Insulin resistance (IR) and hyperinsulinemia both contribute to MetS. Saying that, it is debatable which one of these factors initiates or is the main contributor to MetS (O'Neill and O'Driscoll 2015, Aguilar-Salinas and Viveros-Ruiz 2019). The dominant view is that IR, characterized by the lack of insulin action on peripheral tissues, causes elevation of plasma glucose levels, which in turn will promote the increased demand on pancreatic β-cells to produce and secrete more insulin through a mechanism called β-cell compensation or hyper-responsiveness (Prentki and Nolan 2006, Hudish, Reusch et al. 2019). This compensatory β-cell response leads to hyperinsulinemia which initially restores normal glucose level in the prediabetic state. However, the β-cells eventually become unable to compensate for chronic exposure to excess glucose, lipids and other secretagogues, which leads to β-cell dysfunction and/or apoptosis and the progression toward type 2 diabetes (T2D) and increased diseases associated with MetS (Prentki and Nolan 2006).

This view has been challenged by an alternative hypothesis that islet β-cell hyper-responsiveness is the primary cause of glucose intolerance, at least in some patients. In this view IR can actually be considered as a protective adaptive response of critical tissues, such as the heart,

muscle or liver, against insulin induced metabolic stress (Corkey 2012, Nolan and Prentki 2019). Moreover, increasing evidence indicates that the hyperinsulinemic state contributes disorders associated with MetS, including obesity-related T2D, non-alcoholic fatty liver disease (NAFLD), atherosclerotic cardiovascular disease (ASCVD), and polycystic ovary syndrome (PCOS) (Nolan and Prentki 2019). These different views all suggest that understanding β-cell function and dysfunction in MetS may provide novel methods to treat T2D, NAFLD, cardiovascular disease (CVD), and other MetS complications.

1.1.1 Obesity: the major factor

Obesity is considered by many to be the main pathogenetic factor in MetS, and is associated with IR, β-cell expansion and hyperinsulinemia (Prentki and Nolan 2006, Al-Goblan, Al-Alfi et al. 2014). Obesity is a condition of abnormal or excessive fat accumulation in adipose tissue and results mainly from long term energy imbalance (Ahima 2011). Energy homeostasis, which is a precise balance between energy intake and energy expenditure, is central for the survival of all organisms (Bluher 2019). In the past ages, undernutrition was the main health problem that humans had to adapt to by withstanding longer periods of starvation and mobilizing and storing energy more efficiently (Yanovski 2018). In recent years, a sedentary lifestyle and easy access to food has led to overnutrition emerging as a major health threat, with more people dying from obesity than undernutrition, and resulting to a major obesity pandemic (Bluher 2019).

Many researchers have tried to identify the mechanisms that cause obesity by studying how appetite and regulation of food intake is disturbed in the brains of obese individuals and how adipose tissue dysfunction can cause secondary health problems (Murray, Tulloch et al. 2014, Lee and Shin 2017). One of the major milestones in understanding the molecular regulation of energy homeostasis is the discovery of leptin (Zhang, Proenca et al. 1994), a hormone secreted by adipose

tissue that acts on the hypothalamus to regulate appetite and energy expenditure (Farooqi 2014). The importance of leptin in the pathogenesis of obesity comes from studying monogenic mouse models that harbor mutations in the leptin gene ($Lep^{ob/ob}$ mice) and leptin receptor gene ($Lepr^{db/db}$ mice), which are characterized by severe obesity, hyperinsulinemia and hyperglycemia (Zhang, Proenca et al. 1994, Farooqi and O'Rahilly 2014). From these studies and previous work before leptin was identified [in particular by the groups of Doug Coleman (Coleman 2010), Bernard Jeanrenaud (Rohner-Jeanrenaud and Jeanrenaud 1996) and George Bray (Ryan, Hansen et al. 2016)], it became clear that the brain and other tissues cooperate to regulate energy homeostasis and contribute to the pathogenesis of obesity (Murray, Tulloch et al. 2014). In addition, monogenetic causes of obesity are rare and cannot explain the extent of the obesity pandemic.

Other factors contributing to the pathogenesis of obesity include the adipose tissue itself, which is composed of both adipocytes (triglyceride-filled cells) and other cells including preadipocytes, stem cells, endothelial cells and immune cells. Adipocytes secrete adipokines such as leptin, adiponectin, IL-6, TNFα and IL-10, which regulate adipose tissue expansion, energy balance, and other functions. These adipokines have anti- and pro-inflammatory effects; any dysregulation of adipocyte metabolism and function in obesity leading to changes in adipokine secretion could also alter the immune system and cause inflammation in adipose tissue, liver and pancreatic islets (Sun, Kusminski et al. 2011).

1.1.2 Type 2 Diabetes: the complicating factor

T2D is one of the MetS complications that is associated strongly with obesity. When T2D and obesity coexist, the β-cell becomes unable to compensate fully for IR in other tissues and β-cell dysfunction occurs. T2D is defined as a metabolic disorder of fuel homeostasis characterized by hyperglycemia and altered lipid metabolism caused by IR and islet β-cell dysfunction due to

genetic and environmental factors (Nolan, Damm et al. 2011). T2D is a slowly progressive disease with its symptoms developing gradually with time and only when the blood glucose levels become chronically elevated the symptoms appear. Chronic untreated hyperglycemia can affect the function of many organs, in particular the kidneys, nerves and eyes (Amos, McCarty et al. 1997). Without intervention and treatment, individuals with T2D can develop secondary end-organ complications, which can lead to serious health and social problems that reduce both their quality of life and lifespan. The risk of developing T2D is known to increase with increasing age, obesity and lack of physical activity (Stumvoll, Goldstein et al. 2005). It is often associated with hypertension, dyslipidemia and a strong genetic predisposition. However, T2D genetic is complex and not clearly understood. To date, approximately 500 genetic variants have been linked to T2D, most with a very small effect (Mahajan, Taliun et al. 2018, Adeyemo, Zaghloul et al. 2019, Dwivedi, Lehtovirta et al. 2019, Spracklen, Horikoshi et al. 2020).

While T2D is diagnosed based solely on the sustained presence of hyperglycemia, this is often accompanied by characteristic changes in other metabolic phenotypes. These can be used to identify stable clinical subtypes of T2D that have different characteristics and also different risks of diabetes-related complications and outcomes (Ahlqvist, Prasad et al. 2020). These subtypes are based on: glutamate decarboxylase autoantibodies, BMI, HbA1c, age at diabetes onset, β-cell function and insulin resistance estimated from fasting glucose and C-peptide levels (Ahlqvist, Prasad et al. 2020)

1.1.3 Non-Alcoholic Fatty Liver Disease: the hidden element

Non-alcoholic fatty liver disease (NAFLD) is a spectrum of liver diseases ranging from isolated steatosis, to a more severe non-alcoholic steatohepatitis (NASH) and fibrosis, and cirrhosis. It is characterized by excessive hepatic fat accumulation (steatosis) in the form of triglycerides (TG)

that involves > 5% of hepatocytes histology or radiologically (Kim, Lee et al. 2020), in the absence of secondary causes such as viral hepatitis, excessive alcohol intake or hereditary liver diseases (Yki-Jarvinen 2014). NAFLD is currently the most common form of chronic liver disease in the world, and is particularly common in patients with obesity and T2D (Huang, Behary et al. 2019).

The liver has many metabolic and biosynthetic functions including glucose production through gluconeogenesis and the production of very low-density lipoproteins (VLDL), which transport TGs to peripheral tissues (Birkenfeld and Shulman 2014). NAFLD reaching NASH stage is a major health concern due to the potential progression to cirrhosis and hepatocellular carcinoma which cause an irreversible damage to the liver (Huang, Behary et al. 2019). In contrast, hepatic steatosis is the reversible stage of NAFLD; which is the imbalance between free fatty acid (FFA) absorption and synthesis and FFA oxidation and TG secretion in VLDL. This imbalance will lead to the accumulation of fat in the form of TG and lipid droplets in the hepatocytes. The sources of liver TG include dietary fat (packaged in TG-rich chylomicrons), *de novo* lipogenesis in the liver and lipolysis in adipose tissue (which provides glycerol and FFA). In healthy individuals, insulin suppresses lipolysis and FFA release from peripheral adipose tissue and promotes hepatic VLDL production. However, obese individuals who have increased visceral adipose tissue (VAT) which contributes to increased IR and hyperinsulinemia, frequently have an ineffective response to insulin that results in increased levels of circulating FFAs, hepatic VLDL production and gluconeogenesis (Yki-Jarvinen 2014). IR and obesity are associated with an increase in the quantity of FFA delivered to the liver following an increase in lipolysis in adipocytes (Mittendorfer, Magkos et al. 2009). Furthermore, FFAs captured by hepatocytes can go through oxidation in the mitochondria to produce adenosine triphosphate (ATP), re-esterification to TG and stored in lipid droplets or secreted as VLDL. All these mechanisms, if persisting chronically, will result in

extreme hepatic steatosis and the production of lipotoxic lipids leading to hepatocellular lipotoxicity through oxidative and ER stress, mitochondrial dysfunction and inflammasome activation, leading to hepatocyte inflammation and apoptosis (Marra and Lotersztajn 2013, Birkenfeld and Shulman 2014). Following this stage of steatosis, NASH will occur, and macrophage-like Kupffer cells will be activated by proinflammatory cytokines produced in the liver. The Kupffer cells will further recruit peripheral macrophages, T cells and neutrophils, to escalate the hepatoxicity seen in NASH (Marra and Lotersztajn 2013). Furthermore, myofibroblasts (hepatic stellate cells [HSCs]) will proliferate in response to TNF-α, IL-1β and other proinflammatory cytokines and secrete extracellular matrix proteins leading to progressive fibrosis and eventually cirrhosis (Marra and Lotersztajn 2013).

More recently, the gut microbiota has been implicated both in the pathogenesis of NAFLD and in the progression to NASH via altered metabolic processes and pro-inflammatory effects (Safari and Gerard 2019). One of the important factors that can also play a role in NAFLD pathogenicity are genetic and epigenetic factors with heritability being estimated to be 20-70% (Sookoian and Pirola 2017). Genome-wide association studies (GWAS) found numerous single-nucleotide polymorphisms (SNPs) that independently associate with NAFLD disease severity, progression and risk, including SNPs located in genes such as the patatin-like phospholipase domain containing protein-3 (PNPLA3), glucokinase regulator (GCKR), transmembrane 6 superfamily member 2 (TM6SF2), hydroxysteroid 17β- dehydrogenase (HSD17B13) and membrane bound O-acyltransferase domain-containing 7 (MBOAT7) (Sookoian and Pirola 2017, Eslam and George 2020). Variants in the Apolipoprotein C3 gene also increase NAFLD risk through loss of normal lipoprotein lipase activity in TG-rich lipoproteins (Duseja and Chalasani 2013, Wang, Ye et al. 2020).

1.2 Overview of glucose homeostasis

Glucose homeostasis is a tightly controlled process involving tissues such as the pancreas, liver, subcutaneous and visceral fat, skeletal muscle and the brain. It is regulated by many hormones and small molecules, most importantly insulin and glucagon that are secreted by pancreatic β- and α-cells respectively and that have opposite and balanced actions (Roder, Wu et al. 2016). These hormones maintain blood glucose levels in a very narrow range of 4 to 7 mM in normal individuals both during fasting and feeding. Insulin, an anabolic hormone, promotes glycogenesis, lipogenesis, and the incorporation of amino acids into proteins. Insulin is secreted when blood glucose levels are high during fed conditions. Insulin stimulates glucose uptake and storage as glycogen in muscle and free fatty acids, triglycerides and glucose storage in adipose tissue as triglycerides. In the liver, insulin inhibits gluconeogenesis and promotes the storage of glucose as glycogen. In contrast, glucagon is a catabolic hormone that is secreted when glucose levels are low like during sleep, between meals and fasting to maintain normal glucose levels. Glucagon stimulates the breakdown of glycogen into glucose (glycogenolysis) in liver and muscles and the production of glucose (gluconeogenesis) from lactate, amino acids and glycerol in liver and kidney **(Figure 1.1)** (Roder, Wu et al. 2016). Recently it was shown that intestinal gluconeogenesis could also influence glucose homeostasis. Intestinal gluconeogenesis induced by protein and fiber intake triggers glucose sensing in the portal vein and activates the gut-brain axis to regulate glucose and energy homeostasis (Soty, Gautier-Stein et al. 2017).

In addition to these two main hormones, catecholamines, glucocorticoids and incretins [such as glucagon-like-peptide-1 (GLP-1) and gastric inhibitory polypeptide (GIP) secreted by the gastrointestinal tract], play an important role in regulating glucose tolerance and glucose homeostasis (Vella, Camilleri et al. 2004). GLP-1 is a secreted peptide that acts as a determining

factor in glucose homeostasis due to its ability to reduce appetite, slow gastric emptying, increase insulin secretion and suppress the secretion of glucagon. GLP-1 is secreted by gastrointestinal mucosa L cells in response to meals. The hypoglycemic action of GLP-1 is regulated by its enzymatic degradation by dipeptidyl peptidase IV (DPP-IV) (Nadkarni, Chepurny et al. 2014). This has led to the use of GLP-1 analogs, such as liraglutide, as long-acting incretin mimetics that are resistant to degradation by DPP-IV to improve glycemic control in T2D patients (Htike, Zaccardi et al. 2017, Andreadis, Karagiannis et al. 2018). However, most clinical evidence supporting the use of these incretin mimetics was obtained in short-term studies (Htike, Zaccardi et al. 2017, Andreadis, Karagiannis et al. 2018). In contrast, one study has shown that daily treatment of humanized mice with the incretin mimetic liraglutide for >200 days led to impair insulin secretion and islet function (Abdulreda, Rodriguez-Diaz et al. 2016), raising concerns about the long-term use of GLP-1 analogues in patients with T2D.

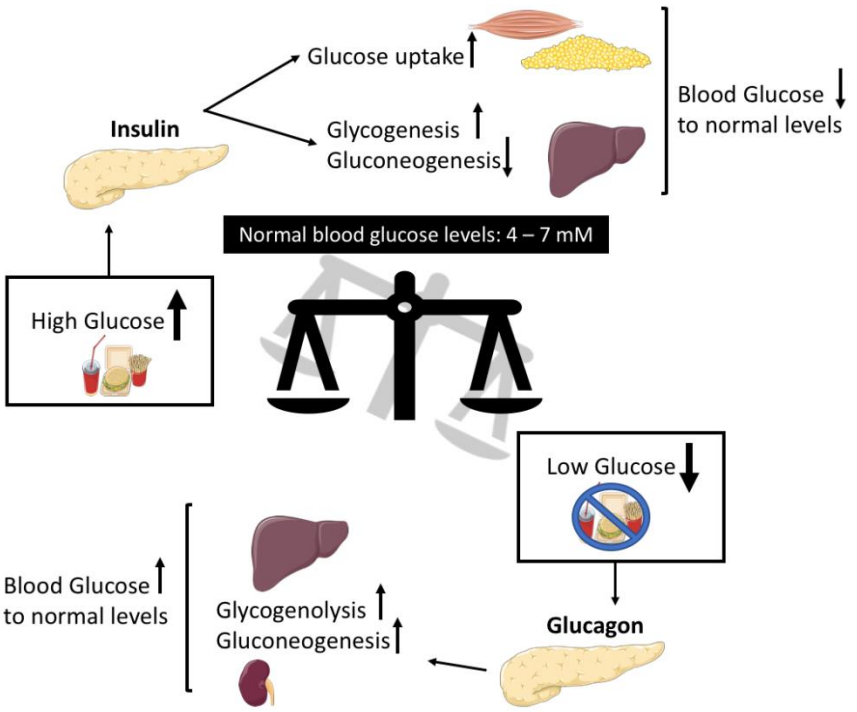

Figure 1.1. Glucose homeostasis.

Insulin and glucagon are the main hormones that regulate blood glucose levels. When blood glucose levels are elevated, for example after eating a meal, the pancreas secretes insulin that increases glucose uptake by tissues including muscle and fat and promotes glycogenesis and suppresses gluconeogenesis in the liver. When blood glucose levels decrease, for example when fasting, the pancreas secretes glucagon to increase glucose production from the liver and the kidney. Adapted from (Roder, Wu et al. 2016).

1.3 Insulin action and resistance

Insulin resistance (IR) is a pathologic condition in which insulin's effect in promoting the uptake and storage of glucose and other fuels is blunted (Campbell and Newgard 2021). IR or insulin insensitivity is controlled by genetic and environmental risk factors (Murea, Ma et al. 2012). IR develops mostly in people who live an inactive lifestyle, like people who are overweight or obese. Individuals with IR often have an elevated fasting glucose, but some have normal fasting blood

glucose and normal postprandial glucose tolerance. In fact, most IR-obese individuals do not develop hyperglycemia, unless β-cell dysfunction occurs and the β-cell can no longer compensate for hyperglycemia (Kahn, Hull et al. 2006). (See Section 1.7). Obesity, T2D, NAFLD, dyslipidemia, hypertension and atherosclerosis have IR as a common denominator (Samuel and Shulman 2016).Individuals with IR often have other health problems such as high blood pressure, increased waist circumference, increased low density lipoproteins (LDL), increased cholesterol and TG levels, decreased high density lipoprotein (HDL) levels, sleep disorders, rapid mood swings and reduced fertility (Samuel and Shulman 2016). In adipose tissue, IR is associated with increased circulating release of FFA and cytokines, which are factors that contribute to the development of IR in the liver and muscles (Kahn and Flier 2000). The IR state in the body causes in the liver an increase in the production of glucose, TG and VLDL whereas in the skeletal muscle, glucose uptake is decreased.

1.3.1 Insulin action in the body

Insulin is an essential anabolic hormone in the body that regulates essential wide range of metabolic pathways. In the liver, insulin increases glycogen synthesis and glycolysis and reduces gluconeogenesis; and also promotes the expression of lipogenic genes and decreases the expression of gluconeogenic genes. In muscle, insulin increases glucose utilization and storage by increasing glucose uptake and glycogen synthesis. In adipose tissue, insulin suppresses TG hydrolysis (lipolysis) which decreases the release of FFA and glycerol into the blood and increases glucose and TG uptake leading to increased lipogenesis and fat storage. Insulin stimulates these metabolic changes by activating an intracellular signaling cascade involving protein phosphorylation (Czech 2017). This signaling cascade is initiated by the binding of insulin to the α-subunit of its receptor leading to a conformational change and activation of the β-subunit. The

β-subunit has kinase activity that can autophosphorylate receptor tyrosine residues leading to the phosphorylation and activation of the insulin receptor substrates IRS1 and IRS2. Tyrosine phosphorylated IRS interacts with phosphatidylinositol 3,4,5 kinase (PI3K) to phosphorylate phosphatidylinositol (4,5)-bisphosphate (PIP2) to phosphatidylinositol (3,4,5)-trisphosphate (PIP3). The increased levels of PIP3 result in its binding to PIP3-dependent protein kinase (PDK), which in turn activates protein kinase B (also known as AKT), which is able to diffuse in the cytoplasm to stimulate transfer of glucose transporters (GLUT4) to the cell membrane where they increase uptake of extracellular glucose molecules (Fazakerley, Krycer et al. 2019). In insulin dependent tissues such as muscle and adipose tissue, GLUT4 translocation is an important step for insulin-dependent glucose utilization. In addition to regulating glucose uptake by increasing glucose transport, insulin also regulates enzymes in the gluconeogenesis, lipolysis and lipogenesis pathways (Fazakerley, Krycer et al. 2019). Overall, insulin also induces the storage of glucose as TG by activating enzymes such as acetyl-CoA carboxylase (ACC), fatty acid synthase (FAS) and pyruvate dehydrogenase (PDH) to stimulate lipogenesis in hepatocytes and adipocytes. In parallel, insulin inhibits lipolysis by decreasing the activity of hormone-sensitive lipase (HSL) (Meijssen, Cabezas et al. 2001).

1.3.2 Insulin resistance and obesity associated T2D

Obesity is a risk factor for diseases such as T2D, atherosclerotic heart disease and hypertension through of its association with IR (Wondmkun 2020). Specifically, in T2D associated with obesity, many factors contribute to IR, including oxidative stress, lipotoxicity and inflammation (Wondmkun 2020). In obesity-associated T2D, IR leads to decreased insulin stimulated glucose transport *via* GLUT4 in adipocytes and skeletal muscle as well as increased hepatic glucose production (Kahn and Flier 2000). Furthermore, increased production of TNFα and FFAs by

adipocytes in obese individuals leads to the dysregulation of insulin signaling pathway, resulting in IR in the liver and skeletal muscle (Borst 2004). This induces oxidative stress and inflammation associated with obesity which will further increase IR (Borst 2004, Hurrle and Hsu 2017). Furthermore, chronic hyperglycemia in obesity associated T2D increases the production of reactive oxygen species (ROS) (Nishikawa, Edelstein et al. 2000) which contribute to reduced insulin-stimulated GLUT4 translocation and glucose uptake. Antioxidants, such as α-lipoic acid, prevent the harmful effects of ROS on glucose transport *in vivo* and *in vitro* (Pisoschi and Pop 2015).

Chronically increased plasma levels of FFA secreted from adipose tissue can lead to lipotoxicity which affects insulin signaling in other tissues (Kahn and Flier 2000). High levels of FFA can directly stimulate IRS1 and IRS2 phosphorylation on Ser residues, which inactivates IRS and interferes with insulin-stimulated glucose transport by modulating the transcription and stability of GLUT4 mRNA (Armoni, Harel et al. 2005). In addition, FFAs can easily enter the cell to be oxidized to produce energy as ATP or to be re-esterified for storage as TG. Interestingly, an increase in plasma FFA levels is associated with intracellular TG accumulation leading to IR in peripheral tissues (Boden, Lebed et al. 2001); and also leads to an accumulation of many FFA-derived metabolites including ceramides and diacylglycerol (DAG) (Erion and Shulman 2010). Ceramides, produced from the metabolism of long chain saturated fatty acids, are thought to act as major players in IR *via* inhibition of AKT activation and GLUT4 translocation (Sokolowska and Blachnio-Zabielska 2019).

Inflammation is another factor which induces IR *via* different mechanisms (Kahn and Flier 2000). Obesity and T2D are associated with chronic low-grade inflammation characterized by an increase in pro-inflammatory markers, including leptin, adiponectin, and cytokines such as TNFα

and IL-6, in the circulation and in adipose tissue produced by activated M1 macrophages (Weisberg, McCann et al. 2003). The pro-inflammatory cytokine TNFα is thought to play a significant role in IR. TNFα activates a variety of kinases, such as JNK, IKKβ, and the IL-1 receptor-associated kinase, which directly or indirectly increase the IRS phosphorylation and decrease the activity of PI3K and AKT (Borst 2004). In addition to pro-inflammatory cytokines, ROS production and ER stress also activate JNK and IKKβ (Matulewicz and Karczewska-Kupczewska 2016). All these effects induce serine phosphorylation of IRS1 and contribute to IR.

1.4 Overview of energy metabolism in obesity and type 2 diabetes

Maintaining energy homeostasis requires a balance between energy consumption and expenditure (Woods, Seeley et al. 1998), which can be disturbed by excessive food intake, causing obesity. Obesity is a major risk factor for T2D as it contributes to IR and β-cell failure due to the exhaustion of insulin stores and fuel surfeit mediated glucolipotoxicity (Prentki and Nolan 2006, Nolan, Damm et al. 2011). β-cell failure also depends on genetic predisposition and/or environmental factors (Prentki and Nolan 2006, Sladek, Rocheleau et al. 2007). Research on genetic factors of T2D have identified many polymorphisms in genes involved in the growth and function of β-cells (Sladek, Rocheleau et al. 2007), supporting the view that and excessive supply of nutrients and β-cell dysfunction are key elements involved in the development of T2D.

Alterations in glucose and lipid metabolism by the glycerolipid / free fatty acid (GL/FFA) cycle (Prentki and Madiraju 2008, Prentki and Madiraju 2012, Prentki, Matschinsky et al. 2013), which is implicated in balancing glucose and lipid metabolism and is central to energy homeostasis in many tissues (Nye, Hanson et al. 2008, Zechner, Zimmermann et al. 2012), may play an important role in the pathogenesis of obesity and T2D. The main route for glucose utilization is

oxidation *via* glycolysis and the Krebs cycle to produce ATP. However, a high intake of nutrients, for example by people with obesity or T2D, can lead to excessive production of ROS in the mitochondria and to ER overload, which eventually causes oxidative and ER stresses. Ceramides, ROS, DAG and other metabolites are known to influence insulin action and resistance and are potentially toxic to various cells when they accumulate (Poitout and Robertson 2002, Nolan and Prentki 2008).

1.5 The GL/FFA cycle in heath and disease

Lipid and glucose metabolism are linked through a central pathway called the GL/FFA cycle, which is implicated in fuel storage and mobilization, and metabolic signaling in tissues such as liver, islets and adipose tissue (Prentki and Madiraju 2008), and also thermogenesis in adipose tissue (Poursharifi, Attane et al. 2020).

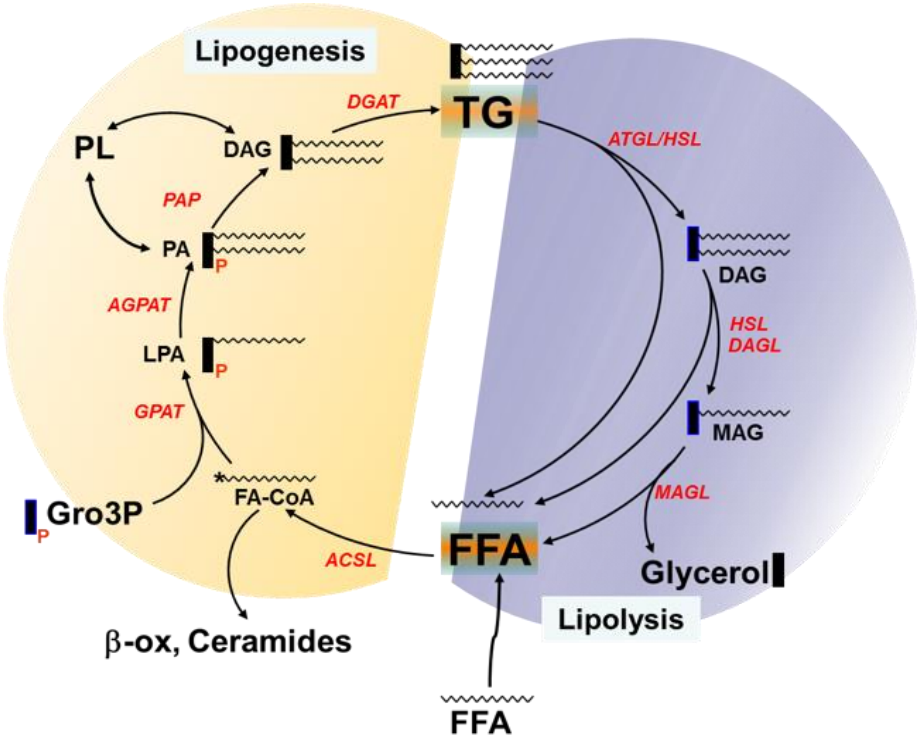

Figure. 1.2. The glycerolipid / free fatty acid cycle.

It is composed of two arms: lipogenic arm (in orang) and a lipolitic arm (in purple). Glycerol-3-phosphate (Gro3P) and fatty acid-CoA (FA-CoA) are the staring substrates. A more detailed description of this cycle is in the text. The abbreviations are: ATGL/HSL, adipose triglyceride lipase/ hormone-sensitive lipase; DAG, diacylglycerol; DAGL, diacylglycerol lipase; MAG, monoacylglycerol; MAGL, monoacylglycerol lipase; FFA, free fatty acid; ACSL, long-chain acyl-CoA synthetase; β-ox, β-oxidation; Gro3P, glycerol-3-phosphate; GPAT, glycerol-3-phosphate acyl transferase; AGPAT, 1-acyl-sn-glycerol-3-phosphate acyltransferase; FA-CoA, fatty acyl-CoA; LPA, lysophosphatidic acid; PA, phosphatidic acid; PAP, phosphatidic acid phosphatase; Pl, phosphatidylcholine; TG, triglycerides. Adapted from (Prentki and Madiraju 2008).

1.5.1 Overall view of the GL/FFA cycle

The GL/FFA cycle is an esterification process of FFA with glycerol to form TG through lipogenesis, followed by the hydrolysis of TG to regenerate glycerol and FFAs through lipolysis

(Figure 1.2) (Prentki and Madiraju 2012). The cycle is initiated by combining glycerol-3-phosphate (Gro3P) from glucose metabolism with FFA in the form of acyl-CoA. In each complete turn of the cycle, seven phosphodiester bonds from ATP are consumed, leading to energy released as heat. The lipogenic arm of the GL/FFA cycle is initiated by an enzyme called glycerol-3-phosphate acyl transferase (GPAT) which allows the synthesis of lysophosphatidic acid (LPA) from FFA in the form of acyl-CoA (FA-CoA) and Gro3P. GPAT is a membrane protein with 4 isoforms, and GPAT 3 and 4 account for 80-90% of the total activity in most tissues (Wendel, Lewin et al. 2009). Overexpression of GPAT3 in INS832/13 β-cell line increases TG and DAG content and increases the severity of glucolipotoxicity (El-Assaad, Joly et al. 2010). The next step in the lipogenesis arm is the formation of phosphatidic acid (PA) from LPA, catalyzed by 1-acyl-sn-glycerol-3-phosphate acyltransferase (AGPAT) which is also a membrane enzyme, present in several isoforms, mostly located in the ER (Takeuchi and Reue 2009). The dephosphorylation of PA to DAG is catalyzed by the phosphatidic acid phosphatases, lipins, located in the cytosol, the ER and the nucleus (Bou Khalil, Blais et al. 2010). The final stage of lipogenesis is the synthesis of TG from DAG, catalyzed by DAG acyltransferases (DGAT) -1 and 2 (Yu and Ginsberg 2004).

The lipolytic arm of the GL/FFA cycle is initiated by hydrolysis of the stored TG in lipid droplets to DAG and FFA by adipose triglyceride lipase (ATGL). DAG is then hydrolysed by hormone sensitive lipase (HSL) generating monoacylglycerol (MAG) (Zechner, Strauss et al. 2005, Mairal, Langin et al. 2006), which is further hydrolyzed by MAG lipase and/or α / β-domain containing hydrolase-6 (ABHD6) to produce glycerol and FFA, the two end-products of lipolysis.

A particularly interesting aspect of the GL/FFA cycle is that it is likely to provide a crucial link between intracellular energy homeostasis and cellular signaling processes (Prentki and Madiraju 2008). Other than TG, the metabolites generated by the GL/FFA cycle are considered

lipid signaling molecules. For example, the esterification step of the GL/FFA cycle can produce the lipid signaling molecules LPA and PA (Noguchi, Ishii et al. 2003). LPA levels increase in the islets of mice fed a high-fat diet: the resulting LPA can signal via plasma membrane receptors (Moolenaar, van Meeteren et al. 2004) and can impair glucose homeostasis and insulin secretion (Rancoule, Attane et al. 2013). Similarly, the activation of mammalian target of rapamycin (mTOR) by PA (Foster 2007) is likely to have important physiological consequences as mTOR is a major cellular stress sensor that is involved in cellular energy hemostasis (Tsang, Qi et al. 2007). FFAs, which are the end-products of lipolysis in the GL/FFA cycle, are known signaling molecules that can activate G protein-coupled receptor 40 (GPR40) and G protein-coupled receptor 120 (GPR120) (Nolan, Leahy et al. 2006), uncoupling proteins (Sluse, Jarmuszkiewicz et al. 2006), and PPARs (Jump 2004). MAG, another GL/FFA cycle metabolite can act as a metabolic coupling factor (MCF) leading to glucose-stimulated insulin secretion (GSIS) (Zhao, Mugabo et al. 2014). Moreover, MAG has been proposed to promote brown fat activation and white fat browning by activating PPARα and PPARγ (Zhao, Mugabo et al. 2016). Notably, recent work on an ABHD6 adipose tissue specific KO, shows that elevated 2-MAG levels increases GL/FFA cycle activity in visceral fat depots *via* 2-MAG/PPARα signaling and contributes to cold-induced thermogenesis (Poursharifi, Attane et al. 2020). Furthermore, the production of Gro3P from glycolysis provides substrate for cytosolic Gro3P dehydrogenase (GPDH): which may link the GL/FFA cycle to the control of cytoplasmic redox potential and glycolytic flow *via* the re-oxidation of reduced NAD (NADH).

1.5.2 Role of the GL/FFA cycle in obesity induced T2D

Altered GL/FFA cycling is one of the mechanisms proposed to explain the failure of the pancreatic β-cell in T2D. Overexpressing HSL in β-cells stimulates lipolysis and reduces TG content in mouse

islets when the animals are fed a high fat diet, resulting in glucose intolerance and impaired GSIS (Mulder, Sorhede-Winzell et al. 2003). Similarly, rodent models with hyperglycemia and glucose intolerance, such as DIO mice (Peyot, Pepin et al. 2010, Delghingaro-Augusto, Decary et al. 2012), show defective GSIS associated with an altered balance between lipogenesis and lipolysis in the GL/FFA cycle (Prentki and Madiraju 2012). In addition, enhanced GL/FFA cycling is involved in β-cell compensation in Zucker fatty (ZF) rat islets, an increase in insulin secretion induced by glucose and palmitate correlates well with increased FFA esterification, lipolysis and expression of lipolytic enzymes, as well as a stimulation of fatty acid oxidation, (Nolan, Leahy et al. 2006).

It is well known that accumulation of TG, DAG and malonyl-CoA (Mal-CoA) in muscle and decreased FFA oxidation can contribute to the development of IR in obese and T2D rodent models (Ruderman and Prentki 2004, Petersen and Shulman 2018). Furthermore, the subcutaneous adipose tissue (SAT) of obese and IR patients exhibit an increased expression of genes involved in lipogenesis and lipolysis, suggesting that enhanced GL/FFA cycle activity in SAT contributes to counteract obesity-associated IR (Gauthier, Rabasa-Lhoret et al. 2014). Finally, activation of GL/FFA cycle may help maintain normal blood glucose levels in obese individuals by increasing insulin secretion and decreasing IR (Prentki and Madiraju 2012). Taken together, these evidence show the importance of the GL/FFA cycle in controlling glucose and lipid metabolism and demonstrate how alterations in this cycle could lead to metabolic dysfunction and T2D.

1.6 Insulin secretion and its regulation in health

The main role of the pancreatic β-cell is to control glycemia by secreting insulin in response to circulating levels of blood glucose and other nutrients as well as neurohormonal agonists. The pancreatic β-cell has distinct metabolic characteristics from most other cell types that allow it to

utilize higher levels of glucose. The β-cell expresses GLUT2 in the plasma membrane which is an insulin-independent glucose transported that has a low affinity (high Km) and high transport capacity for glucose which ensures a high flow of glucose entry into the cell (Hiriart and Aguilar-Bryan 2008). β-cells also express glucokinase (a high Km hexokinase) which functions as a glucose sensor whose activity is not allosterically inhibited by its catalytic product, glucose-6-phosphate (G6P), thus enabling the β-cell to continuously utilize glucose (Matschinsky 2002). The β-cell also has low lactate dehydrogenase and monocarboxylate (lactate/pyruvate) transport activity (Ishihara, Wang et al. 1999) and a high activity of the mitochondrial malate/aspartate shuttle (Rubi, del Arco et al. 2004), which supports the mitochondrial oxidation of NADH and $FADH_2$ to increase ATP production. Moreover, the β-cell has high activity of both pyruvate dehydrogenase and pyruvate carboxylase, which ensures coexistence of anaplerotic and oxidative glucose/pyruvate metabolism (Sugden and Holness 2011). All of these specific metabolic characteristics aim to enhance the mitochondrial tricarboxylic acid cycle (TCA) cycle activity, oxidative phosphorylation, and efficient ATP production in β-cells.

Insulin secretion by the β-cell is stimulated and regulated mainly by glucose, however other nutrients, hormones and neurotransmitters play important roles. Lipid metabolism, *via* the formation of long-chain acyl-CoAs and the GL/FFA cycle (Deeney, Gromada et al. 2000, Nolan, Leahy et al. 2006, Prentki and Madiraju 2012) or via GPR40 (Latour, Alquier et al. 2007) can enhance insulin secretion. Amino acids can also increase insulin secretion, either by modulating lipid metabolism, or by directly depolarizing the plasma membrane but only in the presence of glucose (Prentki, Matschinsky et al. 2013). All these will be discussed further in this section.

1.6.1 Insulin synthesis and exocytosis

The insulin gene encodes a single chain precursor protein called pre-proinsulin that matures into active insulin through a series of proteolytic reactions (Omar-Hmeadi and Idevall-Hagren 2021). Insulin synthesis is regulated by glucose at the level of transcription and translation. Transcription factors such as pancreatic and duodenal homeobox-1 (PDX-1), MafA, paired box gene 6 (PAX6) and B-2 / Neurogenic differentiation 1 (NeuroD1) regulate the transcription of the insulin gene (Hagman, Hays et al. 2005, Fu, Gilbert et al. 2013). After the pre-proinsulin mRNA is translated, the N-terminal signal peptide (rich in water-soluble residues) is recognized by signal recognition particles that direct the ribosome to the rough ER and facilitate pre-proinsulin translocation across the ER membrane, where the signal peptide is removed (Dodson and Steiner 1998, Magro and Solimena 2013). In the rough ER, pre-proinsulin is cut into proinsulin by specific peptidases. Proinsulin then leaves the rough ER in micro-vesicles and joins the trans-Golgi network, where it is packaged into secretory vesicles and it is cleaved into insulin and C-peptide: vesicles bud from the Golgi apparatus and become mature granules that will be stored until they are signaled to be released or are degraded by the lysosomes when insulin demands are low. Since C-peptide has a longer half-life than insulin, the plasma C-peptide concentration can be used to evaluate the secretory potential of the β-cell (Fu, Gilbert et al. 2013).

1.6.2 Glucose stimulate insulin secretion

Glucose stimulates insulin secretion through a triggering pathway and an amplifying pathway (Campbell and Newgard 2021). The triggering pathway is activated by glucose entry to the β-cell; glucose is then phosphorylated to G6P by glucokinase and further metabolized by glycolysis and the tricarboxylic acid (TCA) cycle to provides reducing equivalents (NADH, $FADH_2$) for the respiratory chain within mitochondria to produce ATP (Herman and Kahn 2006). An increase in

glucose metabolism in the β-cell following an increase in blood glucose leads a higher ATP/ADP ratio, closure of ATP-sensitive K^+ channels (K_{ATP}), depolarization of the plasma membrane, and activation of voltage- gated Ca^{2+} channels. The subsequent rise in intracellular Ca^{2+} levels triggers the fusion of insulin granules to the plasma membrane and their exocytosis **(Figure 1.3)** (Herman and Kahn 2006, Nolan, Damm et al. 2011). This pathway represents the first phase of GSIS: it is rapid and peaks within 5 minutes, and results primarily from the exocytosis of granules that were stored close to the plasma membrane (Prentki, Matschinsky et al. 2013, Campbell and Newgard 2021).

The amplifying pathway is the second phase of GSIS and involves a secondary set of stimuli that allow the continuation of insulin secretion at a lower and sustained rate independent of the K_{ATP} channels. It is affected by changes in protein kinase A (PKA) activity and the concentration of cAMP, phospholipase C and plasma membrane phosphoinositides (Tengholm 2012); as well as different MCFs, such as the generation of mitochondrial NADH, long chain-CoA esters, pyruvate cycling, Mal-CoA, MAG-1 and others (Prentki, Matschinsky et al. 2013). In the mitochondria, rapid glucose oxidation increases the ATP/ADP ratio and stimulates insulin secretion. During glucose stimulation, TCA cycle intermediates, including citrate and malate, accumulate in the β-cell and act as precursors for MCFs **(Figure 1.3)**. A constant refill of TCA cycle metabolites by a process called anaplerosis is required to maintain increased levels of mitochondrial derived MCFs during glucose oxidation (Prentki, Matschinsky et al. 2013). One of the important metabolic signaling cycles that increases anaplerosis is pyruvate cycling (Fransson, Rosengren et al. 2006). In this cycle, GTP generated during glucose stimulation is utilized by the mitochondrial isoform of phosphoenolpyruvate carboxykinase (PEPCK) to synthesize phosphoenolpyruvate (PEP) from oxaloacetate (Campbell and Newgard 2021). Although the

synthesis of a new molecule of PEP from pyruvate requires one ATP and one GTP, PEP has a very high free energy. This may allow the β-cell to continue to synthesize ATP as a direct product of the pyruvate kinase (PK) reaction to produce pyruvate, even at maximum mitochondrial phosphorylation potential (Huang, Malhi et al. 2015). Pyruvate from this reaction enter the mitochondria rapidly *via* the pyruvate carboxylase (PC) reaction, where it forms oxaloacetate, to restart the cycle and reload TCA cycle metabolites. Studies have shown that PC expression levels can directly affect GSIS (Farfari, Schulz et al. 2000, Jensen, Joseph et al. 2006). Furthermore, increased activity of the membrane-associated PK which converts ADP and PEP into ATP and pyruvate is sufficient to close K_{ATP} channels in mouse β-cells (Abulizi, Cardone et al. 2020, Lewandowski, Cardone et al. 2020). The mitochondrial electron transport chain (ETC) is closely linked to GSIS by affecting the β-cell energy state and ATP production (Prentki, Matschinsky et al. 2013). The ETC plays direct role in generating MCFs, including ATP, ADP, AMP, and ROS. As a result, inhibition of the individual ETC complexes is associated with reduced GSIS (Prentki, Matschinsky et al. 2013).

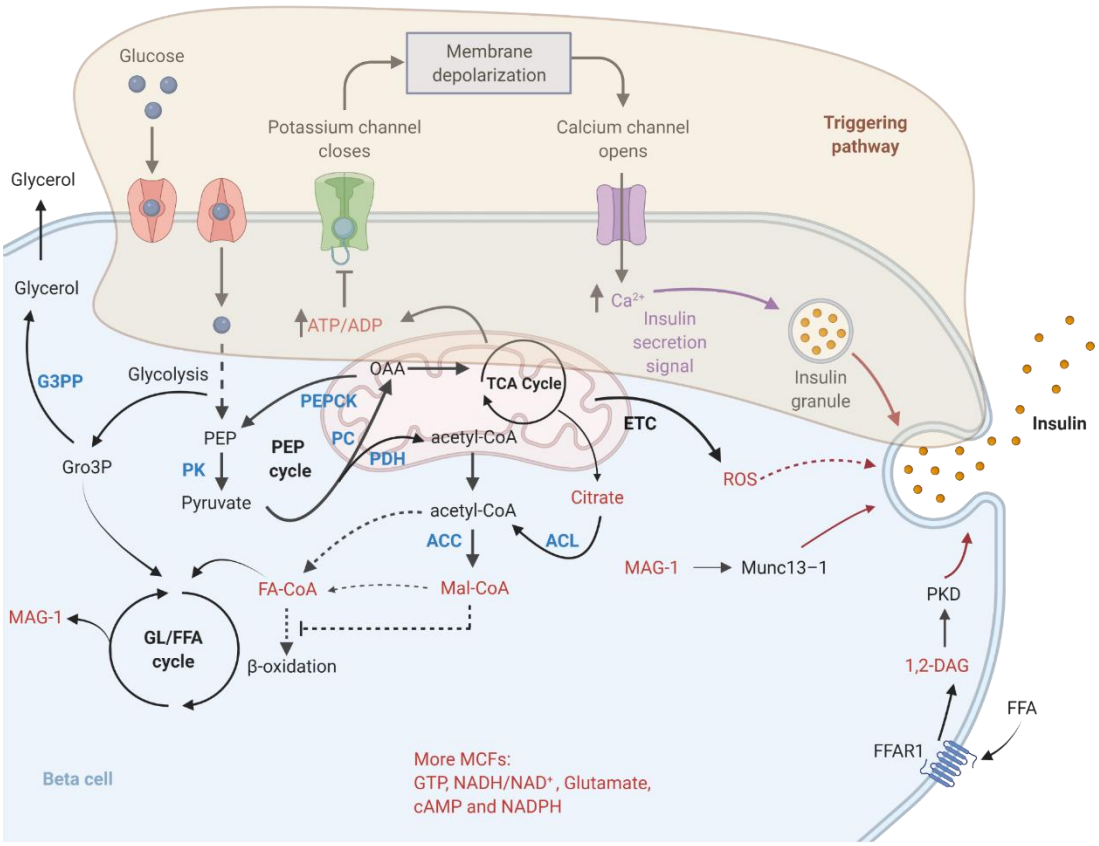

Figure. 1.3. Mechanisms involved in insulin secretion by pancreatic β-cells.

Glucose-stimulated insulin secretion (GSIS) is mediated first by a triggering pathway (brown bubble). Glucose enters β-cells *via* GLUT1 (human) or GLUT2 (rodent) transporters; glucose is metabolized *via* the glycolytic pathway, followed by oxidation *via* the tricarboxylic acid (TCA) cycle generating ATP and increasing ATP/ADP ratio, which results in the closure of KATP channels, membrane depolarization and opening of voltage-gated calcium channels and increased intracellular calcium that triggers insulin granule exocytosis. The amplifying pathway is represented by the production of different metabolic coupling factors (MCFs) indicated in red. FFA can also stimulate insulin secretion in the present of glucose through the lipolysis arm of the GL/FFA cycle that generates 1-MAG, which activates Munc13–1 (insulin exocytosis facilitator); and through the activation of free fatty acid-activated receptor-1 (FFAR-1) that results in a signaling cascade of 1,2-DAG/PKD (protein kinase D), stimulating insulin exocytosis. Adapted from (Nolan, Damm et al. 2011, Prentki, Corkey et al. 2020) using BioRender.

1.6.3 Fatty acid amplification of GSIS

FFAs stimulate insulin secretion from β-cells in the presence of permissive concentrations of glucose (approximately 5 mM). FFA can have different effects on insulin secretion depending on the concentration of glucose and the exposure time of β-cell to FFA. For example, insulin secretion is enhanced when β-cells are incubated with FFA for a short-term at high glucose concentrations. However, under the same hyperglycemic conditions, long-term incubation with FFA induces glucolipotoxicity and leads to β-cell dysfunction (see Section 1.7). The non-toxic acute effect of FFAs on insulin secretion can be explained by several mechanisms (Nolan, Leahy et al. 2006, Prentki, Corkey et al. 2020). One mechanism involves FFAR1 (FFA-activated receptor-1, also known as GPR40) which is expressed at high levels in β-cells **(Figure 1.3)**. FFAR1 is activated by medium to long chain FFA resulting in metabolism of PIP2 to produce inositol triphosphate (IP3) and 1,2 DAG which activates a signaling cascade that stimulates insulin exocytosis. IP3 is involved in the mobilization of Ca^{2+} from ER stores and 1,2 DAG can activate protein kinase D (PKD1) and some protein kinase C enzymes to stimulate insulin exocytosis (Campbell and Newgard 2021). Key evidence for a role of FFAR1 in FFA induced secretion raised from the observation that FFAR1 KO mice show reduced FFA amplification of GSIS *in vivo* and *ex vivo* (Kebede, Alquier et al. 2008). On the other hand, FFAR1 overexpression in β-cells enhances GSIS and improves glucose tolerance in normal and diabetic mice (Alquier and Poitout 2009).

A second mechanism involves the ACC/Mal-CoA/CPT-1 (carnitine palmitoyltransferase 1) signaling network **(Figure 1.3)** (Prentki, Corkey et al. 2020). This network is activated under conditions were high glucose level leads to enhanced anaplerotic input into the TCA cycle via the carboxylation of pyruvate to oxaloacetate via pyruvate carboxylase This in turn leads to an increase in mitochondrial levels of citrate that subsequently escapes the mitochondria to the cytoplasm

(cataplerosis) and then citrate is converted rapidly to acetyl-CoA via ATP-citrate lyase. ACC then convert acetyl-CoA into Mal-CoA and elevated levels of Mal-CoA in the β-cell at high glucose is known to inhibit FA oxidation via its interaction with CPT-1, the rate limiting step of FA β-oxidation. FFA can then be re-directed to esterification in the lipogenic arm of the GL/FFA cycle, resulting, following lipolysis, in the generation of many MCFs, including 1-MAG that can activate Munc13–1, an insulin exocytosis coordinator (Zhao, Mugabo et al. 2014). In most tissues MAGL is the main MAG hydrolase; however, in β-cells, MAGL is poorly expressed in comparison to ABHD6 (Zhao, Poursharifi et al. 2015). As a result, ABHD6 is the predominant enzyme converting MAG to FFA and glycerol in those cells; and ABHD6 knockdown enhances GSIS and ABHD6 overexpression reduces GSIS in the β-cell (Zhao, Poursharifi et al. 2015).

A third mechanism that leads to FFA amplification of GSIS involves the GL/FFA cycle particularly the lipogenic arm of the GL/FFA cycle that forms glycerol-3-phosphate (Gro3P) from glucose **(Figure 1.3)**. Since the cytosolic concentration of Gro3P is controlled by glycerol-3-phosphate phosphatase (G3PP) (Mugabo, Zhao et al. 2016); and differences in the expression levels of G3PP can regulate GSIS in rat islets *in vitro* (Mugabo, Zhao et al. 2016) (see Section 1.10).

1.6.4 Amino acids and insulin secretion

Amino acids such as glutamine and arginine also regulate insulin secretion through a mechanism that involves their metabolism by mitochondria. Glutamine in the cytosol can be converted into glutamate by glutaminase. Glutamate converted to α-ketoglutarate by glutamate dehydrogenase can enter the TCA cycle, which leads to the production of ATP and MCFs that stimulate insulin secretion (Prentki, Matschinsky et al. 2013). Furthermore, Leucine can also stimulate insulin secretion when it is catabolized to acetyl-CoA, which activates glutamate dehydrogenase and

direct more α-ketoglutarate to enter the TCA cycle. Finally, arginine can promote insulin secretion *via* depolarization of the plasma membrane to cause Ca^{2+} influx in the cytosol (Broca, Brennan et al. 2003). *In vitro*, insulin secretion is only stimulated by amino acids when they are individually present at high concentrations or present in combination at physiological concentrations (Newsholme and Krause 2012). However, amino acids derived from dietary proteins in combination with glucose, will stimulate insulin secretion *in vivo* (Newsholme, Bender et al. 2007).

1.7 β-cell adaptation and failure in obesity associated T2D

A functional pancreatic β-cell is essential for glucose homeostasis. The adaptation of β-cells to insulin secretion demands, which varies during different metabolic challenges and IR states, is also crucial to maintain euglycemia. Many studies have underlined the fact that some obese patients with IR only develop T2D when there is evidence of β-cell failure (Prentki and Nolan 2006, Nolan and Prentki 2019). Therefore, the ability of the β-cells to compensate for IR is a determining factor in the prediction of T2D susceptibility. Thus, the β-cell acts as a nutrient sensor that adapts to changes in insulin demands *via* the intracellular metabolism of various nutrients in the β-cell. Nonetheless, in conditions associated with the MetS where there is chronic fuel excess and β-cell metabolic stress and islet inflammation, β-cells initially show a compensatory response via a combination of factors, including increased cell proliferation and changes in gene expression (e.g. metabolic, exocytosis and insulin genes) that result in augmented insulin secretion to meet the elevated metabolic demand, but eventually exhaustion of β-cell can occur leading to β-cell dysfunction and failure (Prentki, Peyot et al. 2020).

1.7.1 β-cell adaptation

In overweight and prediabetes, where a condition of nutrient overload is associated with increased IR, increased insulin secretion is required to control blood glucose levels. As the metabolic dysfunction or IR becomes more severe, the demand for increased insulin secretion is met by a compensatory β-cell response that is characterized by increased secretion from β-cells and hyperinsulinemia that attempts to normalize blood glucose levels. This compensation is achieved *via* several changes in the islets, including proliferation of the β-cells and an expansion of their functional mass (Hudish, Reusch et al. 2019). In addition, β-cells compensate by increasing insulin synthesis, upregulating glucose metabolism pathways linked to insulin secretion, and inducing the unfolded protein response (UPR), a defense system that helps preserve β-cell function and survival under conditions of overnutrition and IR.

The enhanced β-cell response to glucose is associated with upregulation of several glycolytic enzymes leading to increased glycolysis and glucose oxidation. For example, in obese IR animal models such as the ZF rat, β-cell adaptation to IR is characterized by increased glucokinase mRNA levels and enzymatic activity of (Wortham and Sander 2016). The activity of enzymes involved in pyruvate cycling processes like PC is also increased during β-cell compensation (Lewandowski, Cardone et al. 2020), which leads to accumulation of mitochondrial metabolites implicated in the production of MCFs that enhance GSIS. In obese individuals, increased circulating levels of FFAs and TG create pressure on the β-cell to compensate to avoid lipotoxicity, for example by increasing β-cell FFA oxidation to limit TG accumulation (Nolan, Leahy et al. 2006). Furthermore, increased circulating FFA can enhance GL/FFA cycling in β-cells, which increases production of lipid signaling molecules such as MAG, DAG and FA-CoA that function as MCFs to promote insulin secretion (Prentki and Madiraju 2008). Increased plasma

FFA levels also activate FFAR1, which can contribute to enhanced insulin secretion (Kebede, Alquier et al. 2008).

In β-cells, many changes in the expression of genes encoding metabolic enzymes are central in the adaptation to nutrient overload. Transcription factors identified as the main regulators of lipid and glucose metabolism during β-cell adaptation include SREBP1c, PPARα, PPARδ and LXR (Newsholme and Krause 2012). For example, SREBP1c, links lipogenesis to GSIS by activating target genes encoding lipogenic enzymes such as FAS and ACC. Srebp1c β-cell KO mice show reduced an adaptive response to high glucose levels that is associated with a failure to upregulate lipogenic genes (Diraison, Ravier et al. 2008). PPARδ, which is a transcriptional activator of β-oxidation genes in several tissues in response to FFA is a central player in the induction of β-oxidation and GSIS by FFA (Ravnskjaer, Frigerio et al. 2010). Maintenance of β-cell function for insulin biosynthesis also requires efficient functioning of the UPR machinery. A study of C57BL/6NTac mice fed HFD showed an increased expression of genes known to promote β-cell function and differentiation, including upregulation of UPR genes to protect against decompensating ER stress responses (Gupta, Jetton et al. 2017). An *ex vivo* study in mouse and human islets showed that the UPR functions as a sensor for insulin demand and could induce β-cell proliferation through activation of ATF6 (Sharma, O'Donnell et al. 2015).

Additional factors that contribute to β-cell compensation include an increase in GLP-1 levels, which is known to promote β-cell proliferation and inhibit β-cell apoptosis (Yusta, Baggio et al. 2006). Increased neural stimulation of the endocrine pancreas can also contribute to the compensatory increase in insulin secretion and growth of β-cells (Faber, Deem et al. 2020). Finally, autocrine actions of insulin and IGF1 and IGF2 may also contribute to β-cell proliferation and

survival by signalling through IRS2 (Modi, Jacovetti et al. 2015) and the PKB/AKT cascade (Jetton, Lausier et al. 2005).

1.7.2 β-cell dysfunction and failure

Extensive studies have shown that chronic exposure of β-cells to high concentrations of glucose (glucotoxicity) and FFA (lipotoxicity) alone or in combination (glucolipotoxicity) alters the function and survival of the pancreatic β-cell (El-Assaad, Buteau et al. 2003, Hagman, Hays et al. 2005, Prentki, Peyot et al. 2020). Although the β-cell initially adapts to nutrient excess by secreting more insulin and increasing β-cell proliferation and mass, prolonged exposure to excess nutrients can lead to β-cell dysfunction and death through processes such as glucotoxicity and lipotoxicity (Prentki and Nolan 2006, Prentki, Peyot et al. 2020). The overload of nutrients on the β-cell can contribute to the development of MetS including obesity, T2D and NAFLD (Nolan and Prentki 2019).

1.7.2.1 Glucotoxicity

Glucotoxicity is a condition in which chronic exposure to hyperglycemia (15–30 mM) results in impairment of β-cell function, including reduced insulin secretion and insulin gene expression and increased β-cell apoptosis and death (Unger and Grundy 1985, Jonas, Bensellam et al. 2009, Bensellam, Laybutt et al. 2012). Continuous β-cell overstimulation with glucose results in β-cell exhaustion and depletion of insulin reserves. Most of the work that demonstrated the effect of chronically elevated glucose levels on β-cell function was done on pancreatic β-cell lines (Prentki, Peyot et al. 2020), and identified the following mechanisms of glucotoxicity in the β-cell.

- ***Oxidative stress:*** leads to ROS accumulation that damages cellular DNA, proteins and lipids (Bensellam, Laybutt et al. 2012). Mitochondria are one of the main sources of

cellular ROS, as superoxide is produced during oxidative phosphorylation as a by-product of ATP synthesis. Different studies have shown that high glucose exposure leads to increase ROS formation and expression of oxidative stress markers such as heme oxygenase-1 in both mouse and human islets (Jonas, Bensellam et al. 2009, Lu, Koshkin et al. 2010, Bensellam, Laybutt et al. 2012). Furthermore, β-cells have low capacity to scavenge ROS due to the low expression of antioxidant enzymes, which makes them susceptible to oxidative damage (Grankvist, Marklund et al. 1981, Tiedge, Lortz et al. 1997, Prentki, Peyot et al. 2020). Overexpression of antioxidant genes and antioxidant supplementation have been shown to protect against oxidative stress damage in β-cells (Lu, Koshkin et al. 2010). For example, isolated rat islets were protected against glucotoxicity using the antioxidants N-acetylcysteine and aminoguanidine (Tanaka, Gleason et al. 1999). The same agents also decreased markers of oxidative stress and improved glucose tolerance in Zucker Diabetic Fatty rats (Tanaka, Gleason et al. 1999).

- ***ER stress:*** is a critical cause of β-cell failure; and an efficient and functional unfolded protein response (UPR) is required to maintain a functional β-cell for insulin biosynthesis. The UPR related to the ER stress. The UPR is a cellular stress response that is triggered to downregulate protein synthesis, folding and overall workload under ER stress. UPR components, such as TXNIP and CHOP, were elevated in β-cells following chronic high glucose exposure, indicative of increase ER stress (Bensellam, Laybutt et al. 2012). However, the UPR may fail to maintain ER homeostasis in β-cells and activate apoptosis under severe ER stress conditions seen as a result of chronic hyperglycemia (Szegezdi, Logue et al. 2006, Tang, Koulajian et al. 2012).

- ***Glycation:*** is a spontaneous and non-enzymatic reaction between reducing sugars such as glucose with amine residues on plasma proteins which normally occurs as a result of long standing hyperglycemia in diabetes (Bensellam, Laybutt et al. 2012). Glycation of proteins can lead to alteration in their enzymatic activity and receptor binding and functioning. As a result, protein glycation and formation of advanced glycation end products (AGEs) can contribute to the pathogenesis of diabetes and its complications including nephropathy, retinopathy, neuropathy and cardiomyopathy (Singh, Bali et al. 2014). Hyperglycemia was shown to promote protein glycation and AGE production in mouse islets (Pascal, Veiga-da-Cunha et al. 2010). Interestingly, inhibition of AGEs can prevent hyperglycemia-induced impairment of insulin gene expression and GSIS (Tajiri, Moller et al. 1997). AGEs can also induce β-cell failure by promoting ROS production and oxidative stress leading to loss of β-cell function (Lin, Zhang et al. 2012, Singh, Bali et al. 2014).
- ***Inflammation:*** results in elevated numbers of macrophages infiltrating islets of patients with T2D, accompanied by increased levels of cytokines like IL-1β and IL-6 (Donath, Ehses et al. 2005, Ehses, Perren et al. 2007, Boni-Schnetzler, Thorne et al. 2008). It is known that increased production of IL-1β upregulates Fas receptor, a member of the TNF receptor family that can mediate cell death by apoptosis (Miwa, Asano et al. 1998, Donado, Cao et al. 2020). Non-diabetic human islets incubated *in vitro* in media with high glucose concentrations show an increase IL-1β production, which upregulates Fas expression leading to β-cell dysfunction and death (Maedler, Sergeev et al. 2002). Interestingly, treatment with a specific IL-1β receptor antagonist improved β-cell function and greatly reduced hyperglycemia in T2D subjects in a clinical trial (Herder and Donath 2015). In these studies, it is important to remember that inflammation can both cause or be caused

by glucotoxicity, ER stress and oxidative stress (Donath, Ehses et al. 2005, Prentki and Nolan 2006).

- ***β-cell dedifferentiation:*** and loss of identity can result from chronic exposure to elevated glucose levels, which is demonstrated by changes in expression of key transcription factors and β-cell differentiation markers like PDX-1, MafA, NeuroD1, HIF1 α, Pax6, GCK and Glut2 that occur in β-cells exposed to elevated glucose concentrations (Laybutt, Hawkins et al. 2007, Bensellam, Laybutt et al. 2012, Prentki, Peyot et al. 2020). These changes in gene expression and β-cell dedifferentiation in T2D could be an adaptive mechanism to allow the β-cells to survive this chronic increase in glucose and protect itself from irreversible damage.

1.7.2.2 Lipotoxicity and glucolipotoxicity

Lipotoxicity is a condition that is associated with dysregulation of lipid homeostasis that leads to increased levels of plasma lipids (including TG, FFA, cholesterol and ceramides), that cause the deterioration of β-cell function and survival (Poitout and Robertson 2008). The lipotoxicity concept emerged from studies showing that exposure of β-cells to high levels of lipids (a mixture of palmitate and oleate) caused deterioration of β-cell function (Unger 1995). In contrast, some *in vitro* and *ex vivo* studies showed that high levels of lipids were relatively beneficial to the β-cells, particularly when glucose was not simultaneously elevated (Briaud, Harmon et al. 2001, El-Assaad, Joly et al. 2010). For example, a study in obese ZF rats indicated that elevated FFA levels and hyperlipidemia may be important signals that enable β-cell adaptation to IR (Nolan, Leahy et al. 2006). It is certainly possible that β-cells are susceptible to lipotoxic damage at normal glucose levels, particularly if there is a pre-existing defect in the detoxification process, such as a defects in FA oxidation (Prentki and Nolan 2006). In addition, different FFAs have different effects on

the induction of β-cell apoptosis *in vitro*; with chronic elevation of saturated FFAs (such as palmitate and stearate) leading to β-cell apoptosis and chronic elevation of mono-unsaturated FFAs (such as oleate) protecting the β-cell from apoptosis (El-Assaad, Buteau et al. 2003). In contrast, *in vivo* rodent studies, where the FFAs were delivered by intralipid infusion, revealed overall minimal effects on β-cell GSIS and gene expression with no signs of significant toxicity (Steil, Trivedi et al. 2001). Even though, there is a lack of *in vivo* evidence that demonstrates that high FFA levels alone can interfere in β-cell function, there is emerging evidence showing that the toxic effects of lipids occurs in the presence of high levels of glucose (Poitout and Robertson 2008, Prentki, Matschinsky et al. 2013).

In recognition that the toxic effects of FFAs on tissues will only appear when glucose levels are also elevated, the term glucolipotoxicity was proposed to describe the combined toxic effect of glucose and FFAs when present in the β-cell simultaneously (Prentki, Joly et al. 2002). The combined exposure is thought to be required since β-cell can adapt to acute elevated glucose concentrations *via* changes in gene expression to enhance GSIS and gluoco-detoxification (Farfari, Schulz et al. 2000); and to elevated FFAs under low glucose concentration because the levels of the glucose-derived Mal-CoA that inhibits FFA oxidation are low. The presence of high levels of glucose, (resulting in increased levels of Mal-CoA) will prevent FFA oxidation and therefore FFA detoxification, while at the same time promoting esterification of FFAs leading to complex lipids, including cytotoxic lipids such as DAG and phosphatidate (Prentki and Corkey 1996, Prentki, Joly et al. 2002). Glucolipotoxicity is defined as the synergistic chronic effect of elevated concentrations of glucose and FFA in inducing β-cell dysfunction including decreased GSIS and decreased total β-cell insulin content. Many *in vitro* and *in vivo* studies support the concept of glucolipotoxicity and its role in β-cell dysfunction (Prentki, Peyot et al. 2020).

1.7.3 Fuel excess detoxification pathways

The mechanisms leading to β-cell dysfunction and toxicity under conditions where there are high levels of glucose and lipids (glucolipotoxicity) have been widely studied (Unger and Grundy 1985, Unger 1995, Prentki and Corkey 1996, Prentki, Peyot et al. 2020). However, little is known about the mechanisms that β-cells use to detoxify excess nutrients and protect against toxicity. Unlike other cell types, the β-cell senses circulating levels of glucose and other nutrients constantly to release insulin when needed. This means that β-cells have to allow entry and metabolize large amounts of these nutrients to adjust insulin secretion to changes in their levels in the circulation. These nutrients activate many metabolic pathways simultaneously and generate many metabolic intermediates, some of which are toxic (El-Assaad, Buteau et al. 2003, Poitout and Robertson 2008); however, β-cells can't reduce glucose entry to protect themselves against hyperglycemia and have limited capacity to store excess fuels (Poitout and Robertson 2008, Prentki, Matschinsky et al. 2013). On the other hand, β-cells can modify potentially toxic molecules and/or excrete them; or redirect excess glucose and FFA carbons to other metabolic pathways. This allows β-cells to protect themselves from nutrient excess and to monitor their glucose metabolic flux to regulate insulin secretion. For example, while high intracellular levels of FFAs and free cholesterol are toxic (Oh, Bae et al. 2018); FFAs can be converted into cholesterol esters or TG and stored in the form of lipid droplets or exported out of β-cells; and excess free cholesterol can be excreted through the β-cell via ATP-binding cassette transporter-A1 (ABCA1). Interestingly, suppression of ABCA1 was found to cause cholesterol accumulation, decreased insulin secretion and altered glucose homeostasis in mice β-cells (Brunham, Kruit et al. 2007). Furthermore, 70% of glucose carbons in β-cells are directed to glycerolipids in the presence of high glucose levels (MacDonald, Dobrzyn et al. 2008). The relative importance of these different nutrient detoxification pathways

and the underlying molecular mechanisms are not well understood. Thus, the new concepts of gluco- lipo- and glucolipo- detoxification were established and are being studied as part of this thesis. These concepts and their potential mechanisms are discussed in the following sections.

1.7.3.1 The GL/FFA cycle

In addition to its role in insulin secretion, the GL/FFA cycle could be involved in detoxification of excess nutrients. Since the GL/FFA cycle is an energy-requiring process, its activation can prevent an energy overload caused by a possible excessive supply of nutrients in the β-cell. Also, stimulation of the GL/FFA cycle can lower ROS production by redirecting a significant amount of glucose entering the cell away from mitochondrial oxidation (Prentki and Madiraju 2008). Furthermore, the cycle acts as a lipodetoxification mechanism via the release of FFAs from the hydrolysis of TGs, which can either be eliminated outside the cell or oxidized in the mitochondria (Martins, Miyasaka et al. 2004).

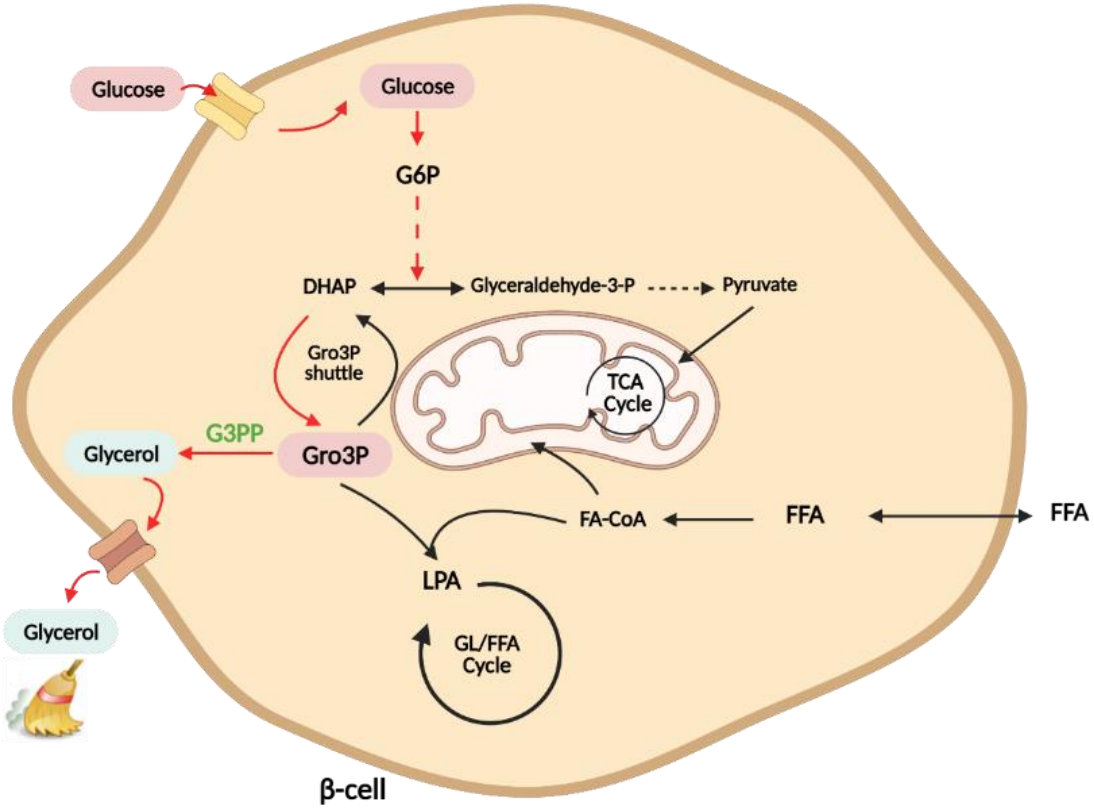

Figure 1.4. G3PP directly hydrolyzes Gro3P to release glycerol.

Red arrows represent the direction of glucose carbons towards glycerol through Gro3P by the action of G3PP, which acts as an important glucodetoxification mechanism to eliminate excess glucose carbons in the β-cell. Abbreviations: DHAP, dihydroxyacetone phosphate; FA-CoA, fatty acyl-CoA; FFA, free fatty acid; G3PP, glycerol 3-phosphate phosphatase; G6P, glucose 6-phosphate; GL/FFA cycle, glycerolipid/free fatty acid cycle; Glyceraldehyde-3-P, glyceraldehyde-3-phosphate; Gro3P, glycerol 3-phosphate; TCA cycle, tricarboxylic acid cycle. Adapted from (Mugabo, Zhao et al. 2016) using BioRender.

1.7.3.2 Glycerol production and release

As β-cells express low levels of glycerokinase, the detoxification of glucose as glycerol involves the export of glycerol outside the cell through membrane aquaglyceroporins (AQPs) (Matsumura, Chang et al. 2007). In β-cells the action of G3PP provides an important glucodetoxification mechanism by directing glucose carbons towards glycerol **(Figure 1.4)** (Mugabo, Zhao et al. 2016).

Knockdown of G3PP *in vitro* increase the severity of glucotoxicity and glucolipotoxicity, whereas G3PP overexpression reduced the toxic actions of glucose and excess FFA in terms of apoptosis (Mugabo, Zhao et al. 2016).

1.8 Overview of liver metabolism in health and nutrient excess

Liver is a key organ for energy metabolism and homeostasis that consists of different cell types including Kupffer cells, stellate cells and endothelial cells (Vasconcellos, Alvarenga et al. 2016). Of these, hepatocytes represent ~ 80% of liver cells (Si-Tayeb, Noto et al. 2010) and play a central role in liver metabolism and detoxification. Kupffer cells are part of the tissue monocyte macrophage defense system and remove particulate matter from blood by their phagocytic action (Nguyen-Lefebvre and Horuzsko 2015). Stellate cells produce extracellular matrix and collagen and store vitamin A in lipid droplets. They are activated in response to liver injury and participate in fibrogenesis by depositing collagen (Khomich, Ivanov et al. 2019).

Liver metabolic activity is closely controlled by the pancreatic hormones insulin, glucagon; corticosteroids and catecholamines; and several gastrointestinal hormones (Rui 2014). Since the liver's portal vein is the direct recipient of all blood leaving the digestive system, the liver plays a critical role in metabolizing and storing diet-derived carbohydrates, lipids, and proteins (Harkins and Ahmad 2022). In the fed state **(Figure 1.5)** , insulin stimulates glycogenesis resulting in glucose being stored in the liver in the form of glycogen (Rui 2014). Insulin also stimulates lipogenesis in hepatocytes and esterification of FFAs with glycerol-3-phosphate (Gro3P) to generate TG. FFAs can be stored as TG, phospholipids and cholesterol esters. These complex lipids are either stored in lipid droplets and membrane structures or secreted as VLDL. Unlike glucose and FFA, amino acids cannot be stored in the liver; and are metabolized through

deamination to provide energy or to be used for synthesis of non-essential amino acids or glucose. Amino acid metabolism in the liver produces ammonia, a toxic metabolite that can be converted to urea (less toxic) that is excreted in urine as a waste product of digestion.

In the fasted state, when blood concentrations of glucose begin to decline, glucagon stimulates hepatocytes to break down the glycogen (glycogenolysis) and to export glucose to the bloodstream to be used by other tissues. The liver can also synthesize glucose from other molecules such as glycerol, lactate, pyruvate and amino acids (gluconeogenesis) which occurs during longer periods of fasting. Maintenance of blood glucose levels within a narrow range is an important function of the liver. During a prolonged fast, hepatic gluconeogenesis is the main source of endogenous glucose production. Furthermore, in prolonged fasting/starvation the liver converts the FFAs released by lipolysis from adipose tissue into ketone bodies through mitochondrial β-oxidation and ketogenesis. During starvation, ketone bodies provide an important source of energy for the brain and heart **(Figure 1.5)** (Rui 2014).

Many transcription factors and co-activators, including, ChREBP, SREBP, LXR, PPARa, PGC-1α, CREB, FOXO1 and CRTC2, control the expression of enzymes that catalyze metabolic processes in the liver and control its energy metabolism in the fasted and fed states (Yamashita, Takenoshita et al. 2001, Horton, Goldstein et al. 2002, Moran-Salvador, Lopez-Parra et al. 2011, Calkin and Tontonoz 2012). Dysfunction in the regulation of liver metabolism can lead to IR, T2D and NAFLD (Kitade, Chen et al. 2017, Huang, Behary et al. 2019).

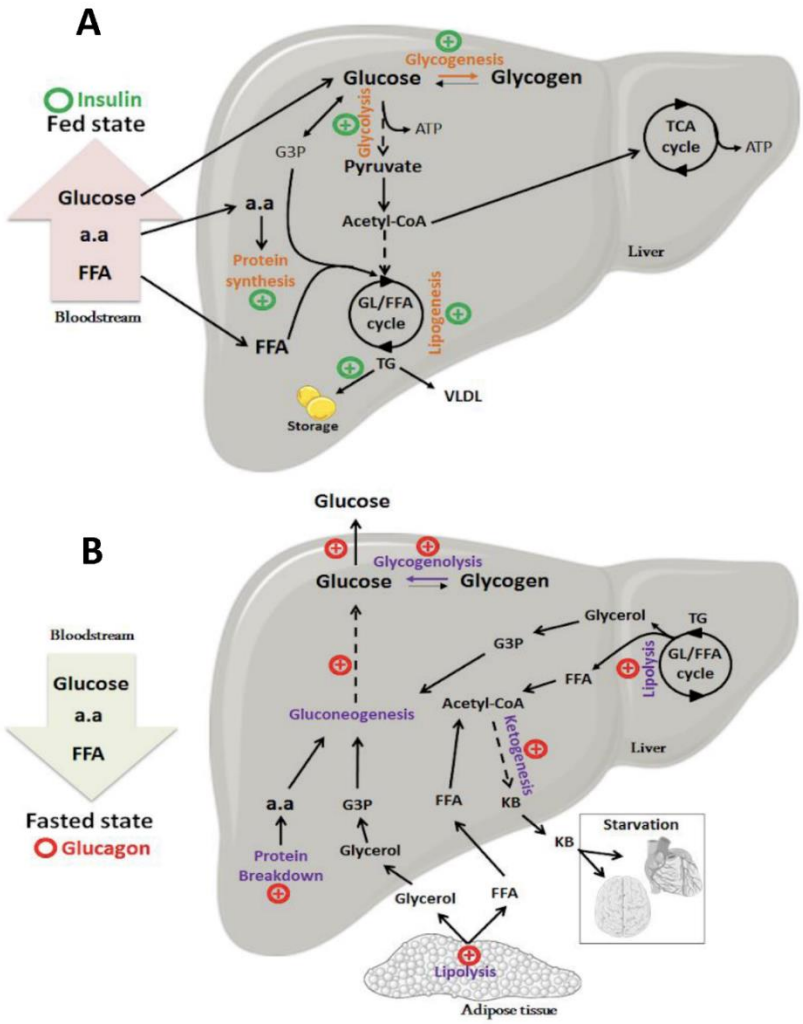

Figure 1.5. Major metabolic pathways in the liver during the fed and fasted state.

(A) In the fed state, circulating levels of glucose, amino acids (a.a) and free fatty acid (FFA) are high and insulin stimulated the uptake of these macronutrients in the live rand activates pathways (in orange) to normalize their levels in blood. **(B)** In the fasted state, glucagon upregulates pathways in the liver and adipose tissue (purple) to increase glucose, amino acid and FFA blood levels. Abbreviations: a.a, amino acids; ATP, adenosine triphosphate; FFA, free fatty acid; GL/FFA cycle, glycerolipid/free fatty acid cycle; Gro3P, glycerol 3-phosphate; TCA cycle, tricarboxylic acid cycle; TG, triglyceride; VLDL, very low-density lipoprotein; KB, ketone bodies.

1.8.1 Hepatic glucose metabolism in health

The liver plays a major role in overall body glucose metabolism by balancing glucose production from different substrates and glucose storage in the form of glycogen (Sharabi, Tavares et al. 2015, Adeva-Andany, Perez-Felpete et al. 2016). The liver is responsible for 80% of endogenous glucose production, with the rest being provided by the kidney (Gerich 2010). The nutritional state of the body (fed/fasted) and the duration of that state (short fasting or starvation) both determine whether the liver acts as a glucose producing or glucose storage organ (Sharabi, Tavares et al. 2015). For example, during short-term fasting, changes in metabolite flux controlled by protein modifications or allosteric effectors are made to maintain normoglycemia. In contrast, prolonged fasting leads to changes in mRNA expression of key enzymes in the glycolysis and gluconeogenesis pathways. However, all nutritional stats are subject mainly to a hormonal regulation by the opposing hormones insulin and glucagon (Rui 2014).

Since the liver plays a central role in glucose production, it is important to highlight the metabolite fluxes that control gluconeogenesis and hepatic glucose production (HGP). The liver can shift from net hepatic glucose storage to net glucose output by regulating the activity of key gluconeogenic or glycolytic enzymes (Sharabi, Tavares et al. 2015). In total, 7 out of 10 reactions that are common between glycolysis and gluconeogenesis are reversible. The remaining three reactions are irreversible and are paired with unique and opposing reactions for gluconeogenesis, each catalyzed by specific enzymes. To achieve a net flux toward gluconeogenesis or glycolysis, the liver must regulate the enzymes involved in these three reactions and their glycolytic equivalents by allosteric effectors, at the gene expression level or by covalent modifications. If these opposite reactions were to act at the same rate, they will create a futile metabolic cycle that will result in energy expenditure and waste (Sharabi, Tavares et al. 2015).

The three irreversible reactions in glycolysis are: 1) the conversion of G6P to glucose, 2) the conversion of fructose 1,6-bisphosphate (F1,6P) to fructose-6-phosphate (F6P) and 3) the conversion of pyruvate to PEP.

1) **Glucose/G6P:** Glucose enters hepatocytes via GLUT2, an insulin-independent membrane glucose transporter (Seyer, Vallois et al. 2013). It is then phosphorylated by glucokinase (GCK), a liver specific hexokinase, to generate G6P, which cannot be transported back by GLUT2 and is retained inside the hepatocyte (Kamata, Mitsuya et al. 2004). GCK is unique among the hexokinases, in that it is not inhibited by its product (G6P), so that GCK activity is determined by its mRNA expression (Iynedjian 2009). In the gluconeogenic pathway, GCK is opposed by glucose-6-phosphatase (G6Pase), which hydrolyzes G6P to glucose (Han, Kang et al. 2016). G6P can also be generated *via* glycogenolysis and gluconeogenesis. G6P acts as a branch point that serves as an intermediate for glucose uptake, storage and production. It is a precursor for glycogen synthesis and is also metabolized through glycolysis to generate pyruvate, which can enter the mitochondria to be oxidized to generate ATP through the TCA cycle and oxidative phosphorylation. Pyruvate and Gro3P can also be used in *de novo* lipogenesis to synthesize FFAs, leading to glucose being stored as TG. G6P is also metabolized via the pentose phosphate pathway to generate NADPH which is required for lipogenesis and biosynthesis of other bioactive molecules (Sharabi, Tavares et al. 2015).

2) **F6P/F1,6P:** The conversion of F6P to F1,6P, catalyzed by phosphofructokinase 1 (PFK1) which is a highly regulated enzyme, (along with its opposing gluconeogenic enzyme, fructose 1,6-bisphoshpatase (FBPase) is first committed step in glycolysis and a key determinant of net glycolytic or gluconeogenic flux (Mor, Cheung et al. 2011). The

activities of PFK1 and FBPase are regulated by hormones and nutritional states and the allosteric effector, fructose 1,6-bisphosphate (F2,6P) (Van Schaftingen, Hue et al. 1980). Under conditions that favor glucose utilization, F2,6P levels are high, PFK1 is activated and FBPase is inhibited and glycolysis is favoured. Low F2,6P levels occur when there is a demand for glucose production, leading to inhibition of PFK1 and activation of FBPase, which tilts the balance toward gluconeogenesis (Sharabi, Tavares et al. 2015).

3) **PEP/pyruvate:** The final step in glycolysis involves the conversion of PEP to pyruvate by PK. PEPCK is the opposing gluconeogenic enzyme and catalyzes the conversion of oxaloacetate generated by oxidation of cytosolic malate by malate dehydrogenase, to PEP (Sharabi, Tavares et al. 2015). The activity of these enzymes is also regulated by hormones and nutritional states: in the fed state, insulin activates PK by inhibiting its phosphorylation by reducing cAMP levels; while in the fasted state, glucagon inhibits PK activity by increasing levels of cAMP (Engstrom 1978). PK is can also be allosteric activated by fructose-1,6-BP (Flory, Peczon et al. 1974).

1.8.2 Hepatic fat metabolism in health

Fatty acids released from adipose tissue (in the fasting state) or absorbed from the intestine after digestion can be captured by hepatocytes and esterified with Gro3P from glycolysis to generate TG or with cholesterol to produce cholesterol esters (Alves-Bezerra and Cohen 2017). The liver also can convert glucose into fatty acids through *de novo* lipogenesis (Alves-Bezerra and Cohen 2017). TG and cholesterol esters are either stored in lipid droplets in hepatocytes or secreted into the circulation in the form of VLDL.

Lipogenesis begins with the oxidation of glucose to pyruvate in the glycolytic pathway. Pyruvate is transported to the mitochondria and metabolized by pyruvate dehydrogenase to form

acetyl-CoA, which is combined with oxaloacetate by citrate synthase to form citrate in the first step of the Krebs cycle. The citrate destined for lipogenesis does not continue in the cycle, but is exported (cataplerosis) to the cytoplasm and retransformed into acetyl-CoA and oxaloacetate by ATP-citrate lyase (ACL). Oxaloacetate is reduced to malate, which is converted to pyruvate by malic enzyme, thereby releasing NADPH. The pyruvate is recycled in the mitochondria and carboxylated by PC to form oxaloacetate, leading to a continuous synthesis of citrate. In the cytoplasm, acetyl-CoA is carboxylated by ACC to form mal-CoA. Mal-CoA and NADPH are used as precursors for the synthesis of palmitic acid by fatty acid synthase (FAS) (Rui 2014).

Lipogenesis is controlled by transcriptional regulation of glycolytic and lipogenic genes. Many transcription regulators, including ChREBP, SREBP, LXR, PPARγ and PPARδ, have been shown to regulate these pathways (Rui 2014, Alves-Bezerra and Cohen 2017).

1.8.3 Liver metabolism under nutri-stress

Under conditions of chronic excess of glucose and lipids, many aspects of liver metabolism change due to the increase of hepatic IR and HGP. Many studies have shown that increased HGP in T2D patients is the major contributor to hyperglycemia in the fasting state (DeFronzo, Simonson et al. 1982, Campbell, Mandarino et al. 1988, Gerich, Mitrakou et al. 1990, Magnusson, Rothman et al. 1992). In T2D patients, glucose homeostasis is altered in response to β-cell dysfunction and to IR in the liver, muscle and adipocytes (Prentki and Nolan 2006, Nolan, Damm et al. 2011, Roder, Wu et al. 2016). Thus, when insulin fails to suppress HGP by the liver, it results in hyperglycemia T2D patients (Fisher and Kahn 2003). Several mechanisms have been suggested to explain the pathogenesis of IR in the liver (Samuel and Shulman 2012, Johnson and Olefsky 2013). One potential mechanism is inflammation, based on the observation that obese individuals showed a

marked increase in hepatic macrophages that contributed to hepatic IR (Obstfeld, Sugaru et al. 2010, Johnson and Olefsky 2013). Another mechanism is ectopic lipid accumulation, which can be considered as a driver for IR in the liver (Samuel and Shulman 2012). In addition, IR in other tissues could contribute to hepatic IR. For example, IR in muscle can result in more glucose being redirected to the liver; while IR in adipose tissue leads to increased lipolysis which increases the substrate available for gluconeogenesis and HGP. Progression of these changes in liver metabolism can lead to the development of NAFLD (Birkenfeld and Shulman 2014, Kitade, Chen et al. 2017).

1.9 Overview of glycerol and glycerol 3-phosphate metabolism

The importance of glycerol comes by acting as a precursor of glycerol 3-phosphate (Gro3P), which is a key metabolite for glucose and lipid metabolism (Lin 1977, Xue, Chen et al. 2017). Circulating glycerol levels were thought to depend on the hydrolysis of TG through the lipolysis arm of the GL/FFA cycle; from glyceraldehyde, an intermediate in fructose metabolism by the action of alcohol dehydrogenase; or to a small extent from the diet (Xue, Chen et al. 2017). However, the recent identification of the mammalian G3PP introduces a new pathway for glycerol formation through the direct hydrolysis of the glycolytic intermediate Gro3P (Mugabo, Zhao et al. 2016). Glycerol utilization and metabolism occurs mainly in the liver and kidney and to a lesser extent in skeletal muscle, brain and pancreatic islets; and is determined mainly by the amount and activity of glycerol kinase (GK) in these tissue (Lin 1977). For example, since GK has little activity in adipocytes, glycerol resulting from lipolysis cannot be reused in fat cells (Guan, Li et al. 2002).

Gro3P is produced both from the phosphorylation of glycerol by GK and via glycolysis thru dihydroxyacetone-3-phosphate (DHAP) which is reduced to Gro3P by cytosolic Gro3P dehydrogenase (GPD1) **(Figure 1.6)**. In the mitochondria, Gro3P can be oxidized via the

mitochondrial Gro3P dehydrogenase (GPD2), transferring the electrons to the electron transport chain, and generating DHAP in the cytoplasm. In the GPD2 reaction, flavin adenine dinucleotide (FAD) is reduced to $FADH_2$ (Ronnow and Kielland-Brandt 1993), which enters into mitochondrial respiration to finally generate ATP (Estabrook and Sacktor 1958, Lee and Lardy 1965). This conversion between Gro3P and DHAP, called the Gro3P shuttle, transfers cytosolic reducing equivalents to the mitochondrial oxidative phosphorylation pathway (Lin 1977, Mracek, Drahota et al. 2013, Shi, Wang et al. 2018).

In mammalian cell, Gro3P can enter the Gro3P shuttle or the lipogenic pathway **(Figure 1.6)**. Until recently, Gro3P derived from glycolysis was thought to be hydrolyzed directly to glycerol *via* the action of G3PP (Mugabo, Zhao et al. 2016). This allows Gro3P to provide the backbone for either glucose *via* gluconeogenesis in some tissues, or for TG *via* the GL/FFA cycle; and to transfer electrons from the cytosol to the mitochondria for oxidative phosphorylation through the Gro3P shuttle (Nelson and Robergs 2007, Xue, Chen et al. 2017). Overall, glycerol and Gro3P metabolism in mammalians is controlled by a team of enzymes and pathways that work together to optimize their utilization and availability **(Figure 1.6)**.

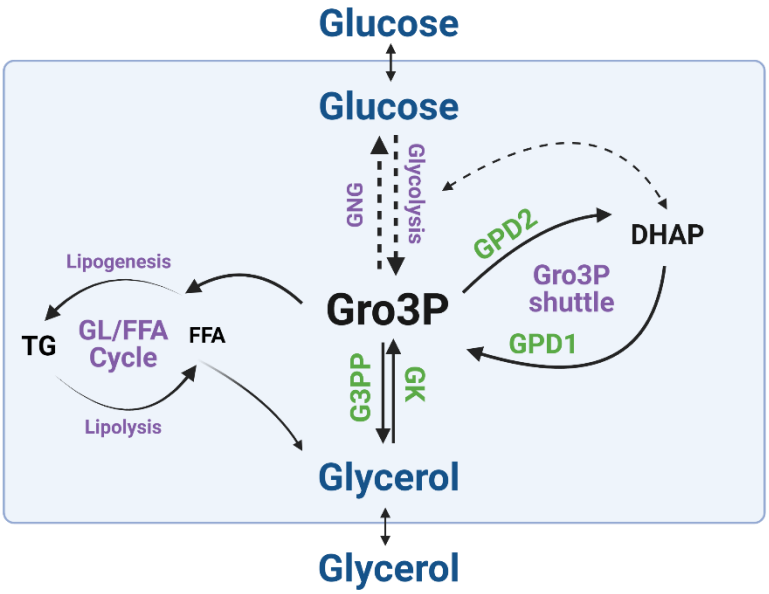

Figure 1.6. Overview of glycerol 3-phosphate metabolism in mammalian.

Glycerol-3-phosphate (Gro3P) can be formed from glucose during glycolysis, glycerol through glycerol kinase (GK) or from the Gro3P shuttle. Gro3P is at the crossroads of glucose and lipid metabolism and is one of the starting substrates for the GL/FFA cycle. Gro3P availability in the cytosol is controlled by a team of enzymes (in green) and pathways (in purple). Abbreviations: GK, glycerol-3-phosphate phosphatase (G3PP), cytosolic Gro3P dehydrogenase (GPD1) and mitochondrial Gro3P dehydrogenase (GPD2) using BioRender.

1.10 Mammalian glycerol 3-phosphate phosphatase/PGP a novel enzyme in intermediate metabolism

As discussed is Section 1.9, Gro3P is a key metabolite for glucose and lipid metabolism whose availability is controlled by many enzymes including G3PP. This section will focus on the recently identified enzyme G3PP and its role in the control of glucose, lipid and energy metabolism in mammalian cells.

1.10.1 Identification of glycerol-3-phosphate phosphatase in mammalians

It is well established that lipolysis, measured as FFA and glycerol release, is implicated in the regulation of GSIS by pancreatic β-cells (Mulder, Yang et al. 2004, Nolan, Leahy et al. 2006). The first critical step in converting TG to glycerol and fatty acids is conducted by ATGL (Prentki and Madiraju 2008, Trites and Clugston 2019). In whole-body ATGL-KO mice (Peyot, Guay et al. 2009) and in β-cell specifc ATGL-KO mice (Attane, Peyot et al. 2016), glycerol release from pancreatic islets was significantly elevated at high concentrations of glucose, suggesting that the glycerol did not originate from lipolysis. Furthermore, the powerful pan-lipase inhibitor orlistat completely inhibited lipolysis and GSIS in β-cells, measured over a range of glucose concentrations (4, 10, 16, and 25 mM glucose) (Mugabo, Zhao et al. 2016). In contrast, when glycerol was measured under the same conditions but with glucose ≤10 mM, glycerol release was inhibited by orlistat, which suggested that β-cells are able to produce glycerol from glucose *via* non-lipolytic pathways (Mugabo, Zhao et al. 2016). A thorough search for mammalian candidate proteins that are homologous to the known yeast and bacterial G3PP enzymes (Norbeck, Pahlman et al. 1996, Larrouy-Maumus, Biswas et al. 2013), identified one specific protein, previously described as phosphoglycolate phosphatase (PGP).

1.10.2 The G3PP/PGP gene and protein in various organisms

PGP is an evolutionarily conserved enzyme that can hydrolyze various phospho-metabolites. (Possik, Madiraju et al. 2017, Gohla 2019). In lower organisms and plants there are separate genes for PGP, that hydrolyzes 2-phosphoglycolate (2-PG), and G3PP, which hydrolyzes Gro3P. However, in animal species, a single gene product (*PGP*) appears to catalyze the hydrolysis of both and Gro3P and possibly other phospho-substrates.

Microorganisms: In bacteria, separate genes for PGP and G3PP exist (Teresa Pellicer, Felisa Nunez et al. 2003, Zheng, Zhao et al. 2008, Larrouy-Maumus, Biswas et al. 2013). PGP takes part in the hydrolysis of toxic 2-PG, produced during the repair of the 3'end of damaged DNA (Teresa Pellicer, Felisa Nunez et al. 2003). A distinct bacterial G3PP, belonging to the same phylogenic tree as PGP, is involved in glycerophospholipid recycling and catabolism (Larrouy-Maumus, Biswas et al. 2013) and in the utilization of glycerol (Lindner, Meiswinkel et al. 2012).

Yeast: *Saccharomyces cerevisiae* harbors a PGP homologue (Pho13) and two distinct G3PP enzymes. Yeast Pho13 deletion mutants display an elevated pentose phosphate pathway activity and a high capacity to ferment xylose (Kim, Xu et al. 2015) and to form ethanol (Bamba, Hasunuma et al. 2016). A recent study ascribed a metabolite repair function to Pho13, in the dephosphorylation of the toxic glycolytic by-products 4-phosphoerythronate (4-PE) and 2-PG (Collard, Baldin et al. 2016). Yeast G3PP enzymes are involved in glycerol production and are required for survival in stress conditions such as salinity, oxidative, anoxia, and butanol (Norbeck, Pahlman et al. 1996, Pahlman, Granath et al. 2001, Fan, Whiteway et al. 2005).

Plasmodium: Deletion of PGP in *Plasmodium falciparum* has been shown (Dumont, Richardson et al. 2019) to cause elevation of dihydroxyacetone-3-phosphate (DHAP), a metabolite of glycolysis and intermediates of pentose phosphate pathway in addition to 2-phospholactate and 4-PE, two toxic by-products of glycolysis. It was suggested that PGP acts as a metabolite repair enzyme by hydrolyzing the toxic products, and regulates the central carbon metabolism and drug sensitivity of plasmodium (Dumont, Richardson et al. 2019). Purified PGP from *Plasmodium berghei* was shown to dephosphorylate 2-phospholactate and 2-PG, *in vitro*, even though these metabolites could not be measured in a PGP deletion mutant as the knockout was lethal for this parasite (Nagappa, Satha et al. 2019). The precise physiological function of PGP in plasmodium

species is not clear, although it was speculated that it may play a role in the control of glycolysis, which is an essential source of ATP in this organism (Nagappa, Satha et al. 2019).

Plants: In plants, photorespiration generates large amounts of 2-PG inside the chloroplast, which can strongly inhibit the Calvin cycle. In *Arabidopsis thaliana* 13 different genes coding for different PGP isoforms have been annotated, but only two of these have been characterized. Plants with deletion of PGP-1, expressed in the chloroplasts of leaves, were not viable in normal air but could survive in 1% CO_2 atmosphere, whereas deletion of PGP-2, expressed in the cytosol, had no visible effect on the plant survival (Schwarte and Bauwe 2007, Timm, Woitschach et al. 2019). Thus, degradation of 2-PG in the chloroplast by PGP-1 is essential in Arabidopsis. In addition to these PGP genes, two glycerophosphatases with 95% identical amino acid sequence, coded by *AtGpp1* and *AtGpp2,* were described in Arabidopsis and were proposed to regulate formation of glycerol in the cytosol and in plastids (Caparros-Martin, Reiland et al. 2007). Even though the expression of AtGpp1 and AtGpp2 is not affected by osmotic, ionic or oxidative stress conditions, plants with gain of function in AtGpp2 show improved tolerance to salt, osmotic and oxidative stress (Caparros-Martin, Reiland et al. 2007).

Flies and nematodes: It is not known whether there are distinct PGP and G3PP enzymes in *Drosophila melanogaster* or *Caenorhabditis elegans*. Deletion of CG5567, a homologue of PGP, led to elevated triglycerides in *Drosophila* larvae grown on high sugar, without any effect on mortality or development (Dwyer 2020). However, the protein product of CG5567 is yet to be characterized in *Drosophila*. In *C. elegans*, three phosphoglycolate phosphatase homologs (*pgph1, 2, 3*) have been identified (Possik, Madiraju et al. 2017). Exposing *C. elegans* to hyperosmotic stress or excess glucose induces expression of these genes, and is accompanied by elevated glycerol production, supporting that the three PGP homologs in the worm act as G3PPs that are

essential for glycerol production and adaptation to hyperosmotic and metabolic stresses (Lee, Murphy et al. 2009, Rohlfing, Miteva et al. 2010).

Arctic fish: Two potential G3PP enzymes have been identified in the arctic fish *Osmerus mordax*, which is capable of acclimation to cold temperature by the production of large quantities of glycerol (Ditlecadet, Short et al. 2011, Raymond 2015). Since these fish G3PP isoforms were found to show optimal activity at acidic pH, their physiological role in glycerol production at near neutral pH was questioned (Raymond 2015).

Mammals: The mammalian PGP gene consists of two exons and one intron and maps to chromosome 16 in humans, chromosome 17 in mice and chromosome 10 in rats (Seifried, Bergeron et al. 2016, Segerer, Engelmann et al. 2018). PGP encodes a 321 amino acid long cytosolic protein that is a member of the superfamily of haloacid dehalogenase (HAD)-like hydrolases (Possik, Madiraju et al. 2017). The mammalian *PGP* gene product has been described with different names and functions. It was first described in human red blood cells (RBC) as phosphoglycolate phosphatase (PGP), based on its sequence similarity to the plant and bacterial PGP enzymes, along with its similar substrate specificity (i.e., high activity towards 2-PG) (Rose 1981, Yu, Pendley et al. 1990). Later, this protein was called as aspartate-based, ubiquitous, Mg^{2+}-dependent phosphatase (AUM), as it showed hydrolytic activity for peptides containing phosphotyrosine (Seifried, Knobloch et al. 2014, Seifried, Bergeron et al. 2016, Segerer, Engelmann et al. 2018, Gohla 2019). However, the very low cellular levels of 2-PG under physiological conditions and the ~1,000-fold lower catalytic efficiency of purified PGP towards phosphotyrosine peptides compared to classical tyrosine phosphatases, the proposed physiological role of mammalian PGP in the hydrolysis of either 2-PG or phosphotyrosine residues is questionable. Studies from our lab demonstrated that PGP functions as a G3PP, hydrolysing Gro3P,

produced normally in all the cells *via* glycolysis and available in sufficient concentrations (1-5 mM) to serve as a PGP substrate (Mugabo, Zhao et al. 2016, Possik, Madiraju et al. 2017). Hence, the name G3PP is more appropriate for the *PGP* gene product, and is accepted by most protein databases (Uniprot, NCBI Protein, PDB, etc.).

1.10.3 Substrates and enzymatic activities of G3PP/PGP

G3PP/PGP is known to hydrolyze 2-PG, formed by pyruvate kinase in RBC **(Figure 1.7 in blue)** (Rose, Grove et al. 1986).; and has also been shown to dephosphorylate 4-PE and 2-phospholactate, toxic by-products of glyceraldehyde-3-phosphate dehydrogenase (GAPDH) and pyruvate kinase respectively **(Figure 1.7 in blue)**. However, 4-PE and 2-phospholactate are undetectable in cells under normal conditions but accumulate only when G3PP/PGP expression is suppressed (Collard, Baldin et al. 2016, Dumont, Richardson et al. 2019, Kempaiah Nagappa, Satha et al. 2019). Purified recombinant mouse PGP protein showed high catalytic efficiency with 2-PG, 4-PE, and 2-phospholactate, but relatively lower activity with Gro3P (Collard, Baldin et al. 2016, Mugabo, Zhao et al. 2016). The purified enzyme also shows very high activity with the non-physiological substrate p-nitrophenol phosphate (Seifried, Knobloch et al. 2014). Thus, the observed catalytic efficiencies of purified G3PP/PGP *in vitro* may not have much relevance based on the physiological availability of these substrates. Therefore, because the intracellular concentration of Gro3P ranges from 1–5 mM and the Km of G3PP/PGP for Gro3P is ∼1.4 mM, Gro3P is a more physiologically relevant G3PP/PGP substrate) (Mugabo, Zhao et al. 2016) than 2-PG, 4-PE or 2-phospholactate, which are either undetectable or present in low micromolar levels in normal cells (Collard, Baldin et al. 2016, Mugabo, Zhao et al. 2016, Possik, Madiraju et al. 2017, Gohla 2019).

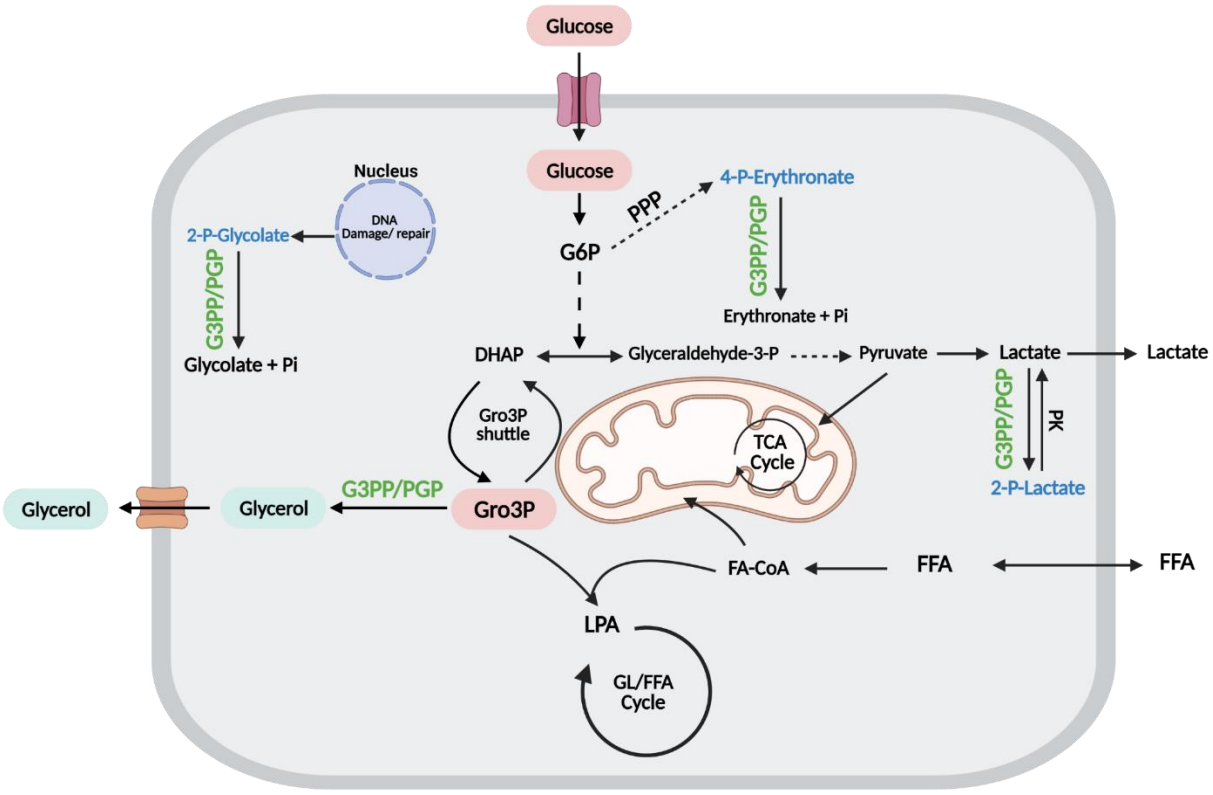

Figure 1.7. Substrates and enzymatic activities of G3PP/PGP.

Potential G3PP/PGP substrates are shown in blue: 2-phosphoglycolate (2-P-Glycolate), 2-phospholactate (2-P-Lactate) and 4-phosphoerythronate (4-P-Erythronate). Physiological substrate is glycerol-3-phosphate (Gro3P). Abbreviations: DHAP, dihydroxyacetone phosphate; FA-CoA, fatty acyl-CoA; FFA, free fatty acid; G3PP/PGP, glycerol 3-phosphate phosphatase/phosphoglycolate phosphatase; G6P, glucose 6-phosphate; GL/FFA cycle, glycerolipid/free fatty acid cycle; Glyceraldehyde-3-P, glyceraldehyde-3-phosphate; TCA cycle, tricarboxylic acid cycle; PK, pyruvate kinase; PPP, pentose phosphate pathway. Adapted from (Possik, Madiraju et al. 2017) using BioRender.

1.10.4 Candidates biological action of G3PP/PGP related to its Gro3Pase activity

There are many lines of evidence in mammalian cells showing the important role played by G3PP in controlling Gro3P levels and indicating its biological action in different cells.

1.10.4.1 Pancreatic islets and hepatocytes

Cellular levels of Gro3P in hepatocytes (Mugabo, Zhao et al. 2016) and INS-1(832/13) cells (Lamontagne, Al-Mass et al. 2017, Mugabo, Zhao et al. 2017) under normal glucose supply are sufficient to serve as the substrate for the G3PP enzyme. In most cells, DHAP formed during glycolysis is partly converted to Gro3P. Gro3P can also be formed from glycerol by GK in cells expressing this enzyme such as liver, kidney and muscle (Lin 1977). Altering G3PP protein expression can control cellular levels of Gro3P with impact on several metabolic pathways (Mugabo, Zhao et al. 2016). For example, overexpression of human G3PP increased glycerol production from glucose, in parallel with markedly decreased Gro3P levels, glycolysis and glucose driven respiration in rat pancreatic islets, INS-1(832/13) cells and rat hepatocytes, while suppression of G3PP in these cells produced the opposite effects (Mugabo, Zhao et al. 2016). The level of G3PP expression in pancreatic β-cells and hepatocytes was also inversely related to glycerolipid production. Thus, for cells grown at normal glucose concentrations, G3PP can control glucose and lipid metabolism (Mugabo, Zhao et al. 2016). In contrast, increased G3PP activity was shown to lower glycerol-driven gluconeogenesis in isolated rat hepatocytes and in rats overexpressing G3PP in the liver (Mugabo, Zhao et al. 2016, Possik, Madiraju et al. 2017). These results demonstrate that G3PP is a key player in the control of lipid and glucose metabolism in β-cells and hepatocytes.

1.10.4.2 Embryonic cells with inactive mutant G3PP

Since G3PP/PGP regulates Gro3P levels, G3PP/PGP inactivation should alter glycerolipid metabolism. Mice with a knock-in mutant of catalytically inactive G3PP/PGP ($PGP^{D34N/D34N}$) had increased levels of DAGs and TGs in e8.5 embryos, indicating that these knock-in embryos had increased lipogenesis from Gro3P accumulation (Segerer, Hadamek et al. 2016). Deletion of the

Drosophila PGP ortholog caused significant elevation in triglycerides and altered glycolysis in the larvae, showed no effect on development (Dwyer 2020). Therefore, G3PP/PGP likely regulates glucose and glycerolipid metabolism by controlling Gro3P levels during development: this function of G3PP appears to be essential for development in higher organisms.

1.10.4.3 Cancer cells

Studies on cancer cell lines provided further evidence for a role of G3PP/PGP in controlling glucose metabolism. Deletion of *PGP* in HCT116 human colorectal cancer cells led to ~40% reduction in glucose utilization and lactate production together with 75% decline in fructose 2,6-diphosphate levels. These changes could all be restored by the re-expression of G3PP/PGP in HCT116 cells (Collard, Baldin et al. 2016). Furthermore, G3PP/PGP deletion was also associated with inhibition of the pentose phosphate pathway and accumulation of 6-phosphogluconate in HCT116 cells. These changes were associated with the accumulation of two toxic side products of glycolysis (2-phospholactate and 4-PE), which can also inhibit glycolysis and the pentose phosphate pathway, it was proposed that G3PP/PGP is required to maintain the metabolic integrity of HCT116 cells by hydrolyzing and removing the toxic metabolites (Collard, Baldin et al. 2016). However, the concentrations of 2-phospholactate and 4-PE in cells with normal PGP activity were much below their Km (~170 to 250µM respectively), questioning the ability of G3PP/PGP to detoxify these metabolites at low concentrations. The accumulation of toxic glycolytic metabolites and their possible removal by G3PP/PGP is probably relevant only in cancer cells (Possik, Madiraju et al. 2017).

1.11 Rationale of the thesis

Obesity is a risk factor for type 2 diabetes (T2D) that contributes to IR and pancreatic β-cell failure through the exhaustion of insulin stores and fuel surfeit mediated glucolipotoxicity (Prentki and Nolan 2006, Nolan, Damm et al. 2011). Alterations in glucose and lipid metabolism, including the GL/FFA cycle (Prentki and Madiraju 2008, Prentki and Madiraju 2012, Prentki, Matschinsky et al. 2013), which is implicated in balancing glucose and lipid metabolism and central to energy homeostasis in many tissues (Nye, Hanson et al. 2008, Zechner, Zimmermann et al. 2012), play an important role in the pathogenesis of obesity and T2D. The GL/FFA cycle involves FA esterification with glycerol to synthesize mono-, di-, & triacylglycerols and phospholipids (lipogenesis), followed by their sequential hydrolysis releasing the FFA (lipolysis), that can then be re-esterified (Prentki and Madiraju 2008, Prentki and Madiraju 2012, Prentki, Matschinsky et al. 2013). Glycerol-3-phosphate (Gro3P), formed from glucose during glycolysis is at the crossroads of glucose and lipid metabolism and is one of the starting substrates for the GL/FFA cycle. Availability of Gro3P and fatty acyl-CoA regulates the flux through the GL/FFA cycle and the associated production of lipids and metabolic signals.

In mammalian cells, Gro3P is thought to undergo either esterification *via* lipogenesis or oxidation *via* glycolysis. Direct hydrolysis of Gro3P to release glycerol, which happens in plants and microbes, was not known to occur in mammalian cells. Recently, a novel glycerol-3-phosphate phosphatase (G3PP, encoded by the phosphoglycolate phosphatase [PGP] gene) was identified and characterized in mammalian cells and shown to directly hydrolyze glycolysis-derived Gro3P to glyceol (Mugabo, Zhao et al. 2016). G3PP, by regulating cytosolic Gro3P levels, can play a role in the control of glycolysis, glucose oxidation, cellular redox and ATP production, gluconeogenesis, glycerolipid synthesis and FA oxidation in pancreatic islet β-cells and

hepatocytes (Mugabo, Zhao et al. 2016). The elevated activity of G3PP *ex vivo* was shown to decrease gluconeogenesis in hepatocytes and to reduce both glucose stimulated insulin secretion under elevated glucose levels and the effects of glucolipotoxicity in β-cells. Overexpression of G3PP in rat liver *in vivo,* using an adenoviral construct, reduced body weight gain, hepatic glucose production and plasma triglycerides and increased HDL (Mugabo, Zhao et al. 2016). In parallel, Collard et al. have shown that PGP reduces cellular levels of 4-Phosphoerythronate and 2-phospho-L-lactate, compounds which are by-products of glyceraldehyde 3-phosphate dehydrogenase and pyruvate kinase respectively (Collard, Baldin et al. 2016). This action of PGP/G3PP was shown to antagonize the activity of the pentose phosphate pathway and glycolysis in a cancer cell line, leading to the hypothesis that it may act as a 'metabolite repair enzyme' by eliminating toxic by-products of central carbon metabolism (Beaudoin and Hanson 2016). Taken together, these results implicate G3PP as a novel player in the control of energy and intermediary metabolism, insulin secretion and the response to metabolic stress. However, the precise molecular basis of G3PP's role in intermediary metabolism and its regulation under physiological and pathological conditions in different tissues are not known.

A key scientific objective of this thesis is to test whether G3PP has a biological function *in vivo* that is linked to glucose or lipid metabolism of or detoxification of excess glucose that is related to its Gro3P hydrolysis activity in pancreatic β-cells and hepatocytes *ex vivo*.

Aims:

Chapter II: To examine the role of G3PP in the regulation of insulin secretion, metabolic stress and glucose and lipid metabolism in mouse pancreatic β-cells *in vivo*.

Chapter III: To examine the role of G3PP in the regulation of glucose and lipid metabolism and metabolic stress in mouse hepatocytes *in vivo*.

Chapter IV: To examine if controlled overexpression of G3PP affect glucose and lipid metabolism and protects against metabolic stress in mouse hepatocytes *in vivo*.

Bridging Chapters I and II

Initial studies (overexpression and knockdown *in vitro*) indicated that G3PP plays a role in islet metabolism, insulin secretion and protection against glucolipotoxicity (Mugabo, Zhao et al. 2016). My goal was to examine the importance of G3PP in regulating insulin secretion, metabolic stress, and glucose and lipid metabolism in mouse pancreatic β-cells *in vivo*. As G3PP deletion/inactivation is known be embryonic lethal, these parameters were studied in detail using β-cell specific inducible G3PP-KO (BKO) mice. This inducible model was generated by crossing floxed G3PP mice crossed with MCre mice to generate a line with β-cell specific G3PP-KO (BKO) after TMX injection. Male BKO mice fed normal diet for 20 weeks and body weight and food intake were monitored. We performed a detailed study of *in vivo* insulin and glucose homeostasis. Blood glucose, glycerol, insulin, triglycerides and FFA levels were measured using commercial kits. Pancreatic islets from MCre and BKO mice fed normal diet were examined *ex vivo* for insulin secretion in response to various fuel and to glucotoxicity conditioned. We also conducted metabolomics studies in islets from BKO and MCre mice, which we correlated with altered glucose, lipid and mitochondrial metabolism in the islets.

Chapter II: Glycerol-3-phosphate phosphatase operates a glycerol shunt in pancreatic β-cells that controls insulin secretion and metabolic stress

Anfal Al-Mass[1,2], Pegah Poursharifi[2], Marie-Line Peyot[2], Roxane Lussier[2], Emily J Levens[2], Julian Guida[2], Yves Mugabo[2], Elite Possik[2], Rasheed Ahmad[3], Fahd Al-Mulla[3], Robert Sladek[1], S. R. Murthy Madiraju[2], Marc Prentki[2*]

[1] Department of Medicine, McGill University, Montréal, QC, Canada.

[2] Departments of Nutrition, Biochemistry and Molecular Medicine, University of Montreal, and Montreal Diabetes Research Center, Centre de Recherche du Centre Hospitalier de l'Université de Montréal (CRCHUM), Montréal, QC, Canada.

[3] Departments of Immunology, Microbiology, Genetics and Bioinformatics, Dasman Diabetes Institute, Dasman 15462, Kuwait.

*__Corresponding author:__
Marc Prentki, PhD
Professor of Nutrition, Biochemistry and Molecular Medicine, Université de Montréal
Room R08-412, Tour Viger, 900 rue Saint Denis
Montreal, QC H2X 0A9, Canada.
Email: marc.prentki@umontreal.ca

Short title: G3PP and glucodetoxification in β-cells

Keywords: Glycerol-3-phosphate phosphatase, Glycerol shunt, Glucose-stimulated insulin secretion, Glucodetoxification, Pancreatic beta cell, Type 2 diabetes, Obesity

Published in: Molecular Metabolism 2022 (**Al-Mass, A.**, Poursharifi, P., Peyot, M. L., Lussier, R., Levens, E. J., Guida, J., Mugabo, Y., Possik, E., Ahmad, R., Al-Mulla, F., Sladek, R., Madiraju, S., & Prentki, M. (2022). Glycerol-3-phosphate phosphatase operates a glycerol shunt in pancreatic β-cells that controls insulin secretion and metabolic stress. Molecular metabolism, 60, 101471. https://doi.org/10.1016/j.molmet.2022.101471)

2.1 Abstract

Objective: The recently identified glycerol-3-phosphate (Gro3P) phosphatase (G3PP) in mammalian cells, encoded by the *PGP* gene, was shown to regulate glucose, lipid and energy metabolism by hydrolyzing Gro3P and to control glucose-stimulated insulin secretion (GSIS) in β-cells, *in vitro*. However, whether G3PP regulates β-cell function and insulin secretion *in vivo* is not known.

Methods: We now examined the role of G3PP in the control of insulin secretion *in vivo*, β-cell function and glucotoxicity in inducible β-cell specific G3PP-KO (BKO) mice. Inducible BKO mice were generated by crossing floxed-G3PP mice with Mip-Cre-ERT (MCre) mice. All the *in vivo* studies were done using BKO and control mice fed normal diet and the *ex vivo* studies were done using pancreatic islets from these mice.

Results: BKO mice, compared to MCre controls, showed increased body weight, adiposity, fed insulinemia, enhanced *in vivo* GSIS, reduced plasma triglycerides and mild glucose intolerance. Isolated BKO mouse islets incubated at high (16.7 mM), but not at low or intermediate glucose (3 and 8 mM), showed elevated GSIS, Gro3P content as well as increased levels of metabolites and signaling coupling factors known to reflect β-cell activation for insulin secretion. BKO islets also showed reduced glycerol release and increased O_2 consumption and ATP production at high glucose only. BKO islets chronically exposed to elevated glucose levels showed increased apoptosis, reduced insulin content and decreased mRNA expression of β-cell differentiation markers, *Pdx-1*, *MafA* and *Ins-2*.

Conclusions: The results demonstrate that β-cells are endowed with a "*glycerol shunt*", operated by G3PP that regulates β-cell metabolism, signaling and insulin secretion *in vivo*, primarily at elevated glucose concentrations. We propose that the glycerol shunt plays a role in preventing insulin hypersecretion and excess body weight gain and contributes to β-cell mass preservation in the face of hyperglycemia.

2.2 Introduction

Hyperinsulinemia and IR contribute to obesity, type 2 diabetes (T2D) and associated metabolic disorders (Nolan and Prentki 2019, Thomas, Corkey et al. 2019). Pancreatic β-cells secrete insulin

primarily in response to increasing blood glucose levels, through the production of metabolic coupling factors (MCF) that promote insulin granule exocytosis. Disturbed glucose and lipid metabolism, including the glycerolipid/ free fatty acid (GL/FFA) cycle (Prentki and Madiraju 2008, Prentki and Madiraju 2012, Prentki, Matschinsky et al. 2013), which is implicated in the regulation of insulin secretion and energy homeostasis (Nye, Hanson et al. 2008, Zechner, Zimmermann et al. 2012, Poursharifi, Attane et al. 2020), contribute to the pathogenesis of obesity and T2D. The GL/FFA cycle, known to produce several MCF, in particular monoacylglycerol (Poursharifi, Madiraju et al. 2017), consists of two arms: lipogenesis implicated in the synthesis of glycerolipids, and lipolysis during which glycerolipids, in particular triglycerides (TG) are hydrolyzed to FFA and glycerol (Prentki and Madiraju 2008, Prentki and Madiraju 2012). Lipogenesis involves the esterification of fatty acyl-CoA with glycerol-3-phosphate (Gro3P), which in β-cells is formed mostly from glucose via glycolysis. The GL/FFA cycle is driven largely by the availability of Gro3P and fatty acyl-CoA (Prentki and Madiraju 2008, Prentki and Madiraju 2012, Prentki, Matschinsky et al. 2013).

We recently reported that mammalian cells harbor a Gro3P phosphatase (G3PP), which by hydrolyzing Gro3P to glycerol, controls the availability of Gro3P for various metabolic pathways, in particular TG synthesis (lipogenesis segment of GL/FFA cycle), the Gro3P-electron shuttle to mitochondria and flux through lower glycolysis (Mugabo, Zhao et al. 2016). G3PP in mammalian cells, previously known as phosphoglycolate phosphatase, is encoded by *PGP* and we demonstrated that it primarily uses Gro3P as its intracellular substrate under normal physiological conditions. However, this enzyme is also able to use other phosphate esters, including phosphoglycolate as substrates, under stress conditions (Segerer, Hadamek et al. 2016, Possik, Madiraju et al. 2017, Possik, Al-Mass et al. 2021). Our earlier *in vitro* studies primarily in INS1-β-cells showed that G3PP activity is inversely proportional to glucose-stimulated insulin secretion (GSIS) at elevated glucose concentrations. We found that increased expression of G3PP in β-cells diverts a significant part of the glucose carbons towards the formation of glycerol, which is not metabolized due to low glycerol kinase activity (Prentki and Madiraju 2008, Xue, Chen et al. 2017) and leaves the β-cell. Thus, elevated G3PP in β-cells prevents hypersecretion of insulin under excess glucose conditions by lowering the flux through the GL/FFA cycle, lower-glycolysis and mitochondrial oxidation (which are important sources of MCF), while the reverse was noticed with the suppression of G3PP (Mugabo, Zhao et al. 2016). In addition, glucotoxicity and

glucolipotoxicity in β-cells were aggravated when G3PP expression was suppressed, whereas the cells were protected when G3PP was over-expressed, suggesting an important role of G3PP in the detoxification of glucose and protection of β-cells under nutrient-excess conditions (Mugabo, Zhao et al. 2016).

However, the role of β-cell G3PP in the control of insulin secretion and energy homeostasis *in vivo* is not known, nor do we know the range of glucose concentrations where the enzyme is active. In addition, if we have learned much about the pathways and biochemical basis of glucotoxicity, little is known as to how mammalian cells cope, adapt and detoxify excess glucose in the body (Prentki, Peyot et al. 2020). Deletion of G3PP activity in the whole body was found to be embryonically lethal (Segerer, Hadamek et al. 2016), and therefore we have generated β-cell specific G3PP knockout (BKO) mice in which deletion of *PGP*/G3PP gene is induced in the adult stage, in order to avoid any developmental effects. The present *in vivo* and *ex vivo* studies, in which islets were exposed to low, intermediate and high glucose reveal the existence in the β-cell of a "glycerol shunt" operated by G3PP implicated in β-cell metabolism, signaling and insulin secretion as well as in the control of metabolic stress, and that this novel pathway primarily functions at high but not normal or low glucose concentrations.

2.3 Materials and Methods

Generation of G3PP conditional KO mice and breeding strategy

Heterozygous G3PP-lox/lox mice in which exons 1 and 2 of *PGP* (coding for G3PP protein) gene are flanked with LoxP sites were generated by Ingenious Targeting Laboratory (Stony Brook, NY). The donor targeting vector was designed so that the first loxP sequence is inserted on the 5' side of exon 1 and the second at the 3' end of the FRT-flanked Neo selection cassette (after exon 2) **(Figure 2.1*A*)**. The targeting vector was then transfected by electroporation to FLP C57BL/6 ES cells. Positive targeted ES clones, where the Neo cassette was removed by the FLP recombinase, were microinjected into Balb/c blastocysts to generate chimeras. These chimeras were crossed to wildtype (WT) C57Bl/6N to generate heterozygous G3PP-lox/+ mice. Heterozygous G3PP-lox/+ mice were bred to produce homozygous G3PP-lox/lox ($G3PP^{flox/flox}$) mice. Homozygous G3PP-lox/lox were then crossed with heterozygous Mip-CreERT2 mice (Wicksteed, Brissova et al. 2010)

to obtain Mip-CreERT2/+, G3PP-flox/+ and G3PP-flox/+ mice. These mice were further mated to get MipCre-ERT2/+, WT, G3PP-flox/flox and Mip-CreERT2/+; G3PP-flox/flox mice. The presence of the WT or the floxed *PGP* allele was evaluated in DNA from ear punch tissue fragments using the following primers: NDEL1: 5'- ACCTCTTGCCTGCCCTTCAAGG-3'; NDEL2: 5'- TTGACCCATTTCAGTCTCA GCAACAGG-3', and the presence of Cre transgene using the following primers: forward: 5'- CCTGGCGATCCCTGAACATGTCCT-3', Reverse: 5'- TGGACTATAAAGCTGGTGGGCAT -3'. Specific amplification of a 452 bp DNA fragment corresponding to the floxed- *PGP* allele, a 312 bp fragment corresponding to the WT *PGP* allele and the presence of the Mip-Cre transgene by a 267 bp DNA fragment was verified by genomic PCR **(Figure 2.1*B*)**.

Animals

All mice were on C57BL/6N genetic background. At 8 weeks of age, wild-type (WT), $G3PP^{flox/flox}$ (fl/fl), Mip-CreERT2 (MCre) and Mip-$CreERT2/^{+}$;$G3PP^{flox/flox}$ male mice received tamoxifen (TMX) intraperitoneal injections for 5 consecutive days (50 mg/kg body weight, dissolved in 90% corn oil plus 10% ethanol) to induce Cre recombinase and β-cell specific deletion of G3PP in the Mip-$CreERT2/^{+}$; $G3PP^{flox/flox}$ mice (BKO). After 5 days of TMX injections, mice were placed in individual cages and fed normal chow diet (15% fat by energy; Harlan Teklad, Madison, WI, USA) for 12 weeks. Body weight and food intake were measured weekly. Specific deletion of G3PP expression in pancreatic islets without any change in other tissues was ascertained in the BKO mice, as compared to WT, MCre and fl/fl control mice **(Figure 2.1*C*)**. Body composition (lean and fat mass) after 12 weeks after TMX injection was measured by magnetic resonance imaging (EchoMRI Analyzer-700). Animals were housed individually at room temperature (23°C) with a 12 h light/12 h dark cycle. 20-week-old mice were anesthetized by intraperitoneal injection of ketamine (100 mg/kg)/xylazine (10 mg/kg), followed by cardiac puncture and euthanasia via cervical dislocation. Various tissues, including adipose depots, liver, kidney, etc., were immediately collected and kept frozen for further analyses. All procedures were approved by the institutional committee for the protection of animals (Comité Institutionnel de Protection des Animaux du Centre Hospitalier de l'Université de Montréal).

Pancreatic islet isolation.

Pancreatic islets were isolated from BKO, WT, MCre and fl/fl mice as previously described (Peyot, Roubtsova et al. 2021). After isolation, the islets were kept in RPMI medium supplemented with 2 mM glutamine, 1 mM sodium pyruvate, 10 mM HEPES (pH 7.4), penicillin (100U/ml)/ streptomycin (100µg/ml), 10% FBS and containing 5 mM glucose (glucose concentration during overnight recovery was 8 mM for glucotoxicity experiments) for overnight recovery and then employed for *ex-vivo* insulin secretion experiments and other measurements as detailed below.

Western blotting

Mouse tissues and pancreatic islets were lysed in RIPA buffer (10 mM Tris-HCl, 1 mM EDTA, 0.5 mM EGTA, 1% Triton X-100, 0.1% sodium deoxycholate, 0.1% sodium dodecylsulfate and 140 mM NaCl) and the protein extracts were used for western blot analysis to validate β-cell specific G3PP deletion (G3PP primary antibody: PGP antibody E-10, sc-390883; secondary antibody: m-IgGκ BP-HRP, sc-516102). For all tissues, α-tubulin was used as the gel loading control.

Intraperitoneal glucose tolerance test (IPGTT)

IPGTT was performed on 16-week-old male G3PP-BKO, WT, MCre and fl/fl mice. Glucose (2 g/kg body weight) was injected intraperitoneally in conscious mice at 13:00 hours after 6 h of food withdrawal. Glycemia was measured in the tail blood at time 0, 15, 30 and 60 min following glucose administration using a glucometer (Contour blood glucometer, Bayer). Insulin levels were also measured in the tail blood.

Insulin tolerance test (ITT)

ITT was performed on 19-week-old male G3PP-BKO, WT, MCre and fl/fl mice. Insulin (0.75 U/kg body weight, Humulin; Lilly, Indianapolis, USA) was injected intraperitoneally (IPITT) in conscious mice at 13:00 hours, after 4h of food withdrawal. Glycemia was measured in the tail blood at time 0, 15, 30, 45, 60, 90 and 120 min using glucometer. Blood was collected from the tail at time 0 min to measure plasma insulin levels.

Plasma parameters

Twenty week old mice fed a normal diet were anesthetized as described above and blood was collected through cardiac puncture at 08:00 hour. Plasma glucose, insulin, non-esterified fatty acids (NEFA), TG and glycerol were measured (Attane, Peyot et al. 2016).

***Ex vivo* insulin secretion**

After overnight recovery, islets were transferred in complete RPMI medium containing 3 mM glucose for 2h and preincubated for 45 min at 37°C in Krebs Ringer buffer (135 mM NaCl, 3.6 mM KCl, 0.5 mM NaH_2PO_4, 0.5 mM $MgCl_2$ and 1.5mM $CaCl_2$ with 10 mM HEPES (pH 7.4) and 2 mM $NaHCO_3$) (KRBH) containing 0.5% defatted-BSA, 2 mM glutamine, 50 µM L-carnitine and 3 mM glucose. Batches of 10 islets, in triplicates, were incubated for 1h at 3, 8 and 16 mM glucose in the presence or absence of palmitate/oleate (0.15 mM/each, complexed with BSA) and at 3 mM glucose plus 35 mM KCl. Insulin release was normalized for the total islet insulin content.

Glycerol release

Batches of 100 islets that were preincubated for 1h in KRBH containing 0.5% defatted-BSA, 2 mM glutamine), 50 µM L-carnitine and 4 mM glucose. After preincubation, the islets were incubated for 2h at 4 and 16 mM glucose. Glycerol release into the medium was determined using [γ-^{32}P]ATP (Perkin Elmer Life Sciences) and glycerol kinase (Sigma) (Bradley and Kaslow 1989).

Oxygen consumption and mitochondrial function

Isolated mouse islets (batches of 75 islets) were transferred to XF24 islet capture microplates in 4 mM KRBH (0.07% defatted-BSA, 2 mM glutamine and 50 µM L-carnitine). After basal respiration measurement in a XF24 respirometer (Seahorse Bioscience) for 20 min, glucose levels were increased to 16 mM and O_2 consumption was measured for another 1h. Then oligomycin (to assess uncoupled respiration), FCCP (to estimate maximal respiration), and antimycin/rotenone (to measure non-mitochondrial respiration) were added successively.

Glucotoxicity

After overnight recovery in RPMI medium containing 8 mM glucose and 10% FBS, 150 -200 islets were incubated for 7 days at 11 and 30 mM glucose in serum-free RPMI medium with 0.5% BSA. Media were changed on alternate days. After 7 days incubation, islets were collected to measure insulin content, gene expression and apoptosis (Cell Death Detection kit, Roche, Basel, Switzerland) (Li, Karaca et al. 2017).

RNA extraction and quantitative PCR

Total RNA was extracted from 150 islets (RNeasy Micro Kit, Qiagen). Following reverse-transcription to cDNA, expression of different genes was determined by quantitative PCR using SYBR Green (Qiagen (QuantiTect)). All gene expression analyses were conducted in duplicate and normalized to the expression of *18S*. Sequences for the primers used are listed in Supplementary Table S2.1.

Targeted metabolomics

Isolated islets (250) were incubated in 1.5 ml tubes under similar conditions as for the *ex vivo* insulin secretion experiments. After incubation, media were collected to measure insulin secretion and 675 µl of ice-cold extraction buffer (80% methanol, 2 mM ammonium acetate, pH 9.0) was quickly added to the islets and mixed by vortex, followed by sonication in a cup-horn (Q700 Sonicator, Qsonica, Newtown, CT) at 150 watts for 1 min (cycles of 10s on, 10s off) in an ethanol-ice bath. Islet extracts were centrifuged at 4°C for 10 min at 20,000×g, and 600 µl supernatant from each condition was collected in separate ice-cold glass tubes to which water (168 µl) was added. Polar metabolites were extracted with 960 µL of chloroform:heptane (3:1, v/v) by 2 × 10s vigorous mixing by vortex followed by 10-min incubation on ice and 15 min centrifugation at 4°C at 4,500×g. The upper aqueous phase (540 µL) was transferred in a cold 1.5 ml tube, followed by centrifugation and the supernatants (400 µL) were collected. All the samples were frozen in liquid nitrogen and freeze-dried, and stored at −80°C until used. The dried samples were reconstituted in 20 µL of Milli-Q water at 4°C, and 5 µL injections were employed in duplicate for analysis on an LC-electrospray ionization-MS/MS system (Agilent 1200 SL and a triple-quadrupole mass spectrometer (4000Q TRAP MS/MS, Sciex)) (Mugabo, Zhao et al. 2016). Peak areas were used for relative quantification of identified metabolites.

Statistical analyses

Data were analyzed using GraphPad Prism 6 (GraphPad Software, San Diego, CA). Results are expressed as means ± SEM. Statistical differences between two groups were assessed by unpaired, two-tailed Student's *t* test, and between multiple groups using one-way or two-way analyses of variance (ANOVA) with Bonferroni post-hoc test, as indicated. A p value < 0.05 was considered statistically significant.

Study approval

All the procedures for mice studies were performed in accordance with the Institutional Committee for the Protection of Animals at the University of Montréal CRCHUM.

2.4 Results

In the present study, we employed Mip-Cre-ERT (MCre) mice as the control group for the G3PP-BKO mice considering that the MCre mice express Cre recombinase in response to tamoxifen, unlike the fl/fl and WT mice. Additionally, MCre mice were previously shown to display expression of human growth hormone sequences (Oropeza, Jouvet et al. 2015), which may influence islet function. Thus, it was previously suggested that for β-cell specific gene knockout studies using Mip-Cre-ERT mice (Wicksteed, Brissova et al. 2010), the better controls are the Mip-Cre-ERT mice than the WT or flox/flox (for the concerned gene) mice (Bergeron, Ghislain et al. 2018). However, we compared the different control groups and found that WT and fl/fl mice have similar phenotype with regard to *in vivo* **(Supplemental Figure S2.1)** and *ex vivo* **(Supplemental Figures S2.2 and S2.4)** parameters. This justifies the use of MCre mice as control mice in this study.

G3PP-BKO mice show increased body weight gain, fat mass and fed insulinemia

G3PP-BKO mice fed a standard chow diet till 20 weeks of age showed significant increase in body weight gain **(Figure 2.1*D* and *E*)** and fat mass **(Figure 2.1*F*)** with no change in food intake **(Figure 2.1*G*)** compared to MCre control mice. Even though there was no change in fed glycemia, fed insulinemia was significantly higher in the BKO mice with C-peptide levels showing no statistically significant difference **(Figure 2.1*H*)**. However, BKO mice showed lower plasma TG level with no changes in glycerol and FFA **(Figure 2.1*H*)**. In accordance with the increased fat

mass, we found that BKO mice have larger visceral adipose depots **(Figure 2.1*I*)** and higher visceral adipose tissue weight **(Supplemental Figure 2.1*E*)**. There was no significant change in other tissue weights in BKO mice compared to controls and also among the different controls **(Supplemental Figure 2.1*E*)**. The TG content of visceral adipose tissue and skeletal muscle was higher in the BKO mice **(Figure 2.1*J*)**.

G3PP-BKO mice show increased insulin secretion *in vivo* and mild glucose intolerance

As the BKO mice displayed elevated fed insulinemia, we assessed glucose tolerance in these mice. Glucose tolerance, assessed by IPGTT, in the BKO mice was found to be modestly impaired, as indicated by the significantly elevated plasma glucose levels only at 30 min after intraperitoneal glucose injection, with larger AUC-glucose at 60 min, although no changes were seen at 15 min after the glucose load, compared to MCre controls **(Figure 2.2*A*)**. Furthermore, plasma insulin levels were higher in the BKO mice at all the time points following glucose injection compared to control mice **(Figure 2.2*B*)**. These results indicated that BKO mice secrete more insulin than control mice under similar hyperglycemic conditions. The IPITT suggested that the BKO mice fed a chow diet have unaltered insulin sensitivity **(Figure 2.2*C*)**, despite showing elevated insulin secretion in response to a glucose load.

G3PP-BKO islets show increased insulin secretion and mitochondrial metabolism only at high glucose concentration

In order to examine if the *in vivo* deletion of *PGP* gene in mice impacts β-cell function, and if so in which glucose concentration range, we measured insulin secretion in BKO and control mouse islets *ex-vivo*, in response to different concentration of glucose with and without FFA. Insulin secretion at 3 mM (basal, hypoglycemia) and 8 mM (intermediate/physiological in mice) glucose concentration was similar between BKO and MCre control islets **(Figure 2.3*A*)**. However, at high glucose concentration (16 mM) BKO islets showed markedly increased insulin secretion compared to the control islets **(Figure 2.3*A*)**, indicating that G3PP activity is more relevant in the control of GSIS under hyperglycemic conditions. Similar results were obtained in the presence of FFA **(Figure 2.3*B*)**. KCl-induced insulin secretion showed no statistically significant difference in the BKO islets **(Figure 2.3*C*)**. G3PP deletion in β-cells had no effect on insulin content **(Figure 2.3*D*)**, but markedly lowered glucose-dependent glycerol release **(Figure 2.3*E*)**.

Considering that G3PP, by controlling the availability of Gro3P for mitochondrial electron shuttle, can regulate mitochondrial respiration, we investigated mitochondrial respiration in the BKO islets. Our results showed that in the BKO islets, both oxygen consumption and ATP production were elevated at high glucose concentration but unchanged at low glucose, without affecting H^+ leak **(Figure 2.3*F*-*H*)**. The above results indicated that G3PP deletion in β-cells enhances mitochondrial oxidative phosphorylation and GSIS only at high glucose concentration and not at low or physiological basal concentrations.

Metabolite profiling in G3PP-BKO islets exposed to varying glucose concentrations

To gain insight into the mechanism by which G3PP deletion altered β-cells function, we conducted targeted metabolomics to measure metabolites related to glycolysis, Krebs cycles and additional pathways in BKO and control islets exposed to low, intermediate and high glucose, and correlated the data to GSIS **(Figure 2.4*A*)**. Results showed that the levels of G3PP substrate Gro3P as well as its precursor dihydroxyacetone phosphate (DHAP) increased with increasing glucose concentration in both BKO and control islets and were markedly higher in the BKO only at high glucose concentration **(Figure 2.4*B* and *C*)**. This increase in Gro3P and DHAP levels positively correlated with GSIS in both BKO and MCre islets **(Figure 2.4*A*)**. On the other hand, neither G3PP deletion in β-cells nor glucose concentration had any effect on the islet levels of another known substrate for G3PP, 2-phosphoglycolate (2-PG), which was very low **(Figure 2.4*D*)**.

Lactate, an indicator of glycolytic flux, increased with increasing glucose concentration and was higher in BKO islets at 16 mM glucose, compared to the control islets **(Figure 2.4*E*)**. Similarly, ATP level, an important MCF for insulin secretion, was higher in the BKO islets at 16 mM glucose in association with a small rise in the ATP/ADP ratio **(Figure 2.4*F*-*H*)**. BKO islets showed elevated acetyl-CoA levels compared to MCre islets at all glucose concentrations **(Figure 2.4*I*)**, whereas malonyl-CoA, an important MCF (Prentki, Joly et al. 2002) was found to be higher in BKO islets at 16 mM glucose **(Figure 2.4*J*)**. Interestingly, malonyl-CoA levels also correlated with GSIS results **(Figure 2.4*A*)**, and implicated the elevated malonyl-CoA, together with ATP, as plausible MCF and the associated pathways as responsible for the elevated GSIS in the BKO islets. Among the Krebs cycle intermediates measured, only malate showed an increase in the BKO islets at 16 mM glucose, whereas no major changes were noticed in the levels of isocitrate/citrate and succinate compared to the control islets **(Figure 2.4*K*-*M*)**. There were no differences in AMP,

adenosine, GMP, NADH, NAD, NADPH, NADP, GSH, GSSG, fumarate and arginine **(Supplemental Figure S2.3)** and in NADH/NAD, NADPH/NADP, GSH/GSSH, cAMP and amino acid levels **(Figure 2.4*N-U*)** between the groups. These results showed that G3PP deletion led to increased glycolytic flux in the β-cell, accompanied by elevated acetyl-CoA and malonyl-CoA production and mitochondrial ATP formation, which are known to act as MCF and contribute to enhanced GSIS.

G3PP-BKO islets are more susceptible to chronic glucotoxicity

All the above *in-vivo* and *ex-vivo* metabolic measurements in the BKO mice and islets revealed that G3PP activity is more relevant in the β-cell at high glucose concentration. Therefore, we examined if G3PP activity impacts the toxic effect of chronic exposure of islets to high glucose levels (glucotoxicity). After incubation of BKO and MCre islets for 7 days at 11 mM glucose (close to fed glucose concentration in mice) and 30 mM glucose (glucotoxicity condition), the BKO islets exposed to 30 mM glucose looked more transparent compared to the control islets **(Supplementary Figure S2.4*A*)**. The BKO islets exposed to high glucose showed a significant decrease in insulin content after 7 days incubation **(Figure 2.5*A*)**. Furthermore, BKO islets showed a marked increase in apoptosis in comparison to control islets after 7 days exposure to glucotoxic conditions **(Figure 2.5*B*)**. In order to better understand the mechanisms underlying the changes in BKO islets, we measured the expression of different genes related to insulin, β-cell identity and ER stress. The results revealed that the BKO islets showed a significant decrease in the expression levels of *Ins-2* and *Pdx-1* under glucotoxic conditions compared to control islets **(Figure 2.5*C* and *D*)**. Expression of *Mafa* showed a more pronounced decrease close to significance ($p = 0.056$) than *Ins-2* and *Pdx-1* in the BKO islets **(Figure 2.5*E*)**. There were no differences in these genes, insulin content or apoptosis in WT versus fl/fl mice **(Supplemental Figure 2.4*B* and *C*)**. In addition, genes related to glucotoxicity (*Txnip*) and ER stress (*Bip*) showed significantly increased expression under glucotoxicity conditions **(Figure 2.5*G* and *H*; Supplementary Figure S2.5*F* and *G*)** but no difference between groups.

2.5 Discussion

Glucose is the primary nutrient for β-cell stimulation and its metabolism via glycolysis plays a critical role in the regulation of insulin secretion, in part through the production of Gro3P, a

metabolite that links glycolysis to GL/FFA cycling, the Gro3P shuttle and direct glycerol release by G3PP (Prentki and Madiraju 2008, Prentki and Madiraju 2012, Prentki, Matschinsky et al. 2013, Possik, Madiraju et al. 2017). However, chronic exposure to excess glucose is toxic to β-cell function (Prentki, Peyot et al. 2020), and our earlier *in vitro* studies largely done in the tumoral β-cell line INS1-832/13 suggested that G3PP in b-cells helps in the elimination of excess glucose carbons in the form of glycerol (Mugabo, Zhao et al. 2016). However, we do not know the glucose concentration range in which the flux from glucose to glycerol via G3PP and Gro3P hydrolysis is most active, independently of lipolysis. The question is important as G3PP shunts glucose carbons from glycolysis into glycerol that escapes the β-cell, due to low glycerol kinase activity in these cells (Prentki and Madiraju 2008, Xue, Chen et al. 2017). This is an ideal detoxification pathway of excess glucose because glucose carbons leave the cell early-on in their metabolism following glucose entry and its trapping in the form of glucose-6-phosphate by glucokinase, and also because glycerol is a neutral polar molecule that can reach high levels without toxicity (Gaudet, Arsenault et al. 2000). We propose to name this pathway the *"glycerol shunt",* a new name for a pathway of intermediary metabolism in mammalians whatever is the cell type. It may be highly relevant for cardiometabolic disorders and healthy aging at large as we recently demonstrated, using the nematode *C. elegans,* that G3PP plays key role in the defense against various stresses, including glucotoxicity (Possik, Schmitt et al. 2022). In *C. elegans* a mild enhancement in G3PP activity mimics the beneficial effects of calorie restriction, without affecting food intake and fertility (Possik, Schmitt et al. 2022). Moreover, a recent human genetic study identified *PGP*/G3PP genetic variants to be associated with longevity in centenarians, together with variants in another gene closely related to glucose metabolism, *FN3KRP* coding for fructosamine-3-kinase related protein (Torres, Nygaard et al. 2021). We now provide *in vivo* and *ex vivo* evidence indicating that G3PP controls glucose metabolism, insulin secretion and glucotoxicity in normal β-cells, using an inducible β-cell specific G3PP-KO mouse model.

The loss of G3PP activity in the β-cells in adult mice leads to mild hyperinsulinemia, even when the mice are fed chow diet and their fed glycemia is comparable to control groups (WT, MCre and fl/fl). This sustained elevated plasma insulin levels in the BKO mice can explain the increased anabolism and energy storage, particularly in the fat, and also the elevated body weight gain, which are not due to altered food intake. The reduced plasma TG levels and increased TG content in visceral fat and skeletal muscle in the BKO mice also suggest that fat is sequestered in

peripheral tissues due to the enhanced plasma insulin levels. Thus, insulin activates lipoprotein lipase and promotes fat esterification and inhibits adipose lipolysis, particularly during fasting period (Czech, Tencerova et al. 2013). The possibility that the mild glucose intolerance in the BKO mice is due to the increased TG storage in fat and muscle tissues needs to be ascertained. Overall these results suggest that compromised activity of G3PP in β-cells can lead to hyperinsulinemia-driven obesity.

We further verified that the *in vivo* elevated insulinemia in BKO mice is due to intrinsic β-cell effect. Thus, *ex vivo* insulin secretion in isolated islets from the BKO mice at three glucose concentrations corresponding to hypoglycemia, normoglycemia and hyperglycemia, 3, 8, and 16 mM respectively, is significantly elevated only at the highest concentration of glucose. At 8 mM glucose a trend towards higher secretion *ex vivo* was noted both in the absence and presence of exogenous fatty acids but it did not reach statistical significance. This increase in secretion at high glucose was associated with a marked decline in glycerol production and increase in cellular levels of Gro3P, which is the starting substrate for GL/FFA cycle. Thus, the increased availability of Gro3P in BKO islets is expected to augment the flux through the GL/FFA cycle, particularly through its lipogenic segment, leading to the production of lipid MCF (e.g., diacylglycerol and monoacylglycerol) necessary for the lipid amplification of GSIS (Prentki and Madiraju 2012), thereby contributing to the enhanced insulin secretion in BKO islets and hyperinsulinemia in BKO mice. Moreover, the high glucose concentration dependency for the elevated insulin secretion is not masked by the presence of FFA, suggesting that Gro3P accumulation is the driving force for the enhanced GSIS in BKO islets, likely through the GL/FFA cycle. The present findings emphasize that G3PP deletion in β-cells has no significant impact at low and intermediate/physiological glucose concentration (3 and 8 mM) on GSIS and on the glycolytic and Krebs cycle metabolites, compared to the control islets. Only at high, 16 mM glucose there is a significant increase in Gro3P and DHAP levels in BKO islets. It is likely that at intermediate glucose concentration, β-cells use Gro3P effectively for the Gro3P shuttle, lipogenesis and lower-glycolysis, without much build-up of this substrate. Furthermore, deletion of G3PP also led to elevated glycolysis in the islets, specifically at high glucose concentration, probably due to increased diversion of Gro3P towards lower glycolysis and lactate production. G3PP deficient islets displayed increased levels of some Krebs cycle intermediates and mitochondrial respiration only at high glucose concentration, as evidenced by elevated O_2 consumption and ATP production,

likely because of augmented pyruvate production and Gro3P shuttle mediated electron supply to mitochondrial electron transport chain, coupled with oxidative phosphorylation. Thus, it is relevant to note that the NADH/NAD levels in BKO islets are lower at 16 mM glucose, without any change in NADH levels, suggesting an efficient transfer of reducing equivalents from cytosol to mitochondria via the Gro3P shuttle. The increased ATP availability also can explain, in part, enhanced GSIS in the BKO islets through the closure of K_{ATP} channels (Prentki, Matschinsky et al. 2013).

In addition, the augmented GSIS in BKO islets can also be due to the accelerated acetyl-CoA carboxylase (ACC)/malonyl-CoA (Mal-CoA)/ carnitine palmitoyltransferase 1 (CPT-1) signaling network (Saggerson 2008, Prentki, Matschinsky et al. 2013, Prentki, Corkey et al. 2020) as there is a marked increase in the levels of acetyl-CoA, the substrate for ACC, and malonyl-CoA, produced by ACC, under high glucose levels in the BKO islets. Overall, the results provide a mechanism as to how deletion of G3PP in β-cells results in enhanced insulin secretion. Thus, G3PP deletion activates multiple pathways known to mediate GSIS, including ATP production, the GL/FFA cycle and ACC/malonyl-CoA/CPT-1 network to achieve augmented insulin secretion at high glucose concentrations and these effects are related to the elevated Gro3P levels and reduced activity of the glycerol shunt (Figure 6).

The results also emphasized that Gro3P is the more plausible physiological substrate for G3PP in the β-cell as 2-PG levels, the other suggested G3PP substrate, were found to be very low and did not change in control and BKO islets at all tested glucose concentrations (Possik, Madiraju et al. 2017, Possik, Al-Mass et al. 2021). Earlier *in vitro* studies in cancer cell lines suggested that G3PP/PGP may act as a 'metabolite repair enzyme' by eliminating toxic by-products of glycolysis, 4-phosphoerythronate and 2-phospho-L-lactate (Collard, Baldin et al. 2016). However, we did not notice any toxicity of G3PP-deleted β-cells at physiological glucose concentration, both *in vivo* and *ex vivo*. Instead, these β-cells displayed more efficient metabolic activation and insulin secretion, showing indirectly that under normal conditions, the above toxic metabolites do not accumulate or cause toxicity in the BKO β-cells (Possik, Madiraju et al. 2017, Possik, Al-Mass et al. 2021).

As the studies above indicated that lack of G3PP in β-cells impacts metabolism and insulin secretion only at elevated glucose concentrations, we found it to be of importance to determine if

this enzyme plays a role in preventing β-cell glucotoxicity and nutri-stress (Prentki, Peyot et al. 2020), a term encompassing the toxic actions of all nutrients in excess: carbohydrates, lipids and proteins, reflected by elevated blood levels of glucose, TG and FFA as well as some amino acids. Chronic exposure of isolated BKO islets to 30 mM glucose increased apoptosis compared to MCre islets and reduced insulin content and the expression of *Ins2*, *Pdx1* and *Mafa* that are crucial for β-cell function (Ye, Tai et al. 2006, Poitout, Amyot et al. 2010, Prentki, Peyot et al. 2020). Reduced expression of these genes is known to induce dedifferentiation, a feature of β-cells dysfunction (Poitout, Amyot et al. 2010, Prentki, Peyot et al. 2020). In addition, it appears that the elevated apoptosis in the BKO mouse islet β-cells rendered the islets more transparent, probably due to the degradation of intracellular structures, as known to occur in the lens fiber cells during development (Wride 2000). These findings are in accordance with the view that G3PP in the β-cell plays a role in glucodetoxification, maintaining the differentiated state and the expression of the insulin gene, *Ins2*. Additional exhaustive studies in animal models of diabetes with β-cell specific KO or graded overexpression of G3PP and with G3PP activators are needed to establish the role of the glycerol shunt as a pathway to be harnessed to prevent β-cell glucotoxicity and perhaps prevent or reverse type 2 diabetes. Whether β-cell specific deletion of G3PP exerts effects on other islet cells and thereby influences the secretion of glucagon and other peptides also needs to be examined in future studies.

In conclusion, the data demonstrate that the *PGP* gene product encodes for a protein that shows Gro3P phosphatase activity and that deletion of this gene specifically in pancreatic β-cells impacts glucose metabolism, β-cell function and GSIS, only at high glucose concentration (Figure 6). The present *in vivo* and *ex vivo* studies confirm our earlier conclusions based on in vitro studies using rat islets and INS cell line (Mugabo, Zhao et al. 2016). The data identify a novel metabolic pathway, the *glycerol shunt*, implicated in glucodetoxification and fuel partitioning via the metabolic fate of Gro3P and DHAP. We propose that in β-cells G3PP operated glycerol shunt expels excessive glucose carbons as glycerol to prevent more than necessary secretion of insulin that could cause obesity and possibly hypoglycemia, as well as β-cell dysfunction and death under chronic hyperglycemic conditions. The findings are potentially of general interest as we know very little about fuel excess detoxification pathways at large, whatever is the cell type, and because of

the recently emerging view that G3PP is implicated in healthy aging (Torres, Nygaard et al. 2021, Possik, Schmitt et al. 2022).

Author contributions

AAM, MLP, SRMM, and MP designed research; AAM, PP, MLP, RL, EL, JG and YM conducted experiments; AAM, MLP, SRMM, and MP analyzed data; PP, MLP, EP, RS, RA and FAM reviewed and edited the manuscript and AAM, SRMM and MP wrote the paper.

Acknowledgments

This study was supported by funds from Canadian Institutes of Health Research (to M.P. and S.R.M.M.), and from Dasman Diabetes Research Institute/ Montreal Medical International (to M.P, MSRM, RA and FA-M). M.P. was recipient up to 2019 of a Canada Research Chair in Diabetes and Metabolism. AA-M is supported by a scholarship from Kuwait University. PP was recipient of postdoctoral fellowships from the Fondation Valifonds, the Montreal Diabetes Research Center, the CRCHUM and Mitacs. We thank the core facilities for Cellular Physiology, Metabolomics and Rodent Phenotyping of the CRCHUM/Montreal Diabetes Research Center. We thank Jennifer Estall (University of Montreal, Canada), Erik Joly (CRCHUM) and Julien Lamontagne (CRCHUM) for helpful advice and discussion. We also thank Isabelle Chénier and Heidi Erb for technical assistance with animal experiments. Figure 6 was created with BioRender.com.

Conflict of interest

The authors have declared that no conflict of interest exists.

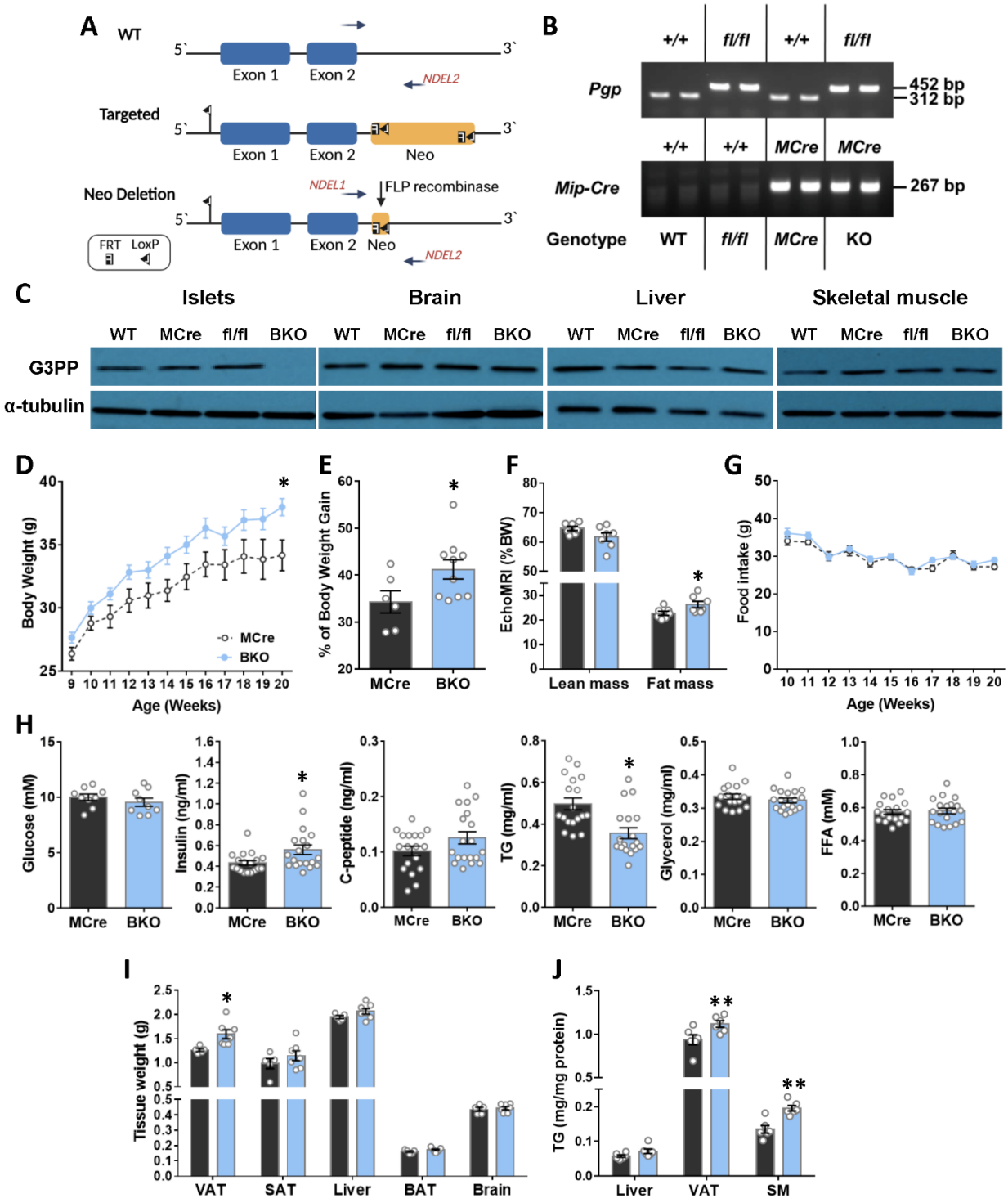
A
WT
5`
3`
Exon 1
Exon 2
NDEL2
Targeted
Neo
Neo Deletion
NDEL1
FLP recombinase
FRT
LoxP
B
+/+
fl/fl
MCre
Pgp
452 bp
312 bp
Mip-Cre
267 bp
Genotype
WT
KO
C
Islets
Brain
Liver
Skeletal muscle
G3PP
α-tubulin
D
Body Weight (g)
Age (Weeks)
MCre
BKO
E
% of Body Weight Gain
F
EchoMRI (%BW)
Lean mass
Fat mass
G
Food intake (g)
H
Glucose (mM)
Insulin (ng/ml)
C-peptide (ng/ml)
TG (mg/ml)
Glycerol (mg/ml)
FFA (mM)
I
Tissue weight (g)
VAT
SAT
Liver
BAT
Brain
J
TG (mg/mg protein)
SM

Figure 2.1. Increased body weight gain, fat mass and fed insulinemia with reduction in fed plasma TG in male BKO mice.

(A) Schematic representation of gene targeting strategy for the generation of the G3PP-lox conditional allele. Wild-type, targeted and G3PP-lox alleles are represented. The loxP recombination sites inserted at the 5' side of exon 1 and 3' side of exon 2 in PGP gene, the FRP-flanked Neo-cassette FRP sites, and the NDEL1/NDEL2 primers for PCR genotyping are indicated. The breeding of mice to produce BKO mice is described in Methods. **(B)** The presence of the WT, Mip-Cre transgene or the floxed PGP alleles was evaluated in DNA from ear punch tissue fragments using the primers described in Methods. A specific amplification of a 452 bp DNA fragment corresponds to the floxed- PGP allele, a 312 bp fragment corresponds to the WT PGP allele and the presence of a 267 bp DNA fragment corresponds to the Mip-Cre transgene, as verified by genomic PCR. **(C)** G3PP deletion was validated using protein extracts from islets, brain, liver and skeletal muscle (SM) from mice, 4 weeks after deletion and used for western blot (WT, n=4; fl/fl, n=3; MCre, n=3; BKO, n=3). For all tissues α-tubulin was used as a housekeeping protein. Mice were kept on chow diet for 12 weeks after G3PP deletion following TMX treatment. **(D)** Body weight (Mcre, n=6; BKO, n=10). **(E)** Percentage of body weight gain (MCre, n=6; BKO, n=10). **(F)** Lean and fat mass expressed as percentage of BW (MCre, n=7; BKO, n=7 (one BKO mouse out of 8, died during experiment)). **(G)** Food intake (MCre, n=6; BKO, n=10). **(H)** Plasma parameters in fed state (For glycemia: MCre, n= 9 and BKO=9; for insulin, C-peptide, TG, glycerol and FFA, MCre, n=18; BKO, n=19). **(I)** Weights of visceral adipose tissue (VAT), subcutaneous adipose tissue (SAT), liver, brown adipose tissue (BAT) and brain (MCre, n=6; BKO, n=7). **(J)** TG content for liver, VAT and skeletal muscle (SM) (MCre, n=6; BKO, n=7). Data are mean ± SEM. $*p < 0.05$, $**p < 0.01$ vs MCre (Two-way ANOVA (Panel D and G) and Student's t test (Panel E, F, H, I and J)).

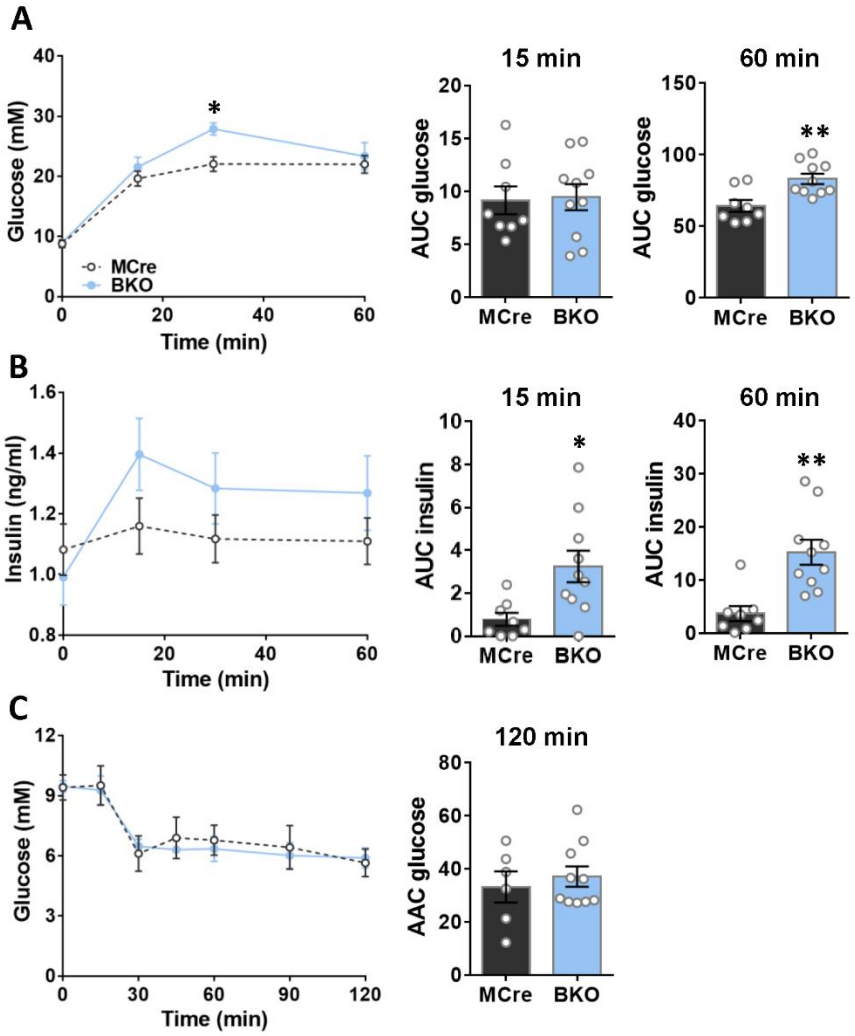

Figure 2.2. Increased *in vivo* glucose induced insulin secretion with mild glucose intolerance and normal insulin sensitivity in BKO mice.

(A) Glycemia during IPGTT in male mice, 16 weeks after G3PP deletion (MCre, n=8; BKO, n=10). Inset depicts area under the curve (AUC) for glycemia after 15 min and 60 min. **(B)** Insulinemia during IPGTT in male mice (MCre, n=8; BKO, n=10). Inset depicts AUC for insulinemia after 15 min and 60 min. **(C)** Glycemia during ITT in mice, 19 weeks after G3PP deletion (MCre, n=6; BKO, n=10). Inset depicts area above the curve (AAC) after 120 min. Data are means ± SEM. *$p < 0.05$, **$p < 0.01$ vs MCre (Two-way ANOVA and Student's t test (for AUC and AAC)).

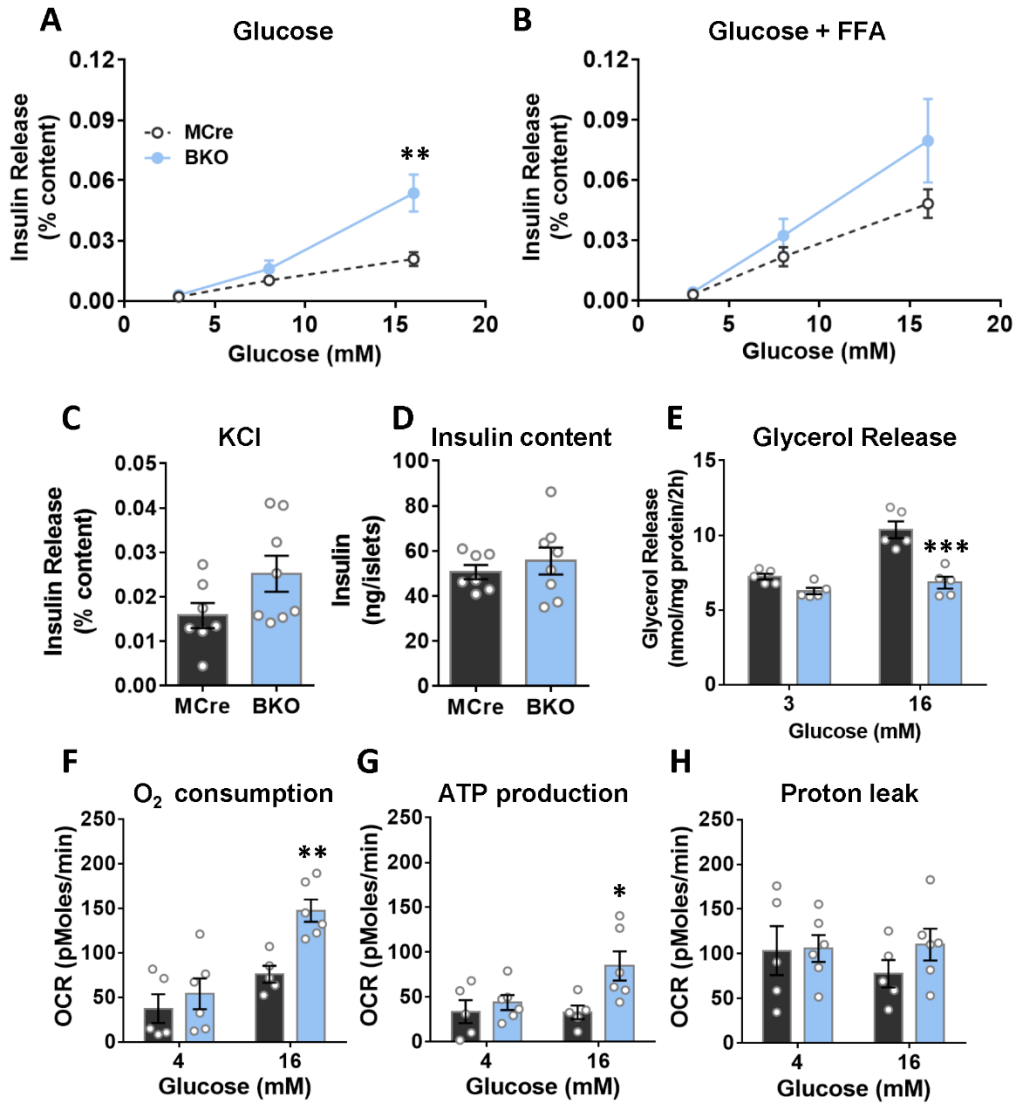

Figure 2.3. Assessment of *ex vivo* glucose induced insulin secretion and metabolic parameters in BKO versus control mouse islets after 12 weeks of G3PP deletion.

(A) Insulin secretion at 3, 8 and 16 mM glucose. **(B)** Insulin secretion as in A, but in the presence of palmitate/oleate (0.125 mM each). **(C)** Insulin secretion at 3 mM glucose plus 35 mM KCl. **(D)** Total insulin content. For A, B, C and D: MCre, n=7; BKO, n=8. **(E)** Glycerol release (MCre, n=5; BKO, n=5). **(F)** Oxygen consumption. **(G)** ATP production. **(H)** H^+ leak (MCre, n=5; BKO, n=6). *p < 0.05, **p < 0.01, and ***P < 0.001 vs. MCre (Two-way ANOVA (Panel A and B) and Student's t test (Panel C-H)).

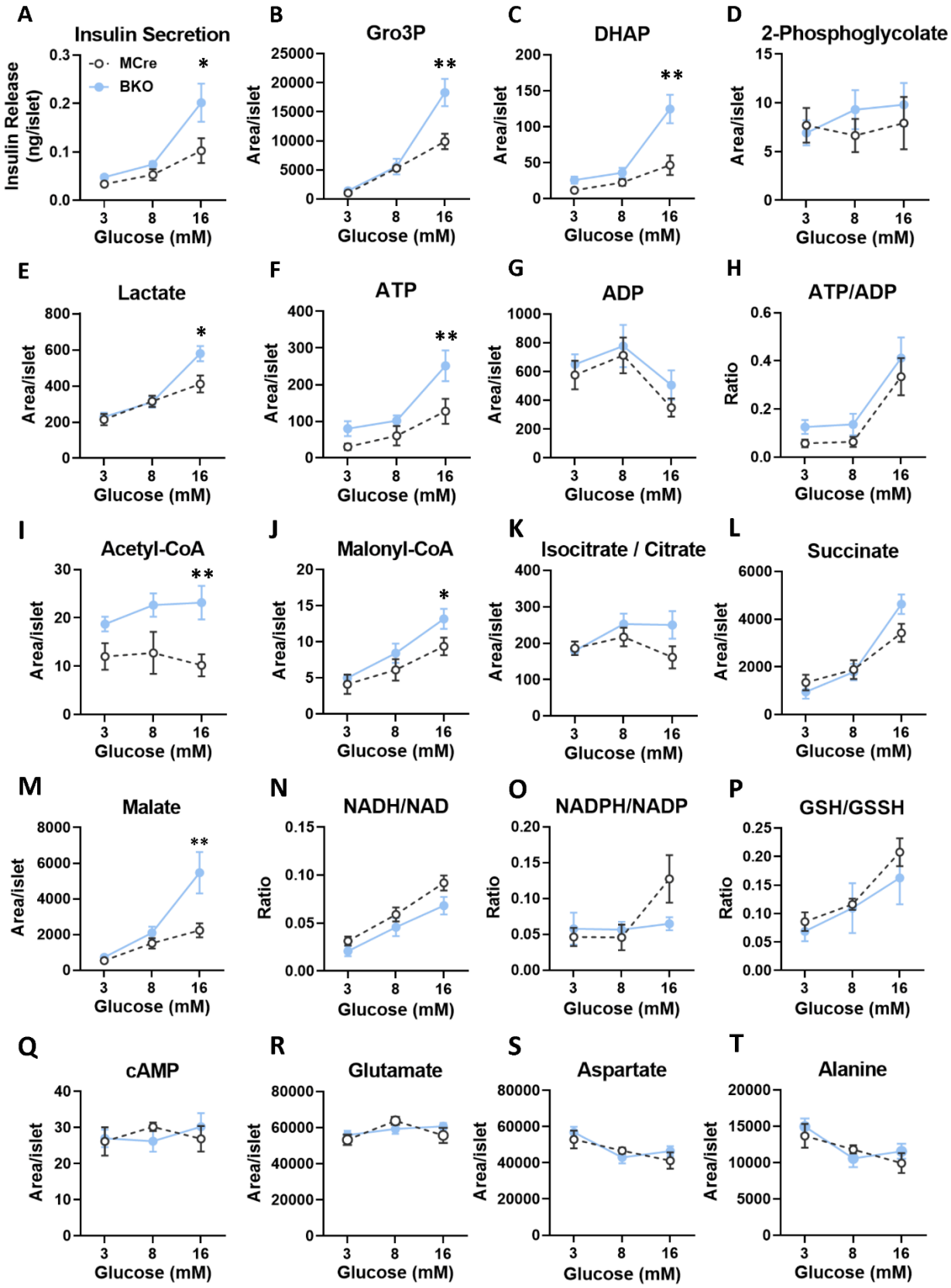
A
Insulin Secretion
MCre
BKO
Insulin Release (ng/islet)
Glucose (mM)
B
Gro3P
Area/islet
C
DHAP
D
2-Phosphoglycolate
E
Lactate
F
ATP
G
ADP
H
ATP/ADP
Ratio
I
Acetyl-CoA
J
Malonyl-CoA
K
Isocitrate / Citrate
L
Succinate
M
Malate
N
NADH/NAD
O
NADPH/NADP
P
GSH/GSSH
Q
cAMP
R
Glutamate
S
Aspartate
T
Alanine

Figure 2.4. Targeted metabolomics analyses in BKO and control islets, 12 weeks after G3PP deletion.

(A) Insulin secretion at 3, 8 and 16 mM glucose after 1h incubation for the metabolomics experiments. At the end of incubation, metabolites were extracted and analyzed by LC-MS/MS. **(B)** Gro3P. **(C)** Dihydroxyacetone-phosphate (DHAP). **(D)** 2-Phosphoglycolate. **(E)** Lactate. **(F)** ATP. **(G)** ADP. **(H)** ATP/ADP. **(I)** Acetyl-CoA. **(J)** Malonyl-CoA. **(K)** Isocitrate /citrate. **(L)** Succinate. **(M)** Malate. **(N)** NADH/NAD. **(O)** NADPH/NADP. **(P)** GSH/GSSH. **(Q)** cAMP. **(R)** Glutamate. **(S)** Aspartate. **(T)** Alanine. Islets from 3 mice were pooled for one measurement and there were 5 such measurements for MCre and BKO, separately. A total of 15 mice were used in each group. Means ± SEM (n= 5 for each group). **p* < 0.05 and ***p* < 0.01 vs. MCre (Two-way ANOVA).

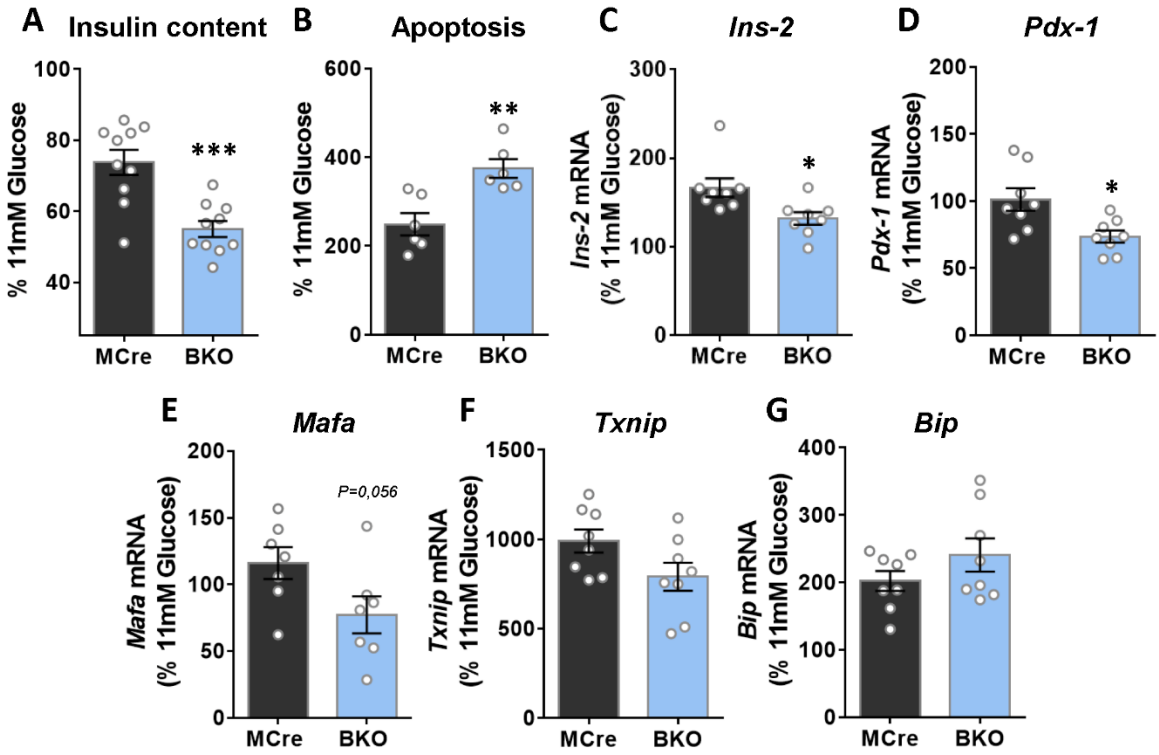

Figure 2.5. Assessment of chronic glucotoxicity in BKO and control islets.

Islets incubated at 11 and 30 mM glucose for 7 days (Islets from 2 mice were pooled for one measurement). After the 7-days incubation, islets were collected to measure: **(A)** insulin content (MCre, n=10 from 20 mice; BKO, n=10 from 20 mice), **(B)** apoptosis (MCre, n=6 from 12 mice; BKO, n=6 from 12 mice) and (C-G) gene expression (mRNA) by rt-PCR (MCre, n=8 from 16 mice; BKO, n=8 from 16 mice). **(C)** *Ins-2*, **(D)**, *Pdx-1* **(E)** *Mafa*, **(F)** *Txnip* and **(G)** *Bip*. Data are presented as % of 11mM glucose from the data shown in Figure S2.5. Means ± SEM. *$p < 0.05$, **$p < 0.01$, and ***$p < 0.001$ vs. MCre (Student's *t* test).

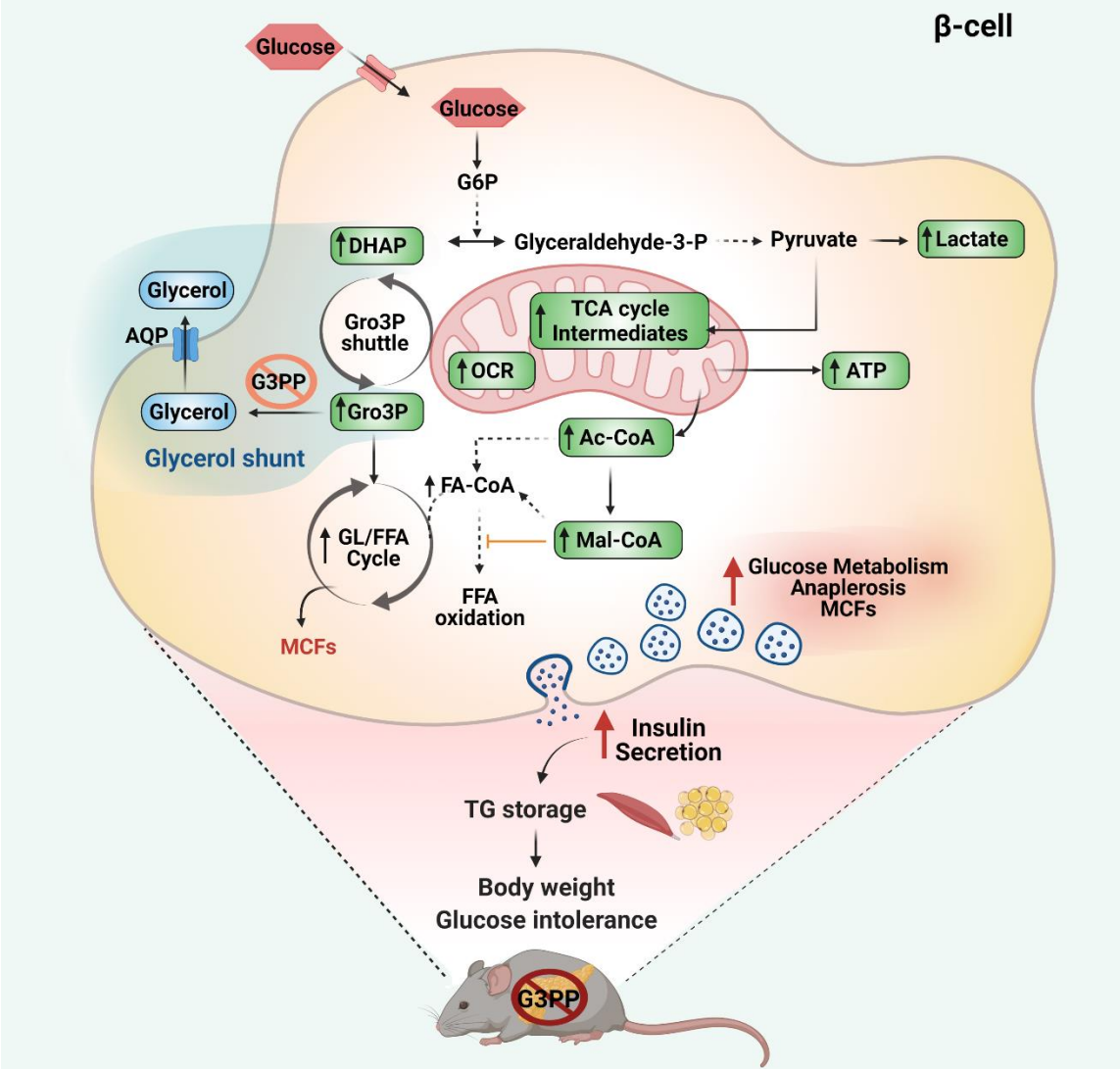

Figure 2.6. Model depicting the effect of G3PP β-cell specific deletion on energy homeostasis and body weight via increasing insulin secretion under high glucose concentration.

The abbreviations are: Ac-CoA, acetyl-CoA; AQP, aquaporin channel; ATP, adenosine triphosphate; DHAP, dihydroxyacetone phosphate; FA-CoA, fatty acyl-CoA; FFA, free fatty acid; G3PP, glycerol 3-phosphate phosphatase; G6P, glucose 6-phosphate; GL/FFA cycle, glycerolipid/ free fatty acid cycle; Glyceraldehyde-3-P, glyceraldehyde-3-phosphate; Gro3P, glycerol 3-phosphate; Mal-CoA, malonyl-CoA; MCF, metabolic coupling factor; OCR, oxygen consumption rate; TCA cycle, tricarboxylic acid cycle; TG, triglyceride.

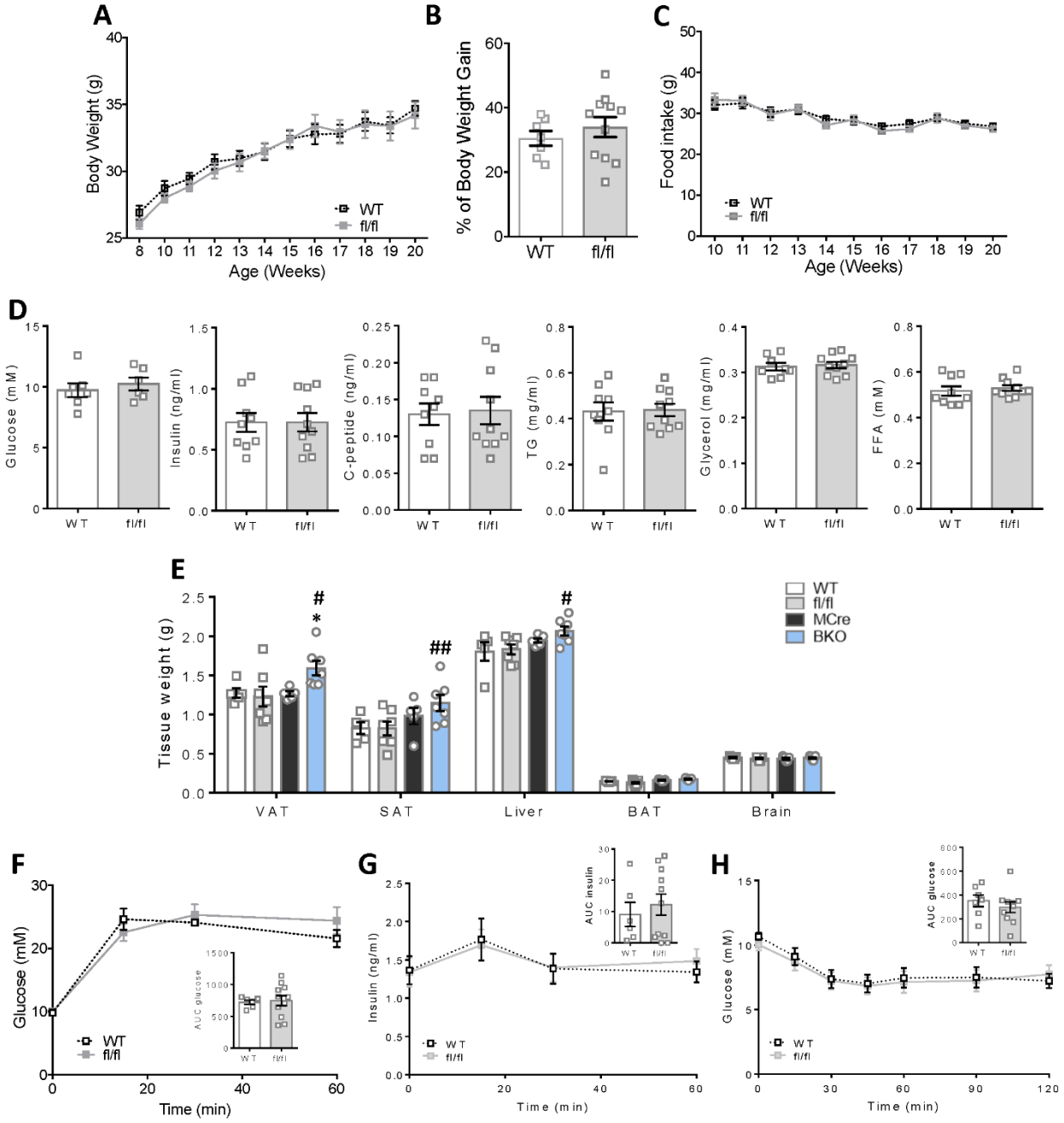
A
Body Weight (g)
Age (Weeks)
WT
fl/fl
B
% of Body Weight Gain
C
Food intake (g)
Age (Weeks)
D
Glucose (mM)
Insulin (ng/ml)
C-peptide (ng/ml)
TG (mg/ml)
Glycerol (mg/ml)
FFA (mM)
E
Tissue weight (g)
WT
fl/fl
MCre
BKO
VAT
SAT
Liver
BAT
Brain
F
Glucose (mM)
Time (min)
AUC glucose
G
Insulin (ng/ml)
Time (min)
AUC insulin
H
Glucose (mM)
Time (min)
AUC glucose

Figure S2.1. *In vivo* parameters of WT and G3PP-fl/fl mice.

(A) Body weight. **(B)** Percentage of body weight gain. **(C)** Food intake (For A, B and C: WT, n=7; fl/fl, n=11). **(D)** Plasma parameters in fed mice (For glycemia: WT, n=9; fl/fl, n=6; for insulin, C-peptide, TG, glycerol and FFA: WT, n=9; fl/fl, n=10). **(E)** Tissue weights of VAT, SAT, liver, BAT and brain (WT, n=5; fl/fl, n=7; MCre, n=6; BKO, n=7). **(F)** Glycemia during IPGTT (WT, n=6; fl/fl, n=11); inset depicts area under the curve (AUC) for glycemia after 120 min. **(G)** Insulinemia during IPGTT (WT, n=6; fl/fl, n=11); inset depicts AUC for insulinemia after 120 min. **(H)** Glycemia during ITT (WT, n=7; fl/fl, n=9 out of 11 mice as two mice showing stress were removed). Inset depicts area above the curve (AAC) after 120 min. Means ± SEM. *$P < 0.05$ vs. MCre and #$P < 0.05$ and ##$P < 0.01$ vs. WT and fl/fl (Two-way ANOVA (Panel A, C, F, G and H), Student's *t* test (Panel B and D) and One-way ANOVA (Panel E)).

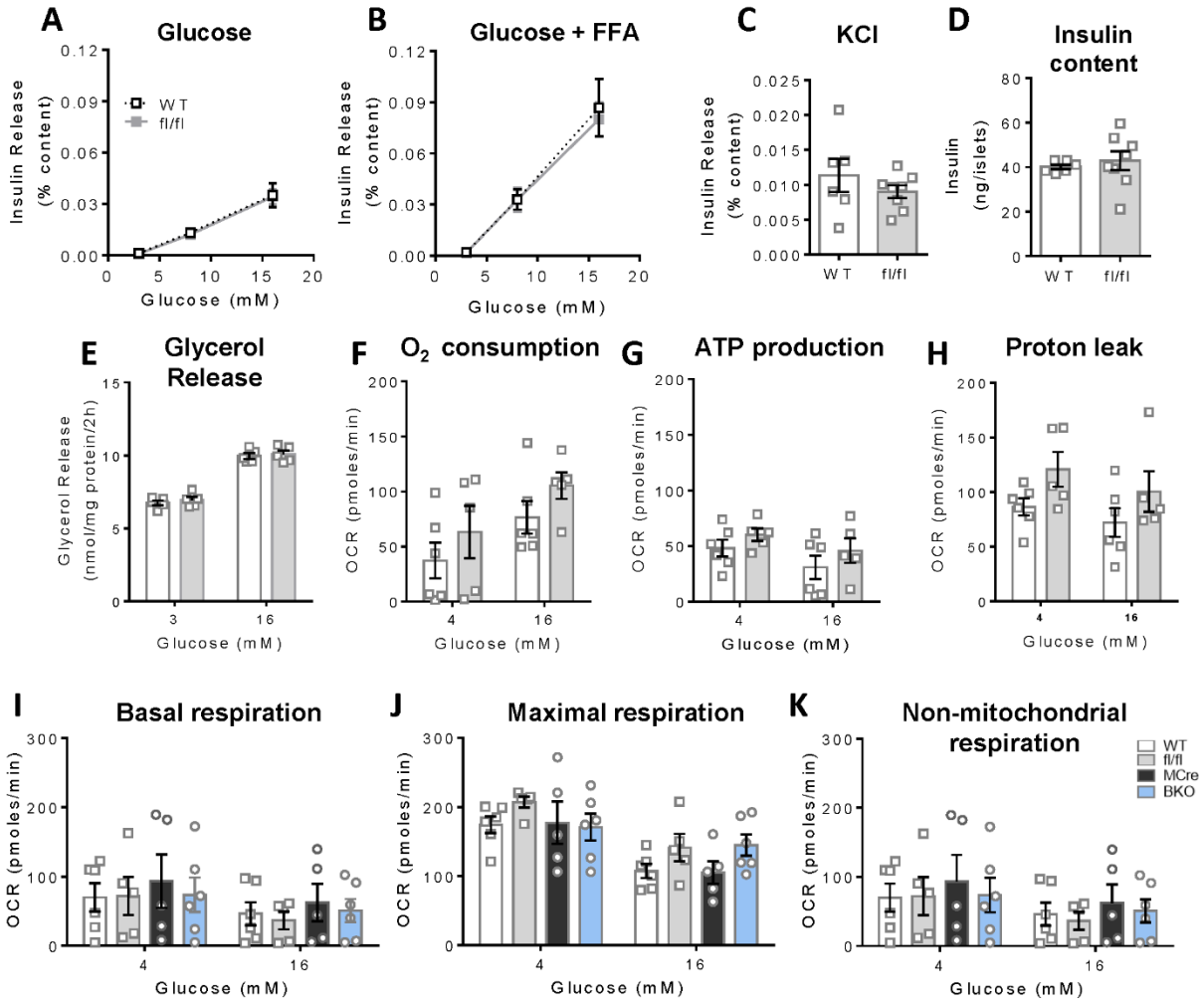

Figure S2.2. *Ex vivo* insulin secretion, glycerol release and O_2 consumption in WT and G3PP-fl/fl mouse islets.

(A) Insulin secretion at 3, 8 and 16 mM glucose. **(B)** Insulin secretion as in A, but with added palmitate/oleate (0.125 mM each). **(C)** Insulin secretion at 3 mM glucose plus 35 mM KCl. **(D)** Total insulin content (For A, B, C and D: WT, n=6; fl/fl, n=8). (E) Glycerol release (WT, n=5; fl/fl, n=5). **(F)** O_2 consumption. **(G)** ATP production. **(H)** H^+ leak (For F, G and H: WT, n=6; fl/fl, n=5). **(I)** Basal respiration. **(J)** Maximal respiration. **(K)** Non-mitochondrial respiration (For I, J and K: WT, n=6; fl/fl, n=5; MCre, n=5; BKO, n=6). Means ± SEM. (Two-way ANOVA (Panel A and B), Student's *t* test (Panel C-H) and One-way ANOVA (Panel I-K)).

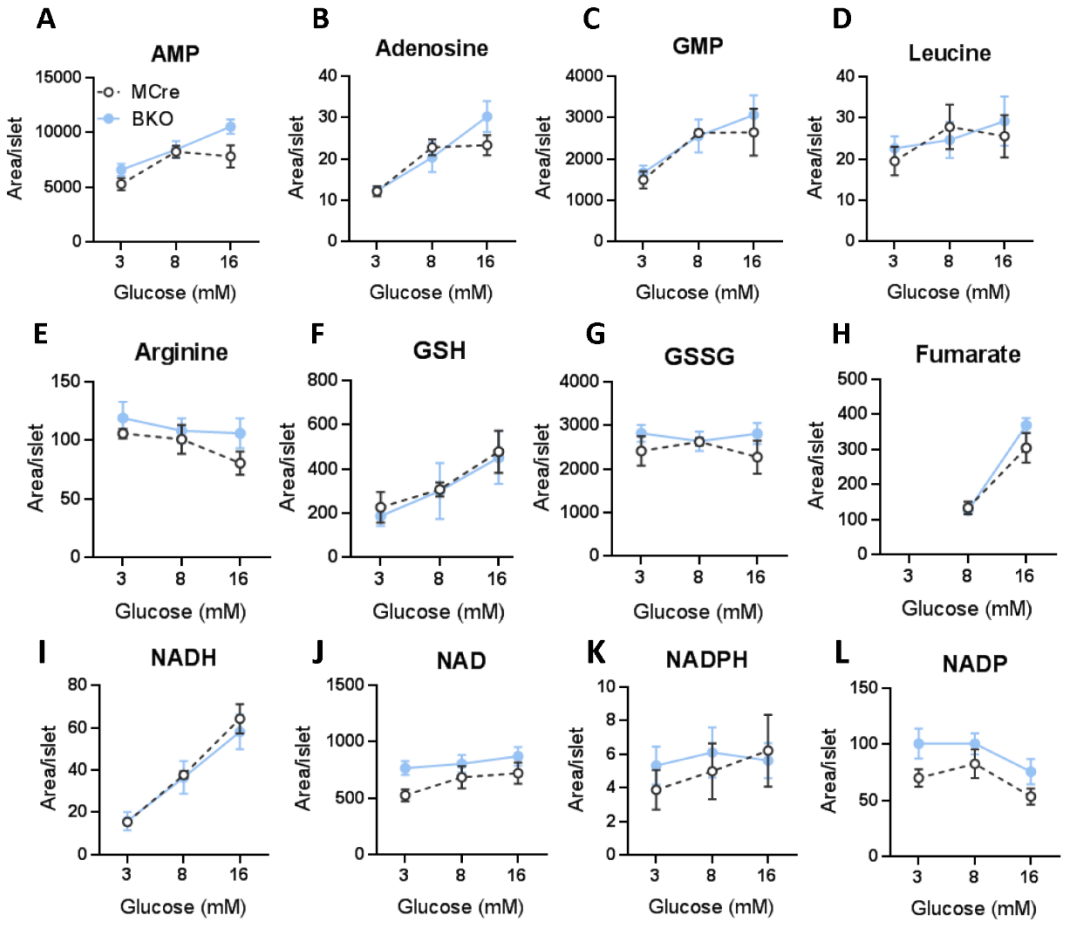

Figure S2.3. Targeted metabolomics determination in islets incubated at various glucose concentrations.

BKO and control mouse islets were exposed to 3, 8 and 16 mM glucose for 1h. Then, metabolites were extracted and analyzed by LC-MS/MS: **(A)** ANP, **(B)** adenosine, **(C)** GMP, **(D)** leucine, **(E)** arginine, **(F)** GSH, **(G)** GSSG, **(H)** fumarate, **(I)** NADH, **(J)** NAD, **(K)** NADPH, **(L)** NADP. Islets from 3 mice were pooled for one measurement and there were 5 such measurements for MCre and BKO, separately. A total of 15 mice were used in each group. Means ± SEM (n= 5 for each group) (Two-way ANOVA).

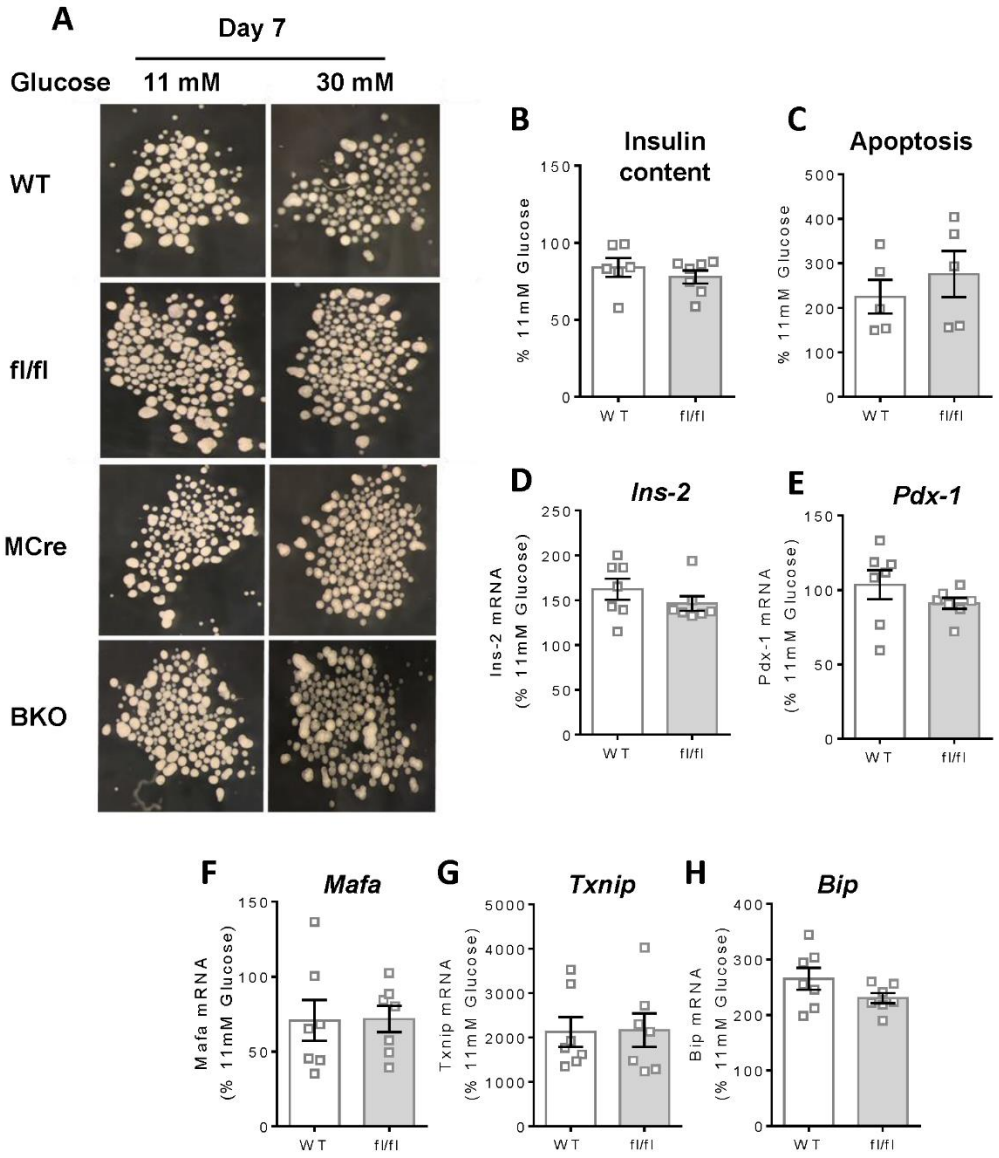

Figure S2.4. Glucotoxicity in WT and G3PP-fl/fl mouse islets.

(A) Representative images of islets incubated at 11 and 30 mM glucose for 7 days. Islets incubated as In A (Islets from 2 mice were pooled for one measurement) were collected to measure: **(B)** insulin content (WT, n=6 from 12 mice; fl/fl, n=7 from 14 mice), **(C)** apoptosis and (D-H) gene expression (WT, n=5 from 10 mice; fl/fl, n=5 from 10 mice) (mRNA) by rt-PCR: **(D)** *Ins-2*, **(E)** *Pdx-1*, **(F)** *Mafa*, **(G)** *Txnip* and **(H)** *Bip*. Data are presented as % of 11mM glucose from the data shown in Figure S2.5; Means ± SEM (Student's *t* test).

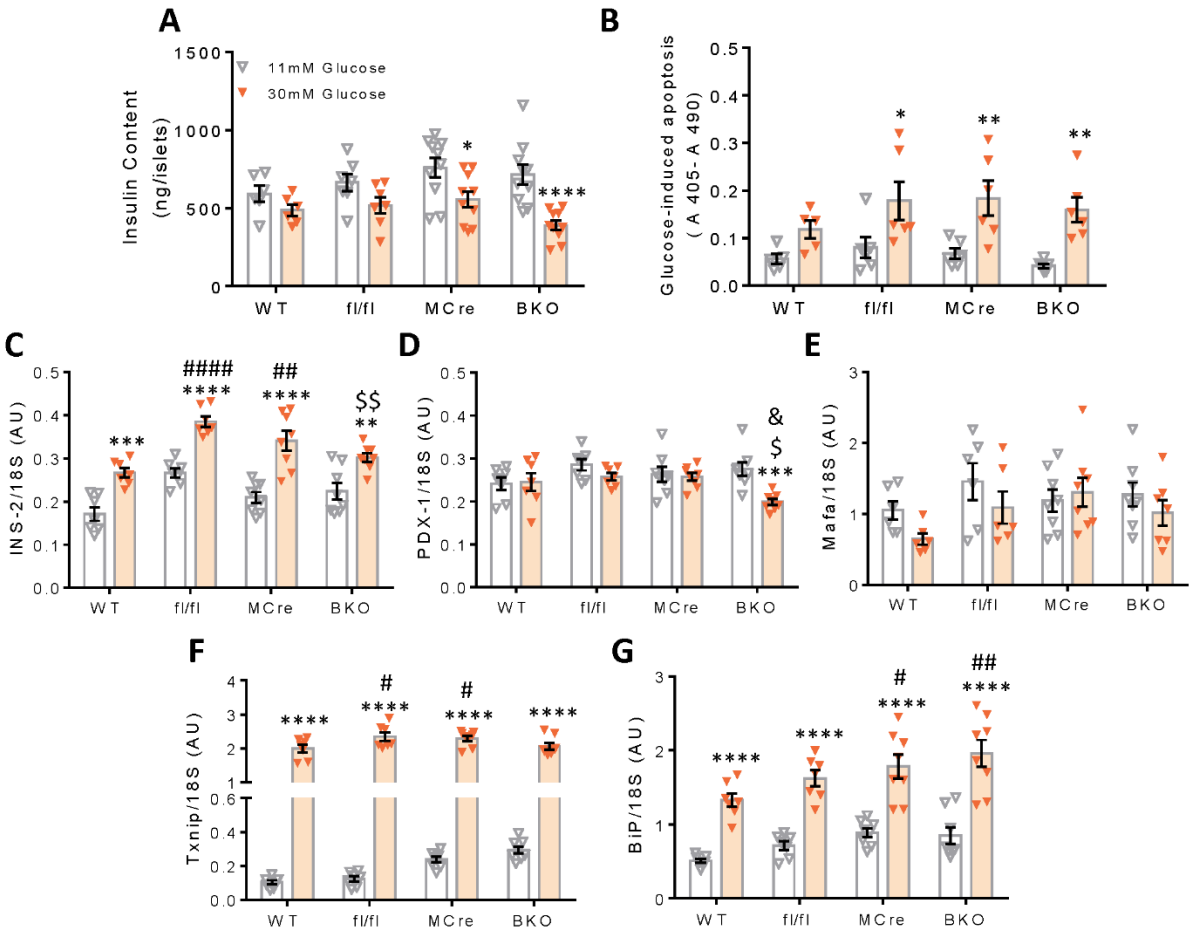

Figure S2.5. Glucotoxicity in BKO islets and control mouse islets.

Islets (Islets from 2 mice were pooled for one measurement) were incubated at 11 and 30 mM glucose for 7 days and were collected to measure: **(A)** Insulin content (WT, n=7; fl/fl, n=7; MCre, n=8; BKO, n=8). **(B)** Apoptosis (WT, n=6; fl/fl, n=7; MCre, n=10; BKO, n=10). (C-G) Gene expression (WT, n=5; fl/fl, n=5; MCre, n=6; BKO, n=6), mRNA measured by rt-PCR: **(C)** *Ins-2*, **(D)** *Pdx-1*, **(E)** *Mafa*, **(F)** *Txnip* and **(G)** *Bip*. Means ± SEM. *P < 0.05, **P < 0.01, ***P < 0.001 and ****P < 0.0001 vs. 11mM of the same genotype and #P < 0.05, ##P < 0.01, ###P < 0.001 and ####P < 0.0001 vs. 30mM WT and $P < 0.05 and $$P < 0.01 vs. 30mM fl/fl and &P < 0.05 vs. 30mM MCre (Two-way ANOVA).

Table S2.1. Primer sequences used for RT-PCR.

Gene	Primer sequences (5’-3’)
Ins-2	F:TGGAGGCTCTCTACCTGGTG
	R:TCTACAATGCCACGCTTCTG
Mafa	F:GTGCTGGAGGATCTGTACTGG
	R:ATGGTGGTGATGGTGATGG
Pdx-1	F:GGTATAGCCGGAGAGATGC
	R:CTGGTCCGTATTGGAACG
Bip	F:TGCAGCAGGACATCAAGTTC
	R:TACGCCTCAGCAGTCTCCTT
Txnip	F:CGAGTCAAAGCCGTCAGGAT
	R:TTCATAGCGCAAGTAGTCCAAAGT
18s	F:CTG AGA AAC GGC TAG CAC ATC
	R:GGC CTC GAA AGA GTC CTG TAT

References:

Attane, C., Peyot, M. L., Lussier, R., Poursharifi, P., Zhao, S., Zhang, D., . . . Prentki, M. (2016). A beta cell ATGL-lipolysis/adipose tissue axis controls energy homeostasis and body weight via insulin secretion in mice. *Diabetologia, 59*(12), 2654-2663.

Bergeron, V., Ghislain, J., Vivot, K., Tamarina, N., Philipson, L. H., Fielitz, J., & Poitout, V. (2018). Deletion of protein kinase D1 in pancreatic beta-cells impairs insulin secretion in high-fat diet-fed mice. *Diabetes, 67*(1), 71-77.

Bradley, D. C., & Kaslow, H. R. (1989). Radiometric assays for glycerol, glucose, and glycogen. *Anal Biochem, 180*(1), 11-16.

Collard, F., Baldin, F., Gerin, I., Bolsee, J., Noel, G., Graff, J., . . . Bommer, G. T. (2016). A conserved phosphatase destroys toxic glycolytic side products in mammals and yeast. *Nat Chem Biol, 12*(8), 601-607.

Czech, M. P., Tencerova, M., Pedersen, D. J., & Aouadi, M. (2013). Insulin signalling mechanisms for triacylglycerol storage. *Diabetologia, 56*(5), 949-964.

Gaudet, D., Arsenault, S., Perusse, L., Vohl, M. C., St-Pierre, J., Bergeron, J., . . . Rioux, J. D. (2000). Glycerol as a correlate of impaired glucose tolerance: dissection of a complex system by use of a simple genetic trait. *Am J Hum Genet, 66*(5), 1558-1568.

Li, N., Karaca, M., & Maechler, P. (2017). Upregulation of UCP2 in beta-cells confers partial protection against both oxidative stress and glucotoxicity. *Redox Biol, 13*, 541-549.

Mugabo, Y., Zhao, S., Seifried, A., Gezzar, S., Al-Mass, A., Zhang, D., . . . Prentki, M. (2016). Identification of a mammalian glycerol-3-phosphate phosphatase: role in metabolism and signaling in pancreatic beta-cells and hepatocytes. *Proc Natl Acad Sci U S A, 113*(4), E430-439.

Nolan, C. J., & Prentki, M. (2019). Insulin resistance and insulin hypersecretion in the metabolic syndrome and type 2 diabetes: time for a conceptual framework shift. *Diab Vasc Dis Res, 16*(2), 118-127.

Nye, C. K., Hanson, R. W., & Kalhan, S. C. (2008). Glyceroneogenesis is the dominant pathway for triglyceride glycerol synthesis in vivo in the rat. *J Biol Chem, 283*(41), 27565-27574.

Oropeza, D., Jouvet, N., Budry, L., Campbell, J. E., Bouyakdan, K., Lacombe, J., . . . Estall, J. L. (2015). Phenotypic characterization of MIP-CreERT1Lphi mice with transgene-driven islet expression of human growth hormone. *Diabetes, 64*(11), 3798-3807.

Peyot, M. L., Roubtsova, A., Lussier, R., Chamberland, A., Essalmani, R., Murthy Madiraju, S. R., . . . Prat, A. (2021). Substantial PCSK9 inactivation in beta-cells does not modify glucose homeostasis or insulin secretion in mice. *Biochim Biophys Acta Mol Cell Biol Lipids, 1866*(8), 158968.

Poitout, V., Amyot, J., Semache, M., Zarrouki, B., Hagman, D., & Fontes, G. (2010). Glucolipotoxicity of the pancreatic beta cell. *Biochim Biophys Acta, 1801*(3), 289-298.

Possik, E., Al-Mass, A., Peyot, M. L., Ahmad, R., Al-Mulla, F., Madiraju, S. R. M., & Prentki, M. (2021). New mammalian glycerol-3-phosphate phosphatase: role in beta-cell, liver and adipocyte metabolism. *Front Endocrinol (Lausanne), 12*, 706607.

Possik, E., Madiraju, S. R. M., & Prentki, M. (2017). Glycerol-3-phosphate phosphatase/PGP: role in intermediary metabolism and target for cardiometabolic diseases. *Biochimie, 143*, 18-28.

Possik, E., Schmitt, C., Al-Mass, A., Bai, Y., Côté, L., Morin, J., . . . Prentki, M. (2022). Phosphoglycolate phosphatase homologs act as glycerol-3-phosphate phosphatase to control stress and healthspan in C. elegans. *Nature Communications, 11;13(1):177*.

Poursharifi, P., Attane, C., Mugabo, Y., Al-Mass, A., Ghosh, A., Schmitt, C., . . . Prentki, M. (2020). Adipose ABHD6 regulates tolerance to cold and thermogenic programs. *JCI Insight, 5*(24), e140294.

Poursharifi, P., Madiraju, S. R. M., & Prentki, M. (2017). Monoacylglycerol signalling and ABHD6 in health and disease. *Diabetes Obes Metab, 19 Suppl 1*, 76-89.

Prentki, M., Corkey, B. E., & Madiraju, S. R. M. (2020). Lipid-associated metabolic signalling networks in pancreatic beta cell function. *Diabetologia, 63*(1), 10-20.

Prentki, M., Joly, E., El-Assaad, W., & Roduit, R. (2002). Malonyl-CoA signaling, lipid partitioning, and glucolipotoxicity: role in beta-cell adaptation and failure in the etiology of diabetes. *Diabetes, 51 Suppl 3*, S405-413.

Prentki, M., & Madiraju, S. R. (2008). Glycerolipid metabolism and signaling in health and disease. *Endocr Rev, 29*(6), 647-676.

Prentki, M., & Madiraju, S. R. (2012). Glycerolipid/free fatty acid cycle and islet beta-cell function in health, obesity and diabetes. *Mol Cell Endocrinol, 353*(1-2), 88-100.

Prentki, M., Matschinsky, F. M., & Madiraju, S. R. (2013). Metabolic signaling in fuel-induced insulin secretion. *Cell Metab, 18*(2), 162-185.

Prentki, M., Peyot, M. L., Masiello, P., & Madiraju, S. R. M. (2020). Nutrient-induced metabolic stress, adaptation, detoxification, and toxicity in the pancreatic beta-cell. *Diabetes, 69*(3), 279-290.

Saggerson, D. (2008). Malonyl-CoA, a key signaling molecule in mammalian cells. *Annu Rev Nutr, 28*, 253-272.

Segerer, G., Hadamek, K., Zundler, M., Fekete, A., Seifried, A., Mueller, M. J., . . . Gohla, A. (2016). An essential developmental function for murine phosphoglycolate phosphatase in safeguarding cell proliferation.

Thomas, D. D., Corkey, B. E., Istfan, N. W., & Apovian, C. M. (2019). Hyperinsulinemia: an early indicator of metabolic dysfunction. *J Endocr Soc, 3*(9), 1727-1747.

Torres, G. G., Nygaard, M., Caliebe, A., Blanche, H., Chantalat, S., Galan, P., . . . Nebel, A. (2021). Exome-wide association study identifies FN3KRP and PGP as new candidate longevity genes. *J Gerontol A Biol Sci Med Sci, 76*(5), 786-795.

Wicksteed, B., Brissova, M., Yan, W., Opland, D. M., Plank, J. L., Reinert, R. B., . . . Dempsey, P. J. (2010). Conditional gene targeting in mouse pancreatic ss-cells: analysis of ectopic Cre transgene expression in the brain. *Diabetes, 59*(12), 3090-3098.

Wride, M. A. (2000). Minireview: apoptosis as seen through a lens. *Apoptosis, 5*(3), 203-209.

Xue, L. L., Chen, H. H., & Jiang, J. G. (2017). Implications of glycerol metabolism for lipid production. *Prog Lipid Res, 68*, 12-25.

Ye, D. Z., Tai, M. H., Linning, K. D., Szabo, C., & Olson, L. K. (2006). MafA expression and insulin promoter activity are induced by nicotinamide and related compounds in INS-1 pancreatic beta-cells. *Diabetes, 55*(3), 742-750.

Zechner, R., Zimmermann, R., Eichmann, T. O., Kohlwein, S. D., Haemmerle, G., Lass, A., & Madeo, F. (2012). Fat signals--lipases and lipolysis in lipid metabolism and signaling. *Cell Metab, 15*(3), 279-291.

Bridging Chapters II and III

Results from Chapter II showed that G3PP plays a role in glucodetoxification, the prevention of insulin hypersecretion, acts as a defense against excess body weight gain and contributes to preserve β-cell mass in the face of hyperglycemia. Furthermore, initial studies (overexpression and knockdown *in vitro*) indicated that G3PP plays a role in hepatocyte metabolism. My aim in this chapter was to examine the importance of G3PP in the regulation of glucose and lipid metabolism and metabolic stress in mouse hepatocytes *in vivo*. Thus, here I investigate it by using adeno-associated virus 8 (AAV8) expressing Cre recombinase under the control of the thyroid hormone-binding globulin (TBG) promoter to suppress the expression of G3PP in the hepatocytes of adult G3PP fl/fl mice specifically. First, we validated that G3PP deletion in hepatocytes cultured *ex vivo* showed the same metabolic defects that had been previously identified using primary rat hepatocytes grown *in vitro*. Then, we studied adult mice fed with normal diet for 10 weeks and under hyperglycemia conditions using a glucose infusion for 55h. Body weight and food intake were monitored during the 10 weeks. Since my goal was to examine the importance of G3PP in the regulation of glucose and lipid metabolism and metabolic stress in mouse hepatocytes *in vivo*, I obtained comprehensive metabolic profiles including blood glucose, glycerol, insulin, triglycerides, plasma FFA and cholesterol levels, plasma liver enzymes along with liver weight, TG content and inflammation markers.

Chapter III: The hepatic glycerol shunt orchestrated by glycerol-3-phosphate phosphatase controls liver metabolism, fuel deposition and glucodetoxification under hyperglycemia

Anfal Al-Mass[1,2], Pegah Poursharifi[2], Marie-Line Peyot[2], Roxane Lussier[2], Isabelle Chenier[2], Yat Hei Leung[2], Anindya Ghosh[2], Abel Oppong[2], Elite Possik[2], Yves Mugabo[2], Rasheed Ahmad[3], Robert Sladek[1], S. R. Murthy Madiraju[2*], Fahd Al-Mulla[3], Marc Prentki[2*]

[1] Department of Medicine, McGill University, Montréal, QC, Canada.

[2] Departments of Nutrition, Biochemistry and Molecular Medicine, University of Montreal, and Montreal Diabetes Research Center and CRCHUM, Montréal, QC, Canada.

[3] Departments of Immunology, Microbiology, Genetics and Bioinformatics, Dasman Diabetes Institute, Dasman 15462, Kuwait.

Primary Corresponding author
Marc Prentki, PhD
Professor of Nutrition, Université de Montréal,
CRCHUM, Room R08-412, Tour Viger, 900 rue Saint Denis
Montreal, QC H2X 0A9, Canada.
Email: marc.prentki@umontreal.ca

Short title: G3PP and metabolic regulation in liver

Keywords: Glycerol-3-phosphate phosphatase; Glycerol shunt; Glucodetoxification; Liver; Hepatocytes; lipogenesis, triglycerides, cholesterol, glycogen, inflammation, NAFLD

A version of this chapter is published in: Molecular Metabolism 2022. (**Al-Mass, A.,** Poursharifi, P., Peyot, M. L., Lussier, R., Chenier, I., Leung, Y. H., Ghosh, A., Oppong, A., Possik, E., Mugabo, Y., Ahmad, R., Sladek, R., Murthy Madiraju, S. R., Al-Mulla, F., & Prentki, M. (2022). Hepatic glycerol shunt and glycerol-3-phosphate phosphatase control liver metabolism and glucodetoxification under hyperglycemia. Molecular metabolism, 66, 101609. https://doi.org/10.1016/j.molmet.2022.101609)

3.1 Abstract

Objective: Glycerol-3-phosphate (Gro3P) phosphatase (G3PP) hydrolyzes Gro3P to glycerol that exits the cell, thereby operating a "glycerol shunt", a metabolic pathway that we identified recently in mammalian cells. We have investigated the role of G3PP and the glycerol shunt in the regulation of glucose metabolism and lipogenesis in mouse liver.

Methods: We generated hepatocyte-specific G3PP-KO mice (LKO), by injecting AAV8-TBG-i*Cre* to male G3PP$^{fl/fl}$ mice. Controls received AAV8-TBG-*eGFP*. Both groups were fed chow diet for 10 weeks. Hyperglycemia (16-20 mM) was induced by glucose infusion for 55 h. Hepatocytes were isolated from normoglycemic mice for *ex vivo* studies, and targeted metabolomics was carried out in mice liver after glucose infusion.

Results: LKO mice showed no change in body weight, food intake, fed and fasted glycemia but had increased fed plasma triglycerides. Hepatic glucose production from glycerol was increased in fasted LKO mice. Isolated LKO hepatocytes displayed reduced glycerol production and elevated triglyceride and lactate production at high glucose concentration. Hyperglycemia in LKO mice led to increased liver weight and accumulation of triglycerides, glycogen and cholesterol together with elevated levels of Gro3P, dihydroxyacetone phosphate, acetyl-CoA and some Krebs cycle intermediates in liver. Hyperglycemic LKO mice liver showed elevated expression of proinflammatory cytokines and M1-macrophage markers accompanied by increased plasma triglycerides, LDL/VLDL, urea and uric acid and myocardial triglycerides.

Conclusions: The glycerol shunt orchestrated by G3PP acts as a glucose excess detoxification pathway in hepatocytes by preventing metabolic disturbances caused by hyperglycemia that contribute to enhanced liver fat, glycogen storage, inflammation and lipid build-up in the heart. We propose G3PP as a novel therapeutic target for hepatic disorders linked to nutrient excess.

3.2 Introduction

Chronic nutritional excess results in metabolic disorders such as obesity, type 2 diabetes (T2D), ectopic accumulation of triglycerides (TG) and non-alcoholic fatty liver disease (NAFLD). Prolonged fuel surfeit causes hyperinsulinemia, fat build-up and metabolic stress in various organs, leading to insulin resistance, β-cell failure and T2D. (Kitade, Chen et al. 2017, Nolan and Prentki

2019, Huang, Behary et al. 2020, Prentki, Peyot et al. 2020). Central to these metabolic diseases are disturbances in glucose, lipid and energy metabolism in association with deranged insulin homeostasis and inflammation (Nolan and Prentki 2019, Prentki, Corkey et al. 2020, Prentki, Peyot et al. 2020). The pathogenesis of NAFLD starts with the disturbed lipid metabolism in liver, accumulation of TG and enhanced inflammation, which progressively lead to fibrosis, non-alcoholic steatohepatitis (NASH), cirrhosis and hepatocellular carcinoma (Day and James 1998, Duseja and Chalasani 2013, Birkenfeld and Shulman 2014, Esler and Bence 2019, Huang, Behary et al. 2019). Several studies from our lab (Prentki and Nolan 2006, Prentki and Madiraju 2008, Prentki and Madiraju 2012, Prentki, Matschinsky et al. 2013, Prentki, Corkey et al. 2020, Prentki, Peyot et al. 2020) and elsewhere (Zechner, Zimmermann et al. 2012, Oberhauser and Maechler 2021) highlighted the significance of the glycerolipid/free fatty acid (GL/FFA) cycle in T2D, obesity and pancreatic β-cell function. The GL/FFA cycle with its lipogenesis and lipolysis arms, connects lipid and glucose metabolism via glucose-derived glycerol-3-phosphate (Gro3P) and FFA-derived fatty acyl-CoA, the substrates for lipogenesis (Prentki and Madiraju 2008, Poursharifi, Attane et al. 2020). Chronic nutrient surfeit promotes the accumulation of TG in liver by augmenting the lipogenic segment of the GL/FFA cycle by providing Gro3P and FFA (Prentki and Madiraju 2008, Prentki, Matschinsky et al. 2013, Prentki, Peyot et al. 2020).

Glucose-derived Gro3P links glucose, lipid and energy metabolism in all cells, as it is produced during glycolysis, serves as a substrate for glycerolipid synthesis and participates in the electron shuttle between cytosol and mitochondria (Mugabo, Zhao et al. 2016, Possik, Madiraju et al. 2017). We earlier discovered a novel mammalian metabolic enzyme, lying at the heart of intermediary metabolism, Gro3P phosphatase (G3PP) and demonstrated that G3PP directly converts part of the excess glucose-derived Gro3P to less toxic glycerol, which leaves the cell (Mugabo, Zhao et al. 2016). We named this novel metabolic pathway the *glycerol shunt* that possibly helps in glucodetoxification in pancreatic β-cells (Al-Mass, Poursharifi et al. 2022) and demonstrated that G3PP-glycerol shunt pathway confers better healthspan and lifespan in *C. elegans* (Possik, Schmitt et al. 2022). Hydrolytic control of intracellular Gro3P by G3PP adds another layer of metabolic regulation that was not recognized previously in mammalian cells. Our earlier *in vitro* studies support a role for G3PP in liver glucose and lipid metabolism and showed an inverse relationship between G3PP expression and lipogenesis in isolated rat hepatocytes (Mugabo, Zhao et al. 2016) and that the impact of G3PP activity on metabolism is more evident

at high glucose concentrations when intracellular Gro3P rises to sufficiently high levels to become available for G3PP (Mugabo, Zhao et al. 2016). Despite the significant evidence for G3PP mediated regulation of metabolism in hepatocytes *in vitro*, the role of this enzyme *in vivo* in liver is not known. We earlier observed that supra-physiological overexpression (more than 50 fold) of G3PP in rat liver *in vivo*, led to decreased gluconeogenesis from glycerol and plasma TG and elevated plasma glycerol (Mugabo, Zhao et al. 2016). Though these limited studies were compatible with an *in vivo* function of G3PP in Gro3P hydrolysis, the pathophysiological significance of G3PP in liver remains to be discovered. Our recent studies demonstrated that β-cell specific G3PP deletion in normal diet fed mice enhances glucose stimulated insulin secretion, promotes glucose oxidation and lipogenesis in the islets, and renders the islets susceptible to glucotoxicity in terms of excess insulin secretion and apoptosis and these changes are associated with elevated islet Gro3P levels (Al-Mass, Poursharifi et al. 2022). Considering that G3PP is well expressed in the liver (Mugabo, Zhao et al. 2016) and that this tissue plays central role in energy metabolism and metabolic disorders associated with fuel excess, the present studies were conducted to address the precise *in vivo* role of G3PP in liver glucose and fat metabolism and test the view that the glycerol shunt is implicated in hepatic glucodetoxification.

3.3 Materials and Methods

Animals

G3PP$^{lox/lox}$ mice in which exons 1 and 2 of *PGP* (coding for G3PP protein) gene are flanked with LoxP sites were generated by Ingenious Targeting Laboratory (Stony Brook, NY). At 8 weeks of age, male G3PP $^{flox/flox}$ (fl/fl) mice received a single tail vein injection of 5×10^{10} genome copies (GC)/mouse of AAV8-TBG-i*Cre* (Vector Biolabs: VB1724) or AAV8-TBG-*eGFP* (Vector Biolabs: VB1743) or saline **(Figure 3.1*A*)**. The TBG (Thyroxine Binding Globulin) promoter drives hepatocyte-specific gene expression (Yan, Yan et al. 2012). Mice were placed in individual cages and fed a normal chow diet (15% fat by energy; Envigo RMS (Canada) limited. T2918) ad libitum for 10 weeks. Body weight and food intake were measured weekly. All procedures were approved by the Institutional committee for the protection of animals (Comité Institutionnel de Protection des Animaux du Centre Hospitalier de l'Université de Montréal).

Western blot analysis for the validation of hepatocyte specific G3PP deletion

After 4 weeks following AAV8 viral infection, mice were anesthetized and the livers were perfused with collagenase buffer for hepatocyte preparation (see below for details) and visceral adipose tissue, brain and skeletal muscle were collected. Mouse tissues and isolated hepatocytes were lysed in RIPA buffer (10 mM Tris-HCl, 1 mM EDTA, 0.5 mM EGTA, 1% Triton X-100, 0.1% sodium deoxycholate, 0.1% sodium dodecylsulfate and 140 mM NaCl) and the protein extracts were used for western blot analysis to validate hepatocyte-specific G3PP deletion (G3PP primary antibody: PGP Antibody (E-10) (sc-390883), secondary antibody: m-IgGκ BP-HRP (sc-516102) both from Santa Cruz Biotechnology). For all tissues, α-tubulin was used as the gel loading control.

Oral glycerol load test

Mice were fasted for 16 h, after 4 weeks following AAV8 infection, and were administered glycerol at 5 mg/g BW (using 87% wt/vol, glycerol in water) by gavage. Blood was collected from tail vein at baseline and at 5, 10, 15, 20, 30, 45 and 60 min following the glycerol load and blood glucose was measured using a glucometer.

Pyruvate load test

After completing the glycerol load test at 4 weeks following AAV8 infection, mice were rested for 2 weeks. At 6 weeks after AAV8 infection, mice were fasted for 16h and sodium pyruvate (at 1 mg/g BW, in water) was injected intraperitoneally. Blood was collected from the tail vein at baseline and 5, 10, 15, 20, 30, 45, and 60 min following the pyruvate load and blood glucose was measured using a glucometer.

Hepatocyte isolation

Hepatocytes were isolated from mice 4 weeks after AAV8 infection, by *in situ* collagenase (type XI; Sigma) perfusion (Mugabo, Zhao et al. 2016) and were seeded in DMEM complete media (Sigma D5030) (pH 7.4) without phenol red, supplemented with 0.48 mM of sodium bicarbonate, 5 mM glucose, 1 mM sodium pyruvate, 2 mM glutamine, penicillin streptomycin, 0.2% BSA, 1 nM insulin and 100 nM dexamethasone) using Collagen I Coated Plate (A11428-01) (Mugabo, Zhao et al. 2016). *Ex-vivo* experiments were done after 16 h following seeding.

Gluconeogenesis in hepatocytes, *ex vivo*

Primary mouse hepatocytes, attached to the collagen plates for 16 h following seeding, were washed twice with PBS and starved in DMEM without glucose for 3 h. Then the cells were washed with PBS, followed by incubation for 3 h in glucose production medium (pH 7.4) consisting of glucose-free DMEM without phenol red, supplemented with 15 mM Hepes and 2 mM L-glutamine, and 10 mM glycerol or 20 mM sodium lactate plus 2 mM sodium pyruvate. After incubation, the medium was collected for glucose measurement (Autokit Glucose; Wako) and the hepatocytes were collected for protein measurement (Mugabo, Zhao et al. 2016).

Triglyceride, glycerol and lactate production in hepatocytes, *ex vivo*

Primary mouse hepatocytes, attached to the collagen plates, were washed with PBS and incubated in DMEM complete media containing 5 or 25mM glucose for 2 h. After incubations, media and cells were collected to measure glycerol and lactate release and TG and lactate content, respectively, as described before (Mugabo, Zhao et al. 2016).

***In vivo* glucose infusion**

After 4 weeks following infection of the G3PP$^{lox/lox}$ mice with AAV8-TBG-*Cre* (LKO) or AAV8-TBG-*eGFP* (control), a cannula was inserted in the right jugular vein **(Figure 3.3*A*)**. The mice were subcutaneously injected with carprofen (20 mg/kg) combined with saline (around 3ml) to reduce pain, prior to surgery and were anesthetised with isoflurane. Cages were placed on a heating pad with a cold spot (1/3 cold). Diet gel (DietGel 31M: 72-08-5022) was given to the mice during the post-operation period with pellets in the bottom of the cages for the entire time. In the post-operation period, mice were infused with 5U heparinized saline (7 µl/hr) to make sure that the canula remained unclogged. The mice were given a second injection of carprofen (20 mg/kg) and 3ml of saline on the first post-operative day. Following surgery, fresh diet gel was given daily and the mice were also given saline daily based on their hydration status, evaluated by their appearance and attitude in the cage (Bekkevold, Robertson et al. 2013). Five days following surgery, the mice were infused with dextrose 70%. The glucose infusion rate (GIR) started at 30 mg/Kg/min and was adjusted every 3 h during the day and once during the night to maintain the blood glucose at predetermined level (14-16 mM). During the glucose infusion, blood and urine (Chew and Chua 2003) were collected twice daily. The glucose infusion was continued for 55 h and then the mice were euthanized using ketamine/xylazine and blood, liver and heart were collected at necropsy.

Liver analytes

Livers from glucose-infused mice were collected and snap-frozen in liquid nitrogen. TG was measured after lipid extraction (Mugabo, Zhao et al. 2016) using a triglyceride reagent (Sigma-Aldrich cat: T2449). Liver glycogen and total cholesterol were determined by colorimetric assays (Abcam Glycogen Assay Kit, ab65620; and Abcam Cholesterol Assay Kit, ab65390).

Plasma analytes

Lipid profile (Cobas kits used: cholesterol, ref: 04718917 190; triglycerides (TGs), ref: 04657594 190; high density lipoproteins (HDL), ref: 07528604 190; low density lipoproteins (LDL), ref: 07005806 190) and liver function markers (Cobas kits used: alanine aminotransferase (ALT), ref: 04718569 190; alkaline phosphatase (ALP), ref: 04657373 190; albumin, ref: 04657357 190; aspartate aminotransferase (AST), ref: 04657543 190; urea, ref: 04657616 190; uric acid, ref: 04657608 190) were measured in the plasma from glucose-infused mice using a Cobas C111 analyzer (Roche, Switzerland) (Ochoa-Sanchez, Oliveira et al. 2021). Plasma insulin (insulin: AL204, Perkin Elmer). Plasma LDL/VLDL (Cholesterol Assay Kit - HDL and LDL/VLDL (ab65390)). Inflammation markers (IL-6: AL504, Perkin Elmer, TNFα: AL505, Perkin Elmer and CRP: ab157712, ABCAM). Plasma LDL/VLDL, insulin and inflammation markers were done using EnVision from Perkin Elmer at the Metabolomic Core Facility of CRCHUM.

RNA extraction and quantitative PCR

Total RNA was extracted from the livers of glucose-infused mice (RNeasy Micro Kit, Qiagen). Following reverse-transcription to cDNA, expression of various genes was determined by quantitative PCR using SYBR Green (Qiagen QuantiTect). All gene expression analyses were conducted in duplicate and normalized to the expression of *18s*. PCR primer sequences are listed in Supplementary Table S3.1.

Targeted metabolomics

Liver samples from glucose-infused mice were snap-frozen in liquid nitrogen and stored at −80°C. All metabolites described in this study were extracted and measured using an LC-electrospray ionization-MS/MS system (Agilent 1200 SL and a triple-quadrupole mass spectrometer (4000Q TRAP MS/MS, Sciex) as described before (Mugabo, Zhao et al. 2016, Cassim, Raymond et al.

2018). Peak areas were used for relative quantification of the identified metabolites. All these analyses were done at the CRCHUM Metabolomic Core Facility.

Statistical analyses

Data were analyzed using GraphPad Prism 6 (GraphPad Software, San Diego, CA). Results are expressed as means ± SEM. Differences between two groups were assessed by unpaired, two-tailed Student's *t* test, and between multiple groups using one-way or two-way analyses of variance (ANOVA) with Bonferroni correction, as indicated. A p value < 0.05, following correction for multiple testing as appropriate, was considered statistically significant.

3.4 Results

Phenotypic characterization of G3PP-LKO mice on chow diet

G3PP protein levels were markedly decreased in LKO hepatocytes compared to controls (G3PP *fl/fl* mice injected with AAV8-TBG-GFP viral vector or saline vehicle) without any change in G3PP expression in extrahepatic tissues (brain, adipose, kidney, heart and muscles) obtained from LKO mice four weeks following AAV8 infection **(Figure 3.1*B*)**. G3PP-LKO mice fed chow diet for 10 weeks following AAV8-TBG-i*Cre* injection, showed no change in body weight gain or food intake **(Figure 3.1*C* and *D*)** and no differences in fed and fasted glycemia compared to the two control mice **(Figure 3.1*E*)**. At the end of the study, LKO mice showed no change in the weights of liver **(Figure 3.1*F*)** or other tissues **(Figure S3.1*A*)** compared to control animals. There were also no differences in the plasma levels of liver function markers (such as alanine aminotransferase, ALT; alkaline phosphatase, ALP; and albumin), total cholesterol, high density lipoprotein (HDL) and low density lipoprotein (LDL) between LKO and control mice **(Figure S3.1*B*)**. However, the LKO mice showed significantly elevated plasma TG but with only a slight increase in liver TG content (*P=0.1*), compared to the control mice **(Figure 3.1*G* and *H*)**.

Increased glucose production following a glycerol load in LKO mice

In order to assess if deletion of G3PP in hepatocytes affects gluconeogenesis *in vivo*, we conducted glycerol and pyruvate load test after 16 h fasting to deplete glycogen stores. A small but significant increase in plasma glucose levels was observed following a glycerol oral load in the LKO mice compared to controls, likely due to elevated hepatic glucose production **(Figure**

3.2*A*). However, LKO mice did not show a change in glucose production following a pyruvate load **(Figure 3.2*B*)**.

LKO hepatocytes show *ex vivo* decreased glycerol release and increased TG content, glycolytic flux and gluconeogenesis.

Isolated LKO hepatocytes showed significantly decreased glycerol release **(Figure 3.2*C*)** and increased TG content **(Figure 3.2*D*)** compared to control hepatocytes when incubated at high glucose (25mM) but not at basal glucose (5mM) concentration. *Ex vivo* gluconeogenesis in the LKO hepatocytes was found to be elevated with glycerol as a substrate compared to controls **(Figure 3.2*E*)** and this increase was also seen using pyruvate/lactate as substrates **(Figure 3.2*E*)**, though this was not seen *in vivo* **(Figure 3.2*B*)**. Furthermore, LKO hepatocytes showed significantly elevated lactate release **(Figure 3.2*F*)** and content **(Figure 3.2*G*)** only at high glucose concentration. These findings indicate an elevated glycolytic flux at high glucose concentrations in the LKO hepatocytes. These *ex vivo* results with LKO mouse hepatocytes are consistent with our previous *in vitro* findings in rat hepatocytes with RNAi-knockdown of G3PP (Mugabo, Zhao et al. 2016) and validate the present LKO mouse model.

G3PP LKO mice show a transient reduction in urinary glycerol, liver lipid and glycogen accumulation, and increased plasma lipids, lipoproteins and urate during provoked chronic hyperglycemia.

Results from LKO hepatocytes, *ex vivo*, suggested that G3PP activity in hepatocytes has more impact on metabolism at high glucose concentrations. In order to assess *in vivo* the influence of elevated glucose supply on liver metabolism in LKO mice, we infused the LKO and control mice with a glucose solution to elevate glycemia above the physiological levels, for a period of 55 h **(Figure 3.3*A*)**. There was no difference in the body weight between the LKO and control mice at baseline (after implantation of an indwelling canula, 5 days before glucose infusion) and at the start and end of glucose infusion **(Figure S3.2*A*)**. Glycemia and glucose infusion rates (GIR) during the infusion were similar in both LKO and control mice **(Figure 3.3*B*-*C*)**. Average blood glucose levels were 10-11 mM during the first 24h of the infusion; 13-15 mM from 24h to 48h; and 18-19 mM from 48h to 55h of infusion for both the groups of mice. Plasma TG during glucose infusion increased with time in both groups, with LKO mice showing a significant increase at the end of the infusion compared to the control mice **(Figure 3.3*D*)**. Plasma glycerol was not different during glucose infusion between the two groups **(Figure 3.3*E*)**. Urinary glucose and glycerol at 6

h post the start of glucose infusions were both elevated by about twofold in the control mice. But this rise in both metabolites did not occur in the LKO mice. However at subsequent times all glucose and glycerol levels in urine returned to basal values and were not different in LKO vs control mice **(Figure 3.3*F*-*G*)**.

At the end of the 55h glucose infusion, liver weight **(Figure 3.4*A*)** and liver TG **(Figure 3.4*B*)**, glycogen **(Figure 3.4*C*)** and total and free cholesterol **(Figure 3.4*D*)** in LKO mice were significantly elevated compared to the control mice. In addition, heart TG levels were also found to be increased in the LKO mice **(Figure 3.4*E*)**. Furthermore, following glucose infusion, plasma levels of TG **(Figure 3.4*F*)**, LDL + VLDL **(Figure 3.4*H*)**, urea **(Figure 3.4*I*)** and uric acid **(Figure 3.4*J*)** were significantly elevated in the LKO mice, but no changes were seen in total cholesterol **(Figure 3.4*G*)** and HDL levels **(Figure S3.2*C*)** compared with control mice. In addition, liver function parameters ALT, AST and albumin in plasma were not changed between groups after glucose infusion **(Figure S3.2*C*)**.

The livers of G3PP-LKO mice show enhanced expression of markers of inflammation and macrophage infiltration following chronic hyperglycemia

Increased TG and cholesterol accumulation in the liver is known to trigger inflammation, a characteristic of NAFLD/NASH (Chen, Varghese et al. 2014). Considering the accumulation of lipids in liver and plasma of glucose infused LKO mice, we measured inflammation markers in the plasma and the expression of the corresponding genes in the liver following glucose infusion. There was no difference in the plasma protein levels of TNFα, IL-6 or CRP between LKO and control mice **(Figure 3.4*K*)** indicating no systemic change in inflammation. However, the mRNA levels of the pro-inflammatory cytokines *Tnfα* and *Il-6* were significantly increased in the hyperglycemic LKO mouse livers compared with control livers **(Figure 3.4*L*)**, whereas no changes were seen in the expression of other pro-inflammatory cytokines, *Il-1B* and *Mcp-1*, or the anti-inflammatory cytokine *Il-10* **(Figure S3.2*D*)**. Moreover, the mRNA levels of pan-macrophage marker *F4/80* and of the M1-macrophage marker *Cd11c* were markedly increased in the LKO livers compared to the control mice **(Figure 3.4*M*)** suggesting elevated macrophage infiltration.

Liver metabolites profiling in the G3PP-LKO and control mice during chronic hyperglycemia

Targeted metabolomics **(Figures 3.5 and S3.3)** was conducted in order to gain insight into the mechanism by which G3PP deletion in hepatocytes impacts liver metabolism and physiology

in vivo under hyperglycemic conditions. The levels of the G3PP substrate, Gro3P and its precursor DHAP **(Figure 3.5A-B)** were significantly increased in the LKO mouse liver after 55 h glucose infusion. However, no change was seen in the ATP/ADP ratios **(Figure 3.5D)** as well as in ATP, ADP, AMP, adenosine, cAMP **(Figure 3.5P)**, GTP and GMP levels **(Figure S3.3C)** in the LKO livers compared to controls. The redox couples NADH/NAD^+ (Figure 5E), GSH/GSSG **(Figure 3.5G)** as well as parameters that reflect the cytosolic redox state, Gro3P/DHAP **(Figure 3.5C)** and pyruvate/lactate **(Figure 3.5H)**, were similar in both LKO and control livers. An increase in acetyl-CoA and malonyl-CoA levels that positively control the Krebs cycle activity, anaplerosis and lipogenesis, and negatively impact fat oxidation, were found to be higher in the LKO group **(Figure 3.5M-N)**. The NADPH/NADP ratio was reduced in the LKO livers **(Figure 3.5F)**, which may reflect increased usage of NADPH for lipogenesis. There was also an increase in the content of some Krebs cycle intermediates, succinate and α-ketoglutarate **(Figure 3.5I-J)** in LKO livers, reflecting increased anaplerosis, but not others, (iso)citrate, malate and fumarate **(Figure 3.5K-L and S3.3A)**. Leucine levels were found to be higher in LKO livers, which may be due to the increased glucose metabolism at elevated glucose in LKO livers **(Figure 3.2F-G)** causing less usage of alternative fuels, amino acids and fatty acids **(Figure 3.5O)**. Other metabolites including pyruvate, lactate, the amino acids alanine, glutamine, glutamate and aspartate were unchanged in the LKO liver **(Figure S3.3A-B)**.

3.5 Discussion

Glucose derived Gro3P via glycolysis is needed for glycerolipid synthesis at large and TG in particular, and also for shuttling electrons from cytosol to mitochondria via the Gro3P shuttle. Thus, regulation of the cytosolic concentration of Gro3P offers a control mechanism with simultaneous three-dimensional effect on glucose, lipid and energy metabolism, as Gro3P is at the nexus of these pathways (Possik, Madiraju et al. 2017, Possik, Al-Mass et al. 2021). Excess supply of glucose can drive elevated production of Gro3P intracellularly and this together with increased availability of FFA, can lead to TG synthesis through the lipogenic arm of the GL/FFA cycle (Prentki and Madiraju 2008, Prentki and Madiraju 2012). Accumulation of fat in the liver leads to insulin resistance and NAFLD, the hepatic component of the metabolic syndrome, that contributes to the development of obesity and T2D (Bugianesi, Moscatiello et al. 2010, Birkenfeld and Shulman 2014). Our earlier *in vitro* studies using isolated rat hepatocytes demonstrated that G3PP

expression controls Gro3P levels, particularly at high glucose concentrations (Mugabo, Zhao et al. 2016). Thus, the G3PP expression level in isolated rat hepatocytes was found to be inversely related to cellular Gro3P levels and TG accumulation, when cells were incubated at elevated (25 mM) glucose (Mugabo, Zhao et al. 2016). These *in vitro* observations prompted us to ascertain the role of hepatic G3PP *in vivo,* under both normoglycemic and hyperglycemic conditions.

We now show that liver specific deletion of G3PP in normoglycemic mice fed chow diet leads to: (1) elevated plasma TG with only a small increase in liver TG levels and no changes in body weight and food intake; (2) a small elevated liver glucose production *in vivo* upon a glycerol load but not with a pyruvate load; (3) decreased glycerol shunt with reduced glycerol release and increased gluconeogenesis and lactate production from isolated hepatocytes *ex vivo*. As the alterations in the phenotype of the normoglycemic LKO mice were found to be relatively mild, we tested the consequences of hepatic G3PP deletion *in vivo* in mice with induced chronic hyperglycemia by glucose infusion. Under hyperglycemia, however, very significant changes were observed in the LKO mice: (1) increased plasma TG, LDL, VLDL cholesterol and urea levels ; (2) increased liver weight, TG, glycogen, total and free cholesterol contents, as well as expression of markers of inflammation and macrophage invasion; (3) TG deposition in the hearts of LKO mice; (4) elevated liver levels of Gro3P, DHAP, acetyl-CoA, malonyl-CoA and some Krebs cycle intermediates and in the NADP/NADPH ratio. Elevated Krebs cycle intermediates reflect increased anaplerosis (the refilling of cycle intermediates) necessary for lipogenesis and the observed increased levels and malonyl-CoA and TG are indicative of increased lipogenesis in the LKO livers. The increased lactate production is indicative of increased glycolysis and the elevated acetyl-CoA is known to activate anaplerosis via its effect on pyruvate carboxylase and is also the precursor of cholesterol, which is elevated in the LKO livers. Overall the results demonstrate that hepatic G3PP is particularly efficient *in vivo* at elevated glucose and that its function is to act as a "glucose excess detoxification machine" or in other words a "glucose excess security valve" in the liver by redirecting the glucose carbons in excess to the glycerol shunt and glycerol release from the hepatocytes. Consistent with this view, in control mice, glycerol level in the urine was elevated by two-fold compared to basal value 6 h after the start of the glucose infusion reaching about 4 mM, and this rise was suppressed in the LKO mice. Noteworthy, glycerol is relatively a less toxic molecule than glucose, when in excess as high levels of glycerol do not cause any apparent toxicity (Lin 1977). Thus upon liver G3PP suppression in mice, there is increased fuel storage in liver in

the form of TG, cholesterol and glycogen, as well as enhanced glycolysis and lipogenesis, both *in vivo* and *ex vivo*.

Hepatocyte G3PP deletion accelerated gluconeogenesis starting from glycerol and pyruvate plus lactate, *ex vivo* in isolated LKO hepatocytes, but surprisingly only with glycerol, *in vivo* and not with pyruvate. It was shown before that glycerol is a better gluconeogenic substrate than lactate or amino acids in mouse liver due to the rapid utilization of glycerol by glycerol kinase (Wang, Kwon et al. 2020). Moreover, it has been shown that lactate is the largest source of gluconeogenic substrate used by kidney (Gerich, Meyer et al. 2001). Therefore, in liver G3PP-KO mice, under *in vivo* whole-body conditions, pyruvate is expected to trigger glucose production mostly from kidneys, whereas glycerol is expected to drive gluconeogenesis mainly in hepatocytes.

Deletion of hepatocyte G3PP led to enhanced diversion of Gro3P towards TG synthesis and VLDL packaging and secretion under hyperglycemic conditions. It is possible that the elevated plasma LDL/ VLDL facilitated the transport of lipids to tissues like heart, where accumulation of TG was noticed in the LKO mice. In the hyperglycemic LKO mice, the elevated plasma level of urea is possibly related to the enhanced production of acetyl-CoA that is needed for the synthesis of N-acetylglutamate, which drives the first step of urea cycle, catalyzed by carbamoylphosphate sythetase-1 in liver (Shi, Allewell et al. 2015). Increased diversion of glucose carbons towards ribose-5-phosphate and phosphoribosylpyrophosphate synthesis in association with elevated NADPH levels was suggested to lead to elevated formation of uric acid in liver (Leyva, Wingrove et al. 1998), and a combination of glucose, fructose and fatty acids are also known to induce uric acid production in HepG2 cells (Zhao, Guo et al. 2016). Thus, in the hyperglycemic LKO mice, the elevated plasma uric acid may be due to increased diversion of glucose towards pentose pathway and NADPH formation. Furthermore, the higher plasma levels of urea and uric acid seen in the LKO mice, are known biomarkers for hepatic steatosis in patients with NAFLD (Liu, Zhang et al. 2013, Oral, Sahin et al. 2019).

Elevated succinate observed in the LKO livers is known to regulate inflammation in many tissues including hepatocytes and the hepatic stellate cells, implicated in NAFLD and liver fibrosis (Mills and O'Neill 2014, Cho 2018). Hyperglycemic LKO mouse livers also showed increased levels of leucine, a branched chain amino acid that accumulates as a physiological adaptation to hepatic stress in NAFLD patients (Lake, Novak et al. 2015). However, the limited duration of hyperglycemic stress did not cause any significant damage to liver as the plasma levels of ALT

and AST in the LKO mice were unchanged and similarly many metabolites, including some Krebs cycle intermediates, adenine and guanine nucleotides, many amino acids, cAMP and the redox couples pyruvate/lactate, Gro3P/DHAP, NADH/NAD and GSH/GSSG were unchanged.

Accumulation of hepatic TG and cholesterol is known to promote the activation of macrophages/Kupffer cells, which exacerbate insulin resistance, as well as induce hepatic inflammation and NAFLD progression (Matsuzawa, Takamura et al. 2007, Chen, Varghese et al. 2014) (Arguello, Balboa et al. 2015). Accordingly, the gene expression of pro-inflammatory cytokines such as TNFα and IL-6, which are known to be released by M1 macrophages and lead to insulin resistance and NAFLD (Odegaard, Ricardo-Gonzalez et al. 2008), is elevated in LKO livers, together with an increased expression of macrophage markers Cd11c (M1macrophage marker) and F4/80 (general macrophage marker). These results suggest an enhanced presence of pro-inflammatory oriented macrophages in the livers of hyperglycemic LKO mice, indicating an increased macrophage recruitment and inflammation in the hyperglycemic LKO liver that may in the long term contribute to NAFLD (Itoh, Suganami et al. 2017, Kitade, Chen et al. 2017).

In conclusion, much knowledge has been accumulated concerning the biochemical basis of nutrient excess toxicity in mammalian cells at large and the liver in particular, that include for example ER stress, mitochondrial dysfunction, AMPK inhibition, cholesterol accumulation, the synthesis of some glycerolipids and ROS production. However, much less is known as to how cells can cope with fuel excess and in particular detoxify glucose when elevated. This is more relevant for the hepatocyte and the pancreatic β-cell that express glucokinase, which has high Km for glucose and Vmax, and which rapidly traps influxing glucose in the cytoplasm in the form of glucose-6-phosphate. Our results, using G3PP LKO mice, identify G3PP and the glycerol shunt as an important glucose excess detoxification pathway in the hepatocyte that when suppressed, under glucotoxic conditions, results in enhanced lipogenesis and accumulation of liver TG, glycogen, and cholesterol, elevated liver inflammation parameters and a rise in plasma TG, uric acid, LDL/VLDL and heart TG (Figure 6). Thus, we propose that the G3PP/glycerol shunt is a novel pathway essential for glucodetoxification and prevention of fat build-up in the liver and that G3PP can be harnessed for metabolic diseases, such as NAFLD/NASH promoted by nutrient excess. Studies in animal models of obesity, diabetes and NAFLD treated with G3PP activators, when they become available, should validate the therapeutic value of G3PP activation.

Author contributions

AAM, MLP, SRMM, and MP designed research; AAM, PP, MLP, RL, IC, YHL, AG and AO conducted experiments; AAM, MLP, SRMM, and MP analyzed data; PP, MLP, EP, YM, RA, FAM and RS critically reviewed and edited the manuscript and AAM, SRMM and MP wrote the paper.

Acknowledgments

This study was supported by funds from Canadian Institutes of Health Research (143308, to M.P. and S.R.M.M.), and from Dasman Diabetes Research Institute/ Montreal Medical International (to M.P, MSRM, RA and FA-M). M.P. was recipient up to 2019 of a Canada Research Chair in Diabetes and Metabolism. AA-M is supported by a scholarship from Kuwait University. PP was recipient of postdoctoral fellowships from the Fondation Valifonds, the Montreal Diabetes Research Center, the CRCHUM and Mitacs. We thank the core facilities for Cellular Physiology, Metabolomics and Rodent Phenotyping of the CRCHUM/Montreal Diabetes Research Center. We thank Jennifer Estall and Christopher Rose (University of Montreal, Canada) for helpful advice and discussion. Figure 1A and 6 was created with BioRender.com.

Conflict of interest

The authors have declared that no conflict of interest exists.

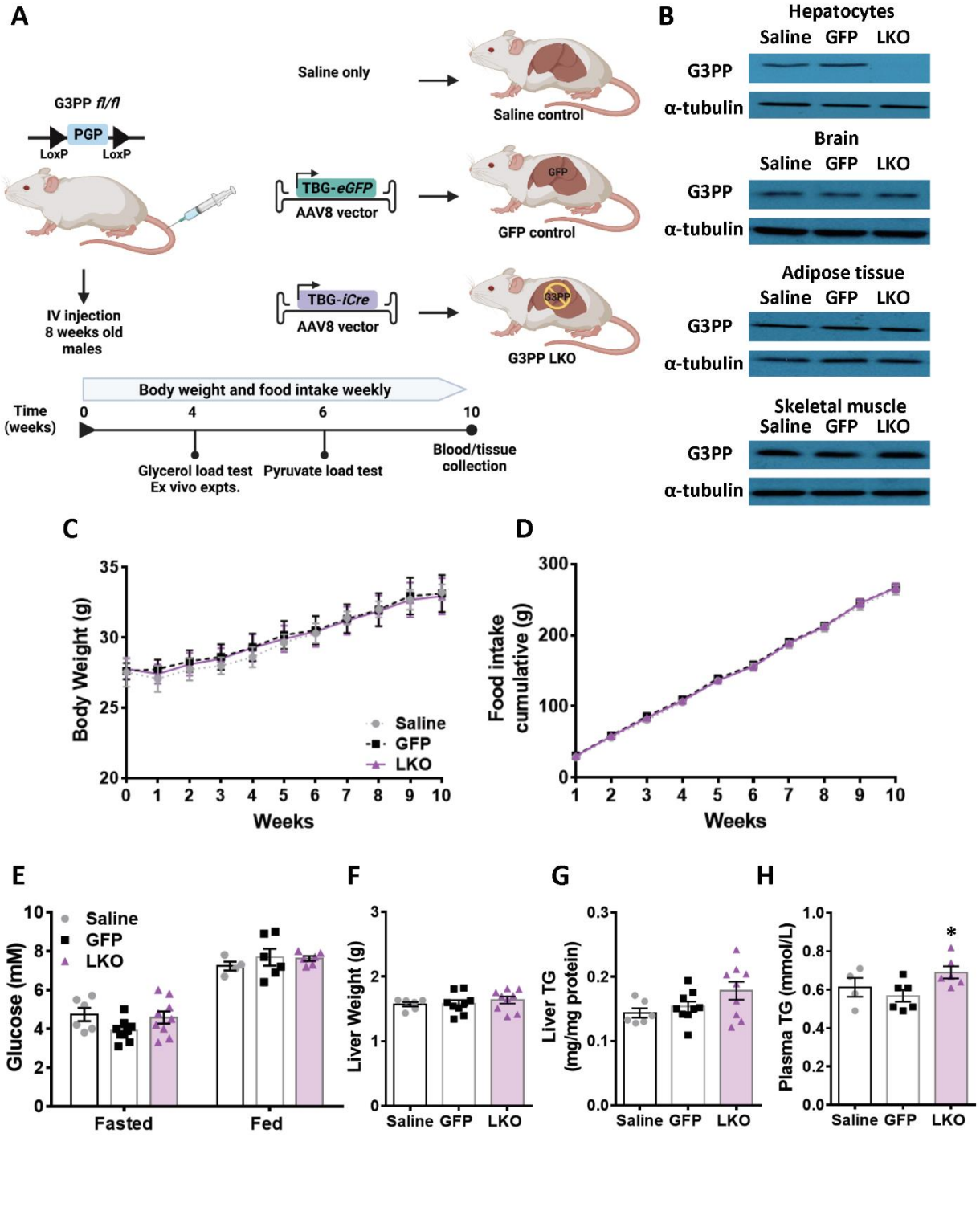
A
G3PP fl/fl
PGP
LoxP
LoxP
IV injection
8 weeks old
males
Saline only
Saline control
TBG-eGFP
AAV8 vector
GFP control
TBG-iCre
AAV8 vector
G3PP LKO
Body weight and food intake weekly
Time
(weeks)
0
4
6
10
Glycerol load test
Ex vivo expts.
Pyruvate load test
Blood/tissue
collection
B
Hepatocytes
Saline GFP LKO
G3PP
α-tubulin
Brain
Saline GFP LKO
G3PP
α-tubulin
Adipose tissue
Saline GFP LKO
G3PP
α-tubulin
Skeletal muscle
Saline GFP LKO
G3PP
α-tubulin
C
Body Weight (g)
Weeks
Saline
GFP
LKO
D
Food intake
cumulative (g)
Weeks
E
Glucose (mM)
Saline
GFP
LKO
Fasted
Fed
F
Liver Weight (g)
Saline GFP LKO
G
Liver TG
(mg/mg protein)
Saline GFP LKO
H
Plasma TG (mmol/L)
*
Saline GFP LKO

Figure 3.1. Generation and phenotyping of hepatocyte specific G3PP-KO (LKO) mice.

(A) Schematic protocol for creating the LKO and control mice and the experimental design in this study. Male, 8 wk old $G3PP^{fl/fl}$ mice were injected with AAV8-TBG-Cre or AAV8-TBG-GFP viral vectors or saline vehicle through the tail vein. Mice were then kept on chow diet for 10 weeks and sacrificed at indicated time and blood and tissues were collected for analyses. **(B)** Validation of G3PP deletion by Western blot using protein extracts from hepatocytes, brain, adipose tissue and skeletal muscle from mice, 4 weeks after IV injections (saline, n=3; GFP, n=3; LKO, n=4); α-tubulin was used as a control of protein loading. **(C)** Body weight, **(D)** food intake, **(E)** fed and fasted glycemia, **(F)** liver weight, **(G)** liver TG content **(H)** Fed plasma triglycerides. N=6-9 per group as shown; means ± SEM; $*p < 0.05$ vs both controls; C, D, two-way ANOVA; E-H one-way ANOVA.

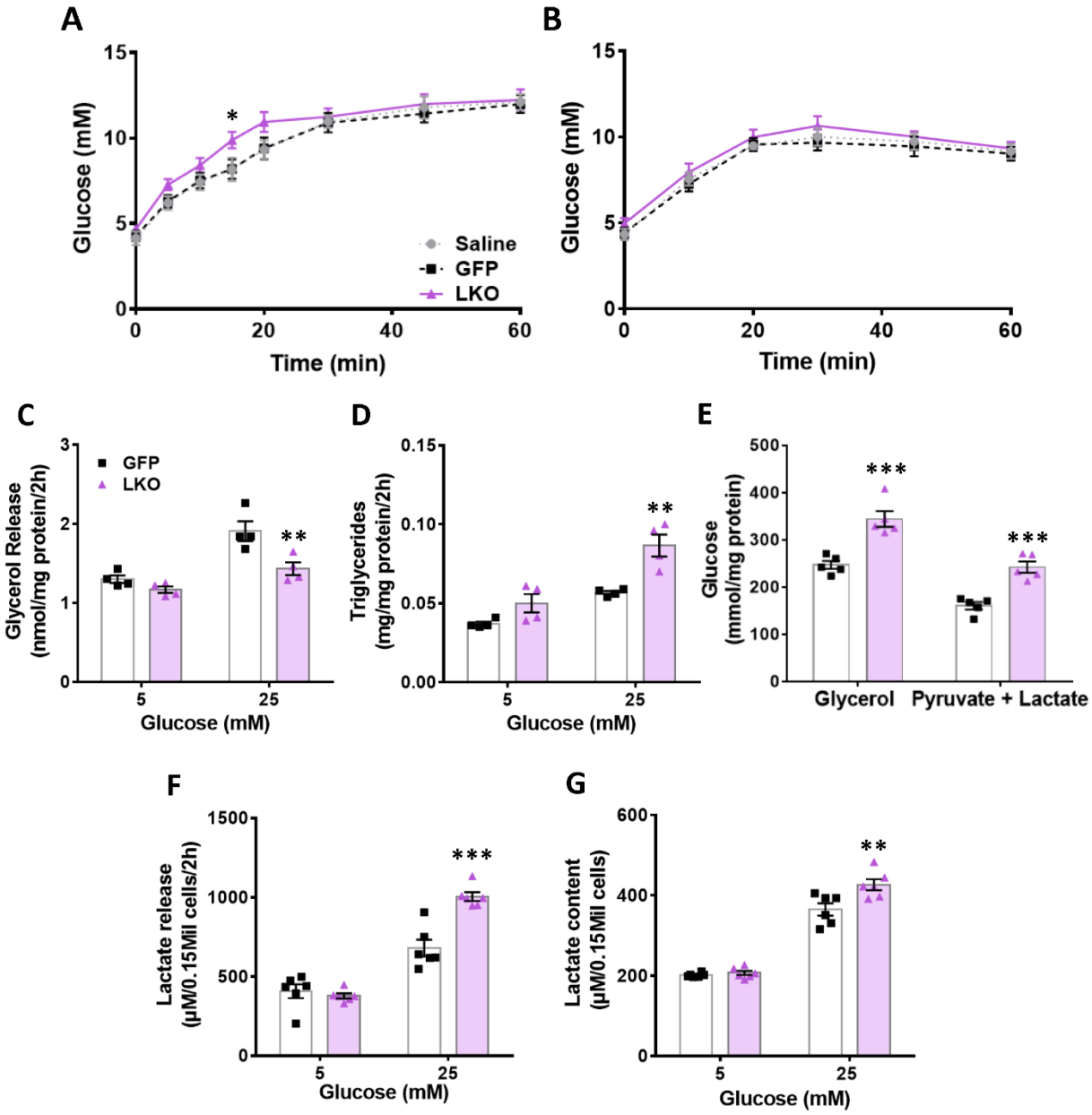
A
B
Glucose (mM)
Time (min)
Saline
GFP
LKO
C
D
E
Glycerol Release (nmol/mg protein/2h)
Triglycerides (mg/mg protein/2h)
Glucose (mmol/mg protein)
Glucose (mM)
Glycerol
Pyruvate + Lactate
F
G
Lactate release (μM/0.15Mil cells/2h)
Lactate content (μM/0.15Mil cells)

Figure 3.2. Isolated LKO hepatocytes show decreased glycerol release and increased TG content, glycolytic flux and gluconeogenesis.

Glycerol (5 mg/g BW, orally) and pyruvate (1 mg/g BW, i.p.) were administered to 16 h fasted LKO and control mice, and tail blood glycemia was measured. **(A)** Glycerol and **(B)** pyruvate load tests (saline, n=6; GFP, n=9; LKO, n=9). Means ± SEM; *$p < 0.05$ vs both controls; two-way ANOVA. Hepatocytes were isolated from LKO and control mice and incubated at 5 and 25 mM glucose, for measuring glycerol release, TG content and lactate content and release. For measuring gluconeogenesis, hepatocytes were glucose starved and incubated with 10 mM glycerol or 20 mM lactate plus 2 mM pyruvate. **(C)** Glycerol release, **(D)** triglyceride content, **(E)** gluconeogenesis from glycerol or pyruvate/lactate, **(F)** lactate release, **(G)** lactate content. n=4-6 per group as shown. *$p < 0.05$, **P < 0.01, and ***$p < 0.001$ vs. control using; one-way ANOVA.

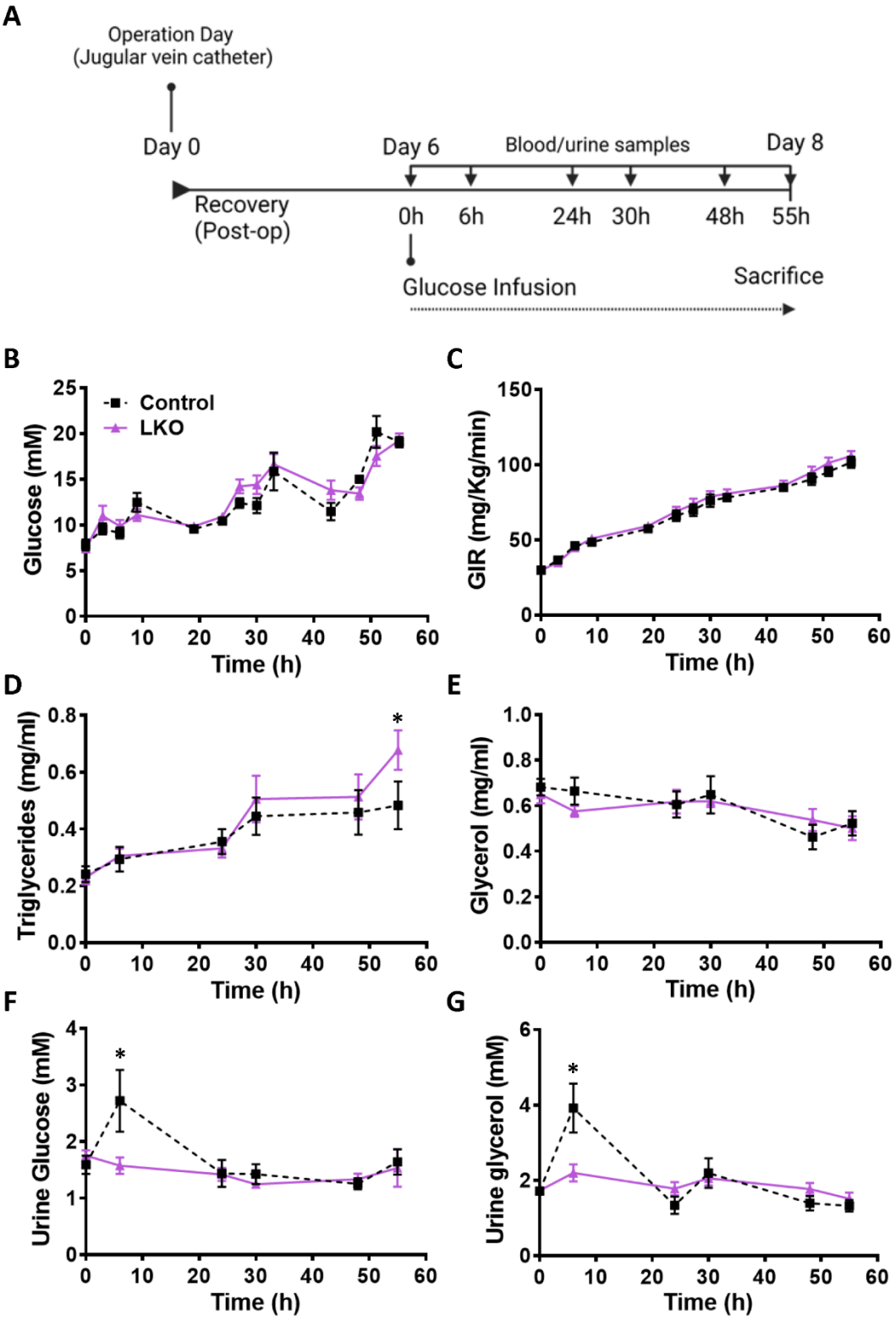
A
Operation Day
(Jugular vein catheter)
Day 0
Recovery
(Post-op)
Day 6
Blood/urine samples
Day 8
0h
6h
24h
30h
48h
55h
Glucose Infusion
Sacrifice
B
Control
LKO
Glucose (mM)
Time (h)
C
GIR (mg/Kg/min)
Time (h)
D
Triglycerides (mg/ml)
Time (h)
E
Glycerol (mg/ml)
Time (h)
F
Urine Glucose (mM)
Time (h)
G
Urine glycerol (mM)
Time (h)

Figure 3.3. *In vivo* glucose infusion causes increased plasma TG and reduced urine glycerol in LKO mice.

(A) Timeline of glucose infusion experiment. Mice were inserted with a catheter in the jugular vein and a continuous intravenous 55h infusion of glucose was maintained. Arterial blood and urine were collected twice a day. **(B)** Blood glucose and **(C)** glucose infusion rate (GIR) were monitored and the infusion rate was adjusted to maintain hyperglycemia. **(D)** Plasma TG. **(E)** Plasma glycerol. **(F)** Glucose in urine. **(G)** Glycerol in urine. Means ± SEM; control, n=6; LKO, n=8); *$p < 0.05$ vs control; Two-way ANOVA.

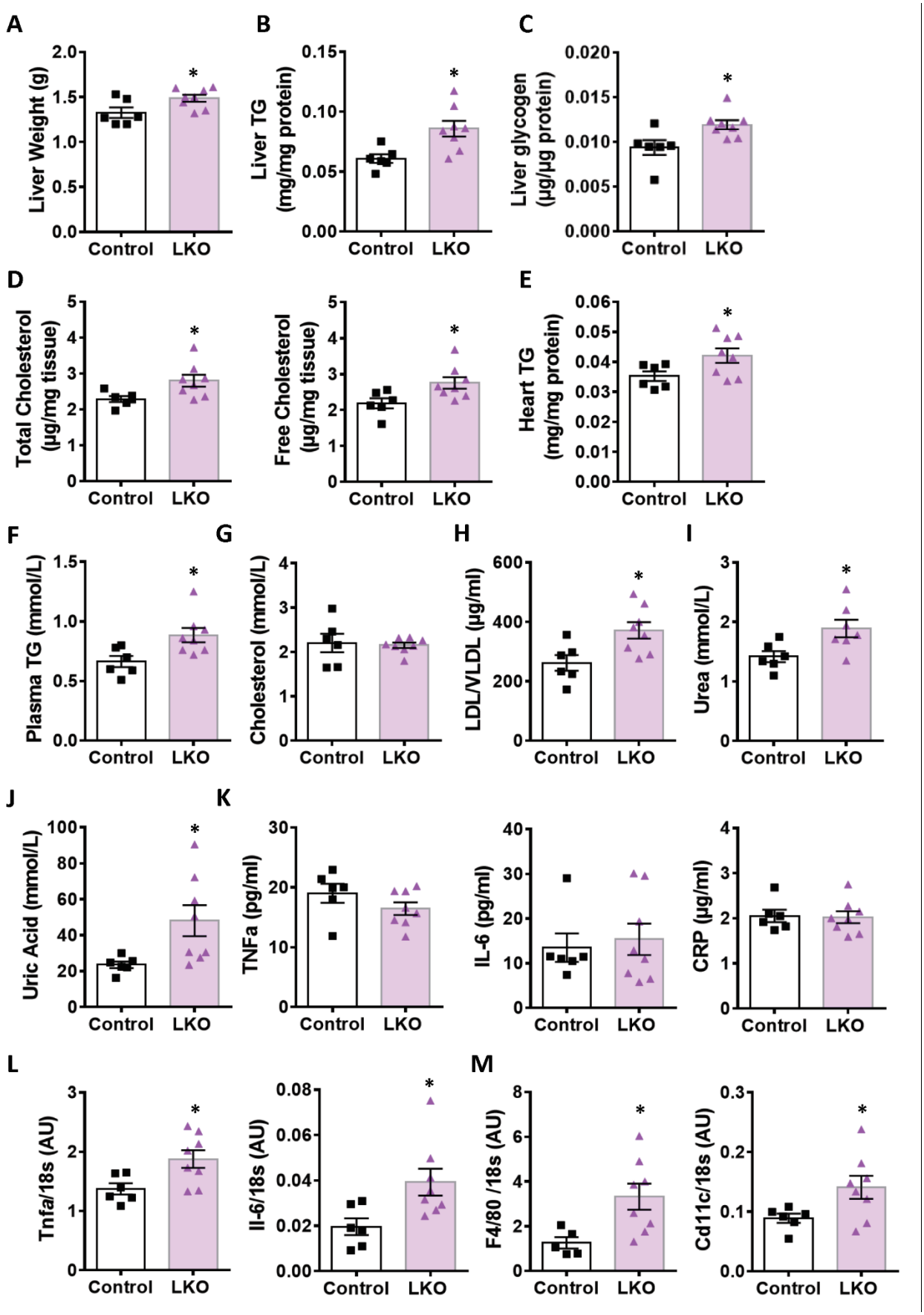
A
Liver Weight (g)
2.0
1.5
1.0
0.5
0.0
Control
LKO
B
Liver TG (mg/mg protein)
0.15
0.10
0.05
0.00
C
Liver glycogen (µg/µg protein)
0.020
0.015
0.010
0.005
0.000
D
Total Cholesterol (µg/mg tissue)
5
4
3
2
1
0
Free Cholesterol (µg/mg tissue)
E
Heart TG (mg/mg protein)
0.06
0.05
0.04
0.03
0.02
0.01
0.00
F
Plasma TG (mmol/L)
1.5
1.0
0.5
0.0
G
Cholesterol (mmol/L)
H
LDL/VLDL (µg/ml)
600
400
200
0
I
Urea (mmol/L)
J
Uric Acid (mmol/L)
100
80
60
40
20
0
K
TNFa (pg/ml)
30
20
10
0
IL-6 (pg/ml)
40
30
20
10
0
CRP (µg/ml)
4
3
2
1
0
L
Tnfa/18s (AU)
Il-6/18s (AU)
0.08
0.06
0.04
0.02
0.00
M
F4/80 /18s (AU)
8
6
4
2
0
Cd11c/18s (AU)
0.3
0.2
0.1
0.0

Figure 3.4. Liver and plasma analytes and inflammation-related liver gene expression in LKO and control mice under hyperglycemia.

(A) Liver weight, **(B)** TG content, **(C)** glycogen content, **(D)** total and free cholesterol. **(E)** Heart TG content. **(F)** Plasma TG, **(G)** cholesterol, **(H)** LDL/VLDL, **(I)** urea, **(J)** and uric acid. **(K)** Plasma inflammation markers: TNFα, IL-6 and C-reactive protein (CRP). **(L)** Liver cytokines mRNA expression of *Tnfa* and *Il-6*. **(M)** Liver mRNA markers of macrophages *F4/80* and *Cd11c*. Means ± SEM (Control, n=6; LKO, n=8). *$p < 0.05$ vs control; Student's *t* test.

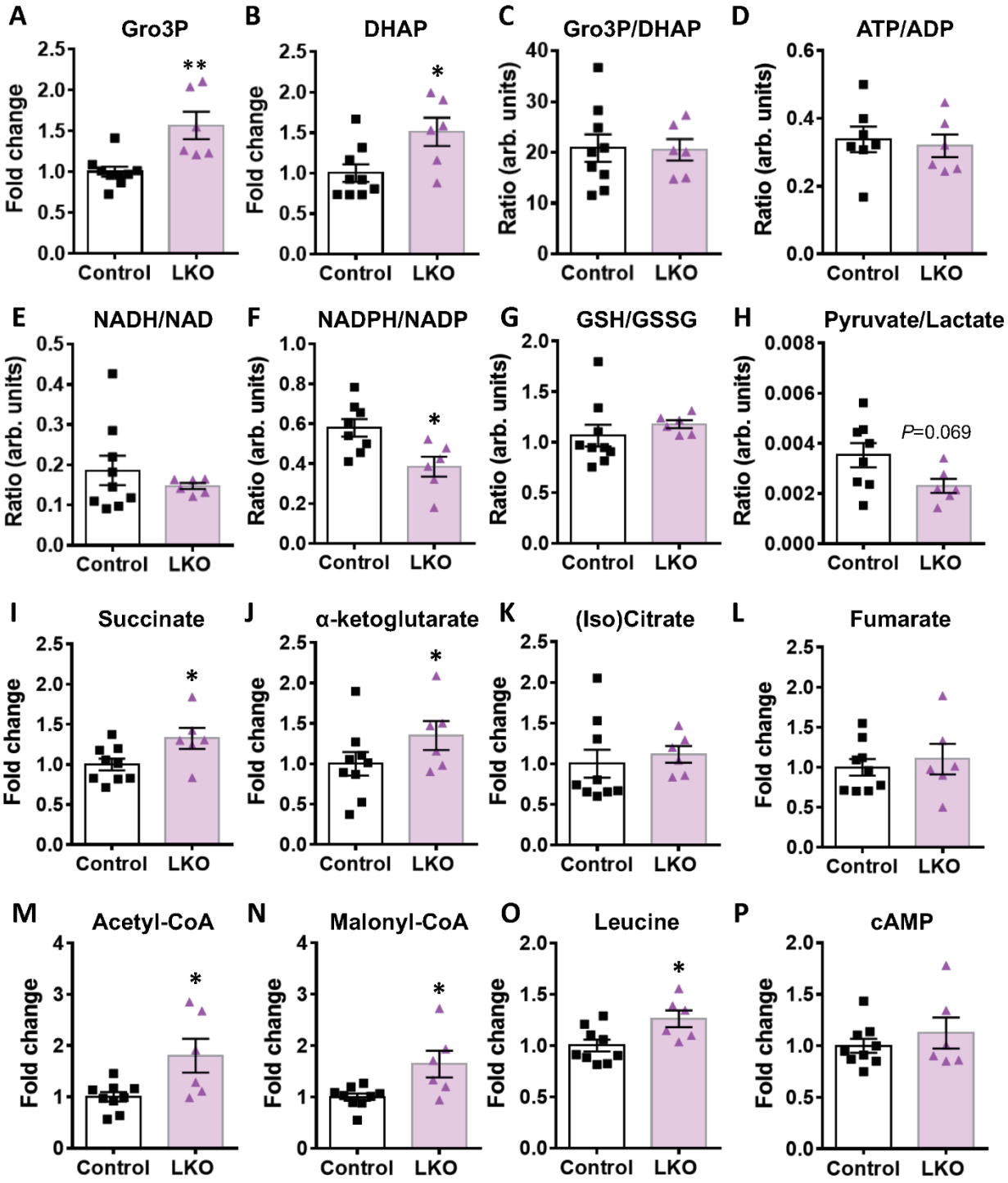
A
Gro3P
Fold change
Control
LKO
B
DHAP
C
Gro3P/DHAP
Ratio (arb. units)
D
ATP/ADP
E
NADH/NAD
F
NADPH/NADP
G
GSH/GSSG
H
Pyruvate/Lactate
P=0.069
I
Succinate
J
α-ketoglutarate
K
(Iso)Citrate
L
Fumarate
M
Acetyl-CoA
N
Malonyl-CoA
O
Leucine
P
cAMP

Figure 3.5. Targeted metabolomic analyses for LKO and control livers following glucose infusion.

The indicated metabolites are expressed as fold increase vs GFP control livers. The ratios of some metabolites and redox couples are shown. **(A)** Gro3P, **(B)** DHAP, **(C)** Gro3P/DHAP, **(D)** ATP/ADP, **(E)** NADH/NAD, **(F)** NADPH/NADP, **(G)** GSH/GSSG, **(H)** pyruvate/lactate, **(I)** succinate, **(J)** α-ketoglutarate, **(K)** (iso)citrate, **(L)** fumarate, **(M)** acetyl-CoA, **(N)** malonyl-CoA, **(O)** leucine and **(P)** cAMP. Means ± SEM (Control, n=9; LKO, n=6). $*p < 0.05$, $**p < 0.01$ vs GFP control; Student's *t* test.

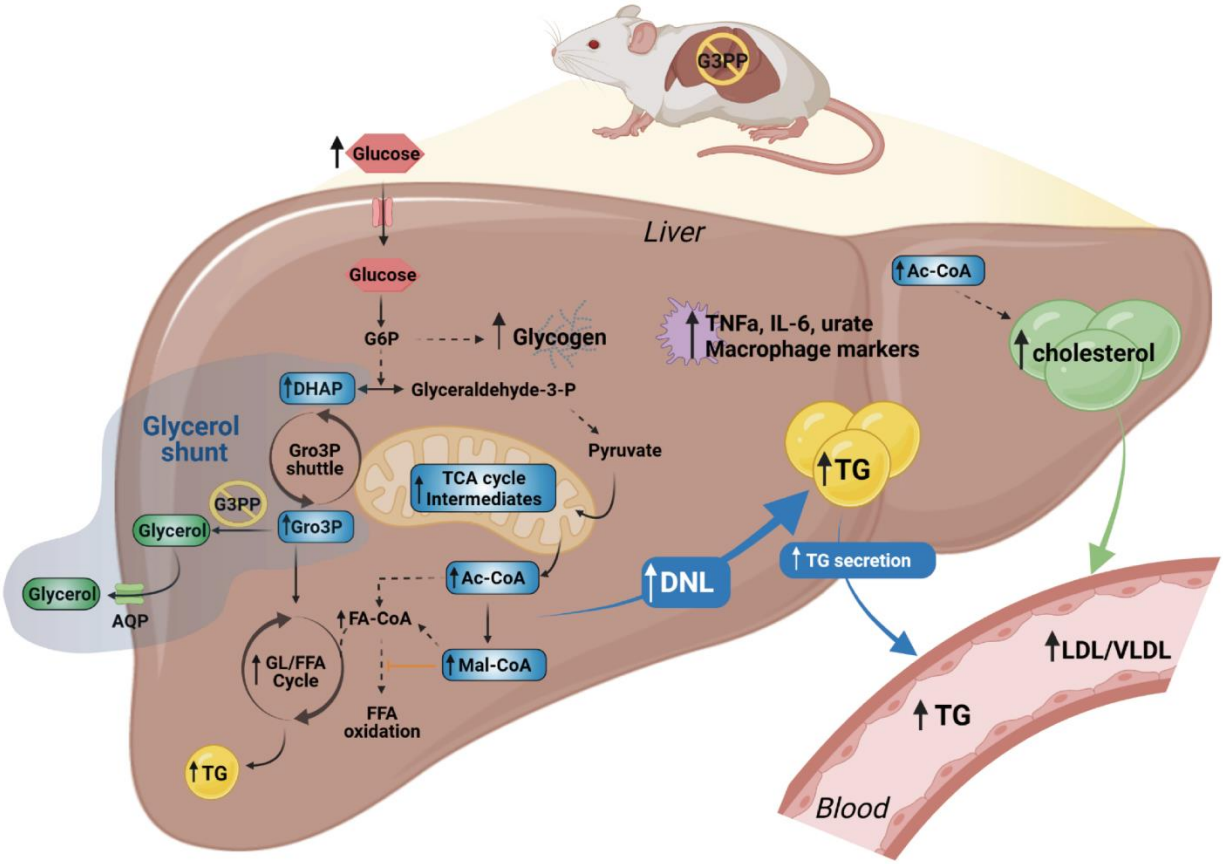

Figure 3.6. Model depicting the effect of G3PP hepatocyte-specific deletion and suppression of the glycerol shunt on liver metabolism under hyperglycemia.

The abbreviations are: Ac-CoA, acetyl-CoA; AQP, aquaglyceroporin; DHAP, dihydroxyacetone phosphate; FA-CoA, fatty acyl-CoA; FFA, free fatty acid; G3PP, glycerol 3-phosphate phosphatase; G6P, glucose 6-phosphate; GL/FFA cycle, glycerolipid/ free fatty acid cycle; Glyceraldehyde-3-P, glyceraldehyde-3-phosphate; Gro3P, glycerol 3-phosphate; Mal-CoA, malonyl-CoA; TCA cycle, tricarboxylic acid cycle; TG, triglyceride; LDL, low-density lipoproteins; VLDL, very low-density lipoproteins; DNL, *de novo* lipogenesis.

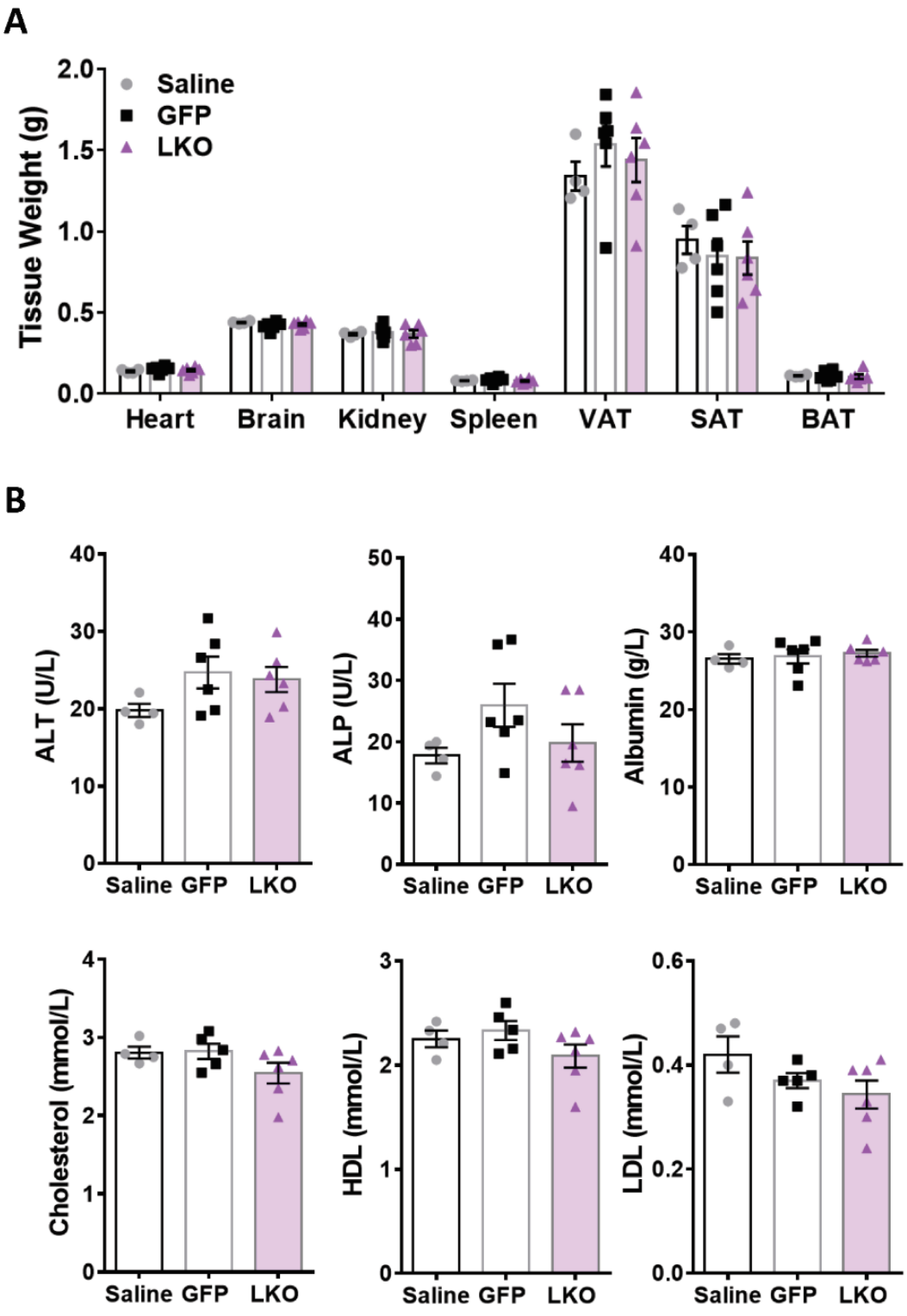
A
Tissue Weight (g)
2.0
1.5
1.0
0.5
0.0
Saline
GFP
LKO
Heart
Brain
Kidney
Spleen
VAT
SAT
BAT
B
ALT (U/L)
ALP (U/L)
Albumin (g/L)
Cholesterol (mmol/L)
HDL (mmol/L)
LDL (mmol/L)
Saline GFP LKO

Figure S3.1. Tissue weights and i*n vivo* plasma liver parameters in LKO and control mice.

Mice were kept on chow diet for 10 weeks after G3PP deletion following AAV injection. **(A)** Tissue weight: heart, brain, kidney, spleen, visceral adipose tissue (VAT), subcutaneous adipose tissue (SAT) and brown adipose tissue (BAT). **(B)** Liver plasma analytes: alanine transaminase (ALT), alkaline phosphatase (ALP), albumin, cholesterol, high-density lipoprotein (HDL) and low-density lipoproteins (LDL). (Saline control, n=4; GFP control, n=6; LKO, n=6). Means ± SEM; One-way ANOVA.

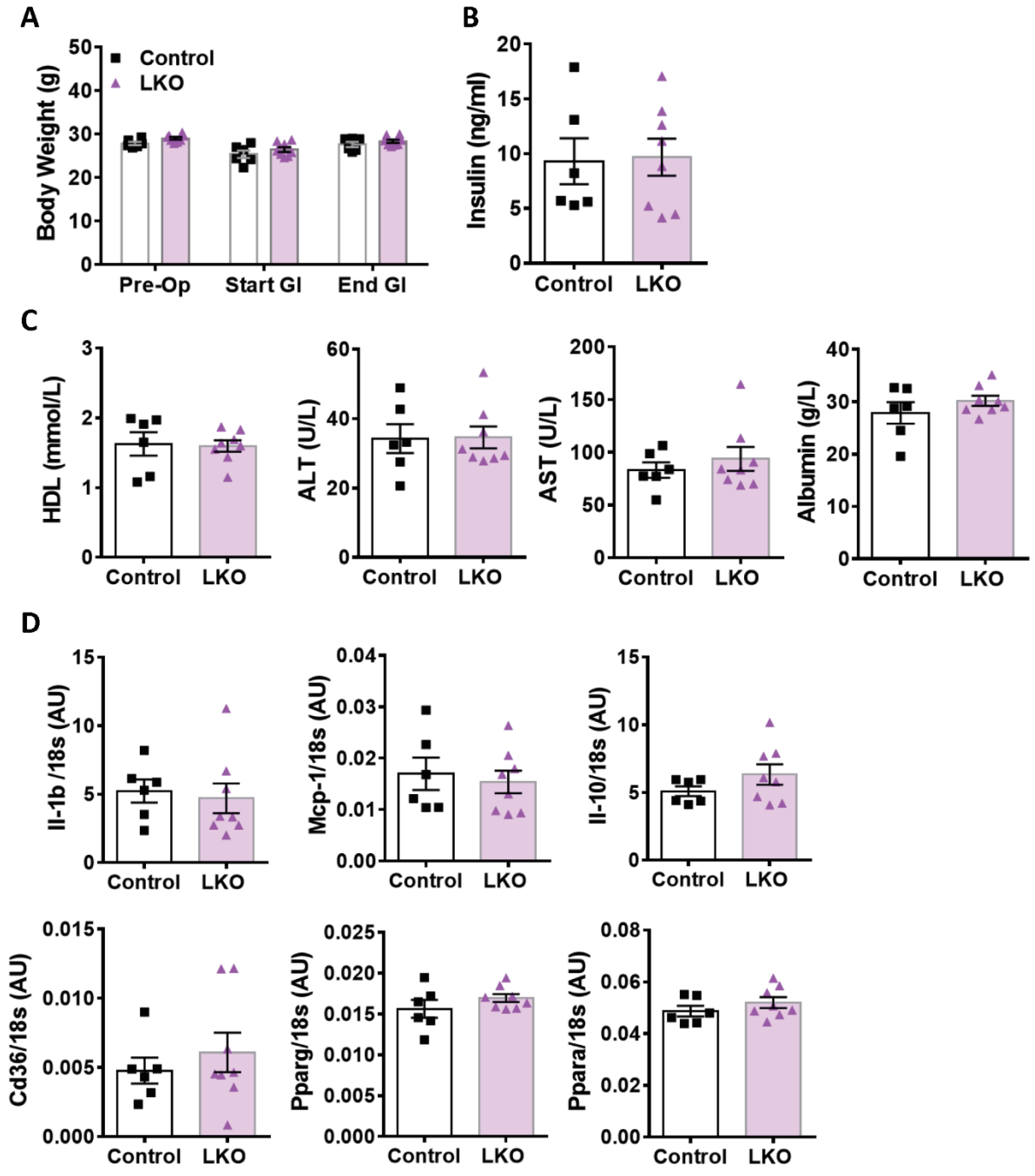

Figure S3.2. Liver function and inflammation parameters in glucose infused LKO and control mice.

(A) Body weight. **(B)** Insulinemia. **(C)** Liver plasma parameters: HDL, ALT, aspartate aminotransferase (AST) and albumin. **(D)** mRNA expression of *Il-1b, Mcp-1, Il-10, Cd36, Pparg* and *Ppara* in the livers. Means ± SEM; Control, n=6; LKO, n=8; Student's *t* test.

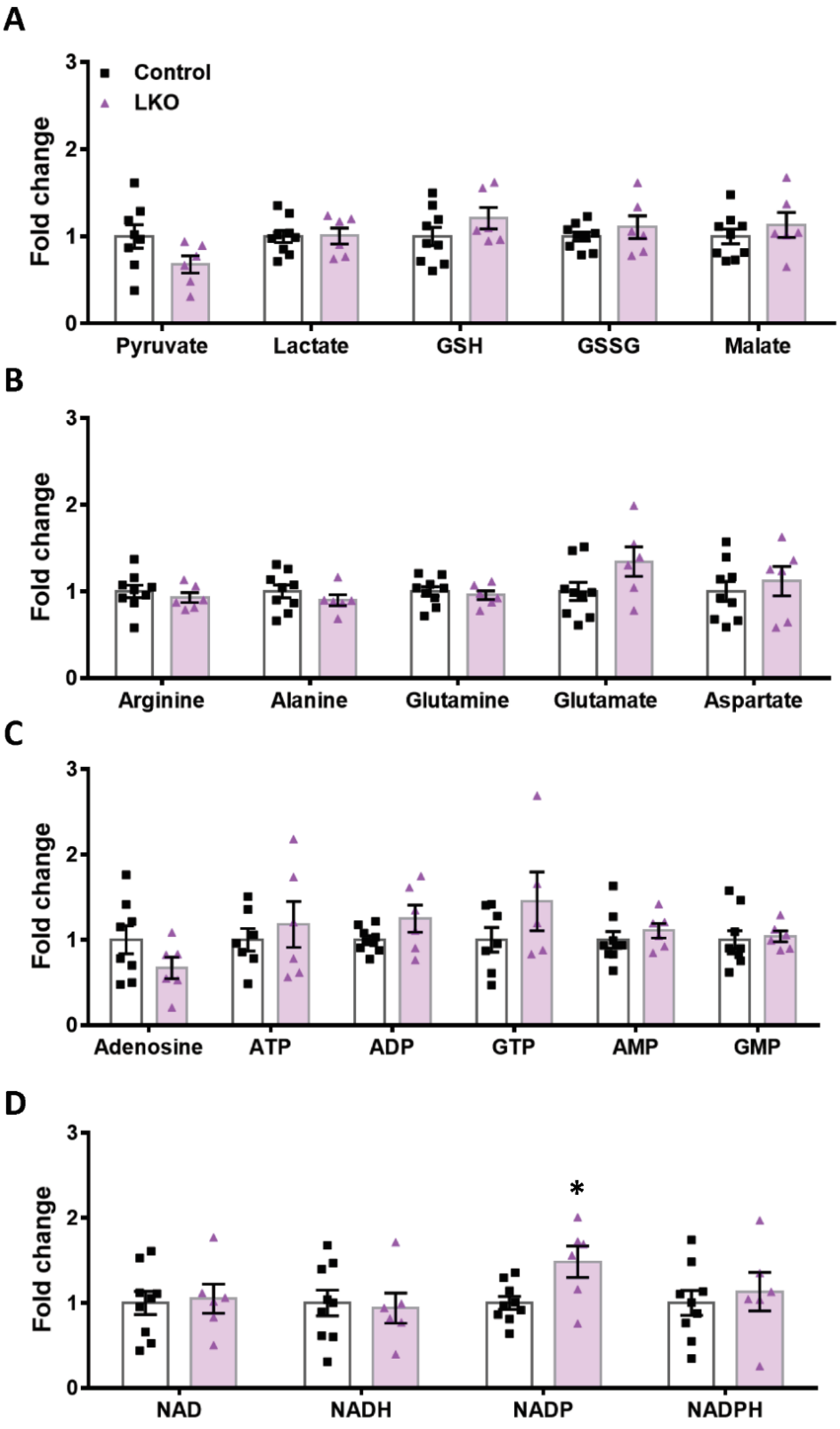
A
Control
LKO
Fold change
3
2
1
0
Pyruvate
Lactate
GSH
GSSG
Malate
B
Fold change
3
2
1
0
Arginine
Alanine
Glutamine
Glutamate
Aspartate
C
Fold change
3
2
1
0
Adenosine
ATP
ADP
GTP
AMP
GMP
D
Fold change
3
2
1
0
*
NAD
NADH
NADP
NADPH

Figure S3.3. Targeted metabolomics analyses in LKO and control livers following glucose infusion.

The indicated metabolites complement those shown in Figure 5 and are expressed as fold increase vs control livers. **(A)** pyruvate, lactate, GSH, GSSG and malate, **(B)** arginine, alanine, glutamine, glutamate and aspartate, **(C)** adenosine, ATP, ADP, GTP, AMP and GMP, **(D)** NAD, NADH, NADP and NADPH. Means ± SEM (Control, n=9; LKO, n=6). *$p < 0.05$ vs control; Student's *t* test.

Table S3.1. Primer sequences used for RT-PCR.

Gene	Primer sequences (5'-3')
Il-6	F:TAGTCCTTCCTACCCCAATTTCC
	R:TTGGTCCTTAGCCACTCCTTC
F4/80	F:TGACTCACCTTGTGGTCCTAA
	R:CTTCCCAGAATCCAGTCTTTCC
Cd11c	F:GTGCTGAGTTCGGACACAGT
	R:AGAGGCCACCTATTTGGTTAGT
Il-10	F:CTTACTGACTGGCATGAGGATCA
	R:GCAGCTCTAGGAGCATGTGG
Tnfa	F:CCAAGGCGCCACATCTCCCT
	R:GCTTTCTGTGCTCATGGTGT
Pparg	F:GGTCAGCTCTTGTGAATGGAA
	R:ATCAGCTCTGTGGACCTCTCC
Ppara	F:GGCCATACACAAGGTCTCCAT
	R:AGAGAATCCACGAAGCCTACC
Mcp-1	F:TAAAAACCTGGATCGGAACCAAA
	R:GCATTAGCTTCAGATTTACGGGT
Il-1B	F:GCAACTGTTCCTGAACTCAACT
	R:ATCTTTTGGGGTCCGTCAACT
Cd36	F:AGGTCTATCTACGCTGTGTTCG
	R:CAATGGTTGTCTGGATTCTGG
18s	F:CTGAGAAACGGCTAGCACATC
	R:GGCCTCGAAAGAGTCCTGTAT

References:

Al-Mass, A., Poursharifi, P., Peyot, M. L., Lussier, R., Levens, E. J., Guida, J., . . . Prentki, M. (2022). Glycerol-3-phosphate phosphatase operates a glycerol shunt in pancreatic beta-cells that controls insulin secretion and metabolic stress. *Mol Metab*, 101471.

Arguello, G., Balboa, E., Arrese, M., & Zanlungo, S. (2015). Recent insights on the role of cholesterol in non-alcoholic fatty liver disease. *Biochim Biophys Acta, 1852*(9), 1765-1778.

Bekkevold, C. M., Robertson, K. L., Reinhard, M. K., Battles, A. H., & Rowland, N. E. (2013). Dehydration parameters and standards for laboratory mice. *J Am Assoc Lab Anim Sci, 52*(3), 233-239.

Birkenfeld, A. L., & Shulman, G. I. (2014). Nonalcoholic fatty liver disease, hepatic insulin resistance, and type 2 diabetes. *Hepatology, 59*(2), 713-723.

Bugianesi, E., Moscatiello, S., Ciaravella, M. F., & Marchesini, G. (2010). Insulin resistance in nonalcoholic fatty liver disease. *Curr Pharm Des, 16*(17), 1941-1951.

Cassim, S., Raymond, V. A., Lacoste, B., Lapierre, P., & Bilodeau, M. (2018). Metabolite profiling identifies a signature of tumorigenicity in hepatocellular carcinoma. *Oncotarget, 9*(42), 26868-26883.

Chen, Y., Varghese, Z., & Ruan, X. Z. (2014). The molecular pathogenic role of inflammatory stress in dysregulation of lipid homeostasis and hepatic steatosis. *Genes Dis, 1*(1), 106-112.

Chew, J. L., & Chua, K. Y. (2003). Collection of mouse urine for bioassays. *Lab Anim (NY), 32*(7), 48-50.

Cho, E. H. (2018). Succinate as a Regulator of Hepatic Stellate Cells in Liver Fibrosis. *Front Endocrinol (Lausanne), 9*, 455.

Day, C. P., & James, O. F. (1998). Hepatic steatosis: innocent bystander or guilty party? *Hepatology, 27*(6), 1463-1466.

Duseja, A., & Chalasani, N. (2013). Epidemiology and risk factors of nonalcoholic fatty liver disease (NAFLD). *Hepatol Int, 7 Suppl 2*, 755-764.

Esler, W. P., & Bence, K. K. (2019). Metabolic Targets in Nonalcoholic Fatty Liver Disease. *Cell Mol Gastroenterol Hepatol, 8*(2), 247-267.

Gerich, J. E., Meyer, C., Woerle, H. J., & Stumvoll, M. (2001). Renal gluconeogenesis: its importance in human glucose homeostasis. *Diabetes Care, 24*(2), 382-391.

Huang, T. D., Behary, J., & Zekry, A. (2019). Non-alcoholic fatty liver disease (NAFLD): a review of epidemiology, risk factors, diagnosis and management. *Intern Med J*.

Huang, T. D., Behary, J., & Zekry, A. (2020). Non-alcoholic fatty liver disease: a review of epidemiology, risk factors, diagnosis and management. *Intern Med J, 50*(9), 1038-1047.

Itoh, M., Suganami, T., Kato, H., Kanai, S., Shirakawa, I., Sakai, T., . . . Ogawa, Y. (2017). CD11c+ resident macrophages drive hepatocyte death-triggered liver fibrosis in a murine model of nonalcoholic steatohepatitis. *JCI Insight, 2*(22).

Kitade, H., Chen, G., Ni, Y., & Ota, T. (2017). Nonalcoholic Fatty Liver Disease and Insulin Resistance: New Insights and Potential New Treatments. *Nutrients, 9*(4).

Lake, A. D., Novak, P., Shipkova, P., Aranibar, N., Robertson, D. G., Reily, M. D., . . . Cherrington, N. J. (2015). Branched chain amino acid metabolism profiles in progressive human nonalcoholic fatty liver disease. *Amino Acids, 47*(3), 603-615.

Leyva, F., Wingrove, C. S., Godsland, I. F., & Stevenson, J. C. (1998). The glycolytic pathway to coronary heart disease: a hypothesis. *Metabolism, 47*(6), 657-662.

Lin, E. C. (1977). Glycerol utilization and its regulation in mammals. *Annu Rev Biochem, 46*, 765-795.

Liu, X., Zhang, H., & Liang, J. (2013). Blood urea nitrogen is elevated in patients with non-alcoholic fatty liver disease. *Hepatogastroenterology, 60*(122), 343-345.

Matsuzawa, N., Takamura, T., Kurita, S., Misu, H., Ota, T., Ando, H., . . . Kaneko, S. (2007). Lipid-induced oxidative stress causes steatohepatitis in mice fed an atherogenic diet. *Hepatology, 46*(5), 1392-1403.

Mills, E., & O'Neill, L. A. (2014). Succinate: a metabolic signal in inflammation. *Trends Cell Biol, 24*(5), 313-320.

Mugabo, Y., Zhao, S., Seifried, A., Gezzar, S., Al-Mass, A., Zhang, D., . . . Prentki, M. (2016). Identification of a mammalian glycerol-3-phosphate phosphatase: role in metabolism and signaling in pancreatic beta-cells and hepatocytes. *Proc Natl Acad Sci U S A, 113*(4), E430-439.

Nolan, C. J., & Prentki, M. (2019). Insulin resistance and insulin hypersecretion in the metabolic syndrome and type 2 diabetes: time for a conceptual framework shift. *Diab Vasc Dis Res, 16*(2), 118-127.

Oberhauser, L., & Maechler, P. (2021). Lipid-Induced Adaptations of the Pancreatic Beta-Cell to Glucotoxic Conditions Sustain Insulin Secretion. *Int J Mol Sci, 23*(1).

Ochoa-Sanchez, R., Oliveira, M. M., Tremblay, M., Petrazzo, G., Pant, A., Bosoi, C. R., . . . Rose, C. F. (2021). Genetically engineered E. coli Nissle attenuates hyperammonemia and prevents memory impairment in bile-duct ligated rats. *Liver Int, 41*(5), 1020-1032.

Odegaard, J. I., Ricardo-Gonzalez, R. R., Red Eagle, A., Vats, D., Morel, C. R., Goforth, M. H., . . . Chawla, A. (2008). Alternative M2 activation of Kupffer cells by PPARdelta ameliorates obesity-induced insulin resistance. *Cell Metab, 7*(6), 496-507.

Oral, A., Sahin, T., Turker, F., & Kocak, E. (2019). Relationship Between Serum Uric Acid Levels and Nonalcoholic Fatty Liver Disease in Non-Obese Patients. *Medicina (Kaunas), 55*(9).

Possik, E., Al-Mass, A., Peyot, M. L., Ahmad, R., Al-Mulla, F., Madiraju, S. R. M., & Prentki, M. (2021). New mammalian glycerol-3-phosphate phosphatase: role in beta-cell, liver and adipocyte metabolism. *Front Endocrinol (Lausanne), 12*, 706607.

Possik, E., Madiraju, S. R. M., & Prentki, M. (2017). Glycerol-3-phosphate phosphatase/PGP: role in intermediary metabolism and target for cardiometabolic diseases. *Biochimie, 143*, 18-28.

Possik, E., Schmitt, C., Al-Mass, A., Bai, Y., Cote, L., Morin, J., . . . Prentki, M. (2022). Phosphoglycolate phosphatase homologs act as glycerol-3-phosphate phosphatase to control stress and healthspan in C. elegans. *Nat Commun, 13*(1), 177.

Poursharifi, P., Attane, C., Mugabo, Y., Al-Mass, A., Ghosh, A., Schmitt, C., . . . Prentki, M. (2020). Adipose ABHD6 regulates tolerance to cold and thermogenic programs. *JCI Insight, 5*(24).

Prentki, M., Corkey, B. E., & Madiraju, S. R. M. (2020). Lipid-associated metabolic signalling networks in pancreatic beta cell function. *Diabetologia, 63*(1), 10-20.

Prentki, M., & Madiraju, S. R. (2008). Glycerolipid metabolism and signaling in health and disease. *Endocr Rev, 29*(6), 647-676.

Prentki, M., & Madiraju, S. R. (2012). Glycerolipid/free fatty acid cycle and islet beta-cell function in health, obesity and diabetes. *Mol Cell Endocrinol, 353*(1-2), 88-100.

Prentki, M., Matschinsky, F. M., & Madiraju, S. R. (2013). Metabolic signaling in fuel-induced insulin secretion. *Cell Metab, 18*(2), 162-185.

Prentki, M., & Nolan, C. J. (2006). Islet beta cell failure in type 2 diabetes. *J Clin Invest, 116*(7), 1802-1812.

Prentki, M., Peyot, M. L., Masiello, P., & Madiraju, S. R. M. (2020). Nutrient-induced metabolic stress, adaptation, detoxification, and toxicity in the pancreatic beta-cell. *Diabetes, 69*(3), 279-290.

Shi, D., Allewell, N. M., & Tuchman, M. (2015). The N-Acetylglutamate Synthase Family: Structures, Function and Mechanisms. *Int J Mol Sci, 16*(6), 13004-13022.

Wang, Y., Kwon, H., Su, X., & Wondisford, F. E. (2020). Glycerol not lactate is the major net carbon source for gluconeogenesis in mice during both short and prolonged fasting. *Mol Metab, 31*, 36-44.

Yan, Z., Yan, H., & Ou, H. (2012). Human thyroxine binding globulin (TBG) promoter directs efficient and sustaining transgene expression in liver-specific pattern. *Gene, 506*(2), 289-294.

Zechner, R., Zimmermann, R., Eichmann, T. O., Kohlwein, S. D., Haemmerle, G., Lass, A., & Madeo, F. (2012). Fat signals--lipases and lipolysis in lipid metabolism and signaling. *Cell Metab, 15*(3), 279-291.

Zhao, L., Guo, X., Wang, O., Zhang, H., Wang, Y., Zhou, F., . . . Ji, B. (2016). Fructose and glucose combined with free fatty acids induce metabolic disorders in HepG2 cell: A new model to study the impacts of high-fructose/sucrose and high-fat diets in vitro. *Mol Nutr Food Res, 60*(4), 909-921.

Bridging Chapters III and IV

Results from Chapter III showed G3PP plays a role in glucodetoxification in the liver and it could play an important role in NAFLD progression. My colleagues had previously shown that overexpression of human G3PP (hG3PP) in rat liver *in vivo*, using an adenoviral construct, lowered body weight gain, hepatic glucose production and plasma triglycerides and increased plasms HDL in animals that were fed standard rat chow. However, these observations were made in short-term studies using the adenoviral construct and G3PP expression was increased more than 100 fold in rat liver. Thus, in this chapter I aimed to examine if controlled overexpression of G3PP affect glucose and lipid metabolism and protects against metabolic stress in mouse hepatocytes *in vivo*. To do so I studied the effects of G3PP protein overexpression at a level close to physiological increase over a longer time period using Adeno-associated virus 8 (AAV8) that expressed human *PGP* (gene name for G3PP) under the control of the thyroid hormone-binding globulin (TBG) promoter to increase G3PP expression in hepatocytes by approximately 3 fold. In this study, I used the same experimental design as in Chapter III.

Chapter IV: Role of Glycerol-3-phosphate phosphatase (G3PP) overexpression in liver

Anfal Al-Mass[1,2], Pegah Poursharifi[2], Marie-Line Peyot[2], Roxane Lussier[2], Isabelle Chenier[2], Abel Oppong[2], S. R. Murthy Madiraju[2], Robert Sladek[1], Marc Prentki[2*]

[1] Department of Medicine, McGill University, Montréal, QC, Canada.

[2] Departments of Nutrition, Biochemistry and Molecular Medicine, University of Montreal, and Montreal Diabetes Research Center, Centre de Recherche du Centre Hospitalier de l'Université de Montréal (CRCHUM), Montréal, QC, Canada.

***Corresponding author:**
Marc Prentki, PhD
Professor of Nutrition, Biochemistry and Molecular Medicine, Université de Montréal
Room R08-412, Tour Viger, 900 rue Saint Denis
Montreal, QC H2X 0A9, Canada.
Email: marc.prentki@umontreal.ca

4.1 Abstract:

Overexpression of the recently identified glycerol-3-phosphate (Gro3P) phosphatase (called G3PP and encoded by the *PGP* gene) in mammalian cells was shown to affect liver intermediary metabolism by controlling the levels of Gro3P under elevated glucose concentrations *ex vivo* and *in vivo*. The *ex vivo* studies were performed using around 100 fold overexpression of G3PP protein in primary rat hepatocytes, which may not represent the G3PP levels found in cells under physiologic conditions. In this study we examined the effect of 3-4 fold overexpression of G3PP in mouse hepatocytes *in vivo* using an adeno-associated virus (AAV8-TBG-hPGP) under normal and hyperglycemic conditions. We found that a 3 fold increase in G3PP protein expression levels leads to a 1.3 fold decrease in lactate release *ex vivo*; but has no major effect of liver metabolism *in vivo*. In our studies, we were unable to confirm that overexpression of G3PP protein led to increased G3PP activity in primary hepatocytes (or hepatocytes *in vivo*). This could reflect the lack of sensitivity of the assays used to measure G3PP activity or the presence of metabolic compensation by the liver. We conclude that a higher level of G3PP overexpression is needed to study the effects of G3PP in liver *in vivo* using transgenic mice or G3PP activator in the future.

4.2 Introduction:

The liver is the main organ that converts glucose and fructose to fatty acid and triglycerides (TG) (Yki-Jarvinen 2014, Han, Kang et al. 2016), which are then either stored as TG in lipid droplets or packaged and secreted in very low density lipoprotein (VLDL) that are transported to white adipose tissue and other tissues for storage. Under conditions where hyperglycemia persists, such as type 2 diabetes (T2D), increased hepatic glucose uptake leads to excessive fat accumulation, insulin resistance, and the progression of non-alcoholic fatty liver disease (NAFLD) (Bugianesi, Moscatiello et al. 2010, Birkenfeld and Shulman 2014, Huang, Behary et al. 2019). Glycerol-3-phosphate phosphatase (G3PP) activity has been shown to be more significant under conditions where glucose concentration is high in the liver and pancreatic β-cell (see results in Chapters 2 and 3) (Mugabo, Zhao et al. 2016, Possik, Al-Mass et al. 2021). By hydrolyzing glycerol-3-phosphate (Gro3P) to glycerol, G3PP can control cytosolic levels of Gro3P and directing glucose carbons away from lipogenesis. This highlights the role of G3PP as a detoxification enzyme under metabolically stressful conditions (Mugabo, Zhao et al. 2016, Possik, Al-Mass et al. 2021). In particular, elevated activity of human G3PP (hG3PP) *ex vivo* was shown to decrease TG content, gluconeogenesis and elevated glycerol release in rat primary hepatocytes and to reduce glucose stimulated insulin secretion in β-cells and protect them from glucolipotoxicity. Overexpression of hG3PP in rat liver *in vivo*, using an adenoviral construct, lowered body weight gain, hepatic glucose production and plasma triglycerides and increased plasms HDL in animals that were fed standard rat chow (Mugabo, Zhao et al. 2016).

One limitation of these short-term studies is that the adenoviral construct used *in vivo* resulted in G3PP expression being increased more than 100-fold in rat liver. Thus, in this project we aimed to study the effects of G3PP protein overexpression that is close to physiological increase over a longer time period. To do so we developed a hepatocyte specific hG3PP overexpression mouse model (LOVX) using Adeno-associated virus 8 (AAV8) that expressed human PGP (gene name for G3PP) under the control of the thyroid hormone-binding globulin (TBG) promoter (Yan, Yan et al. 2012) to increase G3PP expression in hepatocytes by approximately 3 fold. Using this model, we investigated the role of chronic G3PP overexpression in the liver under normal and hyperglycemic conditions.

4.3 Methodology:

Animals. At 8 weeks of age, male C57BL/6N (WT) (Charles River Laboratories) mice received a single injection (1.5×10^{11} GC/mice) of AAV8-TBG-h*PGP* (Vector Biolabs: VB1724) or AAV8-TBG-eGFP (Vector Biolabs: VB1743) by tail vein or a control injection of saline containing no virus **(Figure 4.1*A*)**. The AAV8 construct expresses h*PGP* or eGFP under the control of the TBG promoter, which is hepatocyte specific (Yan, Yan et al. 2012). Mice were placed in individual cages and fed a standard chow diet (15% fat by energy; Harlan Teklad, Madison, WI, USA) for 10 weeks. Body weight and food intake were measured weekly. All procedures were approved by the institutional committee for the protection of animals (Comité Institutionnel de Protection des Animaux du Centre Hospitalier de l'Université de Montréal).

Model validation. Four weeks after AAV infection, mouse tissues like heart, brain, skeletal muscle (SM) and isolated hepatocytes (see 2.5 below for protocol) were collected at necropsy and lysed in RIPA buffer (10 mM Tris-HCl, 1 mM EDTA, 0.5 mM EGTA, 1% Triton X-100, 0.1% sodium deoxycholate, 0.1% sodium dodecylsulfate and 140 mM NaCl) plus phenylmethylsulfonyl fruoride benzylsulfonyl fluoride (PMSF) and ALP cocktail (aprotinin, leupeptin and pepstatin) protease inhibitors. After sonication and centrifugations (13000 rpm for 20 min), protein extracts were used for western blot analysis to validate hepatocyte-specific G3PP overexpression (G3PP primary Antibody: PGP Antibody (E-10) (sc-390883), secondary Antibody. m-IgGκ BP-HRP (sc-516102) both from Santa Cruz). For all tissues, α-tubulin was used as the gel loading control.

Oral Glycerol Load Test. 4 weeks after AAV infection, food was withdrawn from mice for 16 h. Then, 87% (wt/vol) glycerol (5 mg/g BW) was administered orally. Blood glucose was measured from the tail vein at baseline and 5, 10, 15, 20, 30, 45, and 60 min after glycerol load using a glucometer (Bayer Contour).

Pyruvate Load Test. 6 weeks after AAV infection, food was withdrawn from the mice for 16 h. Then, Pyruvate (1 mg/g BW) was Injected IP. Blood glucose was measured from the tail vein at baseline and 5, 10, 15, 20, 30, 45, and 60 min after pyruvate load, and blood glucose was measured by using a glucometer.

Hepatocyte Isolation. Four weeks after AAV infection, hepatocytes were isolated from mice by in situ collagenase (type XI; Sigma) perfusion and using Percoll (Sigma P-1644) gradient to

separate hepatocyte from other cell type in the liver extract. were seeded in DMEM complete media (Sigma D5030) (pH 7.4) without phenol red, supplemented with 3.7g/L of sodium bicarbonate, 5mM glucose, 1mM sodium pyruvate, 2mM glutamine, Penicillin Streptomycin, 0.2% BSA, 1nM insulin and 100nM Dexamethasone) using Collagen I, Coated Plate (A11428-01) (Mugabo, Zhao et al. 2016). *Ex-vivo* experiments were done after 16h of seeding.

Gluconeogenesis in Hepatocytes. After 16h of seeding, primary hepatocytes were washed with PBS solution twice and starved in DMEM without glucose for 3h and then washed with PBS solution, followed by incubation for 3h in glucose production buffer consisting of glucose-free DMEM (pH 7.4) without phenol red, supplemented with 15 mM Hepes and 2 mM L-glutamine, with 10 mM glycerol or 20 mM sodium lactate plus 2 mM sodium pyruvate. Then, the medium was processed for glucose measurement (Autokit Glucose; Wako) and cells were collected for protein (Mugabo, Zhao et al. 2016).

***Ex-vivo* TG, glycerol and lactate.** After 16h, primary hepatocytes were washed with PBS solution and then incubated in DMEM complete media with 5 or 25mM glucose for 2h. Media and cells were collected to measure TG content, glycerol release, lactate content and lactate release. Glycerol release was determined in the media by a radiometric glycerol assay (Bradley and Kaslow 1989) using [γ-32P]ATP and glycerokinase. For TG content, lipid extraction was preformed and TG was measured using Triglyceride kit (Sigma-Aldrich cat: T2449). For lactate content and lactate release was done as described in (Mugabo, Zhao et al. 2016).

***In vivo* glucose infusion.** Four weeks after infection with AAV8-TBG-hPGP (LOVX) or AAV8-TBG-eGFP (control), mice right jugular vein was cannulated 5 days before the beginning of infusion. Mice were given a SC injection of carprofen (20mg/kg) before surgery combined with a SC injection of saline (around 3ml) and anesthetised with isoflurane. Cages were placed on a heating pad with a cold spot (1/3 cold). Diet gel (DietGel 31M: 72-08-5022) was given to the mice during the post-op period with pellets in the bottom of the cages for the entire time. In the post-op period, mice were infused with 5U heparinized saline (7µl/hr) to make sure the jugular vein cannula remained patent. On day 1 post op mice were given a second injection of carprofen (20mg/kg) and 3ml of saline. During post op, hydration was verified daily, and saline was given if needed. Fresh diet gel was also given daily. On the first day of infusion, mice were infused with dextrose 70% with the glucose infusion rate (GIR) starting at 30 mg/kg/min and adjusted every 3h

during the day and once during the night to maintain glycemia at a predetermined hyperglycemic level (14-16mM). During the infusion, blood and urine were collected twice during the day. The infusion ended after 55h; and blood, liver and heart were collected at necropsy.

Liver TG content. Liver was collected and snap frozen in liquid nitrogen. Liver then was homogenized and sonicated and TG was measured after lipid extraction (Mugabo, Zhao et al. 2016) using triglyceride reagent (Sigma-Aldrich cat: T2449).

Plasma parameters. Lipid profile (Cobas kits used: cholesterol, ref: 04718917 190; triglycerides (TGs), ref: 04657594 190; high density lipoproteins (HDL), ref: 07528604 190; low density lipoproteins (LDL), ref: 07005806 190) and liver function markers (Cobas kits used: alanine aminotransferase (ALT), ref: 04718569 190; alkaline phosphatase (ALP), ref: 04657373 190; albumin, ref: 04657357 190; aspartate aminotransferase (AST), ref: 04657543 190; bilirubin, ref: 05589134 190) were measured in the plasma from glucose-infused mice using a Cobas C111 analyzer (Roche, Switzerland). (Ochoa-Sanchez, Oliveira et al. 2021).

Statistical analyses. Data were analyzed using GraphPad Prism 6 (GraphPad Software, San Diego, CA). Results are expressed as means ± SEM. Statistical differences between two groups were assessed using an unpaired, two-tailed Student's *t* test, and between multiple groups using one-way or two-way analyses of variance (ANOVA) with Bonferroni correction for multiple testing, as indicated. A p value < 0.05 was considered statistically significant.

4.4 Results:

G3PP 3 fold protein overexpression in mice hepatocytes show no major phenotype *in vivo* under normal diet.

To validate the LOVX model, we confirmed that G3PP protein levels were about 3 fold higher in hepatocytes compared to control hepatocytes (LOVX 0.7334 ± 0.02137, n=4 vs GFP 0.2589 ± 0.005034, n=4, $p = 0.0001$) and no changes in protein levels in different tissues (whole heart, brain, and skeletal muscle) 4 weeks following AAV infection **(Figure 4.1*B*)**. Mice were fed a normal chow diet for 10 weeks after AAV infection: we observed no significant change in body weight gain (LOVX 26.93 ± 2.853, n=6 vs GFP 25.06 ± 2.602, n=6, $p = 0.6391$) **(Figure 4.1*C*)** or in food intake ($p = 0.9535$ vs GFP) **(Figure 4.1*D*)** between groups. After 10 weeks, observed no significant differences in the weight of the liver, subcutaneous and visceral adipose tissue depots, brain,

kidney and heart, between AAV-infected and control mice **(Figure 4.1*E*)**. Furthermore, the LOVX mice showed no difference in free-running (fed) blood glucose levels (LOVX 6.850 ± 0.1408, n=6 vs GFP 6.633 ± 0.2603, n=6, p = 0.4810) and 16h fasted glycemia (LOVX 4.683 ± 0.1778, n=6 vs GFP 4.750 ± 0.1360, n=6, p = 0.7719) compared to control animals **(Figure 4.1*F*)**. Finally, while previous studies have shown that severe PGP overexpression (more than 10 fold) increased hepatic glucose production in response to glycerol in rat hepatocytes *in vivo* (Mugabo, Zhao et al. 2016); we found that the LOVX mice and control animals had similar responses to oral glycerol and pyruvate loading in tests conducted following 16h fasting to deplete hepatic glycogen stores **(Figure 4.1*G*-*H*)**.

Mouse hepatocytes overexpressing PGP show decreased liver TG content after 4 weeks with no change in plasma lipid profile or liver TG content after 10 weeks.

To see the effect of G3PP overexpression on TG synthesis and storage in the liver, we measured hepatic TG content in tissues collected at necropsy 4 and 10 weeks following AAV infection. Liver TG content was significantly decreased in LOVX mice after 4 weeks compared to control animals (LOVX 0.03381 ± 0.002293, n=3 vs GFP 0.04682 ± 0.002472, n=3, p = 0.0182) **(Figure 4.2*A*)** with no change after 10 weeks (LOVX 0.6350 ± 0.1217, n=6 vs GFP 0.6450 ± 0.05402, n=6, p = 0.9416) **(Figure 4.2*B*)**. Similarly, 10 weeks following infection, G3PP overexpression in hepatocytes does not alter liver biomarkers such as ALT, AST, albumin, ALP and bilirubin **(Figure 4.2*C*)** or plasma lipids including cholesterol, HDL, LDL and TG **(Figure 4.2*D*)**.

LOVX mice hepatocytes *ex vivo* model validation.

To validate if 3 fold G3PP overexpression in hepatocytes affect glucose and lipid metabolism as shown previously using primary rat hepatocyte *in vitro* (Mugabo, Zhao et al. 2016), we conducted *ex vivo* experiments to measure glycerol release, TG content, lactate release and content and gluconeogenesis. LOVX hepatocytes show no significant difference in TG content **(Figure 4.3*A*)** or glycerol release **(Figure 4.3*B*)** after 2h incubation when cultured *ex vivo* in media with low (5G, 5mM) or high (25G, 25mM) glucose concentrations compared to control hepatocytes. Interestingly, LOVX hepatocytes show a significant decrease in lactate release when cultured in high glucose media compared to control hepatocytes (LOVX 551.4 ± 56.49, n=3 vs GFP 808.6 ± 7.170, n=3, p = 0.0006), but no significant difference when cultured under low glucose conditions (LOVX 376.7 ± 46.91, n=3 vs GFP 391.9 ± 22.94, n=3, p = 0.7853) **(Figure 4.3*C*)**. In addition, LOVX hepatocytes and control hepatocytes have similar lactate content when cultured in low (LOVX

108.8 ± 2.030, n=3 vs GFP 107.4 ± 2.017, n=3, p = 0.6572) and high (LOVX 121.4 ± 0.7700, n=3 vs GFP 120.5 ± 5.201, n=3, p = 0.8690) glucose media **(Figure 4.3*D*)**. LOVX hepatocytes also showed no significant difference in gluconeogenesis compared to control cells when glycerol (LOVX 1.293 ± 0.02624, n=3 vs GFP 1.349 ± 0.05310, n=3, *p* = 0.4004) and pyruvate/lactate (LOVX 1.021 ± 0.007111, n=3 vs GFP 1.054 ± 0.01396, n=3, *p* = 0.1018) were used as substrates **(Figure 4.3*E*)**.

LOVX mice shows no major changes in liver metabolism after chronic hyperglycemia

Since our data showed that 3 fold overexpression of G3PP in mouse hepatocytes resulted in limited phenotypic changes both *in vivo* and ex *vivo*, we next investigated whether increased G3PP expression would alter the hepatocyte response to chronic hyperglycemia *in vivo*. Therefore, we challenged the LOVX mice with a glucose infusion to maintain hyperglycemia (14-16 mM) for 48 hours **(Figure 4.4*A*)**. The body weight of LOVX and control mice was not different at baseline or following the glucose infusion **(Figure 4.4*B*)**; and LOVX and control animals maintained similar glycemia and GIR during the infusion period **(Figure 4.4*C*-*D*)**, with blood glucose levels averaging 10-11mM on the first day and 16-17mM on the second day in both groups. During the infusion, plasma TG did not increase with increase glycemia and showed no significant difference between LOVX and control animals **(Figure 4.4*E*)**. However, LOVX mice showed a tendency towards higher plasma glycerol levels than control mice at each time point **(Figure 4.4*F*)**. Furthermore, urine glucose levels were not significantly different between the groups **(Figure 4.4*G*)** and urine glycerol also showed no significant difference between groups during the first day of the study, but tended to be lower in LOVX mice on the second day of infusion **(Figure 4.4*H*)**. At the end of the infusion, LOVX mice show no significant difference in liver weight (LOVX 1.188 ± 0.01855, n=5 vs GFP 1.168 ± 0.03325, n=5, *p* = 0.6206) **(Figure 4.4*I*)**, liver TG (LOVX 0.07863 ± 0.006204, n=5 vs GFP 0.07646 ± 0.006346, n=5, *p* = 0.8124) **(Figure 4.4*J*)** or heart TG (LOVX 0.04014 ± 0.004933, n=5 vs GFP 0.03827 ± 0.005367, n=5, *p* = 0.8041) **(Figure 4.4*K*)** compared to control mice. Taken together, these results show that 3 fold overexpression in mouse hepatocytes have no significant effect on liver metabolism after chronic hyperglycemic stress.

4.5 Discussion

The liver plays a crucial role in gluconeogenesis and lipoprotein synthesis and secretion, both of which depend on the availability of Gro3P in hepatocytes. Our lab previously reported that

suppression of G3PP expression by RNAi in isolated rat primary hepatocytes, resulted in higher levels of Gro3P and glycolysis (as measured by lactate release) and increased glycerolipid synthesis (as indicated by diacylglycerol and triglyceride levels), in hepatocytes incubated at elevated glucose levels (25 mM) but not at low glucose concentrations (5mM) (Mugabo, Zhao et al. 2016). In contrast, hG3PP overexpression in rat hepatocytes showed decrease Gro3P and glycolytic flux at elevated glucose levels (Mugabo, Zhao et al. 2016). Furthermore, we have reported that G3PP activity *in vivo*, plays an important role in fatty liver progression, with increased TG and cholesterol accumulation and increased inflammation being observed under hyperglycemic conditions when G3PP was deleted in mouse liver (see Chapter 2). Moreover, hG3PP overexpression in rat liver *in vivo,* resulted in reduced body weight gain, plasma triglycerides and hepatic glucose production when challenged with glycerol (Mugabo, Zhao et al. 2016). In these studies, PGP was overexpressed for a short term and at extremely high levels; as a result, it is not clear that similar changes would occur if PGP was expressed at a more physiological level, for longer time periods, or in the presence of metabolic stressors such as hyperglycemia.

The AAV8-TBG-h*PGP* in this study allowed us to control *PGP* overexpression in LOVX mice so that it stably increased by 3-4 fold for the duration of the study. Our *in vivo* data showed that LOVX mice had no specific phenotype after 10 weeks on normal diet; and their plasma lipid and liver biomarker profile were indistinguishable from control animals. However, the LOVX showed a significant decrease in liver TG content after 4 weeks of *PGP* overexpression (LOVX 0.03381 ± 0.002293, n=3 vs GFP 0.04682 ± 0.002472, n=3, $p = 0.0182$) compared to GFP controls, that corrected after 10 weeks so that the TG content of LOVX and GFP control mice was equal at the end of the study (LOVX 0.6350 ± 0.1217, n=6 vs GFP 0.6450 ± 0.05402, n=6, $p = 0.9416$). Even though we have studied a smaller number of mice at the earlier time point, this observation could indicate that we had an early effect of G3PP overexpression that became less significant with time. The lack of phenotype in mice fed a normal chow diet is consistent with our earlier ex *vivo* observations that G3PP activity is more important under metabolically stressful conditions such as hyperglycemia. We challenged the LOVX and control mice with hyperglycemia by infusing glucose for 2 days, but did not observe significant changes in liver TG content, nor plasma levels of TG and other liver biomarkers. We did observe a trend towards higher plasma glycerol in LOVX mice compared to control animals that did not reach statistical significance. Since our

studies involved small cohorts of animals, we consider these data to be preliminarily that should be repeated in larger groups of mice.

We further validated the LOVX model *ex vivo* by testing whether if the mouse hepatocytes had that same phenotypic characteristics that were observed in rat hepatocytes (Mugabo, Zhao et al. 2016). We isolated hepatocytes from mice 4 weeks following AAV infection, and incubated them in low (5mM) and high (25mM) glucose media for 2 hours. The LOVX hepatocytes expressed 3 fold more G3PP protein than the control cells, but showed no difference in TG content, glycerol release, lactate content or gluconeogenesis, suggesting that they could generally compensate for *PGP* overexpression at this level. However, lactate release was significantly decreased in the LOVX hepatocytes compared to control hepatocytes, this may indicated that 3 fold increase in G3PP expression can affect the glycolytic flux by directing more glucose carbons to glycerol. In interpreting these negative results, it is important to mention that these experiments were conducted with only 3-5 mice in each group and had statistical power to detect only large effects of *PGP* overexpression. While these effect sizes are smaller/larger than those reported previously by our group (Mugabo, Zhao et al. 2016), our results suggest that a 3 fold increase in PGP expression may have no major impact on the hepatocyte metabolism *in vivo* and *ex vivo* and that higher levels of PGP expression would be required. We also note that we were not able to measure the increase in PGP activity that was caused by a 3-fold increase in PGP expression, and emphasize that future studies would be directed toward obtaining and assessing the metabolic effects of measurable changes in PGP activity rather than simply the response to increased PGP protein levels. These studies could be performed using an inducible transgenic mouse model for G3PP that we are developing or using a chemical activator for G3PP.

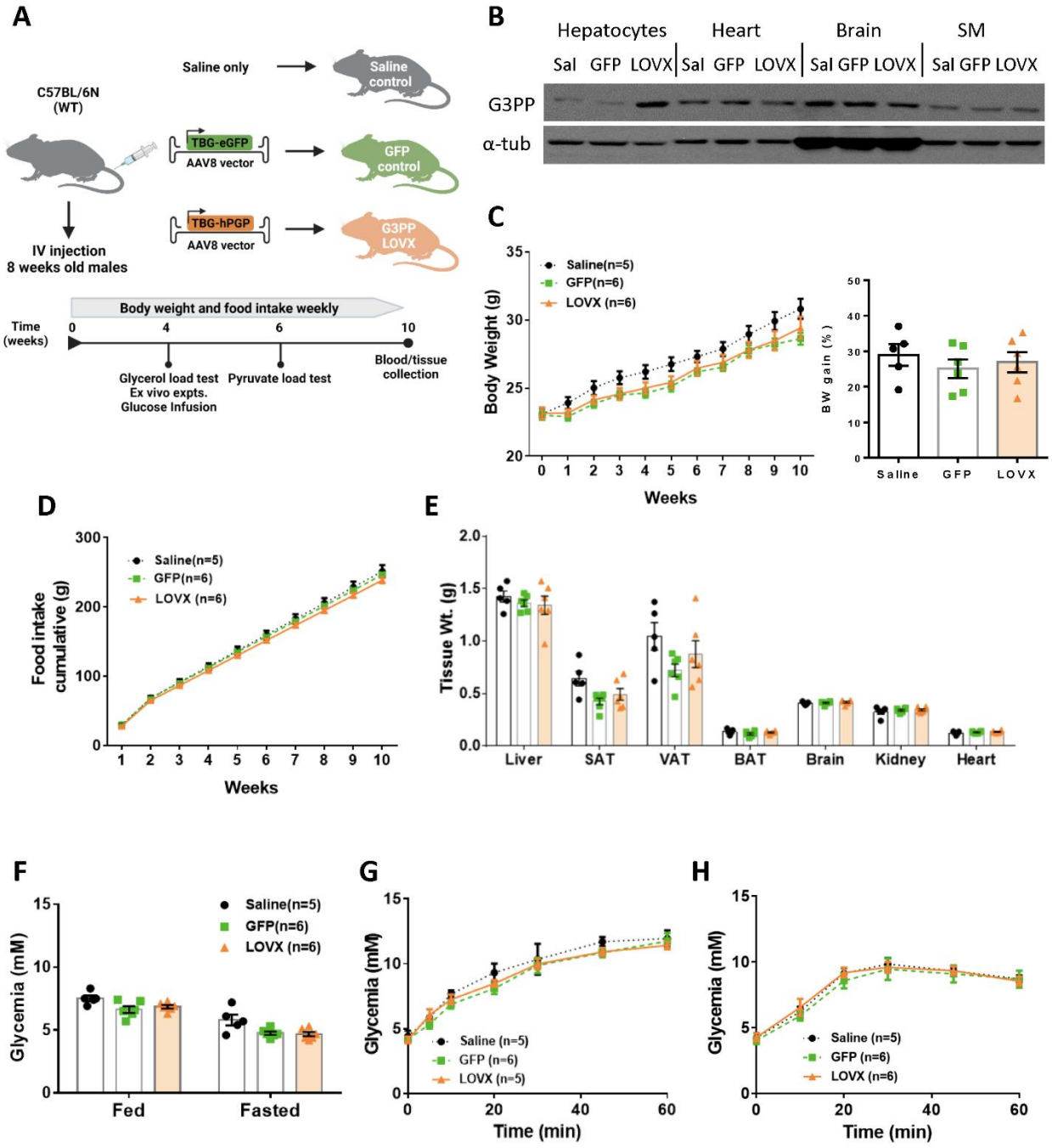
A
Saline only
Saline control
C57BL/6N (WT)
TBG-eGFP
AAV8 vector
GFP control
TBG-hPGP
AAV8 vector
G3PP LOVX
IV injection
8 weeks old males
Body weight and food intake weekly
Time (weeks)
0
4
6
10
Glycerol load test
Ex vivo expts.
Glucose Infusion
Pyruvate load test
Blood/tissue collection
B
Hepatocytes
Heart
Brain
SM
Sal GFP LOVX Sal GFP LOVX Sal GFP LOVX Sal GFP LOVX
G3PP
α-tub
C
Saline(n=5)
GFP(n=6)
LOVX (n=6)
Body Weight (g)
Weeks
BW gain (%)
Saline
GFP
LOVX
D
Saline(n=5)
GFP(n=6)
LOVX (n=6)
Food intake cumulative (g)
Weeks
E
Tissue Wt. (g)
Liver
SAT
VAT
BAT
Brain
Kidney
Heart
F
Saline(n=5)
GFP(n=6)
LOVX (n=6)
Glycemia (mM)
Fed
Fasted
G
Saline (n=5)
GFP (n=6)
LOVX (n=5)
Glycemia (mM)
Time (min)
H
Saline (n=5)
GFP (n=6)
LOVX (n=6)
Glycemia (mM)
Time (min)

Figure 4.1. Effect of G3PP overexpression *in vivo* (G3PP-LOVX model validation).

(A) Experimental scheme showing that WT mice were injected by tail vein with AAV8-TBG-hPGP, AAV8-TBG-eGFP or saline then kept on chow diet for 10 weeks. **(B)** G3PP overexpression was confirmed using protein extracts from hepatocytes, brain, heart and skeletal muscle (SM) from mice, 4 weeks after AAV infection and used for western blot (Saline (Sal), n=3; GFP, n=4; LOVX, n=4). For all tissues α-tubulin was used as a housekeeping protein. **(C)** Body weight and % of weight gain (Saline, n=5; GFP, n=6; LOVX, n=6). **(D)** Food intake (Saline, n=5; GFP, n=6; LOVX, n=6). **(E)** Tissue weight: liver, subcutaneous adipose tissue (SAT), visceral adipose tissue (VAT), brown adipose tissue (BAT), brain, kidney and heart (Saline, n=5; GFP, n=6; LOVX, n=6). **(F)** Fed and fasted glycemia (Saline, n=5; GFP, n=6; LOVX, n=6). **(G)** Glycerol load test (Saline, n=5; GFP, n=6; LOVX, n=5). **(H)** Pyruvate load test (Saline, n=5; GFP, n=6; LOVX, n=6). Data are mean ± SEM. (One-way and Two-way ANOVA).

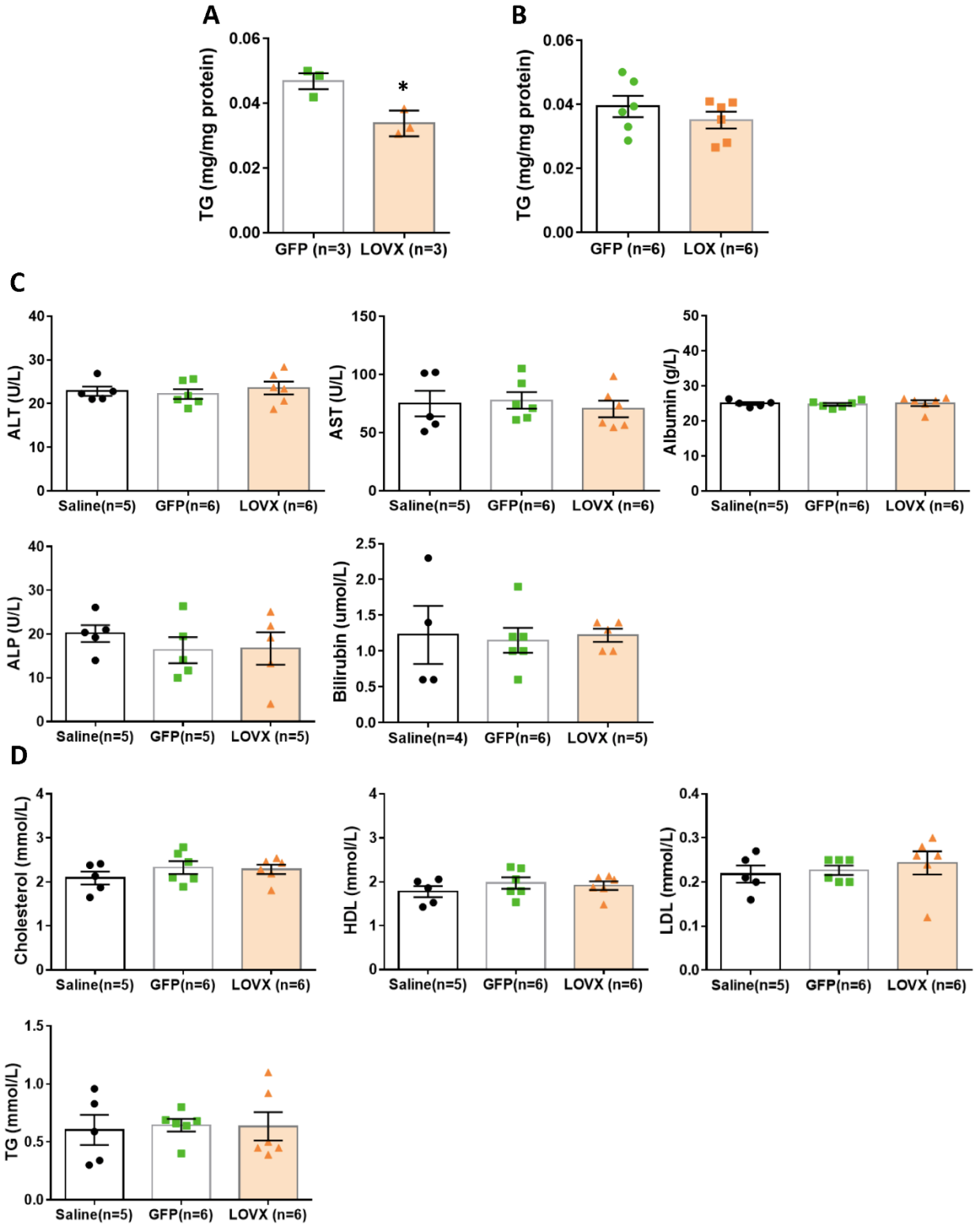
A
TG (mg/mg protein)
0.06
0.04
0.02
0.00
*
GFP (n=3)
LOVX (n=3)
B
TG (mg/mg protein)
0.06
0.04
0.02
0.00
GFP (n=6)
LOX (n=6)
C
ALT (U/L)
40
30
20
10
0
Saline(n=5)
GFP(n=6)
LOVX (n=6)
AST (U/L)
150
100
50
0
Saline(n=5)
GFP(n=6)
LOVX (n=6)
Albumin (g/L)
50
40
30
20
10
0
Saline(n=5)
GFP(n=6)
LOVX (n=6)
ALP (U/L)
40
30
20
10
0
Saline(n=5)
GFP(n=5)
LOVX (n=5)
Bilirubin (umol/L)
2.5
2.0
1.5
1.0
0.5
0.0
Saline(n=4)
GFP(n=6)
LOVX (n=5)
D
Cholesterol (mmol/L)
4
3
2
1
0
Saline(n=5)
GFP(n=6)
LOVX (n=6)
HDL (mmol/L)
4
3
2
1
0
Saline(n=5)
GFP(n=6)
LOVX (n=6)
LDL (mmol/L)
0.4
0.3
0.2
0.1
0.0
Saline(n=5)
GFP(n=6)
LOVX (n=6)
TG (mmol/L)
1.5
1.0
0.5
0.0
Saline(n=5)
GFP(n=6)
LOVX (n=6)

Figure 4.2. Effects of G3PP overexpression on liver and plasma parameters after 10 weeks on normal diet.

(A) Liver TG content 4 weeks after of overexpression (GFP, n=3; LOVX, n=3). **(B)** Liver TG content 10 weeks after of overexpression (GFP, n=6; LOVX, n=6). **(C)** Liver toxicity parameters in plasma: alanine transaminase (ALT), aspartate aminotransferase (AST), albumin, alkaline phosphatase (ALP) and bilirubin (Saline, n=5; GFP, n=6; LOVX, n=6). **(D)** Plasma lipid profile: cholesterol, high-density lipoprotein (HDL), low-density lipoproteins (LDL), triglyceride (TG) (Saline, n=5; GFP, n=6; LOVX, n=6). Data are mean ± SEM. *$p < 0.05$ vs GFP control (Student's *t* test, Panel A-B; One-way ANOVA, Panel C-D).

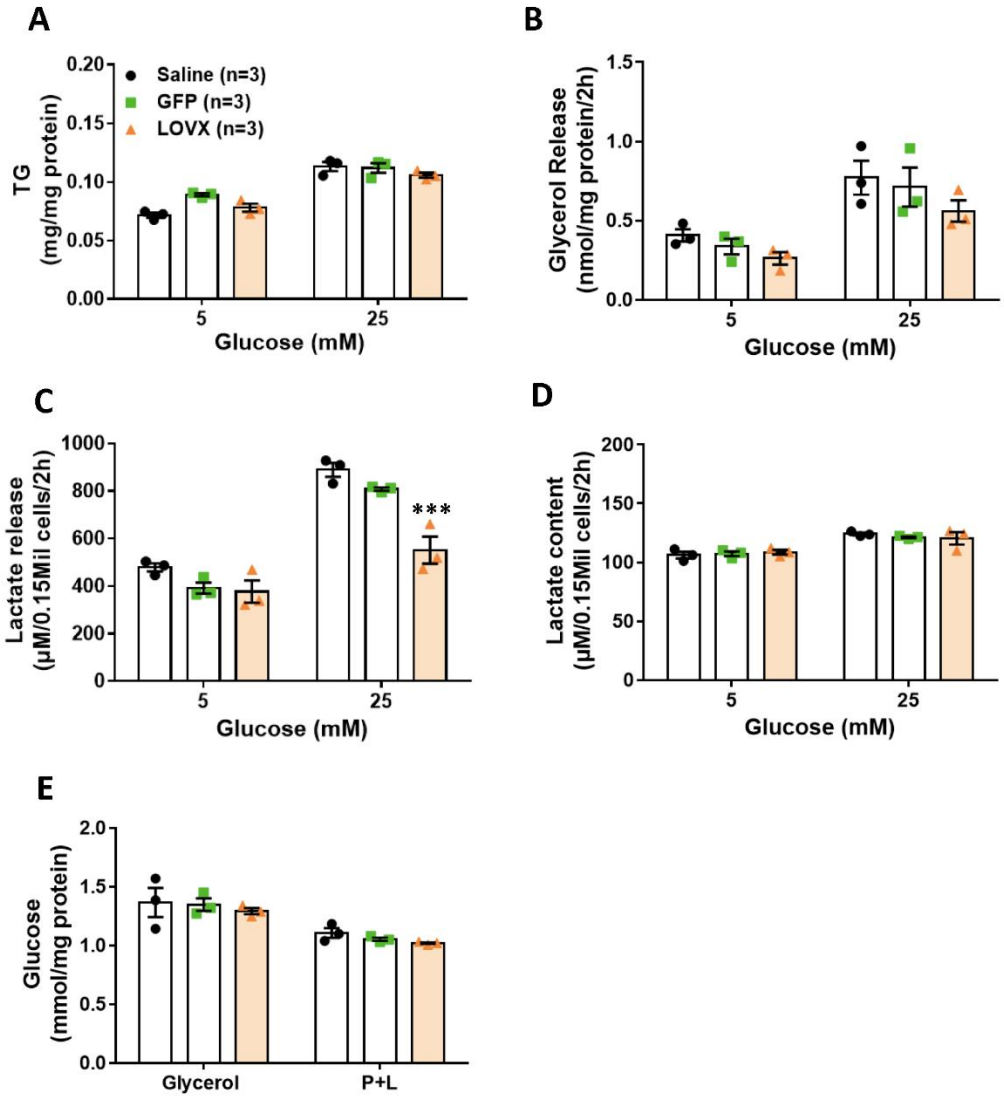

Figure 4.3. *Ex vivo* model validation.

Hepatocytes were extracted following 4 weeks of PGP overexpression and the following parameters were measured directly or in cells cultured *ex vivo* (Saline, n=3; GFP, n=3; LOVX, n=3): **(A)** triglyceride (TG) content, **(B)** glycerol release, **(C)** lactate release, **(D)** lactate content. **(E)** Gluconeogenesis from glycerol or pyruvate/lactate (P+L). ***$p < 0.001$ vs. both controls at 5G (5mM glucose) or 25G (25mM glucose) using One-way ANOVA .

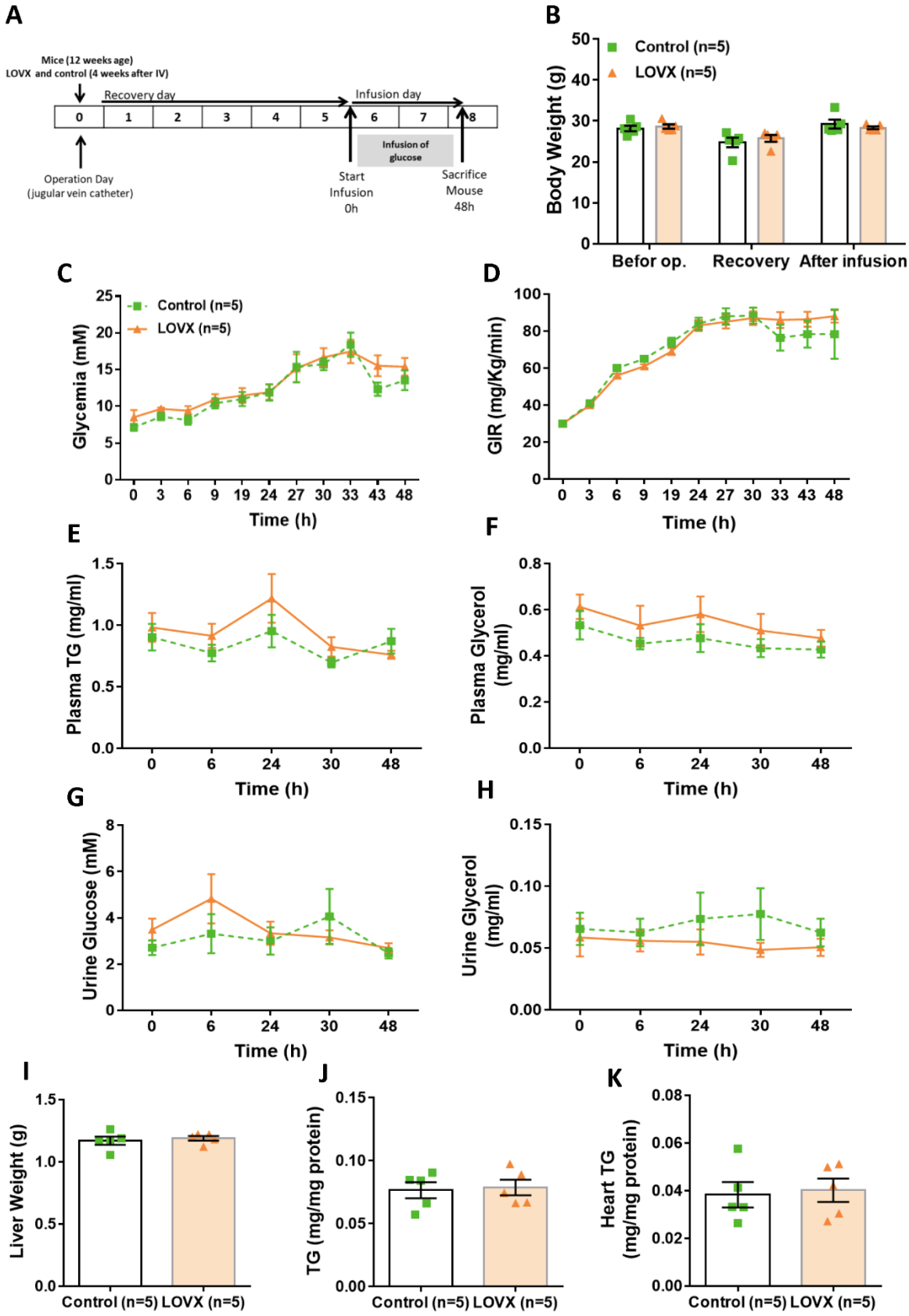
A
Mice (12 weeks age)
LOVX and control (4 weeks after IV)
Recovery day
Infusion day
0
1
2
3
4
5
6
7
8
Infusion of glucose
Operation Day
(jugular vein catheter)
Start Infusion 0h
Sacrifice Mouse 48h
B
Control (n=5)
LOVX (n=5)
Body Weight (g)
Befor op.
Recovery
After infusion
C
Glycemia (mM)
Time (h)
D
GIR (mg/Kg/min)
Time (h)
E
Plasma TG (mg/ml)
Time (h)
F
Plasma Glycerol (mg/ml)
Time (h)
G
Urine Glucose (mM)
Time (h)
H
Urine Glycerol (mg/ml)
Time (h)
I
Liver Weight (g)
Control (n=5) LOVX (n=5)
J
TG (mg/mg protein)
Control (n=5) LOVX (n=5)
K
Heart TG (mg/mg protein)
Control (n=5) LOVX (n=5)

Figure 4.4. Response of LOVX and control mice to *in vivo* glucose infusion for 48h.

(A) Timeline: mice with jugular vein catheter received a continuous intravenous infusion of glucose for 48h with arterial blood and urine samples collected twice daily. **(B)** Body weight was measured weekly. **(C)** Blood glucose was monitored and **(D)** GIR was adjusted as needed during the infusion. The following parameters were measured at the end of the study: **(E)** Plasma TG and **(F)** Plasma glycerol, **(G)** Glucose in urine and **(H)** glycerol in urine. **(I)** Liver weight. **(J)** Liver TG content. **(K)** Heart TG content. Data are mean ± SEM (GFP control, n=5; LOVX, n=5). (Two-way ANOVA, Panel C-H; Student's *t* test, Panel B, I-K).

References:

Birkenfeld, A. L., & Shulman, G. I. (2014). Nonalcoholic fatty liver disease, hepatic insulin resistance, and type 2 diabetes. *Hepatology, 59*(2), 713-723.

Bradley, D. C., & Kaslow, H. R. (1989). Radiometric assays for glycerol, glucose, and glycogen. *Anal Biochem, 180*(1), 11-16.

Bugianesi, E., Moscatiello, S., Ciaravella, M. F., & Marchesini, G. (2010). Insulin resistance in nonalcoholic fatty liver disease. *Curr Pharm Des, 16*(17), 1941-1951.

Han, H. S., Kang, G., Kim, J. S., Choi, B. H., & Koo, S. H. (2016). Regulation of glucose metabolism from a liver-centric perspective. *Exp Mol Med, 48*, e218.

Huang, T. D., Behary, J., & Zekry, A. (2019). Non-alcoholic fatty liver disease (NAFLD): a review of epidemiology, risk factors, diagnosis and management. *Intern Med J*.

Mugabo, Y., Zhao, S., Seifried, A., Gezzar, S., Al-Mass, A., Zhang, D., . . . Prentki, M. (2016). Identification of a mammalian glycerol-3-phosphate phosphatase: role in metabolism and signaling in pancreatic beta-cells and hepatocytes. *Proc Natl Acad Sci U S A, 113*(4), E430-439.

Ochoa-Sanchez, R., Oliveira, M. M., Tremblay, M., Petrazzo, G., Pant, A., Bosoi, C. R., . . . Rose, C. F. (2021). Genetically engineered E. coli Nissle attenuates hyperammonemia and prevents memory impairment in bile-duct ligated rats. *Liver Int, 41*(5), 1020-1032.

Possik, E., Al-Mass, A., Peyot, M. L., Ahmad, R., Al-Mulla, F., Madiraju, S. R. M., & Prentki, M. (2021). New mammalian glycerol-3-phosphate phosphatase: role in beta-cell, liver and adipocyte metabolism. *Front Endocrinol (Lausanne), 12*, 706607.

Yan, Z., Yan, H., & Ou, H. (2012). Human thyroxine binding globulin (TBG) promoter directs efficient and sustaining transgene expression in liver-specific pattern. *Gene, 506*(2), 289-294.

Yki-Jarvinen, H. (2014). Non-alcoholic fatty liver disease as a cause and a consequence of metabolic syndrome. *Lancet Diabetes Endocrinol, 2*(11), 901-910.

Chapter V. Discussion, future directions and conclusions

Hyperglycemia is one of the main characteristics of different metabolic disorders, including obesity-associated T2D (Porte 1999). Excess glucose can simultaneously activate many metabolic pathways that are known to generate many metabolic intermediates and their derivatives, some of which can be toxic (Prentki, Peyot et al. 2020). Different cell types use different mechanisms to eliminate glucose carbons and other toxins; however, little is known about these detoxification mechanisms. In this thesis, I studied one proposed pathway for glucose detoxification, involving G3PP. G3PP was shown previously to control the cytosolic levels of Gro3P, a metabolite formed from glucose during glycolysis that is a starting substrate for the GL/FFA cycle. G3PP sits at the crossroads of glucose and lipid metabolism and can regulate glycolysis, gluconeogenesis, glycerolipid synthesis and FFA oxidation in pancreatic β-cell and hepatocytes. It can also regulate GSIS and glucolipotoxicity in the pancreatic β-cell. It is also important to mention that G3PP is well expressed in the majority of tissues (Mugabo, Zhao et al. 2016). Since G3PP deletion leads to intrauterine growth arrest and embryonic lethality in midgestation (Segerer, Hadamek et al. 2016), I employed tissue-specific inducible KO mouse models to demonstrate that G3PP plays an important role in detoxifying excess glucose in adult pancreatic β-cells and hepatocytes.

Gro3P is the physiological substrate for G3PP

In mammals, G3PP was known to hydrolyze the toxic metabolite 2-PG and was recently shown to act as a 'metabolite repair enzyme' by eliminating toxic by-products of glycolysis and pentose phosphate pathways in cancer cell lines *in vitro* (Collard, Baldin et al. 2016). We considered the possibility that G3PP BKO mice may accumulate toxic by-products in β-cells and develop defective islet function or diabetes; and that similar functional impairment could develop in hepatocytes of G3PP LKO mice and also affect metabolic fitness. However, we did not notice any

signs of toxicity of G3PP deletion in either KO model both *in vivo* and *ex vivo*. BKO mice were as healthy as control animals: both groups gained weight and had equivalent food intake when fed a normal chow diet. In fact, β-cells from BKO mice displayed more efficient metabolic activation and insulin secretion, suggesting that toxic metabolites do not accumulate or cause toxicity in the BKO β-cells fed a normal diet (Possik, Madiraju et al. 2017, Possik, Al-Mass et al. 2021). In particular, 2-PG levels were very low in the BKO islets and did not change in control and BKO islets cultured *ex vivo* at different glucose concentrations. In addition, G3PP deletion in hepatocytes in LKO mice showed no effect on body weight, food intake, liver weight or lipid plasma profile (LDL, HDL and cholesterol) when the KO mice were compared to normal animals fed a normal diet. Markers of hepatocyte damage (ALT, ALP, AST and albumin) were not also different in the LKO and control mice. Moreover, 2-PG levels were not detectable in LKO mouse livers, even during glucose infusion. Interestingly, Gro3P levels were elevated in both LKO mouse liver and BKO mouse islets under conditions of high glucose levels. These results emphasized that Gro3P is a relevant physiological substrate for G3PP and the effects we observed in our models were due to G3PP's activity toward Gro3P rather than toxins such as 2-PG, 4-PE, and 2-phospholactate, particularly under high glucose levels. To confirm this, we need to measure the levels of these by-products in islets or hepatocytes of our models in mice fed a normal diet or stressed by a diet that leads to hyperglycemia.

G3PP deletion phenotype characteristics are consistent between rats and mice

The rationale for this thesis was based on previous findings by our group (Mugabo, Zhao et al. 2016), showing that G3PP played a role in the control of glycolysis, glucose oxidation, cellular redox and ATP production, gluconeogenesis, glycerolipid synthesis and FA oxidation through its effects on cytosolic Gro3P levels in rat β-cells and hepatocytes *in vitro* (Mugabo, Zhao et al. 2016).

Specifically, G3PP knockdown using RNAi in primary rat hepatocytes *in vitro* led to lower glycerol release and higher TG content, lactate release and gluconeogenesis. Furthermore, reduced G3PP activity in both rat islets (RNAi knockdown) and INS-1(832/13) cells (siRNA knockdown) *in vitro* resulted in decreased glycerol release and increased GSIS, ATP production and O_2 consumption under high glucose concentration (Mugabo, Zhao et al. 2016). Therefore, before studying our tissue-specific KO mice *in vivo*, we validated the G3PP deletion phenotype *ex vivo*. BKO islets (inducible KO) showed increased GSIS and mitochondrial metabolism *ex vivo* only at high glucose levels and decreased glucose stimulated glycerol release. In addition, LKO hepatocytes studied *ex vivo* (Using AAV8) showed increased gluconeogenesis, TG content and lactate release with decrease glycerol release in response to high glucose concentration. This shows the role of G3PP is consistent across different models and using different approaches.

In vivo G3PP deletion under normal diet

All the *in vitro* and *ex vivo* data suggest that G3PP activity is more evident under conditions where glucose is elevated **(Figure 5.1)** (Mugabo, Zhao et al. 2016). However, studying the role of G3PP *in vivo* in BKO and LKO mice under normal diet first is important to validate the phenotype, since these are the first *in vivo* studies of tissue specific KO models of G3PP. To do this, the phenotype of BKO and control mice were studied in animals fed normal diet for 12 weeks (until 20 weeks of age). Interestingly, when BKO and control mice were challenged with a glucose load test at sixteen weeks of age, BKO mice showed a significant increase in insulinemia when glycaemia levels were around 20mM for both groups. This is the first *in vivo* evidence that BKO mice respond with higher insulin secretion under similar levels of hyperglycemia. These data were supported by studies of fed animals, where both groups showed similar fed glycaemia but BKO mice showed a significant increase in fed insulinemia. Additionally, BKO mice showed a tendency to have a higher C-peptide

levels, which may indicate that they have higher rate of insulin synthesis and secretion long term (Leighton, Sainsbury et al. 2017). Furthermore, fed plasma TG was significantly lower and TG content in VAT and SM was increased in the BKO mice, likely due to the higher plasma insulin levels which increases TG storage in peripheral tissues (Czech, Tencerova et al. 2013). Consequently, twenty week old BKO mice fed a normal diet showed a significantly larger gain in body weight compared to control mice despite a similar food intake. This increase in body weight was accompanied by an increased fat mass in the BKO mice, which indicating that these mice are more obese than controls due to the hypersecretion of the BKO islets. Moreover, sixteen week old BKO mice fed a normal diet showed mild glucose intolerance when challenged with a glucose load but no change in insulin sensitivity measured by IPITT. This mild glucose intolerance could be caused by the increased TG peripheral tissues and overall increased fat mass in the BKO mice.

On the other hand, the LKO mice and control animals had the same body weight and food intake after 10 weeks on normal diet. LKO mice had normal fed and fasted glycaemia compared to controls; as well as similar liver weights, liver enzymes and plasma lipid profiles. However, LKO mice challenged with an oral glycerol load after an overnight fast showed significantly increased glycemia reflecting an increased hepatic glucose production. This is consistent with previous results showing that G3PP controls gluconeogenesis in hepatocytes cultured *ex vivo* (Mugabo, Zhao et al. 2016). LKO mice challenged with pyruvate, another gluconeogenesis substrate, showed no difference in hepatic glucose production *in vivo*. It is important to mention that the pyruvate loading test can cause elevated blood lactate which may trigger acidosis. Under acidotic conditions, the liver stops making glucose, which can still be made by the kidney (Gerich, Meyer et al. 2001). This could also be the reason also why we did not see any change in glucose levels after pyruvate loading compared to glycerol *in vivo*; however, we would need to measure

blood lactate during the test to validate this hypothesis. On the other hand, we see increased gluconeogenesis stimulated with glycerol or pyruvate/lactate in LKO isolated hepatocytes grown *ex vivo*. Glycerol, as a result of the action of hepatic glycerol kinase, provides a more direct substrate for gluconeogenesis through the formation of Gro3P than substrates such as pyruvate, lactate and amino acids (Wang, Kwon et al. 2020). Thus, the increase in hepatic glucose production in LKO mice is due to the lack of G3PP activity in the liver, where more Gro3P is directed for glucose synthesis. Studying both models under normal diet gave an insight on the role of G3PP under physiological conditions; however, it will be interesting to see what could happen under more metabolically challenging conditions and the role of G3PP in different obese and diabetic models such as *db/db* mice.

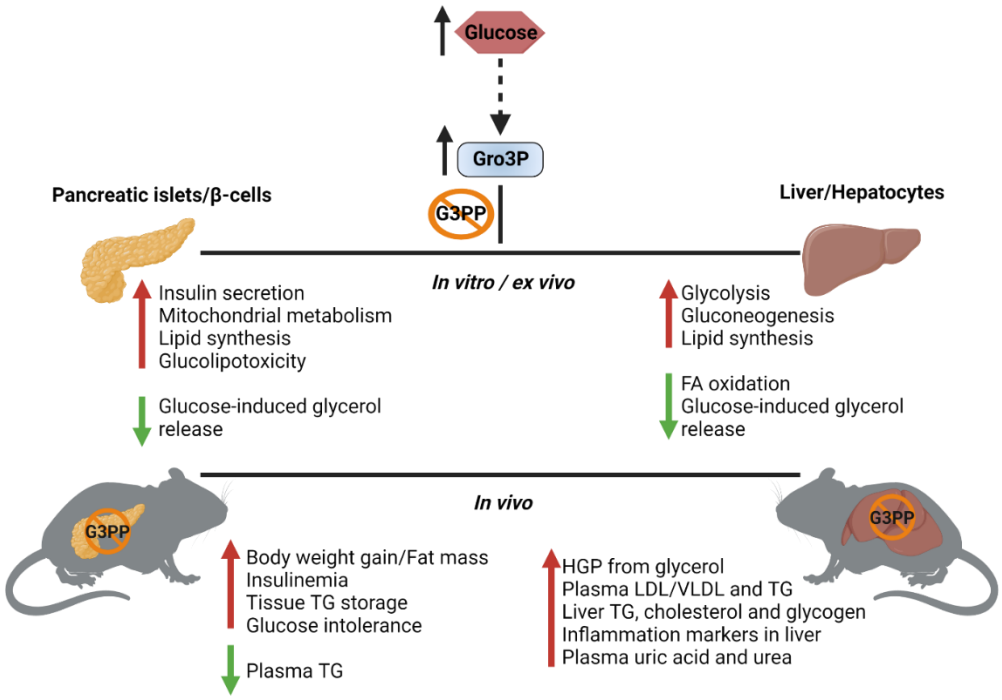

Figure 5.1. Summary of G3PP deletion phenotype in pancreatic β-cells and liver.

The effect of G3PP deletion in pancreatic β-cells and liver hepatocytes under high glucose level *in vitro/ex vivo* and *in vivo*. Abbreviations: Gro3P, glycerol 3-phosphate; G3PP, glycerol 3-

phosphate phosphatase; TG, triglyceride; HGP, hepatic glucose production; LDL, low-density lipoproteins; FA, fatty acid and VLDL, very low-density lipoproteins.

The effect of G3PP deletion in β-cells:

The *in vivo* phenotype of the BKO mice indicated that G3PP deletion in the β-cells leads to increased levels of Gro3P under elevated glucose levels, which pathways like glycolysis and the GL/FFA cycle in β-cells to enhance GSIS. We investigated this further by studying the BKO islets *ex vivo*. BKO islets showed a clear decrease in glucose-induce glycerol release under high glucose concentration compared to the control islets, which validates the functional deletion of G3PP. BKO islets show an enhanced GSIS only at high glucose concentrations (16mM) compared to the control islets **(Figure 5.1)**. These findings highlight that BKO islets show no significant increase in GSIS at intermediate or physiological glucose concentrations. Furthermore, we saw a significant increase in Gro3P levels and the upstream substrate DHAP only when high glucose levels were present and not under intermediate glucose concentrations.

Gro3P metabolism in β-cells is involved in pathways that affect GSIS by generating MCFs, including the GL/FFA cycle, mitochondrial respiration and glucose and lipid metabolism **(Figure 5.1)**. At high glucose levels, BKO islets showed an increase in mitochondrial O_2 consumption and ATP production with no change in basal respiration or proton leak. This is due to the increase in the Gro3P shuttle substrates that affect mitochondrial respiration. Furthermore, ATP levels increased in BKO islets only under high glucose levels but not with intermediate glucose. BKO islets also showed a significant increase in the levels of TCA cycle intermediates, acetyl-CoA and mal-CoA under high glucose levels compared to the control islets; and increased lactate, indicating increased glycolytic flux. Taken together, β-cell G3PP deletion leads to an increase in Gro3P levels

only at high glucose levels; and Gro3P enhances GSIS through the Gro3P shuttle and GL/FA cycle and the production of MCFs.

The effect of G3PP deletion in hepatocytes:

Our *in vivo* data indicated that G3PP activity is more evident under hyperglycemia conditions. TG synthesis depends in part on the availability of Gro3P, which links glycolysis to GL/FFA cycling (Prentki and Madiraju 2008, Prentki and Madiraju 2012). Thus, G3PP by controlling cytosolic levels of Gro3P can control TG synthesis and accumulation in hepatocytes at high glucose levels (Mugabo, Zhao et al. 2016). Our data showed an increase in glycolytic flux in LKO hepatocytes marked by increased lactate content and release only at high glucose concentrations (25mM). Furthermore, LKO hepatocytes had increased TG content at elevated glucose concentrations **(Figure 5.1)**. These findings indicate that more glucose carbons are redirected back to glycolysis or to TG synthesis when G3PP activity is lost. Importantly, LKO hepatocytes show decreased glucose stimulated glycerol release under the same conditions, which further supports that G3PP eliminates glucose carbons to glycerol.

The liver is the major site of gluconeogenesis from substrates such as amino acids, pyruvate, lactate or glycerol released by adipose tissue lipolysis (Adeva-Andany, Perez-Felpete et al. 2016). However, the formation of Gro3P from glycerol by hepatic glycerol kinase provides a more direct substrate for gluconeogenesis than other substrates (Wang, Kwon et al. 2020). G3PP has been shown to control gluconeogenesis *in vitro* (Mugabo, Zhao et al. 2016), which is consistent with our findings that LKO hepatocytes show increased gluconeogenesis in response to both glycerol and pyruvate/lactate as substrates *ex vivo* **(Figure 5.1)**.

Role of G3PP in glucodetoxification

Glucose can enter both β-cells and hepatocytes through GLUT2, which is an insulin-independent transporter. GLUT2 supports a high flow of glucose entry into the cell because it has a low affinity and high transport capacity for glucose (Hiriart and Aguilar-Bryan 2008). This means that both β-cells and hepatocytes cannot reduce glucose entry to protect themselves from glucotoxicity. Nonetheless, they can redirect excess glucose carbons to other metabolic pathways or modify potentially toxic molecules derived from glucose metabolism and/or excrete them outside the cells. One of the potential pathways to eliminate glucose carbons is G3PP which hydrolyzes Gro3P to glycerol, which is not toxic at high levels (Prentki, Peyot et al. 2020).

BKO islets and LKO livers exposed to high glucose levels show increased accumulation of Gro3P and decreased glucose induce glycerol release. This indicates that glucose carbons in the G3PP KO are not being directed to glycerol and then eliminated. We sought to determine whether it is crucial for these cells to have this pathway to detoxify glucose carbon under glucotoxic conditions. It is known that β-cell glucotoxicity can lead to lower insulin content and GSIS; reduced expression of β-cell-specific genes such as the transcription factors *Pdx-1, NeuroD1* and *Mafa,* and the insulin gene; and also decreased β-cell viability and increased apoptosis (Ye, Tai et al. 2006, Prentki, Peyot et al. 2020). Interestingly, BKO islets under gluoctoxic conditions showed reduced insulin content and increased apoptosis. Moreover, the islets had lower expression of *Ins-2*, *Pdx-1* and *Mafa,* indicating that BKO isles β-cells are losing their identity by dedifferentiation, which is a sign of β-cell dysfunction (Prentki, Peyot et al. 2020). These findings indicate that G3PP plays an important role in preventing β-cell glucotoxicity. By directly hydrolysing glucose-derived Gro3P to release glycerol under high glucose, G3PP could act as a detoxification mechanism to protect the β-cell.

Excessive glucose in the liver is converted into TG through the GL/FFA cycle, using Gro3P as a starting substrate along with FA-CoA; which can eventually lead to ectopic fate accumulation in the liver and other tissues (Alves-Bezerra and Cohen 2017). Therefore, the availability of Gro3P is important for TG synthesis; and G3PP could play a role in reducing fat accumulation in the liver by redirecting glucose carbons to glycerol rather than to TG. Consequently, hyperglycemic LKO mice showed higher liver TG content compared to controls. We further investigated other parameters of fatty liver including changes in plasma lipids, and hepatic cholesterol accumulation and inflammation (Arguello, Balboa et al. 2015, Aguilar-Salinas and Viveros-Ruiz 2019). Hyperglycemic LKO mice showed elevated levels of plasma TG and LDL/VLDL; along with higher levels of liver cholesterol, indicating that there is an alteration in cholesterol homeostasis and transport leading to the accumulation of cholesterol in the liver (Arguello, Balboa et al. 2015). Excessive hepatic TG and cholesterol accumulation can promote inflammation by activating macrophages and Kupffer cells (Matsuzawa, Takamura et al. 2007, Chen, Varghese et al. 2014). Hyperglycemic LKO mice showed increased expression of pro-inflammatory cytokines like *Tnfα* and *Il-6* and macrophages markers like *Cd11c* and *F4/80* in the liver.; indicating an increase in macrophage recruitment and inflammation in the LKO liver under hyperglycemia. Furthermore, inflammation is a known effect of glucotoxicity (Prentki and Nolan 2006). Taken together, these findings show that G3PP plays an important role in preventing glucotoxicity and excess fat accumulation in the liver.

These results indicate that G3PP can play a significant role in glucodetoxification in both pancreatic β-cells and the liver. Therefore, it would be interesting to test whether G3PP overexpression in these tissues and cells can protect from glucotoxicity. This was shown *in vitro:* overexpression of hG3PP in β-cells decreased GSIS in response to high glucose levels that could

prevent β-cell exhaustion and protect against glucolipotoxicity (Mugabo, Zhao et al. 2016). Furthermore, overexpression of hG3PP in hepatocytes *in vitro* decreased TG content and lactate release and increased glucose stimulated glycerol released (Mugabo, Zhao et al. 2016). Moreover, overexpression of human G3PP (hG3PP) in rat liver *in vivo,* using an adenoviral construct, resulted in decreased body weight gain in rats that were fed standard chow, along with decreased hepatic glucose production in response to glycerol and plasma TG levels and increased plasms HDL levels. Since these were short-term studies using the adenoviral construct and G3PP expression was increased more than 100-fold in rat liver; we studied the effects of hG3PP protein overexpression at close to physiological levels over a longer time period using AAV8. As discussed in Chapter IV, our model did not show any major phenotype *in vivo* or *ex vivo*, indicating that G3PP overexpression in liver needs to be higher than 3 fold to alter glucose or fat metabolism.

5.1 Future directions

This thesis has shed light on the role of G3PP as a regulator of glucose, lipid and energy metabolism *in vivo* through its phosphatase activity towards Gro3P. My work highlighted the importance of this enzyme in metabolic regulation under stressed conditions such as hyperglycemia, pointing to its potential as a therapeutic target for metabolic diseases like T2D and NAFLD.

In Chapter II, I showed that G3PP deletion in β-cells affects their metabolism and insulin secretion *in vivo,* primarily when glucose concentrations are elevated. However, I studied my BKO mouse model under normal diet, raising the question about how the BKO mice would respond when challenged with a diet that leads to chronic hyperglycemia. I observed that *ex vivo* BKO islets show showed increased apoptosis, reduced insulin content and decreased mRNA expression

of β-cell differentiation markers when chronically exposed to elevated glucose levels. Considering the known role of G3PP in clearing compounds that are potentially toxic to β-cells and other tissues (e.g. 2P-lactate, 4-P erythronate and 2P glycolate), it would be interesting to evaluate BKO mice fed a high sucrose / high fat diet to determine whether the β-cell KO could alter whole body glycerol release, glucose usage and oxidation, fat metabolism and insulin secretion and glucose tolerance. It would also be interesting to examine if controlled overexpression of G3PP in β-cells protects against metabolic stress induced deregulation of insulin secretion and gluco(lipo)toxicity in pancreatic β-cells, *in vivo*. As my initial studies indicated that G3PP overexpression *in vitro* protects against glucolipotoxicity and against excessive stimulation of β-cells by high glucose by reducing insulin secretion (Mugabo, Zhao et al. 2016). Our lab is planning to examine this *in vivo*, using tet-inducible G3PP transgenic (TiG3PP) mice, which will be crossed with Ins1 (Cre) mice (Thorens, Tarussio et al. 2015) to generate β-cell specific Ti-B-G3PP animals. Male Ti-B-G3PP mice (8 weeks old) will be given doxycycline in drinking water and fed normal chow diet and 60% HFD with high sucrose (high fat high sucrose model), for 12 weeks. We will study insulin and glucose homeostasis, both *in vivo* and *ex vivo*; and will correlate our findings with altered glucose, lipid and mitochondrial metabolism in β-cell , insulin secretion in response to various stimuli, insulin content and gene expression, β-cell proliferation, β-cell mass and apoptosis.

In my experiments, I used an inducible model of β-cell specific G3PP-KO mice based on Cre recombinase and evaluated the MCre mice as one of my controls. The MCre mice express a human growth hormone (hGH) minigene in pancreatic isletswhere local hGH secretion is associated with increased insulin content and resistance to streptozotocin-induced hyperglycaemia (Oropeza, Jouvet et al. 2015). In my study, the transgene construct used to generate the MCre mice can produce hGH in islets (Tamarina, Roe et al. 2014); however, I did not observe a specific

phenotype in MCre mice compared with WT and fl/fl mice for all the *in vivo* variables that I studied (discussed in Chapter II). Despite this, it would be worthwhile to validate my findings using another β-cell specific G3PP-KO mouse model such as the Ins1 (Cre) mice that induce complete recombination in β-cells when the animals are born, compared to the MCre mice in which tamoxifen-dependent gene recombination is induced in adult mice (Thorens, Tarussio et al. 2015). This will show that the phenotype is consistent and reproducible, and will give an insight on the effect of G3PP deletion during embryogenesis and islet development on the adult β-cell.

In Chapter III, I showed that G3PP plays an important role in preventing hyperglycemia-induced metabolic stress in the liver which contributes to enhanced fat and glycogen storage and inflammation. These changes in LKO mice were observed after short periods of induced hyperglycemia and raise questions related to the possible effects of prolonged hyperglycemia or diets that are known to induce NAFLD or NASH on the LKO animals. Specifically, will G3PP deletion lead to NAFLD progression under these conditions? A second major step for this project would be to overexpress G3PP in the liver and investigate if controlled overexpression of G3PP in liver normalizes glycemia, protects from liver steatosis or insulin resistance and reduces gluconeogenesis in a high sucrose / high fat mouse model.

In Chapter IV, I overexpressed G3PP by 3 fold in hepatocytes *in vivo* using AAV8-TBG-hPGP and showed that this resulted in a less severe phenotype than a rat model where G3PP was overexpressed ~100 fold using an adenoviral construct (Mugabo, Zhao et al. 2016). This indicates that further optimize of the level of overexpression in the liver would be worthwhile to identify the threshold level of G3PP activity needed to cause metabolic changes *in vivo* (between 3- and 100-fold). Another major advantage of using AAV8-TBG-hPGP is that it allows us to overexpress G3PP in the livers of different well characterized T2D mouse models to see if G3PP

overexpression can reverse the phenotype of animals such as *db/db* mice, which are obese, hyperglycemic and develop fatty liver (Srinivasan and Ramarao 2007).

Finally, it would be important to study the regulation of G3PP by other fuels that can increase levels of intracellular Gro3P, such as fructose. Glucose and fructose are ingested in approximately equal quantities, but many studies have shown that fructose is the major contributor to *de novo* lipogenesis, mainly in the liver which is the major site of fructose metabolism (Hannou, Haslam et al. 2018, Silva, Marques et al. 2019). Fasting fructose concentrations in plasma are typically 0.02-0.04 mM and can increase up to 10-fold after fructose consumption. Fructose is cleared by the intestine (30%) and the liver (70%) (Hannou, Haslam et al. 2018). In the liver, fructose is phosphorylated by fructokinase to form fructose-1-phosphate, which is converted into dihydroxyacetone phosphate and glyceraldehyde-3-phosphate **(Figure 5.2)**. Fructose entry into glycolysis at this intermediate stage differs from glucose entry as it bypasses phosphofructokinase, a major regulatory point in glycolysis. This bypass may lead to an increased availability of glycolysis metabolites, such as Gro3P and pyruvate when fructose is used as a substrate; which could contribute to increase TG production as Gro3P and pyruvate are also lipid biosynthesis precursors (Hannou, Haslam et al. 2018). Because fructose can rapidly increase Gro3P levels in the liver with less regulation compared to glucose **(Figure 5.2)**, it is possible that G3PP can play an important role in NAFLD mediated by Gro3P derived from the high consumption of fructose.

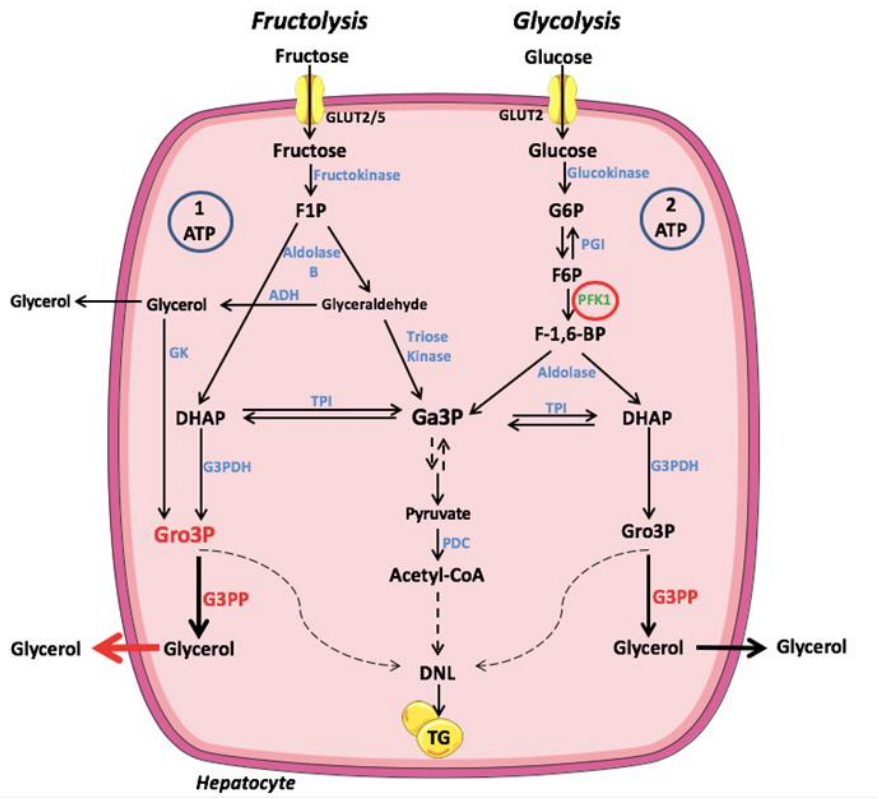

Figure 5.2. Fructose and Glucose metabolism in hepatocyte and role of G3PP

Model depicting the possible role of G3PP in fructose metabolism in hepatocytes. The abbreviations are: Gro3P, glycerol 3-phosphate; G3PP, glycerol 3-phosphate phosphatase; TG, triglyceride; F1P, fructose-1-phosphate; ADH, alcohol dehydrogenases; GK, glycerol kinase; DNL, *de novo* lipogenesis; DHAP, dihydroxyacetone phosphate; Ga3P, glyceraldehyde-3-phosphate; G6P, glucose-6-phosphate; F6P, fructose-6-phosphate; F-1,6-BP, fructose 1,6-bisphosphate; PFK1, phosphofructokinase 1; TPI, triose-phosphate isomerase and G3PDH, glyceraldehyde 3-phosphate dehydrogenase.

5.2 Conclusions

This thesis aimed to provide more insight into the *in vivo* role of G3PP in carbohydrate and lipid metabolism in β-cell and liver, viewing G3PP as a potential detoxification enzyme that eliminates excess glucose carbon as glycerol. I used tissue specific KO mice models and studied them under

normal diet and hyperglycemic conditions with different metabolic challenges *in vivo* and *ex vivo*. The findings in this thesis not only confirm our previous conclusions based on *in vitro* studies using rat islets and hepatocytes (Mugabo, Zhao et al. 2016) but also showed that G3PP played a significant role in hyperglycemic and metabolically stressed mice.

In Chapter II, I demonstrated that G3PP deletion in β-cells affects glucose metabolism, β-cell function and GSIS in BKO mice, but only at high glucose concentrations. BKO mice display increased fed insulinemia, GSIS, body weight, adiposity, reduced glucose tolerance and plasma triglycerides *in vivo*. *Ex vivo*, isolated BKO mouse islets showed elevated GSIS, Gro3P, DHAP and signaling coupling factors reflecting β-cell activation, ATP production and reduced glycerol release, also only at high glucose concentrations. In addition, BKO islets chronically exposed to elevated glucose showed increased apoptosis, reduced insulin content and expression of *Pdx-1*, *Mafa* and *Ins-2* transcripts. This demonstrated that G3PP eliminates excess glucose carbons as glycerol in β-cells to prevent unnecessary excess secretion of insulin that could cause β-cell dysfunction and death under chronic hyperglycemic conditions.

In Chapter III, I demonstrated that G3PP deletion in liver affects glucose and glycerolipid metabolism *in vivo* in LKO mice, particularly under conditions of nutrient excess such as hyperglycemia. Hyperglycemic LKO mice showed enhanced plasma TG, LDL and VLDL and cholesterol levels and increased hepatic weight, TG, glycogen content and expression of inflammatory markers. Furthermore, the levels of Gro3P, DHAP, acetyl-CoA, malonyl-CoA and Krebs cycle intermediates along with the NADP/NADPH ratio were elevated in LKO mouse livers after glucose infusion. This demonstrated that G3PP deletion in hepatocytes increase fat and cholesterol accumulation and inflammation in the liver, which can lead to the development of NAFLD, under conditions of metabolic stress induced by hyperglycemia, seen in diabetic state.

In Chapter IV. I concluded that overexpression of the liver need to be higher than 3 fold to see an effect and this could be done gradually using the AAV8 method or developing a transgenic mice. This is because LOVX mice show minimal phenotypic changes under normal diet and chronic hyperglycemia *in vivo* and no differences in hepatocyte metabolism *ex vivo*.

Overall, the data identify G3PP as a novel metabolic pathway – the *glycerol shunt* – implicated in glucodetoxification and fuel partitioning *via* the metabolic fate of Gro3P and DHAP in both pancreatic β-cells and hepatocytes. Despite the previous beliefs that mammals do not have an enzyme function as G3PP, the work in this thesis and published results (Mugabo, Zhao et al. 2016, Segerer, Hadamek et al. 2016, Possik, Madiraju et al. 2017, Possik, Al-Mass et al. 2021, Possik, Schmitt et al. 2022) shows that such an enzyme does exist and plays a major role in embryonic development, metabolic regulation and different physiological processes. This thesis showed that G3PP activity in pancreatic β-cells is important in regulating GSIS and also in preventing glucotoxicity. Furthermore. G3PP activity in hepatocytes is an important regulator of glucose metabolism and fat storage. G3PP activity can protects against nutrient stress and excess fat accumulation. As a result, by preventing β-cells exhaustion and hyperinsulinemia under metabolic stress conditions and ectopic fat accumulation in the liver G3PP may also be a potential therapeutic target for different metabolic diseases. However, the role and regulation of G3PP in metabolically relevant tissues including VAT, the heart, brain and muscles is still unknown and need further investigation to have full insight on the role of G3PP *in vivo*.

VI. References:

Abdulreda, M. H., R. Rodriguez-Diaz, A. Caicedo and P. O. Berggren (2016). "Liraglutide Compromises Pancreatic beta Cell Function in a Humanized Mouse Model." *Cell Metab* 23(3): 541-546.

Abulizi, A., R. L. Cardone, R. Stark, S. L. Lewandowski, X. Zhao, J. Hillion, L. Ma, R. Sehgal, T. C. Alves, C. Thomas, C. Kung, B. Wang, S. Siebel, Z. B. Andrews, G. F. Mason, J. Rinehart, M. J. Merrins and R. G. Kibbey (2020). "Multi-Tissue Acceleration of the Mitochondrial Phosphoenolpyruvate Cycle Improves Whole-Body Metabolic Health." *Cell Metab* 32(5): 751-766 e711.

Adeva-Andany, M. M., N. Perez-Felpete, C. Fernandez-Fernandez, C. Donapetry-Garcia and C. Pazos-Garcia (2016). "Liver glucose metabolism in humans." *Biosci Rep* 36(6).

Adeyemo, A. A., N. A. Zaghloul, G. Chen, A. P. Doumatey, C. C. Leitch, T. L. Hostelley, J. E. Nesmith, J. Zhou, A. R. Bentley, D. Shriner, O. Fasanmade, G. Okafor, B. Eghan, Jr., K. Agyenim-Boateng, S. Chandrasekharappa, J. Adeleye, W. Balogun, S. Owusu, A. Amoah, J. Acheampong, T. Johnson, J. Oli, C. Adebamowo, S. South Africa Zulu Type 2 Diabetes Case-Control, F. Collins, G. Dunston and C. N. Rotimi (2019). "ZRANB3 is an African-specific type 2 diabetes locus associated with beta-cell mass and insulin response." *Nat Commun* 10(1): 3195.

Aguilar-Salinas, C. A. and T. Viveros-Ruiz (2019). "Recent advances in managing/understanding the metabolic syndrome." *F1000Res* 8.

Ahima, R. S. (2011). "Digging deeper into obesity." *J Clin Invest* 121(6): 2076-2079.

Ahlqvist, E., R. B. Prasad and L. Groop (2020). "Subtypes of Type 2 Diabetes Determined From Clinical Parameters." Diabetes 69(10): 2086-2093.

Al-Goblan, A. S., M. A. Al-Alfi and M. Z. Khan (2014). "Mechanism linking diabetes mellitus and obesity." *Diabetes Metab Syndr Obes* 7: 587-591.

Al-Mass, A., P. Poursharifi, M. L. Peyot, R. Lussier, E. J. Levens, J. Guida, Y. Mugabo, E. Possik, R. Ahmad, F. Al-Mulla, R. Sladek, S. R. M. Madiraju and M. Prentki (2022). "Glycerol-3-

phosphate phosphatase operates a glycerol shunt in pancreatic beta-cells that controls insulin secretion and metabolic stress." *Mol Metab*: 101471.

Alquier, T. and V. Poitout (2009). "GPR40: good cop, bad cop?" *Diabetes* 58(5): 1035-1036.

Alves-Bezerra, M. and D. E. Cohen (2017). "Triglyceride Metabolism in the Liver." *Compr Physiol* 8(1): 1-8.

Amos, A. F., D. J. McCarty and P. Zimmet (1997). "The rising global burden of diabetes and its complications: estimates and projections to the year 2010." *Diabet Med* 14 Suppl 5: S1-85.

Andreadis, P., T. Karagiannis, K. Malandris, I. Avgerinos, A. Liakos, A. Manolopoulos, E. Bekiari, D. R. Matthews and A. Tsapas (2018). "Semaglutide for type 2 diabetes mellitus: A systematic review and meta-analysis." *Diabetes Obes Metab* 20(9): 2255-2263.

Anyamaneeratch, K., P. Rojvirat, W. Sukjoi and S. Jitrapakdee (2015). "Insights into Transcriptional Regulation of Hepatic Glucose Production." *Int Rev Cell Mol Biol* 318: 203-253.

Arguello, G., E. Balboa, M. Arrese and S. Zanlungo (2015). "Recent insights on the role of cholesterol in non-alcoholic fatty liver disease." *Biochim Biophys Acta* 1852(9): 1765-1778.

Armoni, M., C. Harel, F. Bar-Yoseph, S. Milo and E. Karnieli (2005). "Free fatty acids repress the GLUT4 gene expression in cardiac muscle via novel response elements." *J Biol Chem* 280(41): 34786-34795.

Attane, C., M. L. Peyot, R. Lussier, P. Poursharifi, S. Zhao, D. Zhang, J. Morin, M. Pineda, S. Wang, O. Dumortier, N. B. Ruderman, G. A. Mitchell, B. Simons, S. R. Madiraju, E. Joly and M. Prentki (2016). "A beta cell ATGL-lipolysis/adipose tissue axis controls energy homeostasis and body weight via insulin secretion in mice." *Diabetologia* 59(12): 2654-2663.

Bamba, T., T. Hasunuma and A. Kondo (2016). "Disruption of PHO13 improves ethanol production via the xylose isomerase pathway." *AMB Express* 6(1): 4.

Beaudoin, G. A. and A. D. Hanson (2016). "A Guardian Angel Phosphatase for Mainline Carbon Metabolism." *Trends Biochem Sci* 41(11): 893-894.

Bekkevold, C. M., K. L. Robertson, M. K. Reinhard, A. H. Battles and N. E. Rowland (2013). "Dehydration parameters and standards for laboratory mice." *J Am Assoc Lab Anim Sci* 52(3): 233-239.

Bensellam, M., D. R. Laybutt and J. C. Jonas (2012). "The molecular mechanisms of pancreatic beta-cell glucotoxicity: recent findings and future research directions." *Mol Cell Endocrinol* 364(1-2): 1-27.

Bergeron, V., J. Ghislain, K. Vivot, N. Tamarina, L. H. Philipson, J. Fielitz and V. Poitout (2018). "Deletion of protein kinase D1 in pancreatic beta-cells impairs insulin secretion in high-fat diet-fed mice." *Diabetes* 67(1): 71-77.

Birkenfeld, A. L. and G. I. Shulman (2014). "Nonalcoholic fatty liver disease, hepatic insulin resistance, and type 2 diabetes." *Hepatology* 59(2): 713-723.

Bluher, M. (2019). "Obesity: global epidemiology and pathogenesis." *Nat Rev Endocrinol* 15(5): 288-298.

Boden, G., B. Lebed, M. Schatz, C. Homko and S. Lemieux (2001). "Effects of acute changes of plasma free fatty acids on intramyocellular fat content and insulin resistance in healthy subjects." *Diabetes* 50(7): 1612-1617.

Boni-Schnetzler, M., J. Thorne, G. Parnaud, L. Marselli, J. A. Ehses, J. Kerr-Conte, F. Pattou, P. A. Halban, G. C. Weir and M. Y. Donath (2008). "Increased interleukin (IL)-1beta messenger ribonucleic acid expression in beta -cells of individuals with type 2 diabetes and regulation of IL-1beta in human islets by glucose and autostimulation." *J Clin Endocrinol Metab* 93(10): 4065-4074.

Borst, S. E. (2004). "The role of TNF-alpha in insulin resistance." Endocrine 23(2-3): 177-182.

Bou Khalil, M., A. Blais, D. Figeys and Z. Yao (2010). "Lipin - The bridge between hepatic glycerolipid biosynthesis and lipoprotein metabolism." *Biochim Biophys Acta* 1801(12): 1249-1259.

Bradley, D. C. and H. R. Kaslow (1989). "Radiometric assays for glycerol, glucose, and glycogen." *Anal Biochem* 180(1): 11-16.

Briaud, I., J. S. Harmon, C. L. Kelpe, V. B. Segu and V. Poitout (2001). "Lipotoxicity of the pancreatic beta-cell is associated with glucose-dependent esterification of fatty acids into neutral lipids." *Diabetes* 50(2): 315-321.

Broca, C., L. Brennan, P. Petit, P. Newsholme and P. Maechler (2003). "Mitochondria-derived glutamate at the interplay between branched-chain amino acid and glucose-induced insulin secretion." *FEBS Lett* 545(2-3): 167-172.

Brunham, L. R., J. K. Kruit, T. D. Pape, J. M. Timmins, A. Q. Reuwer, Z. Vasanji, B. J. Marsh, B. Rodrigues, J. D. Johnson, J. S. Parks, C. B. Verchere and M. R. Hayden (2007). "Beta-cell ABCA1 influences insulin secretion, glucose homeostasis and response to thiazolidinedione treatment." *Nat Med* 13(3): 340-347.

Bugianesi, E., S. Moscatiello, M. F. Ciaravella and G. Marchesini (2010). "Insulin resistance in nonalcoholic fatty liver disease." *Curr Pharm Des* 16(17): 1941-1951.

Calkin, A. C. and P. Tontonoz (2012). "Transcriptional integration of metabolism by the nuclear sterol-activated receptors LXR and FXR." *Nat Rev Mol Cell Biol* 13(4): 213-224.

Campbell, J. E. and C. B. Newgard (2021). "Mechanisms controlling pancreatic islet cell function in insulin secretion." *Nat Rev Mol Cell Biol*.

Campbell, P. J., L. J. Mandarino and J. E. Gerich (1988). "Quantification of the relative impairment in actions of insulin on hepatic glucose production and peripheral glucose uptake in non-insulin-dependent diabetes mellitus." *Metabolism* 37(1): 15-21.

Caparros-Martin, J. A., S. Reiland, K. Kochert, M. C. Cutanda and F. A. Culianez-Macia (2007). "Arabidopsis thaliana AtGppl and AtGpp2: two novel low molecular weight phosphatases involved in plant glycerol metabolism." *Plant Mol Biol* 63(4): 505-517.

Cassim, S., V. A. Raymond, B. Lacoste, P. Lapierre and M. Bilodeau (2018). "Metabolite profiling identifies a signature of tumorigenicity in hepatocellular carcinoma." *Oncotarget* 9(42): 26868-26883.

Chen, Y., Z. Varghese and X. Z. Ruan (2014). "The molecular pathogenic role of inflammatory stress in dysregulation of lipid homeostasis and hepatic steatosis." *Genes Dis* 1(1): 106-112.

Chew, J. L. and K. Y. Chua (2003). "Collection of mouse urine for bioassays." *Lab Anim* (NY) 32(7): 48-50.

Cho, E. H. (2018). "Succinate as a Regulator of Hepatic Stellate Cells in Liver Fibrosis." *Front Endocrinol (Lausanne)* 9: 455.

Coleman, D. L. (2010). "A historical perspective on leptin." *Nat Med* 16(10): 1097-1099.

Collard, F., F. Baldin, I. Gerin, J. Bolsee, G. Noel, J. Graff, M. Veiga-da-Cunha, V. Stroobant, D. Vertommen, A. Houddane, M. H. Rider, C. L. Linster, E. Van Schaftingen and G. T. Bommer (2016). "A conserved phosphatase destroys toxic glycolytic side products in mammals and yeast." *Nat Chem Biol* 12(8): 601-607.

Corkey, B. E. (2012). "Diabetes: have we got it all wrong? Insulin hypersecretion and food additives: cause of obesity and diabetes?" *Diabetes Care* 35(12): 2432-2437.

Czech, M. P. (2017). "Insulin action and resistance in obesity and type 2 diabetes." *Nat Med* 23(7): 804-814.

Czech, M. P., M. Tencerova, D. J. Pedersen and M. Aouadi (2013). "Insulin signalling mechanisms for triacylglycerol storage." *Diabetologia* 56(5): 949-964.

Daneman, D. (2006). "Type 1 diabetes." *Lancet* 367(9513): 847-858.

Day, C. P. and O. F. James (1998). "Hepatic steatosis: innocent bystander or guilty party?" *Hepatology* 27(6): 1463-1466.

Deeney, J. T., J. Gromada, M. Hoy, H. L. Olsen, C. J. Rhodes, M. Prentki, P. O. Berggren and B. E. Corkey (2000). "Acute stimulation with long chain acyl-CoA enhances exocytosis in insulin-secreting cells (HIT T-15 and NMRI beta-cells)." *J Biol Chem* 275(13): 9363-9368.

DeFronzo, R. A., D. Simonson and E. Ferrannini (1982). "Hepatic and peripheral insulin resistance: a common feature of type 2 (non-insulin-dependent) and type 1 (insulin-dependent) diabetes mellitus." *Diabetologia* 23(4): 313-319.

Delghingaro-Augusto, V., S. Decary, M. L. Peyot, M. G. Latour, J. Lamontagne, N. Paradis-Isler, M. Lacharite-Lemieux, H. Akakpo, O. Birot, C. J. Nolan, M. Prentki and R. Bergeron (2012).

"Voluntary running exercise prevents beta-cell failure in susceptible islets of the Zucker diabetic fatty rat." *Am J Physiol Endocrinol Metab* 302(2): E254-264.

Diraison, F., M. A. Ravier, S. K. Richards, R. M. Smith, H. Shimano and G. A. Rutter (2008). "SREBP1 is required for the induction by glucose of pancreatic beta-cell genes involved in glucose sensing." *J Lipid Res* 49(4): 814-822.

Ditlecadet, D., C. E. Short and W. R. Driedzic (2011). "Glycerol loss to water exceeds glycerol catabolism via glycerol kinase in freeze-resistant rainbow smelt (Osmerus mordax)." *Am J Physiol Regul Integr Comp Physiol* 300(3): R674-684.

Dodson, G. and D. Steiner (1998). "The role of assembly in insulin's biosynthesis." *Curr Opin Struct Biol* 8(2): 189-194.

Donado, C. A., A. B. Cao, D. P. Simmons, B. A. Croker, P. J. Brennan and M. B. Brenner (2020). "A Two-Cell Model for IL-1beta Release Mediated by Death-Receptor Signaling." *Cell Rep* 31(1): 107466.

Donath, M. Y., J. A. Ehses, K. Maedler, D. M. Schumann, H. Ellingsgaard, E. Eppler and M. Reinecke (2005). "Mechanisms of beta-cell death in type 2 diabetes." *Diabetes* 54 Suppl 2: S108-113.

Dumont, L., M. B. Richardson, P. van der Peet, D. S. Marapana, T. Triglia, M. W. A. Dixon, A. F. Cowman, S. J. Williams, L. Tilley, M. J. McConville and S. A. Cobbold (2019). "The Metabolite Repair Enzyme Phosphoglycolate Phosphatase Regulates Central Carbon Metabolism and Fosmidomycin Sensitivity in Plasmodium falciparum." *mBio* 10(6).

Duseja, A. and N. Chalasani (2013). "Epidemiology and risk factors of nonalcoholic fatty liver disease (NAFLD)." *Hepatol Int* 7 Suppl 2: 755-764.

Dwivedi, O. P., M. Lehtovirta, B. Hastoy, V. Chandra, N. A. J. Krentz, S. Kleiner, D. Jain, A. M. Richard, F. Abaitua, N. L. Beer, A. Grotz, R. B. Prasad, O. Hansson, E. Ahlqvist, U. Krus, I. Artner, A. Suoranta, D. Gomez, A. Baras, B. Champon, A. J. Payne, D. Moralli, S. K. Thomsen, P. Kramer, I. Spiliotis, R. Ramracheya, P. Chabosseau, A. Theodoulou, R. Cheung, M. van de Bunt, J. Flannick, M. Trombetta, E. Bonora, C. B. Wolheim, L. Sarelin, R. C. Bonadonna, P. Rorsman, B. Davies, J. Brosnan, M. I. McCarthy, T. Otonkoski, J. O. Lagerstedt, G. A. Rutter,

J. Gromada, A. L. Gloyn, T. Tuomi and L. Groop (2019). "Loss of ZnT8 function protects against diabetes by enhanced insulin secretion." *Nat Genet* 51(11): 1596-1606.

Dwyer, W. (2020). "Characterizing a Phosphoglycolate Phosphatase Ortholog in D. melanogaster." *FASEB Journal* 34(S1): 03428.

Ehses, J. A., A. Perren, E. Eppler, P. Ribaux, J. A. Pospisilik, R. Maor-Cahn, X. Gueripel, H. Ellingsgaard, M. K. Schneider, G. Biollaz, A. Fontana, M. Reinecke, F. Homo-Delarche and M. Y. Donath (2007). "Increased number of islet-associated macrophages in type 2 diabetes." *Diabetes* 56(9): 2356-2370.

El-Assaad, W., J. Buteau, M. L. Peyot, C. Nolan, R. Roduit, S. Hardy, E. Joly, G. Dbaibo, L. Rosenberg and M. Prentki (2003). "Saturated fatty acids synergize with elevated glucose to cause pancreatic beta-cell death." *Endocrinology* 144(9): 4154-4163.

El-Assaad, W., E. Joly, A. Barbeau, R. Sladek, J. Buteau, I. Maestre, E. Pepin, S. Zhao, J. Iglesias, E. Roche and M. Prentki (2010). "Glucolipotoxicity alters lipid partitioning and causes mitochondrial dysfunction, cholesterol, and ceramide deposition and reactive oxygen species production in INS832/13 ss-cells." *Endocrinology* 151(7): 3061-3073.

Engstrom, L. (1978). "The regulation of liver pyruvate kinase by phosphorylation--dephosphorylation." *Curr Top Cell Regul* 13: 28-51.

Erion, D. M. and G. I. Shulman (2010). "Diacylglycerol-mediated insulin resistance." *Nat Med* 16(4): 400-402.

Eslam, M. and J. George (2020). "Genetic contributions to NAFLD: leveraging shared genetics to uncover systems biology." *Nat Rev Gastroenterol Hepatol* 17(1): 40-52.

Esler, W. P. and K. K. Bence (2019). "Metabolic Targets in Nonalcoholic Fatty Liver Disease." *Cell Mol Gastroenterol Hepatol* 8(2): 247-267.

Estabrook, R. W. and B. Sacktor (1958). "alpha-Glycerophosphate oxidase of flight muscle mitochondria." *J Biol Chem* 233(4): 1014-1019.

Faber, C. L., J. D. Deem, C. A. Campos, G. J. Taborsky, Jr. and G. J. Morton (2020). "CNS control of the endocrine pancreas." *Diabetologia* 63(10): 2086-2094.

Fan, J., M. Whiteway and S. H. Shen (2005). "Disruption of a gene encoding glycerol 3-phosphatase from Candida albicans impairs intracellular glycerol accumulation-mediated salt-tolerance." *FEMS Microbiol Lett* 245(1): 107-116.

Farfari, S., V. Schulz, B. Corkey and M. Prentki (2000). "Glucose-regulated anaplerosis and cataplerosis in pancreatic beta-cells: possible implication of a pyruvate/citrate shuttle in insulin secretion." *Diabetes* 49(5): 718-726.

Farooqi, I. S. (2014). "Defining the neural basis of appetite and obesity: from genes to behaviour." *Clin Med (Lond)* 14(3): 286-289.

Farooqi, I. S. and S. O'Rahilly (2014). "20 years of leptin: human disorders of leptin action." *J Endocrinol* 223(1): T63-70.

Fazakerley, D. J., J. R. Krycer, A. L. Kearney, S. L. Hocking and D. E. James (2019). "Muscle and adipose tissue insulin resistance: malady without mechanism?" *J Lipid Res* 60(10): 1720-1732.

Fisher, S. J. and C. R. Kahn (2003). "Insulin signaling is required for insulin's direct and indirect action on hepatic glucose production." *J Clin Invest* 111(4): 463-468.

Flory, W., B. D. Peczon, R. E. Koeppe and H. O. Spivey (1974). "Kinetic properties of rat liver pyruvate kinase at cellular concentrations of enzyme, substrates and modifiers." *Biochem J* 141(1): 127-131.

Foster, D. A. (2007). "Regulation of mTOR by phosphatidic acid?" Cancer Res 67(1): 1-4.

Fransson, U., A. H. Rosengren, F. C. Schuit, E. Renstrom and H. Mulder (2006). "Anaplerosis via pyruvate carboxylase is required for the fuel-induced rise in the ATP:ADP ratio in rat pancreatic islets." *Diabetologia* 49(7): 1578-1586.

Fu, Z., E. R. Gilbert and D. Liu (2013). "Regulation of insulin synthesis and secretion and pancreatic Beta-cell dysfunction in diabetes." *Curr Diabetes Rev* 9(1): 25-53.

Gaudet, D., S. Arsenault, L. Perusse, M. C. Vohl, J. St-Pierre, J. Bergeron, J. P. Despres, K. Dewar, M. J. Daly, T. Hudson and J. D. Rioux (2000). "Glycerol as a correlate of impaired glucose

tolerance: dissection of a complex system by use of a simple genetic trait." *Am J Hum Genet* 66(5): 1558-1568.

Gauthier, M. S., R. Rabasa-Lhoret, D. Prud'homme, A. D. Karelis, D. Geng, B. van Bavel and J. Ruzzin (2014). "The metabolically healthy but obese phenotype is associated with lower plasma levels of persistent organic pollutants as compared to the metabolically abnormal obese phenotype." *J Clin Endocrinol Metab* 99(6): E1061-1066.

Gerich, J. E. (2010). "Role of the kidney in normal glucose homeostasis and in the hyperglycaemia of diabetes mellitus: therapeutic implications." *Diabet Med* 27(2): 136-142.

Gerich, J. E., C. Meyer, H. J. Woerle and M. Stumvoll (2001). "Renal gluconeogenesis: its importance in human glucose homeostasis." *Diabetes Care* 24(2): 382-391.

Gerich, J. E., A. Mitrakou, D. Kelley, L. Mandarino, N. Nurjhan, J. Reilly, T. Jenssen, T. Veneman and A. Consoli (1990). "Contribution of impaired muscle glucose clearance to reduced postabsorptive systemic glucose clearance in NIDDM." *Diabetes* 39(2): 211-216.

Gohla, A. (2019). "Do metabolic HAD phosphatases moonlight as protein phosphatases?" *Biochim Biophys Acta Mol Cell Res* 1866(1): 153-166.

Grankvist, K., S. Marklund and I. B. Taljedal (1981). "Superoxide dismutase is a prophylactic against alloxan diabetes." *Nature* 294(5837): 158-160.

Guan, H. P., Y. Li, M. V. Jensen, C. B. Newgard, C. M. Steppan and M. A. Lazar (2002). "A futile metabolic cycle activated in adipocytes by antidiabetic agents." *Nat Med* 8(10): 1122-1128.

Gupta, D., T. L. Jetton, K. LaRock, N. Monga, B. Satish, J. Lausier, M. Peshavaria and J. L. Leahy (2017). "Temporal characterization of beta cell-adaptive and -maladaptive mechanisms during chronic high-fat feeding in C57BL/6NTac mice." *J Biol Chem* 292(30): 12449-12459.

Hagman, D. K., L. B. Hays, S. D. Parazzoli and V. Poitout (2005). "Palmitate inhibits insulin gene expression by altering PDX-1 nuclear localization and reducing MafA expression in isolated rat islets of Langerhans." *J Biol Chem* 280(37): 32413-32418.

Han, H. S., G. Kang, J. S. Kim, B. H. Choi and S. H. Koo (2016). "Regulation of glucose metabolism from a liver-centric perspective." *Exp Mol Med* 48: e218.

Hannou, S. A., D. E. Haslam, N. M. McKeown and M. A. Herman (2018). "Fructose metabolism and metabolic disease." *J Clin Invest* 128(2): 545-555.

Harkins, J. M. and B. Ahmad (2022). Anatomy, Abdomen and Pelvis, Portal Venous System (Hepatic Portal System). *StatPearls*. Treasure Island (FL).

Herder, C. and M. Y. Donath (2015). "Interleukin-1 receptor antagonist: friend or foe to the heart?" *Lancet Diabetes Endocrinol* 3(4): 228-229.

Herman, M. A. and B. B. Kahn (2006). "Glucose transport and sensing in the maintenance of glucose homeostasis and metabolic harmony." *J Clin Invest* 116(7): 1767-1775.

Hiriart, M. and L. Aguilar-Bryan (2008). "Channel regulation of glucose sensing in the pancreatic beta-cell." *Am J Physiol Endocrinol Metab* 295(6): E1298-1306.

Horton, J. D., J. L. Goldstein and M. S. Brown (2002). "SREBPs: activators of the complete program of cholesterol and fatty acid synthesis in the liver." *J Clin Invest* 109(9): 1125-1131.

Htike, Z. Z., F. Zaccardi, D. Papamargaritis, D. R. Webb, K. Khunti and M. J. Davies (2017). "Efficacy and safety of glucagon-like peptide-1 receptor agonists in type 2 diabetes: A systematic review and mixed-treatment comparison analysis." *Diabetes Obes Metab* 19(4): 524-536.

Huang, J., M. Malhi, J. Deneke and M. E. Fraser (2015). "Structure of GTP-specific succinyl-CoA synthetase in complex with CoA." *Acta Crystallogr F Struct Biol Commun* 71(Pt 8): 1067-1071.

Huang, T. D., J. Behary and A. Zekry (2019). "Non-alcoholic fatty liver disease (NAFLD): a review of epidemiology, risk factors, diagnosis and management." *Intern Med J*.

Huang, T. D., J. Behary and A. Zekry (2020). "Non-alcoholic fatty liver disease: a review of epidemiology, risk factors, diagnosis and management." *Intern Med J* 50(9): 1038-1047.

Hudish, L. I., J. E. Reusch and L. Sussel (2019). "beta Cell dysfunction during progression of metabolic syndrome to type 2 diabetes." *J Clin Invest* 129(10): 4001-4008.

Hurrle, S. and W. H. Hsu (2017). "The etiology of oxidative stress in insulin resistance." *Biomed J* 40(5): 257-262.

Ishihara, H., H. Wang, L. R. Drewes and C. B. Wollheim (1999). "Overexpression of monocarboxylate transporter and lactate dehydrogenase alters insulin secretory responses to pyruvate and lactate in beta cells." *J Clin Invest* 104(11): 1621-1629.

Itoh, M., T. Suganami, H. Kato, S. Kanai, I. Shirakawa, T. Sakai, T. Goto, M. Asakawa, I. Hidaka, H. Sakugawa, K. Ohnishi, Y. Komohara, K. Asano, I. Sakaida, M. Tanaka and Y. Ogawa (2017). "CD11c+ resident macrophages drive hepatocyte death-triggered liver fibrosis in a murine model of nonalcoholic steatohepatitis." *JCI Insight* 2(22).

Iynedjian, P. B. (2009). "Molecular physiology of mammalian glucokinase." *Cell Mol Life Sci* 66(1): 27-42.

Jensen, M. V., J. W. Joseph, O. Ilkayeva, S. Burgess, D. Lu, S. M. Ronnebaum, M. Odegaard, T. C. Becker, A. D. Sherry and C. B. Newgard (2006). "Compensatory responses to pyruvate carboxylase suppression in islet beta-cells. Preservation of glucose-stimulated insulin secretion." *J Biol Chem* 281(31): 22342-22351.

Jetton, T. L., J. Lausier, K. LaRock, W. E. Trotman, B. Larmie, A. Habibovic, M. Peshavaria and J. L. Leahy (2005). "Mechanisms of compensatory beta-cell growth in insulin-resistant rats: roles of Akt kinase." *Diabetes* 54(8): 2294-2304.

Johnson, A. M. and J. M. Olefsky (2013). "The origins and drivers of insulin resistance." *Cell* 152(4): 673-684.

Jonas, J. C., M. Bensellam, J. Duprez, H. Elouil, Y. Guiot and S. M. Pascal (2009). "Glucose regulation of islet stress responses and beta-cell failure in type 2 diabetes." *Diabetes Obes Metab* 11 Suppl 4: 65-81.

Jump, D. B. (2004). "Fatty acid regulation of gene transcription." *Crit Rev Clin Lab Sci* 41(1): 41-78.

Kahn, B. B. and J. S. Flier (2000). "Obesity and insulin resistance." *J Clin Invest* 106(4): 473-481.

Kahn, S. E., R. L. Hull and K. M. Utzschneider (2006). "Mechanisms linking obesity to insulin resistance and type 2 diabetes." *Nature* 444(7121): 840-846.

Kamata, K., M. Mitsuya, T. Nishimura, J. Eiki and Y. Nagata (2004). "Structural basis for allosteric regulation of the monomeric allosteric enzyme human glucokinase." *Structure* 12(3): 429-438.

Kebede, M., T. Alquier, M. G. Latour, M. Semache, C. Tremblay and V. Poitout (2008). "The fatty acid receptor GPR40 plays a role in insulin secretion in vivo after high-fat feeding." *Diabetes* 57(9): 2432-2437.

Kempaiah Nagappa, L., P. Satha, T. Govindaraju and H. Balaram (2019). "Phosphoglycolate phosphatase is a metabolic proofreading enzyme essential for cellular function in Plasmodium berghei." *J Biol Chem* 294(13): 4997-5007.

Khomich, O., A. V. Ivanov and B. Bartosch (2019). "Metabolic Hallmarks of Hepatic Stellate Cells in Liver Fibrosis." *Cells* 9(1).

Kim, J. W., Y. S. Lee, Y. S. Park, B. H. Kim, S. Y. Lee, J. E. Yeon and C. H. Lee (2020). "Multiparametric MR Index for the Diagnosis of Non-Alcoholic Steatohepatitis in Patients with Non-Alcoholic Fatty Liver Disease." *Sci Rep* 10(1): 2671.

Kim, S. R., H. Xu, A. Lesmana, U. Kuzmanovic, M. Au, C. Florencia, E. J. Oh, G. Zhang, K. H. Kim and Y. S. Jin (2015). "Deletion of PHO13, encoding haloacid dehalogenase type IIA phosphatase, results in upregulation of the pentose phosphate pathway in Saccharomyces cerevisiae." *Appl Environ Microbiol* 81(5): 1601-1609.

Kitade, H., G. Chen, Y. Ni and T. Ota (2017). "Nonalcoholic Fatty Liver Disease and Insulin Resistance: New Insights and Potential New Treatments." *Nutrients* 9(4).

Lake, A. D., P. Novak, P. Shipkova, N. Aranibar, D. G. Robertson, M. D. Reily, L. D. Lehman-McKeeman, R. R. Vaillancourt and N. J. Cherrington (2015). "Branched chain amino acid metabolism profiles in progressive human nonalcoholic fatty liver disease." *Amino Acids* 47(3): 603-615.

Lamontagne, J., A. Al-Mass, C. J. Nolan, B. E. Corkey, S. R. M. Madiraju, E. Joly and M. Prentki (2017). "Identification of the signals for glucose-induced insulin secretion in INS1 (832/13) beta-cells using metformin-induced metabolic deceleration as a model." *J Biol Chem* 292(47): 19458-19468.

Larrouy-Maumus, G., T. Biswas, D. M. Hunt, G. Kelly, O. V. Tsodikov and L. P. de Carvalho (2013). "Discovery of a glycerol 3-phosphate phosphatase reveals glycerophospholipid polar head recycling in Mycobacterium tuberculosis." *Proc Natl Acad Sci U S A* 110(28): 11320-11325.

Latour, M. G., T. Alquier, E. Oseid, C. Tremblay, T. L. Jetton, J. Luo, D. C. Lin and V. Poitout (2007). "GPR40 is necessary but not sufficient for fatty acid stimulation of insulin secretion in vivo." *Diabetes* 56(4): 1087-1094.

Laybutt, D. R., Y. C. Hawkins, J. Lock, J. Lebet, A. Sharma, S. Bonner-Weir and G. C. Weir (2007). "Influence of diabetes on the loss of beta cell differentiation after islet transplantation in rats." *Diabetologia* 50(10): 2117-2125.

Lee, S. J., C. T. Murphy and C. Kenyon (2009). "Glucose shortens the life span of C. elegans by downregulating DAF-16/FOXO activity and aquaporin gene expression." *Cell Metab* 10(5): 379-391.

Lee, S. J. and S. W. Shin (2017). "Mechanisms, Pathophysiology, and Management of Obesity." *N Engl J Med* 376(15): 1491-1492.

Lee, Y. P. and H. A. Lardy (1965). "Influence of Thyroid Hormones on L-Alpha-Glycerophosphate Dehydrogenases and Other Dehydrogenases in Various Organs of the Rat." *J Biol Chem* 240: 1427-1436.

Leighton, E., C. A. Sainsbury and G. C. Jones (2017). "A Practical Review of C-Peptide Testing in Diabetes." *Diabetes Ther* 8(3): 475-487.

Lewandowski, S. L., R. L. Cardone, H. R. Foster, T. Ho, E. Potapenko, C. Poudel, H. R. VanDeusen, S. M. Sdao, T. C. Alves, X. Zhao, M. E. Capozzi, A. H. de Souza, I. Jahan, C. J. Thomas, C. S. Nunemaker, D. B. Davis, J. E. Campbell, R. G. Kibbey and M. J. Merrins (2020). "Pyruvate Kinase Controls Signal Strength in the Insulin Secretory Pathway." *Cell Metab* 32(5): 736-750 e735.

Leyva, F., C. S. Wingrove, I. F. Godsland and J. C. Stevenson (1998). "The glycolytic pathway to coronary heart disease: a hypothesis." *Metabolism* 47(6): 657-662.

Li, N., M. Karaca and P. Maechler (2017). "Upregulation of UCP2 in beta-cells confers partial protection against both oxidative stress and glucotoxicity." Redox Biol 13: 541-549.

Lin, E. C. (1977). "Glycerol utilization and its regulation in mammals." *Annu Rev Biochem* 46: 765-795.

Lin, N., H. Zhang and Q. Su (2012). "Advanced glycation end-products induce injury to pancreatic beta cells through oxidative stress." *Diabetes Metab* 38(3): 250-257.

Lindner, S. N., T. M. Meiswinkel, M. Panhorst, J. W. Youn, L. Wiefel and V. F. Wendisch (2012). "Glycerol-3-phosphatase of Corynebacterium glutamicum." *J Biotechnol* 159(3): 216-224.

Liu, X., H. Zhang and J. Liang (2013). "Blood urea nitrogen is elevated in patients with non-alcoholic fatty liver disease." *Hepatogastroenterology* 60(122): 343-345.

Lu, H., V. Koshkin, E. M. Allister, A. V. Gyulkhandanyan and M. B. Wheeler (2010). "Molecular and metabolic evidence for mitochondrial defects associated with beta-cell dysfunction in a mouse model of type 2 diabetes." *Diabetes* 59(2): 448-459.

MacDonald, M. J., A. Dobrzyn, J. Ntambi and S. W. Stoker (2008). "The role of rapid lipogenesis in insulin secretion: Insulin secretagogues acutely alter lipid composition of INS-1 832/13 cells." *Arch Biochem Biophys* 470(2): 153-162.

Maedler, K., P. Sergeev, F. Ris, J. Oberholzer, H. I. Joller-Jemelka, G. A. Spinas, N. Kaiser, P. A. Halban and M. Y. Donath (2002). "Glucose-induced beta cell production of IL-1beta contributes to glucotoxicity in human pancreatic islets." *J Clin Invest* 110(6): 851-860.

Magnusson, I., D. L. Rothman, L. D. Katz, R. G. Shulman and G. I. Shulman (1992). "Increased rate of gluconeogenesis in type II diabetes mellitus. A 13C nuclear magnetic resonance study." *J Clin Invest* 90(4): 1323-1327.

Magro, M. G. and M. Solimena (2013). "Regulation of beta-cell function by RNA-binding proteins." *Mol Metab* 2(4): 348-355.

Mahajan, A., D. Taliun, M. Thurner, N. R. Robertson, J. M. Torres, N. W. Rayner, A. J. Payne, V. Steinthorsdottir, R. A. Scott, N. Grarup, J. P. Cook, E. M. Schmidt, M. Wuttke, C. Sarnowski, R. Magi, J. Nano, C. Gieger, S. Trompet, C. Lecoeur, M. H. Preuss, B. P. Prins, X. Guo, L. F.

Bielak, J. E. Below, D. W. Bowden, J. C. Chambers, Y. J. Kim, M. C. Y. Ng, L. E. Petty, X. Sim, W. Zhang, A. J. Bennett, J. Bork-Jensen, C. M. Brummett, M. Canouil, K. U. Ec Kardt, K. Fischer, S. L. R. Kardia, F. Kronenberg, K. Lall, C. T. Liu, A. E. Locke, J. Luan, I. Ntalla, V. Nylander, S. Schonherr, C. Schurmann, L. Yengo, E. P. Bottinger, I. Brandslund, C. Christensen, G. Dedoussis, J. C. Florez, I. Ford, O. H. Franco, T. M. Frayling, V. Giedraitis, S. Hackinger, A. T. Hattersley, C. Herder, M. A. Ikram, M. Ingelsson, M. E. Jorgensen, T. Jorgensen, J. Kriebel, J. Kuusisto, S. Ligthart, C. M. Lindgren, A. Linneberg, V. Lyssenko, V. Mamakou, T. Meitinger, K. L. Mohlke, A. D. Morris, G. Nadkarni, J. S. Pankow, A. Peters, N. Sattar, A. Stancakova, K. Strauch, K. D. Taylor, B. Thorand, G. Thorleifsson, U. Thorsteinsdottir, J. Tuomilehto, D. R. Witte, J. Dupuis, P. A. Peyser, E. Zeggini, R. J. F. Loos, P. Froguel, E. Ingelsson, L. Lind, L. Groop, M. Laakso, F. S. Collins, J. W. Jukema, C. N. A. Palmer, H. Grallert, A. Metspalu, A. Dehghan, A. Kottgen, G. R. Abecasis, J. B. Meigs, J. I. Rotter, J. Marchini, O. Pedersen, T. Hansen, C. Langenberg, N. J. Wareham, K. Stefansson, A. L. Gloyn, A. P. Morris, M. Boehnke and M. I. McCarthy (2018). "Fine-mapping type 2 diabetes loci to single-variant resolution using high-density imputation and islet-specific epigenome maps." *Nat Genet* 50(11): 1505-1513.

Mairal, A., D. Langin, P. Arner and J. Hoffstedt (2006). "Human adipose triglyceride lipase (PNPLA2) is not regulated by obesity and exhibits low in vitro triglyceride hydrolase activity." *Diabetologia* 49(7): 1629-1636.

Marra, F. and S. Lotersztajn (2013). "Pathophysiology of NASH: perspectives for a targeted treatment." *Curr Pharm Des* 19(29): 5250-5269.

Martins, E. F., C. K. Miyasaka, P. Newsholme, R. Curi and A. R. Carpinelli (2004). "Changes of fatty acid composition in incubated rat pancreatic islets." *Diabetes Metab* 30(1): 21-27.

Matschinsky, F. M. (2002). "Regulation of pancreatic beta-cell glucokinase: from basics to therapeutics." *Diabetes* 51 Suppl 3: S394-404.

Matsumura, K., B. H. Chang, M. Fujimiya, W. Chen, R. N. Kulkarni, Y. Eguchi, H. Kimura, H. Kojima and L. Chan (2007). "Aquaporin 7 is a beta-cell protein and regulator of intraislet glycerol content and glycerol kinase activity, beta-cell mass, and insulin production and secretion." Mol Cell Biol 27(17): 6026-6037.

Matsuzawa, N., T. Takamura, S. Kurita, H. Misu, T. Ota, H. Ando, M. Yokoyama, M. Honda, Y. Zen, Y. Nakanuma, K. Miyamoto and S. Kaneko (2007). "Lipid-induced oxidative stress causes steatohepatitis in mice fed an atherogenic diet." Hepatology 46(5): 1392-1403.

Matulewicz, N. and M. Karczewska-Kupczewska (2016). "Insulin resistance and chronic inflammation." Postepy Hig Med Dosw (Online) 70(0): 1245-1258.

Meijssen, S., M. C. Cabezas, C. G. Ballieux, R. J. Derksen, S. Bilecen and D. W. Erkelens (2001). "Insulin mediated inhibition of hormone sensitive lipase activity in vivo in relation to endogenous catecholamines in healthy subjects." J Clin Endocrinol Metab 86(9): 4193-4197.

Mills, E. and L. A. O'Neill (2014). "Succinate: a metabolic signal in inflammation." Trends Cell Biol 24(5): 313-320.

Mittendorfer, B., F. Magkos, E. Fabbrini, B. S. Mohammed and S. Klein (2009). "Relationship between body fat mass and free fatty acid kinetics in men and women." Obesity (Silver Spring) 17(10): 1872-1877.

Miwa, K., M. Asano, R. Horai, Y. Iwakura, S. Nagata and T. Suda (1998). "Caspase 1-independent IL-1beta release and inflammation induced by the apoptosis inducer Fas ligand." Nat Med 4(11): 1287-1292.

Modi, H., C. Jacovetti, D. Tarussio, S. Metref, O. D. Madsen, F. P. Zhang, P. Rantakari, M. Poutanen, S. Nef, T. Gorman, R. Regazzi and B. Thorens (2015). "Autocrine Action of IGF2 Regulates Adult beta-Cell Mass and Function." Diabetes 64(12): 4148-4157.

Moolenaar, W. H., L. A. van Meeteren and B. N. Giepmans (2004). "The ins and outs of lysophosphatidic acid signaling." Bioessays 26(8): 870-881.

Mor, I., E. C. Cheung and K. H. Vousden (2011). "Control of glycolysis through regulation of PFK1: old friends and recent additions." Cold Spring Harb Symp Quant Biol 76: 211-216.

Moran-Salvador, E., M. Lopez-Parra, V. Garcia-Alonso, E. Titos, M. Martinez-Clemente, A. Gonzalez-Periz, C. Lopez-Vicario, Y. Barak, V. Arroyo and J. Claria (2011). "Role for PPARgamma in obesity-induced hepatic steatosis as determined by hepatocyte- and macrophage-specific conditional knockouts." FASEB J 25(8): 2538-2550.

Mracek, T., Z. Drahota and J. Houstek (2013). "The function and the role of the mitochondrial glycerol-3-phosphate dehydrogenase in mammalian tissues." Biochim Biophys Acta 1827(3): 401-410.

Mugabo, Y., S. Zhao, J. Lamontagne, A. Al-Mass, M. L. Peyot, B. E. Corkey, E. Joly, S. R. M. Madiraju and M. Prentki (2017). "Metabolic fate of glucose and candidate signaling and excess-fuel detoxification pathways in pancreatic beta-cells." J Biol Chem 292(18): 7407-7422.

Mugabo, Y., S. Zhao, A. Seifried, S. Gezzar, A. Al-Mass, D. Zhang, J. Lamontagne, C. Attane, P. Poursharifi, J. Iglesias, E. Joly, M. L. Peyot, A. Gohla, S. R. Madiraju and M. Prentki (2016). "Identification of a mammalian glycerol-3-phosphate phosphatase: role in metabolism and signaling in pancreatic beta-cells and hepatocytes." Proc Natl Acad Sci U S A 113(4): E430-439.

Mulder, H., M. Sorhede-Winzell, J. A. Contreras, M. Fex, K. Strom, T. Ploug, H. Galbo, P. Arner, C. Lundberg, F. Sundler, B. Ahren and C. Holm (2003). "Hormone-sensitive lipase null mice exhibit signs of impaired insulin sensitivity whereas insulin secretion is intact." J Biol Chem 278(38): 36380-36388.

Mulder, H., S. Yang, M. S. Winzell, C. Holm and B. Ahren (2004). "Inhibition of lipase activity and lipolysis in rat islets reduces insulin secretion." Diabetes 53(1): 122-128.

Murea, M., L. Ma and B. I. Freedman (2012). "Genetic and environmental factors associated with type 2 diabetes and diabetic vascular complications." Rev Diabet Stud 9(1): 6-22.

Murray, S., A. Tulloch, M. S. Gold and N. M. Avena (2014). "Hormonal and neural mechanisms of food reward, eating behaviour and obesity." Nat Rev Endocrinol 10(9): 540-552.

Nadkarni, P., O. G. Chepurny and G. G. Holz (2014). "Regulation of glucose homeostasis by GLP-1." Prog Mol Biol Transl Sci 121: 23-65.

Nagappa, L. K., P. Satha, T. Govindaraju and H. Balaram (2019). "Correction: Phosphoglycolate phosphatase is a metabolic proofreading enzyme essential for cellular function in Plasmodium berghei." J Biol Chem 294(44): 16479.

Nelson, J. L. and R. A. Robergs (2007). "Exploring the potential ergogenic effects of glycerol hyperhydration." Sports Med 37(11): 981-1000.

Newsholme, P., K. Bender, A. Kiely and L. Brennan (2007). "Amino acid metabolism, insulin secretion and diabetes." Biochem Soc Trans 35(Pt 5): 1180-1186.

Newsholme, P. and M. Krause (2012). "Nutritional regulation of insulin secretion: implications for diabetes." Clin Biochem Rev 33(2): 35-47.

Nguyen-Lefebvre, A. T. and A. Horuzsko (2015). "Kupffer Cell Metabolism and Function." J Enzymol Metab 1(1).

Nishikawa, T., D. Edelstein, X. L. Du, S. Yamagishi, T. Matsumura, Y. Kaneda, M. A. Yorek, D. Beebe, P. J. Oates, H. P. Hammes, I. Giardino and M. Brownlee (2000). "Normalizing mitochondrial superoxide production blocks three pathways of hyperglycaemic damage." Nature 404(6779): 787-790.

Noguchi, K., S. Ishii and T. Shimizu (2003). "Identification of p2y9/GPR23 as a novel G protein-coupled receptor for lysophosphatidic acid, structurally distant from the Edg family." J Biol Chem 278(28): 25600-25606.

Nolan, C. J., P. Damm and M. Prentki (2011). "Type 2 diabetes across generations: from pathophysiology to prevention and management." Lancet 378(9786): 169-181.

Nolan, C. J., J. L. Leahy, V. Delghingaro-Augusto, J. Moibi, K. Soni, M. L. Peyot, M. Fortier, C. Guay, J. Lamontagne, A. Barbeau, E. Przybytkowski, E. Joly, P. Masiello, S. Wang, G. A. Mitchell and M. Prentki (2006). "Beta cell compensation for insulin resistance in Zucker fatty rats: increased lipolysis and fatty acid signalling." Diabetologia 49(9): 2120-2130.

Nolan, C. J. and M. Prentki (2008). "The islet beta-cell: fuel responsive and vulnerable." Trends Endocrinol Metab 19(8): 285-291.

Nolan, C. J. and M. Prentki (2019). "Insulin resistance and insulin hypersecretion in the metabolic syndrome and type 2 diabetes: time for a conceptual framework shift." Diab Vasc Dis Res 16(2): 118-127.

Norbeck, J., A. K. Pahlman, N. Akhtar, A. Blomberg and L. Adler (1996). "Purification and characterization of two isoenzymes of DL-glycerol-3-phosphatase from Saccharomyces cerevisiae. Identification of the corresponding GPP1 and GPP2 genes and evidence for osmotic

regulation of Gpp2p expression by the osmosensing mitogen-activated protein kinase signal transduction pathway." J Biol Chem 271(23): 13875-13881.

Nye, C. K., R. W. Hanson and S. C. Kalhan (2008). "Glyceroneogenesis is the dominant pathway for triglyceride glycerol synthesis in vivo in the rat." J Biol Chem 283(41): 27565-27574.

O'Neill, S. and L. O'Driscoll (2015). "Metabolic syndrome: a closer look at the growing epidemic and its associated pathologies." Obes Rev 16(1): 1-12.

Oberhauser, L. and P. Maechler (2021). "Lipid-Induced Adaptations of the Pancreatic Beta-Cell to Glucotoxic Conditions Sustain Insulin Secretion." Int J Mol Sci 23(1).

Obstfeld, A. E., E. Sugaru, M. Thearle, A. M. Francisco, C. Gayet, H. N. Ginsberg, E. V. Ables and A. W. Ferrante, Jr. (2010). "C-C chemokine receptor 2 (CCR2) regulates the hepatic recruitment of myeloid cells that promote obesity-induced hepatic steatosis." Diabetes 59(4): 916-925.

Ochoa-Sanchez, R., M. M. Oliveira, M. Tremblay, G. Petrazzo, A. Pant, C. R. Bosoi, M. Perreault, W. Querbes, C. B. Kurtz and C. F. Rose (2021). "Genetically engineered E. coli Nissle attenuates hyperammonemia and prevents memory impairment in bile-duct ligated rats." Liver Int 41(5): 1020-1032.

Odegaard, J. I., R. R. Ricardo-Gonzalez, A. Red Eagle, D. Vats, C. R. Morel, M. H. Goforth, V. Subramanian, L. Mukundan, A. W. Ferrante and A. Chawla (2008). "Alternative M2 activation of Kupffer cells by PPARdelta ameliorates obesity-induced insulin resistance." Cell Metab 7(6): 496-507.

Oh, Y. S., G. D. Bae, D. J. Baek, E. Y. Park and H. S. Jun (2018). "Fatty Acid-Induced Lipotoxicity in Pancreatic Beta-Cells During Development of Type 2 Diabetes." Front Endocrinol (Lausanne) 9: 384.

Omar-Hmeadi, M. and O. Idevall-Hagren (2021). "Insulin granule biogenesis and exocytosis." Cell Mol Life Sci 78(5): 1957-1970.

Oral, A., T. Sahin, F. Turker and E. Kocak (2019). "Relationship Between Serum Uric Acid Levels and Nonalcoholic Fatty Liver Disease in Non-Obese Patients." Medicina (Kaunas) 55(9).

Oropeza, D., N. Jouvet, L. Budry, J. E. Campbell, K. Bouyakdan, J. Lacombe, G. Perron, V. Bergeron, J. C. Neuman, H. K. Brar, R. J. Fenske, C. Meunier, S. Sczelecki, M. E. Kimple, D. J. Drucker, R. A. Screaton, V. Poitout, M. Ferron, T. Alquier and J. L. Estall (2015). "Phenotypic characterization of MIP-CreERT1Lphi mice with transgene-driven islet expression of human growth hormone." Diabetes 64(11): 3798-3807.

Pahlman, A. K., K. Granath, R. Ansell, S. Hohmann and L. Adler (2001). "The yeast glycerol 3-phosphatases Gpp1p and Gpp2p are required for glycerol biosynthesis and differentially involved in the cellular responses to osmotic, anaerobic, and oxidative stress." J Biol Chem 276(5): 3555-3563.

Pascal, S. M., M. Veiga-da-Cunha, P. Gilon, E. Van Schaftingen and J. C. Jonas (2010). "Effects of fructosamine-3-kinase deficiency on function and survival of mouse pancreatic islets after prolonged culture in high glucose or ribose concentrations." Am J Physiol Endocrinol Metab 298(3): E586-596.

Petersen, M. C. and G. I. Shulman (2018). "Mechanisms of Insulin Action and Insulin Resistance." Physiol Rev 98(4): 2133-2223.

Peyot, M. L., C. Guay, M. G. Latour, J. Lamontagne, R. Lussier, M. Pineda, N. B. Ruderman, G. Haemmerle, R. Zechner, E. Joly, S. R. M. Madiraju, V. Poitout and M. Prentki (2009). "Adipose triglyceride lipase is implicated in fuel- and non-fuel-stimulated insulin secretion." J Biol Chem 284(25): 16848-16859.

Peyot, M. L., E. Pepin, J. Lamontagne, M. G. Latour, B. Zarrouki, R. Lussier, M. Pineda, T. L. Jetton, S. R. Madiraju, E. Joly and M. Prentki (2010). "Beta-cell failure in diet-induced obese mice stratified according to body weight gain: secretory dysfunction and altered islet lipid metabolism without steatosis or reduced beta-cell mass." Diabetes 59(9): 2178-2187.

Peyot, M. L., A. Roubtsova, R. Lussier, A. Chamberland, R. Essalmani, S. R. Murthy Madiraju, N. G. Seidah, M. Prentki and A. Prat (2021). "Substantial PCSK9 inactivation in beta-cells does not modify glucose homeostasis or insulin secretion in mice." Biochim Biophys Acta Mol Cell Biol Lipids 1866(8): 158968.

Pisoschi, A. M. and A. Pop (2015). "The role of antioxidants in the chemistry of oxidative stress: A review." Eur J Med Chem 97: 55-74.

Poitout, V., J. Amyot, M. Semache, B. Zarrouki, D. Hagman and G. Fontes (2010). "Glucolipotoxicity of the pancreatic beta cell." Biochim Biophys Acta 1801(3): 289-298.

Poitout, V. and R. P. Robertson (2002). "Minireview: Secondary beta-cell failure in type 2 diabetes--a convergence of glucotoxicity and lipotoxicity." Endocrinology 143(2): 339-342.

Poitout, V. and R. P. Robertson (2008). "Glucolipotoxicity: fuel excess and beta-cell dysfunction." Endocr Rev 29(3): 351-366.

Porte, D., Jr. (1999). "Mechanisms for hyperglycemia in the metabolic syndrome. The key role of beta-cell dysfunction." Ann N Y Acad Sci 892: 73-83.

Possik, E., A. Al-Mass, M. L. Peyot, R. Ahmad, F. Al-Mulla, S. R. M. Madiraju and M. Prentki (2021). "New mammalian glycerol-3-phosphate phosphatase: role in beta-cell, liver and adipocyte metabolism." Front Endocrinol (Lausanne) 12: 706607.

Possik, E., S. R. M. Madiraju and M. Prentki (2017). "Glycerol-3-phosphate phosphatase/PGP: role in intermediary metabolism and target for cardiometabolic diseases." Biochimie 143: 18-28.

Possik, E., C. Schmitt, A. Al-Mass, Y. Bai, L. Cote, J. Morin, H. Erb, A. Oppong, W. Kahloan, J. A. Parker, S. R. M. Madiraju and M. Prentki (2022). "Phosphoglycolate phosphatase homologs act as glycerol-3-phosphate phosphatase to control stress and healthspan in C. elegans." Nat Commun 13(1): 177.

Possik, E., C. Schmitt, A. Al-Mass, Y. Bai, L. Côté, J. Morin, H. Erb, A. Oppong, W. Kahloan, J. A. Parker, S. R. M. Madiraju and M. Prentki (2022). "Phosphoglycolate phosphatase homologs act as glycerol-3-phosphate phosphatase to control stress and healthspan in C. elegans." Nature Communications 11;13(1):177.

Poursharifi, P., C. Attane, Y. Mugabo, A. Al-Mass, A. Ghosh, C. Schmitt, S. Zhao, J. Guida, R. Lussier, H. Erb, I. Chenier, M. L. Peyot, E. Joly, C. Noll, A. C. Carpentier, S. R. M. Madiraju and M. Prentki (2020). "Adipose ABHD6 regulates tolerance to cold and thermogenic programs." JCI Insight 5(24): e140294.

Poursharifi, P., C. Attane, Y. Mugabo, A. Al-Mass, A. Ghosh, C. Schmitt, S. Zhao, J. Guida, R. Lussier, H. Erb, I. Chenier, M. L. Peyot, E. Joly, C. Noll, A. C. Carpentier, S. R. M. Madiraju and M. Prentki (2020). "Adipose ABHD6 regulates tolerance to cold and thermogenic programs." JCI Insight 5(24).

Poursharifi, P., S. R. M. Madiraju and M. Prentki (2017). "Monoacylglycerol signalling and ABHD6 in health and disease." Diabetes Obes Metab 19 Suppl 1: 76-89.

Prentki, M. and B. E. Corkey (1996). "Are the beta-cell signaling molecules malonyl-CoA and cytosolic long-chain acyl-CoA implicated in multiple tissue defects of obesity and NIDDM?" Diabetes 45(3): 273-283.

Prentki, M., B. E. Corkey and S. R. M. Madiraju (2020). "Lipid-associated metabolic signalling networks in pancreatic beta cell function." Diabetologia 63(1): 10-20.

Prentki, M., E. Joly, W. El-Assaad and R. Roduit (2002). "Malonyl-CoA signaling, lipid partitioning, and glucolipotoxicity: role in beta-cell adaptation and failure in the etiology of diabetes." Diabetes 51 Suppl 3: S405-413.

Prentki, M. and S. R. Madiraju (2008). "Glycerolipid metabolism and signaling in health and disease." Endocr Rev 29(6): 647-676.

Prentki, M. and S. R. Madiraju (2012). "Glycerolipid/free fatty acid cycle and islet beta-cell function in health, obesity and diabetes." Mol Cell Endocrinol 353(1-2): 88-100.

Prentki, M., F. M. Matschinsky and S. R. Madiraju (2013). "Metabolic signaling in fuel-induced insulin secretion." Cell Metab 18(2): 162-185.

Prentki, M. and C. J. Nolan (2006). "Islet beta cell failure in type 2 diabetes." J Clin Invest 116(7): 1802-1812.

Prentki, M., M. L. Peyot, P. Masiello and S. R. M. Madiraju (2020). "Nutrient-induced metabolic stress, adaptation, detoxification, and toxicity in the pancreatic beta-cell." Diabetes 69(3): 279-290.

Rancoule, C., C. Attane, S. Gres, A. Fournel, R. Dusaulcy, C. Bertrand, C. Vinel, K. Treguer, M. Prentki, P. Valet and J. S. Saulnier-Blache (2013). "Lysophosphatidic acid impairs glucose

homeostasis and inhibits insulin secretion in high-fat diet obese mice." Diabetologia 56(6): 1394-1402.

Ravnskjaer, K., F. Frigerio, M. Boergesen, T. Nielsen, P. Maechler and S. Mandrup (2010). "PPARdelta is a fatty acid sensor that enhances mitochondrial oxidation in insulin-secreting cells and protects against fatty acid-induced dysfunction." J Lipid Res 51(6): 1370-1379.

Raymond, J. A. (2015). "Two potential fish glycerol-3-phosphate phosphatases." Fish Physiol Biochem 41(3): 811-818.

Roder, P. V., B. Wu, Y. Liu and W. Han (2016). "Pancreatic regulation of glucose homeostasis." Exp Mol Med 48: e219.

Rohlfing, A. K., Y. Miteva, S. Hannenhalli and T. Lamitina (2010). "Genetic and physiological activation of osmosensitive gene expression mimics transcriptional signatures of pathogen infection in C. elegans." PLoS One 5(2): e9010.

Rohner-Jeanrenaud, F. and B. Jeanrenaud (1996). "Obesity, leptin, and the brain." N Engl J Med 334(5): 324-325.

Ronnow, B. and M. C. Kielland-Brandt (1993). "GUT2, a gene for mitochondrial glycerol 3-phosphate dehydrogenase of Saccharomyces cerevisiae." Yeast 9(10): 1121-1130.

Rose, Z. B. (1981). "Phosphoglycolate phosphatase from human red blood cells." Arch Biochem Biophys 208(2): 602-609.

Rose, Z. B., D. S. Grove and S. N. Seal (1986). "Mechanism of activation by anions of phosphoglycolate phosphatases from spinach and human red blood cells." J Biol Chem 261(24): 10996-11002.

Rotondo, F., A. C. Ho-Palma, X. Remesar, J. A. Fernandez-Lopez, M. D. M. Romero and M. Alemany (2017). "Glycerol is synthesized and secreted by adipocytes to dispose of excess glucose, via glycerogenesis and increased acyl-glycerol turnover." Sci Rep 7(1): 8983.

Rubi, B., A. del Arco, C. Bartley, J. Satrustegui and P. Maechler (2004). "The malate-aspartate NADH shuttle member Aralar1 determines glucose metabolic fate, mitochondrial activity, and insulin secretion in beta cells." J Biol Chem 279(53): 55659-55666.

Ruderman, N. and M. Prentki (2004). "AMP kinase and malonyl-CoA: targets for therapy of the metabolic syndrome." Nat Rev Drug Discov 3(4): 340-351.

Rui, L. (2014). "Energy metabolism in the liver." Compr Physiol 4(1): 177-197.

Ryan, D. H., B. C. Hansen and W. T. Cefalu (2016). "George A. Bray, MD: Progress in Obesity-Multidisciplinary Research, Multidimensional Man." Diabetes Care 39(9): 1481-1485.

Safari, Z. and P. Gerard (2019). "The links between the gut microbiome and non-alcoholic fatty liver disease (NAFLD)." Cell Mol Life Sci 76(8): 1541-1558.

Saggerson, D. (2008). "Malonyl-CoA, a key signaling molecule in mammalian cells." Annu Rev Nutr 28: 253-272.

Samuel, V. T. and G. I. Shulman (2012). "Mechanisms for insulin resistance: common threads and missing links." Cell 148(5): 852-871.

Samuel, V. T. and G. I. Shulman (2016). "The pathogenesis of insulin resistance: integrating signaling pathways and substrate flux." J Clin Invest 126(1): 12-22.

Schwarte, S. and H. Bauwe (2007). "Identification of the photorespiratory 2-phosphoglycolate phosphatase, PGLP1, in Arabidopsis." Plant Physiol 144(3): 1580-1586.

Segerer, G., D. Engelmann, A. Kaestner, M. Trotzmuller, H. Kofeler, C. Stigloher, C. Thiele, E. Jeanclos and A. Gohla (2018). "A phosphoglycolate phosphatase/AUM-dependent link between triacylglycerol turnover and epidermal growth factor signaling." Biochim Biophys Acta Mol Cell Biol Lipids 1863(6): 584-594.

Segerer, G., K. Hadamek, M. Zundler, A. Fekete, A. Seifried, M. J. Mueller, F. Koentgen, M. Gessler, E. Jeanclos and A. Gohla (2016). "An essential developmental function for murine phosphoglycolate phosphatase in safeguarding cell proliferation." Sci Rep 6: 35160.

Seifried, A., A. Bergeron, B. Boivin and A. Gohla (2016). "Reversible oxidation controls the activity and oligomeric state of the mammalian phosphoglycolate phosphatase AUM." Free Radic Biol Med 97: 75-84.

Seifried, A., G. Knobloch, P. S. Duraphe, G. Segerer, J. Manhard, H. Schindelin, J. Schultz and A. Gohla (2014). "Evolutionary and structural analyses of mammalian haloacid dehalogenase-

type phosphatases AUM and chronophin provide insight into the basis of their different substrate specificities." J Biol Chem 289(6): 3416-3431.

Seyer, P., D. Vallois, C. Poitry-Yamate, F. Schutz, S. Metref, D. Tarussio, P. Maechler, B. Staels, B. Lanz, R. Grueter, J. Decaris, S. Turner, A. da Costa, F. Preitner, K. Minehira, M. Foretz and B. Thorens (2013). "Hepatic glucose sensing is required to preserve beta cell glucose competence." J Clin Invest 123(4): 1662-1676.

Sharabi, K., C. D. Tavares, A. K. Rines and P. Puigserver (2015). "Molecular pathophysiology of hepatic glucose production." Mol Aspects Med 46: 21-33.

Sharma, R. B., A. C. O'Donnell, R. E. Stamateris, B. Ha, K. M. McCloskey, P. R. Reynolds, P. Arvan and L. C. Alonso (2015). "Insulin demand regulates beta cell number via the unfolded protein response." J Clin Invest 125(10): 3831-3846.

Shi, D., N. M. Allewell and M. Tuchman (2015). "The N-Acetylglutamate Synthase Family: Structures, Function and Mechanisms." Int J Mol Sci 16(6): 13004-13022.

Shi, Y., H. Wang, Y. Yan, H. Cao, X. Liu, F. Lin and J. Lu (2018). "Glycerol-3-Phosphate Shuttle Is Involved in Development and Virulence in the Rice Blast Fungus Pyricularia oryzae." Front Plant Sci 9: 687.

Si-Tayeb, K., F. K. Noto, M. Nagaoka, J. Li, M. A. Battle, C. Duris, P. E. North, S. Dalton and S. A. Duncan (2010). "Highly efficient generation of human hepatocyte-like cells from induced pluripotent stem cells." Hepatology 51(1): 297-305.

Silva, J. C. P., C. Marques, F. O. Martins, I. Viegas, L. Tavares, M. P. Macedo and J. G. Jones (2019). "Determining contributions of exogenous glucose and fructose to de novo fatty acid and glycerol synthesis in liver and adipose tissue." Metab Eng 56: 69-76.

Singh, V. P., A. Bali, N. Singh and A. S. Jaggi (2014). "Advanced glycation end products and diabetic complications." Korean J Physiol Pharmacol 18(1): 1-14.

Sladek, R., G. Rocheleau, J. Rung, C. Dina, L. Shen, D. Serre, P. Boutin, D. Vincent, A. Belisle, S. Hadjadj, B. Balkau, B. Heude, G. Charpentier, T. J. Hudson, A. Montpetit, A. V. Pshezhetsky, M. Prentki, B. I. Posner, D. J. Balding, D. Meyre, C. Polychronakos and P.

Froguel (2007). "A genome-wide association study identifies novel risk loci for type 2 diabetes." Nature 445(7130): 881-885.

Sluse, F. E., W. Jarmuszkiewicz, R. Navet, P. Douette, G. Mathy and C. M. Sluse-Goffart (2006). "Mitochondrial UCPs: new insights into regulation and impact." Biochim Biophys Acta 1757(5-6): 480-485.

Smith, G. I., B. Mittendorfer and S. Klein (2019). "Metabolically healthy obesity: facts and fantasies." J Clin Invest 129(10): 3978-3989.

Sokolowska, E. and A. Blachnio-Zabielska (2019). "The Role of Ceramides in Insulin Resistance." Front Endocrinol (Lausanne) 10: 577.

Sookoian, S. and C. J. Pirola (2017). "Genetic predisposition in nonalcoholic fatty liver disease." Clin Mol Hepatol 23(1): 1-12.

Soty, M., A. Gautier-Stein, F. Rajas and G. Mithieux (2017). "Gut-Brain Glucose Signaling in Energy Homeostasis." Cell Metab 25(6): 1231-1242.

Spracklen, C. N., M. Horikoshi, Y. J. Kim, K. Lin, F. Bragg, S. Moon, K. Suzuki, C. H. T. Tam, Y. Tabara, S. H. Kwak, F. Takeuchi, J. Long, V. J. Y. Lim, J. F. Chai, C. H. Chen, M. Nakatochi, J. Yao, H. S. Choi, A. K. Iyengar, H. J. Perrin, S. M. Brotman, M. van de Bunt, A. L. Gloyn, J. E. Below, M. Boehnke, D. W. Bowden, J. C. Chambers, A. Mahajan, M. I. McCarthy, M. C. Y. Ng, L. E. Petty, W. Zhang, A. P. Morris, L. S. Adair, M. Akiyama, Z. Bian, J. C. N. Chan, L. C. Chang, M. L. Chee, Y. I. Chen, Y. T. Chen, Z. Chen, L. M. Chuang, S. Du, P. Gordon-Larsen, M. Gross, X. Guo, Y. Guo, S. Han, A. G. Howard, W. Huang, Y. J. Hung, M. Y. Hwang, C. M. Hwu, S. Ichihara, M. Isono, H. M. Jang, G. Jiang, J. B. Jonas, Y. Kamatani, T. Katsuya, T. Kawaguchi, C. C. Khor, K. Kohara, M. S. Lee, N. R. Lee, L. Li, J. Liu, A. O. Luk, J. Lv, Y. Okada, M. A. Pereira, C. Sabanayagam, J. Shi, D. M. Shin, W. Y. So, A. Takahashi, B. Tomlinson, F. J. Tsai, R. M. van Dam, Y. B. Xiang, K. Yamamoto, T. Yamauchi, K. Yoon, C. Yu, J. M. Yuan, L. Zhang, W. Zheng, M. Igase, Y. S. Cho, J. I. Rotter, Y. X. Wang, W. H. H. Sheu, M. Yokota, J. Y. Wu, C. Y. Cheng, T. Y. Wong, X. O. Shu, N. Kato, K. S. Park, E. S. Tai, F. Matsuda, W. P. Koh, R. C. W. Ma, S. Maeda, I. Y. Millwood, J. Lee, T. Kadowaki, R. G. Walters, B. J. Kim, K. L. Mohlke and X. Sim (2020). "Identification of type 2 diabetes loci in 433,540 East Asian individuals." Nature 582(7811): 240-245.

Srinivasan, K. and P. Ramarao (2007). "Animal models in type 2 diabetes research: an overview." Indian J Med Res 125(3): 451-472.

Steil, G. M., N. Trivedi, J. C. Jonas, W. M. Hasenkamp, A. Sharma, S. Bonner-Weir and G. C. Weir (2001). "Adaptation of beta-cell mass to substrate oversupply: enhanced function with normal gene expression." Am J Physiol Endocrinol Metab 280(5): E788-796.

Stumvoll, M., B. J. Goldstein and T. W. van Haeften (2005). "Type 2 diabetes: principles of pathogenesis and therapy." Lancet 365(9467): 1333-1346.

Sugden, M. C. and M. J. Holness (2011). "The pyruvate carboxylase-pyruvate dehydrogenase axis in islet pyruvate metabolism: Going round in circles?" Islets 3(6): 302-319.

Sun, K., C. M. Kusminski and P. E. Scherer (2011). "Adipose tissue remodeling and obesity." J Clin Invest 121(6): 2094-2101.

Szegezdi, E., S. E. Logue, A. M. Gorman and A. Samali (2006). "Mediators of endoplasmic reticulum stress-induced apoptosis." EMBO Rep 7(9): 880-885.

Tajiri, Y., C. Moller and V. Grill (1997). "Long-term effects of aminoguanidine on insulin release and biosynthesis: evidence that the formation of advanced glycosylation end products inhibits B cell function." Endocrinology 138(1): 273-280.

Takeuchi, K. and K. Reue (2009). "Biochemistry, physiology, and genetics of GPAT, AGPAT, and lipin enzymes in triglyceride synthesis." Am J Physiol Endocrinol Metab 296(6): E1195-1209.

Tamarina, N. A., M. W. Roe and L. Philipson (2014). "Characterization of mice expressing Ins1 gene promoter driven CreERT recombinase for conditional gene deletion in pancreatic beta-cells." Islets 6(1): e27685.

Tanaka, Y., C. E. Gleason, P. O. Tran, J. S. Harmon and R. P. Robertson (1999). "Prevention of glucose toxicity in HIT-T15 cells and Zucker diabetic fatty rats by antioxidants." Proc Natl Acad Sci U S A 96(19): 10857-10862.

Tang, C., K. Koulajian, I. Schuiki, L. Zhang, T. Desai, A. Ivovic, P. Wang, C. Robson-Doucette, M. B. Wheeler, B. Minassian, A. Volchuk and A. Giacca (2012). "Glucose-induced beta cell

dysfunction in vivo in rats: link between oxidative stress and endoplasmic reticulum stress." Diabetologia 55(5): 1366-1379.

Tengholm, A. (2012). "Cyclic AMP dynamics in the pancreatic beta-cell." Ups J Med Sci 117(4): 355-369.

Teresa Pellicer, M., M. Felisa Nunez, J. Aguilar, J. Badia and L. Baldoma (2003). "Role of 2-phosphoglycolate phosphatase of Escherichia coli in metabolism of the 2-phosphoglycolate formed in DNA repair." J Bacteriol 185(19): 5815-5821.

Thomas, D. D., B. E. Corkey, N. W. Istfan and C. M. Apovian (2019). "Hyperinsulinemia: an early indicator of metabolic dysfunction." J Endocr Soc 3(9): 1727-1747.

Thorens, B., D. Tarussio, M. A. Maestro, M. Rovira, E. Heikkila and J. Ferrer (2015). "Ins1(Cre) knock-in mice for beta cell-specific gene recombination." Diabetologia 58(3): 558-565.

Tiedge, M., S. Lortz, J. Drinkgern and S. Lenzen (1997). "Relation between antioxidant enzyme gene expression and antioxidative defense status of insulin-producing cells." Diabetes 46(11): 1733-1742.

Timm, S., F. Woitschach, C. Heise, M. Hagemann and H. Bauwe (2019). "Faster Removal of 2-Phosphoglycolate through Photorespiration Improves Abiotic Stress Tolerance of Arabidopsis." Plants (Basel) 8(12).

Torres, G. G., M. Nygaard, A. Caliebe, H. Blanche, S. Chantalat, P. Galan, W. Lieb, L. Christiansen, J. F. Deleuze, K. Christensen, K. Strauch, M. Muller-Nurasyid, A. Peters, M. M. Nothen, P. Hoffmann, F. Flachsbart, S. Schreiber, D. Ellinghaus, A. Franke, J. Dose and A. Nebel (2021). "Exome-wide association study identifies FN3KRP and PGP as new candidate longevity genes." J Gerontol A Biol Sci Med Sci 76(5): 786-795.

Trites, M. J. and R. D. Clugston (2019). "The role of adipose triglyceride lipase in lipid and glucose homeostasis: lessons from transgenic mice." Lipids Health Dis 18(1): 204.

Tsang, C. K., H. Qi, L. F. Liu and X. F. Zheng (2007). "Targeting mammalian target of rapamycin (mTOR) for health and diseases." Drug Discov Today 12(3-4): 112-124.

Unger, R. H. (1995). "Lipotoxicity in the pathogenesis of obesity-dependent NIDDM. Genetic and clinical implications." Diabetes 44(8): 863-870.

Unger, R. H. and S. Grundy (1985). "Hyperglycaemia as an inducer as well as a consequence of impaired islet cell function and insulin resistance: implications for the management of diabetes." Diabetologia 28(3): 119-121.

Van Schaftingen, E., L. Hue and H. G. Hers (1980). "Fructose 2,6-bisphosphate, the probably structure of the glucose- and glucagon-sensitive stimulator of phosphofructokinase." Biochem J 192(3): 897-901.

Vasconcellos, R., E. C. Alvarenga, R. C. Parreira, S. S. Lima and R. R. Resende (2016). "Exploring the cell signalling in hepatocyte differentiation." Cell Signal 28(11): 1773-1788.

Vella, A., M. Camilleri and R. A. Rizza (2004). "The gastrointestinal tract and glucose tolerance." Curr Opin Clin Nutr Metab Care 7(4): 479-484.

Wang, J., C. Ye and S. Fei (2020). "Association between APOC3 polymorphisms and non-alcoholic fatty liver disease risk: a meta-analysis." Afr Health Sci 20(4): 1800-1808.

Wang, Y., H. Kwon, X. Su and F. E. Wondisford (2020). "Glycerol not lactate is the major net carbon source for gluconeogenesis in mice during both short and prolonged fasting." Mol Metab 31: 36-44.

Weisberg, S. P., D. McCann, M. Desai, M. Rosenbaum, R. L. Leibel and A. W. Ferrante, Jr. (2003). "Obesity is associated with macrophage accumulation in adipose tissue." J Clin Invest 112(12): 1796-1808.

Wendel, A. A., T. M. Lewin and R. A. Coleman (2009). "Glycerol-3-phosphate acyltransferases: rate limiting enzymes of triacylglycerol biosynthesis." Biochim Biophys Acta 1791(6): 501-506.

Wicksteed, B., M. Brissova, W. Yan, D. M. Opland, J. L. Plank, R. B. Reinert, L. M. Dickson, N. A. Tamarina, L. H. Philipson, A. Shostak, E. Bernal-Mizrachi, L. Elghazi, M. W. Roe, P. A. Labosky, M. G. Myers, Jr., M. Gannon, A. C. Powers and P. J. Dempsey (2010). "Conditional gene targeting in mouse pancreatic ss-cells: analysis of ectopic Cre transgene expression in the brain." Diabetes 59(12): 3090-3098.

Wondmkun, Y. T. (2020). "Obesity, Insulin Resistance, and Type 2 Diabetes: Associations and Therapeutic Implications." Diabetes Metab Syndr Obes 13: 3611-3616.

Woods, S. C., R. J. Seeley, D. Porte, Jr. and M. W. Schwartz (1998). "Signals that regulate food intake and energy homeostasis." Science 280(5368): 1378-1383.

Wortham, M. and M. Sander (2016). "Mechanisms of beta-cell functional adaptation to changes in workload." Diabetes Obes Metab 18 Suppl 1: 78-86.

Wride, M. A. (2000). "Minireview: apoptosis as seen through a lens." Apoptosis 5(3): 203-209.

Xue, L. L., H. H. Chen and J. G. Jiang (2017). "Implications of glycerol metabolism for lipid production." Prog Lipid Res 68: 12-25.

Yamashita, H., M. Takenoshita, M. Sakurai, R. K. Bruick, W. J. Henzel, W. Shillinglaw, D. Arnot and K. Uyeda (2001). "A glucose-responsive transcription factor that regulates carbohydrate metabolism in the liver." Proc Natl Acad Sci U S A 98(16): 9116-9121.

Yan, Z., H. Yan and H. Ou (2012). "Human thyroxine binding globulin (TBG) promoter directs efficient and sustaining transgene expression in liver-specific pattern." Gene 506(2): 289-294.

Yanovski, J. A. (2018). "Obesity: Trends in underweight and obesity - scale of the problem." Nat Rev Endocrinol 14(1): 5-6.

Ye, D. Z., M. H. Tai, K. D. Linning, C. Szabo and L. K. Olson (2006). "MafA expression and insulin promoter activity are induced by nicotinamide and related compounds in INS-1 pancreatic beta-cells." Diabetes 55(3): 742-750.

Yki-Jarvinen, H. (2014). "Non-alcoholic fatty liver disease as a cause and a consequence of metabolic syndrome." Lancet Diabetes Endocrinol 2(11): 901-910.

Yu, K. T., C. Pendley, 2nd, T. Herczeg and R. G. Pendleton (1990). "2,3-Diphosphoglycerate phosphatase/synthase: a potential target for elevating the diphosphoglycerate level in human red blood cells." J Pharmacol Exp Ther 252(1): 192-200.

Yu, Y. H. and H. N. Ginsberg (2004). "The role of acyl-CoA:diacylglycerol acyltransferase (DGAT) in energy metabolism." Ann Med 36(4): 252-261.

Yusta, B., L. L. Baggio, J. L. Estall, J. A. Koehler, D. P. Holland, H. Li, D. Pipeleers, Z. Ling and D. J. Drucker (2006). "GLP-1 receptor activation improves beta cell function and survival following induction of endoplasmic reticulum stress." Cell Metab 4(5): 391-406.

Zechner, R., J. G. Strauss, G. Haemmerle, A. Lass and R. Zimmermann (2005). "Lipolysis: pathway under construction." Curr Opin Lipidol 16(3): 333-340.

Zechner, R., R. Zimmermann, T. O. Eichmann, S. D. Kohlwein, G. Haemmerle, A. Lass and F. Madeo (2012). "Fat signals--lipases and lipolysis in lipid metabolism and signaling." Cell Metab 15(3): 279-291.

Zhang, Y., R. Proenca, M. Maffei, M. Barone, L. Leopold and J. M. Friedman (1994). "Positional cloning of the mouse obese gene and its human homologue." Nature 372(6505): 425-432.

Zhao, L., X. Guo, O. Wang, H. Zhang, Y. Wang, F. Zhou, J. Liu and B. Ji (2016). "Fructose and glucose combined with free fatty acids induce metabolic disorders in HepG2 cell: A new model to study the impacts of high-fructose/sucrose and high-fat diets in vitro." Mol Nutr Food Res 60(4): 909-921.

Zhao, S., Y. Mugabo, G. Ballentine, C. Attane, J. Iglesias, P. Poursharifi, D. Zhang, T. A. Nguyen, H. Erb, R. Prentki, M. L. Peyot, E. Joly, S. Tobin, S. Fulton, J. M. Brown, S. R. Madiraju and M. Prentki (2016). "alpha/beta-Hydrolase Domain 6 Deletion Induces Adipose Browning and Prevents Obesity and Type 2 Diabetes." Cell Rep 14(12): 2872-2888.

Zhao, S., Y. Mugabo, J. Iglesias, L. Xie, V. Delghingaro-Augusto, R. Lussier, M. L. Peyot, E. Joly, B. Taib, M. A. Davis, J. M. Brown, A. Abousalham, H. Gaisano, S. R. Madiraju and M. Prentki (2014). "alpha/beta-Hydrolase domain-6-accessible monoacylglycerol controls glucose-stimulated insulin secretion." Cell Metab 19(6): 993-1007.

Zhao, S., P. Poursharifi, Y. Mugabo, E. J. Levens, K. Vivot, C. Attane, J. Iglesias, M. L. Peyot, E. Joly, S. R. Madiraju and M. Prentki (2015). "alpha/beta-Hydrolase domain-6 and saturated long chain monoacylglycerol regulate insulin secretion promoted by both fuel and non-fuel stimuli." Mol Metab 4(12): 940-950.

Zheng, Y., L. Zhao, J. Zhang, H. Zhang, X. Ma and D. Wei (2008). "Production of glycerol from glucose by coexpressing glycerol-3-phosphate dehydrogenase and glycerol-3-phosphatase in Klebsiella pneumoniae." J Biosci Bioeng 105(5): 508-512.